THÈSE POUR OBTENIR LE GRADE DE DOCTEUR DE MONTPELLIER SUPAGRO

En Biologie Intégrative, Diversité et Amélioration des Plantes (BIDAP)

École doctorale GAIA – Biodiversité, Agriculture, Alimentation, Environnement, Terre, Eau

Portée par

Unité de recherche Biochimie & Physiologie Moléculaire des Plantes ($B_{\&}$PMP)

Transport à longue distance de K^+ et adaptation au stress salin chez le riz: analyses moléculaires et physiologiques de l'implication de canaux K^+

Présentée par Jing ZHOU

Le 13 juillet 2021

Sous la direction de Anne-Aliénor VERY

Devant le jury composé de

M. Manuel NIEVES-CORDONES, Chercheur, CEBAS-CSIC Murcia, Espagne	Rapporteur
M. Rob ROELFSEMA, Chercheur, Univ. Würzburg, Allemagne	Rapporteur
M. Pascal GANTET, Professeur, Univ. Montpellier, France	Président de jury
M. Tomoaki HORIE, Professeur, Univ. Shinshu, Japon	Examinateur
M. Yi WANG, Professeur, China Agricultural Univ., Chine	Examinateur
Mme Anne-Aliénor VERY, CR CNRS, Montpellier	Directrice de thèse

UNIVERSITÉ DE MONTPELLIER

Montpellier SupAgro

THÈSE POUR OBTENIR LE GRADE DE DOCTEUR DE MONTPELLIER SUPAGRO

En Biologie Intégrative, Diversité et Amélioration des Plantes (BIDAP)

École doctorale GAIA – Biodiversité, Agriculture, Alimentation, Environnement, Terre, Eau

Portée par

Unité de recherche Biochimie & Physiologie Moléculaire des Plantes ($B_{\&}$PMP)

Long-distance K^+ transport and adaptation to salt stress in rice: Molecular and physiological analyses of the involvement of K^+ channels

Présentée par Jing ZHOU

Le 13 juillet 2021

Sous la direction de Anne-Aliénor VERY

Devant le jury composé de

M. Manuel NIEVES-CORDONES, Chercheur, CEBAS-CSIC Murcia, Espagne	Rapporteur
M. Rob ROELFSEMA, Chercheur, Univ. Würzburg, Allemagne	Rapporteur
M. Pascal GANTET, Professeur, Univ. Montpellier, France	Président de jury
M. Tomoaki HORIE, Professeur, Univ. Shinshu, Japon	Examinateur
M. Yi WANG, Professeur, China Agricultural Univ., Chine	Examinateur
Mme Anne-Aliénor VERY, CR CNRS, Montpellier	Directrice de thèse

UNIVERSITÉ DE MONTPELLIER

Montpellier SupAgro

Acknowledgement

During my PhD, I have imagined heaps of times how I could write down the gratitude hidden in my heart to thank all of you who have cared and helped me. At this moment, I could get down to doing the actual writing but do not know where to start. A million memories of the care and help I got flashed through my mind, finally freeze-frame in a venerable person, my supervisor Dr **Anne-Aliénor Véry**. Four years ago, she provided me the opportunity to join her group. I am deeply grateful for her supervision and guidance on my thesis work. Her rigorous attitude towards science and optimistic attitude towards challenges have profoundly influenced me. Her support, help, patience, advice, and encouragement have been valuable throughout this entire thesis work but also in my daily life.

I would specially like to thank Dr **Hervé Sentenac**, I have greatly enjoyed and benefited from scientific discussions with him during my PhD. I have also benefited a lot from his precious suggestions on my thesis writing. I really admire him for his rigorous attitude towards science, deep insight, profound knowledge, and his dedication to science.

I would also like to thank **Claire Corratgé-Faillie** and **Martin Boeglin** for helping in electrophysiology experiment. Thanks to **Doan Trung Luu** for his help in In-fusion cloning. Thanks to **Pierre Berthomieu**, **Jean-Christophe Boyer**, **Jean-Benoît Peltier**, **Guilhem Desbrosses** for their help in experiment aspects and lots of precious scientific discussions. Thanks to **Emmanuel Guiderdoni**, **Christian Chaine**, **Eve Lorenzini**, **Christophe Périn** and **Remy Michel** for helping the rice mutant line amplification and rice hybridization. Thanks to **Brigitte Touraine** for her help in HPLC analysis. Thanks to **Carine Alcon** for her expertise and assistance with microscopy. Thanks to **Gaëlle Rolland** for her help in sugar analysis.

In the B&PMP laboratory, I am very thankful for the help and friendship of the present and past members. They are **Houssein Zhour**, **Mahé Larose**, **Thanyakorn Rongsawat**, **Li-Min Wang**, **Li-Na Zhao**, **Ning Tang**, **Yun-Ji Huang**, **Shou-Yang Liu**, **Hui Kyong Cho**…There are too many to mention, however, special thanks go to **Ikram Madani** for her infinite help in my daily life and all her encouragements when I am down.

My thanks to all the members in the B&PMP laboratory that provided assistances on this thesis.

I would like to thank my thesis committee members, Dr **Christophe Maurel**, Dr **Jacques Le Gouis**, and Dr **Thierry Simonneau**, for all of their valuable suggestions, comments, and supports through this entire process.

I would also like to thank Dr **Rob Roelfsema**, Dr **Manuel Nieves-Cordones**, Dr **Pascal Gantet**, Dr **Tomoaki Horie**, and Dr **Yi Wang** for being my jury of this thesis. Their corrections and suggestions greatly improved the readability of this thesis.

My thanks extend to those people who have cared and helped me over the years, especially my supervisors Dr **Cheng-Lei Li** and Dr **Qi Wu** during my Master of Science.

I would like to express my gratitude to the financial support of my thesis provided by China Scholarship Council. Thanks also to INRAE B&PMP laboratory and L'institut Agro for hosting me.

Lastly, I am deeply indebted to my parents for their support throughout all of my studies. In particular I would like to mention my partner for his help, support, and encouragement throughout my study and life to get through those tough times.

***Summary**:* Rice high quality and yield requires the supply of K^+, as that of other macronutrients. Efficient absorption of K^+ by the roots from the soil solution and distribution of this cation within the plant, through long distance circulation via the xylem and phloem vasculature, the ascending flow being driven in part by the transpiration stream, is essential to support biomass and grain yield production, also in stressing environmental conditions such as soil salinity. The aim of my thesis was to study rice K^+ transport systems involved in these key processes, for a better understanding of K^+ transport mechanisms at the whole plant level, towards future development of more productive and salt stress adapted crops. In this study, a reverse genetics approach revealed that the outwardly-rectifying Shaker K^+ channel OsK5.2 is a major determinant of plant growth upon saline conditions. Under salt treatment, qRT-PCR analysis showed that *OsK5.2* expression was weakly affected in roots and rapidly upregulated in leaves. OsK5.2 mediated K^+ efflux from guard cells limiting stomatal aperture was shown to minimize the Na^+ flux arriving in shoots via the transpiration stream. OsK5.2 contribution to K^+ loading into the xylem sap outperformed the negative effect of the decrease in xylem sap flow for shoot K^+ feeding. OsK5.2 combined functions appeared, so, highly beneficial to the leaf K^+ to Na^+ homeostasis upon saline conditions and Na^+ toxicity limitation. OsK5.2 was also revealed to be crucial for plant biomass production under limitation of the day light period, suggesting a role in phloem transport. *OsK5.2* promoter *GUS* reporter fusions indicated localization of *OsK5.2* expression in the phloem companion cells of root and shoot. By tracing K^+ circulation in xylem and phloem saps, using Rb^+, an important physiological contribution of OsK5.2 to K^+ unloading from the phloem in roots was evidenced. In addition, analysis in rice and heterologously in Arabidopsis of another outward Shaker channel expressed in root vasculature, OsK5.1, suggested that this channel might play a role in xylem sap K^+ loading, in addition to OsK5.2.

Keywords: Outward Shaker K^+ channels, long-distance K^+ transport, salt tolerance, reverse genetics, rice, Arabidopsis, physiology, expression studies, heterologous expression

Résumé: L'obtention de hauts rendements chez le riz repose sur l'apport de K^+, comme celui d'autres macronutriments. L'absorption efficace de K^+ par les racines à partir de la solution du sol et la distribution de ce cation dans la plante, par une circulation sur de longues distances via le xylème et le phloème, le flux ascendant étant alimenté en partie par la transpiration, sont essentielles pour la production de biomasse et de grains, également dans des conditions environnementales stressantes telles qu'une forte salinité du sol. L'objectif de ma thèse a été d'étudier les systèmes de transport de K^+ impliqués dans ces processus clés chez le riz, pour une meilleure compréhension des mécanismes de transport de K^+ au niveau de la plante entière, en vue du développement futur de cultures plus productives et adaptées au stress salin. Dans cette étude, une approche de génétique inverse a révélé que le canal Shaker d'efflux de K^+ OsK5.2 est un déterminant majeur du maintien de la croissance des plantes en conditions salines. Sous traitement salin, l'analyse par qRT-PCR a montré que l'expression d'*OsK5.2* était maintenue dans les racines et stimulée dans les feuilles. La fonction d'efflux de K^+ d'OsK5.2 dans les cellules de garde limitant l'ouverture des stomates s'est révélée minimiser le flux de Na^+ arrivant aux parties aériennes via le flux de transpiration. La contribution d'OsK5.2 à la charge en K^+ de la sève xylèmienne surpasse l'effet négatif de la diminution du débit volumétrique dans le xylème pour l'alimentation en K^+ des parties aériennes. Les fonctions combinées d'OsK5.2 se sont donc montrées très bénéfiques à l'homéostasie K^+/Na^+ de la feuille en conditions salines et à la limitation de la toxicité de Na^+. OsK5.2 s'est également révélé crucial pour la production de biomasse en cas de limitation de la période lumineuse journalière, suggèrant un rôle dans le transport phloémien. En exprimant le gène rapporteur *GUS* sous contrôle du promoteur d'*OsK5.2*, il est apparu qu'*OsK5.2* s'exprime dans les cellules compagnes du phloème des racines et des parties aériennes. L'utilisation de Rb^+ pour tracer la circulation de K^+ dans les sèves du xylème et du phloème, a révélé une contribution importante d'OsK5.2 à la décharge de K^+ du phloème dans les racines. Enfin, l'analyse chez le riz et en contexte hétérologue chez Arabidopsis d'un autre canal Shaker d'efflux exprimé dans le système vasculaire des racines, OsK5.1, a suggéré que ce canal pourrait être impliqué, en plus d'OsK5.2, dans la charge en K^+ de la sève xylèmienne chez le riz.

Mots clés: canaux Shaker d'efflux de K^+, transport de K^+ sur de longues distances, tolérance au sel, génétique inverse, riz, Arabidopsis, physiologie, analyses d'expression, expression hétérologue.

List of abbreviations

ABA: abscisic acid

ATP: adenosine triphosphate

cDNA: complementary deoxyribonucleic acid

CDS: coding sequences

C_T: cycle threshold

CTAB: cetyltrimethylammonium bromide

cv: cultivar

D-MEM: Dulbecco's Modified Eagle's Medium

DNA: deoxyribonucleic acid

dNTP: deoxynucleotide triphosphate

DW: dry weight

EDTA: ethylenediaminetetraacetic acid

FW: fresh weight

GUS: β-glucuronidase

HEPES: 4-(2-hydroxyethyl)-1-piperazineethanesulfonic acid

KO: knock-out

LB: Luria-Bertani medium

LTR: long terminal repeat

mRNA: messenger RNA

ms: millisecond

MS: Murashige and Skoog medium

NOS: Nopaline synthase

PCR: polymerase chain reaction

qRT-PCR: real-time quantitative reverse transcription PCR

RNA: ribonucleic acid

RNase: ribonuclease

rpm: revolution per minute

RT-PCR: reverse transcription PCR

SOC: Super Optimal broth with Catabolite repression

SV40: Simian Virus 40

T-DNA: transfer DNA

Tris: tris(hydroxymethyl)aminomethane

Triton X-100: t-octylphenoxypolyethoxyethanol

UTR: untranslated region

WT: wild-type

X-Gluc: 5-Bromo-4-chloro-1H-indol-3-yl β-D-glucopyranosiduronic acid

Table of contents

Chapter I 4

Introduction 4

I.1 The alkali cation potassium (K^+): Roles in the plant 5

I.1.1 K^+ content and distribution in plants 5

I.1.2 The roles of K^+ in the plant 5

I.2 Families of plant K^+ transport systems at the plasma membrane 7

I.2.1 Shaker K^+ channels 8

I.2.2 K^+ transporters 10

I.3 Integration of K^+ transport in Arabidopsis and rice 13

I.3.1 Root K^+ uptake from soil 13

I.3.2 Long-distance transport of K^+ in xylem and phloem 15

I.3.3 K^+ fluxes in guard cells and control of stomatal aperture 18

I.4 K^+ significance in plant tolerance to salinity stress 20

I.4.1 Soil salinization: a major restriction for agriculture 20

I.4.2 The alkali cation Na^+ 20

I.4.3 The components of salt stress (osmotic, ionic) 22

I.4.4 The K^+/Na^+ balance: a determinant of tolerance to salt stress 24

I.4.5 Ion transport systems involved in QTLs of K^+/Na^+ homeostasis under salt stress in Arabidopsis and rice 24

I.5 Objectives of my thesis 26

Chapter II 27

Materials and methods 27

II.1 Plant materials 28

II.2 Plant culture systems 28

II.2.1 Rice culture on terrines 28

II.2.2 Rice culture on individual pots 28

II.2.3 Rice hydroponic culture 29

II.2.4 Arabidopsis culture 29

II.3 Generation of rice double mutants using cross-pollination 30

II.4 Physiological analysis of mutant lines 30
II.4.1 Plant tissue collection and analysis of Na^+, K^+ and Rb^+ contents in rice and Arabidopsis 30
II.4.2 Xylem sap collection and analysis of Na^+, K^+ and Rb^+ concentrations in rice and Arabidopsis 31
II.4.3 Phloem sap collection and analysis in rice 32
II.4.4 Measurement of rice leaf transpiration using multi-potometer 33
II.4.5 Sugar content assay in rice leaf tissues 33
II.5 Molecular biology techniques 33
II.5.1 Genotyping of *Tos17* and T-DNA insertion lines 33
II.5.2 qRT-PCR analysis of gene expression 35
II.5.3 Gene cloning 36
II.6 Histochemical analysis of GUS activity in transgenic plants expressing *promoter::GUS* constructs 40
II.7 Agrobacterium tumefaciens-mediated transformation of *Arabidopsis thaliana* 41
II.7.1 Transformation of competent *A. tumefaciens* cells 41
II.7.2 Arabidopsis transformation by floral dip method 42
II.7.3 Selection of transgenic plant 42
II.8 Heterologous expression in COS-7 cells and electrophysiology 43
II.8.1 COS-7 cell line 43
II.8.2 COS-7 cell culture 43
II.8.3 Cell transfection 44
II.8.4 Whole-cell patch-clamp 44
II.9 Statistical methods 45
Chapter III 46
The outward Shaker channel OsK5.2 is beneficial to the plant salt tolerance through its role in K^+ translocation and its control of leaf transpiration 46
Chapter IV 63
K^+ unloading from phloem sap mediated by the OsK5.2 outward K^+ channel strongly determines shoot K^+ nutrition 63
IV.1 Introduction 64
IV.2 Results 66

IV.2.1 *OsK5.2* is particularly expressed in phloem tissues of sink organs 66
IV.2.2 Reduced K^+ concentration in the phloem sap of *osk5.2* plants in addition to that in the xylem sap and leaf tissues 66
IV.2.3 Using Rb^+ to trace K^+ circulation in the plant and assess OsK5.2 functions 67
IV.2.4 OsK5.2 contributes to xylem sap K^+ loading in the roots via both direct secretion in the stele and K^+ unloading from the phloem sap, its role in phloem being predominant in standard plant growth conditions 69
IV.2.5 Reduced growth of *osk5.2* plant under short-day condition 71
IV.2.6 Reduced fructose content in the leaves of *osk5.2* plants under normal day length 72
IV.3 Discussion 72
Chapter V 77
Study of K^+ transport by OsK5.1 and OsK5.2 in heterologous systems and in *planta* 77
V.1 Introduction 78
V.2 Results 80
V.2.1 *OsK5.1* expression pattern 80
V.2.2 Analysis of tissue K^+ contents and xylem sap K^+ concentrations in wild-type and *osk5.1* mutant plants 80
V.2.3 Production of *atskor* complemented lines expressing p*AtSKOR::OsK5.1* or p*AtSKOR::OsK5.2* constructs 80
V.2.4 Analysis of K^+ translocation towards the shoots in *atskor*/p*AtSKOR::OsK5.1* or *atskor*/p*AtSKOR::OsK5.2* complemented lines 81
V.2.5 Electrophysiological characterization of OsK5.1 and OsK5.2 in COS-7 cells 82
V.3 Discussion 84
Chapeter VI 89
Conclusion and perspectives 89
References 95
Annexes 110
Résumé long de la thèse en français 111

Chapter I

Introduction

I.1 The alkali cation potassium (K^+): Roles in the plant

I.1.1 K^+ content and distribution in plants

K^+ is the most abundant inorganic cation in plants, comprising of up to 10% of total plant's dry weight (Véry & Sentenac, 2003). K^+ is highly mobile within plants, and can be transported over long-distance exhibiting cycling within the vasculature. The previous studies found that K^+ is preferentially distributed in the growing zones and young tissues, and can be rapidly remobilized from older to younger tissues to support growth (Atwell & Steer, 1990; Proe, Midwood, & Craig, 2000). With varying external environment and cell type, the K^+ concentration of plant cells is found in the range of 10 to 500 mM, essentially due to great variability in vacuolar concentration (Marschner, 1995). The vacuole and the cytoplasm are the two major K^+ pools in plant cells. In cytoplasm, the K^+ concentration is relatively constant around 100 mM, which is the optimal concentration for activation of enzymes participating in intermediary metabolism and biosynthesis (Clarkson & Hanson, 1980; Ragel, Raddatz, Leidi, Quintero, & Pardo, 2019). In contrast to the relative stability of K^+ concentration in cytoplasm, K^+ is greatly variable with concentration range of 10 to more than 200 mM in vacuoles in relation to the functions of K^+ in cell expansion and other turgor-driven processes (Marschner, 1995). Since vacuoles occupy approximately 90% of intracellular volume in many plant cells and are the main cellular reservoir for K^+, changes of K^+ concentration in tissue reflect that in vacuole (Barragán et al., 2012). In K^+-sufficient condition, surplus K^+ is stored into the vacuole allowing to lower the osmotic potential, to generate turgor and drive cell expansion. In contrast, in K^+-deficient condition, cytoplasmic K^+ concentration remains relatively constant to maintain the appropriate environment for enzyme reactions as a consequence of K^+ efflux from vacuole. Meanwhile, other cations like sodium (Na^+) present in the cytosol can be accumulated in the vacuole for replacing K^+ (at least in part) in order to maintain turgor. Besides, K^+ concentration might even reach up to 500 mM in some specialized cells as the guard cells of stomata (Marschner, 1995).

I.1.2 The roles of K^+ in the plant

I.1.2.1 Enzyme activation

In 1943, Boyer et al. initially reported that the catalytic activity of pyruvate kinase requires K^+

(Boyer, Lardy, & Phillips, 1943). After that, K^+ was confirmed to be involved in the activation for more than 60 enzyme systems, which are responsible for a series of metabolic processes (Evans & Sorger, 1966; Suelter, 1970). Also, K^+ participates in the activation of H^+-ATPases at the plasma membrane. The activation of the H^+-ATPase creates a transmembrane electrochemical gradient, which provides a sustained driving force for K^+ influx across the plasma membrane leading to cell expansion and osmoregulation (Marschner, 1995; Michelet & Boutry, 1995).

I.1.2.2 Maintenance of cytoplasmic pH homeostasis

The process of nitrate assimilation is an example of illustration of the role of K^+ in cytoplasmic pH homeostasis through charge balance upon cycling between roots and shoots. K^+ is the dominant counterion accompanying NO_3^- transport. After being taken up by roots, most of NO_3^- is assimilated through NO_3^- reduction. To prevent increase in cytosolic pH arising from NO_3^- reduction in the leaves, organic acids, mainly malate, are synthetized. Such carboxylate ions can be translocated through the phloem together with K^+ (to allow charge balance) from the shoots to the roots. There, HCO_3^- ions are excreted to the external solution after organic acid decarboxylation, thus facilitating further uptake of NO_3^- and of the counterion K^+ (Lea & Morot-Gaudry, 2001; Marschner, 2011; Touraine, Muller &Grignon, 1992; van Beusichem, Baas, Kirkby, & Nelemans, 1985).

I.1.2.3 Control of cell membrane potential

Since most cell membranes contain open K^+ channels in resting conditions (*i.e.*, without requiring specific electrical signal), they are strongly permeable to K^+, much more than to Na^+ or other ions. K^+ concentration at both sides of cell membrane have therefore a great influence on cell membrane potential. Electrophysiological studies show indeed that the resting membrane potential of a living plant cell mainly depends on the extracellular K^+ concentration. An increase in extracellular K^+ concentration causes cell membrane depolarization, through increased K^+ uptake. In contrast, the membrane is hyperpolarized when the extracellular K^+ concentration decreases. The hyperpolarization promotes the activation of inwardly-rectifying Shaker K^+ channels (Maathuis & Sanders, 1994; Nieves-Cordones, Al Shiblawi, & Sentenac, 2016; Véry & Sentenac, 2003).

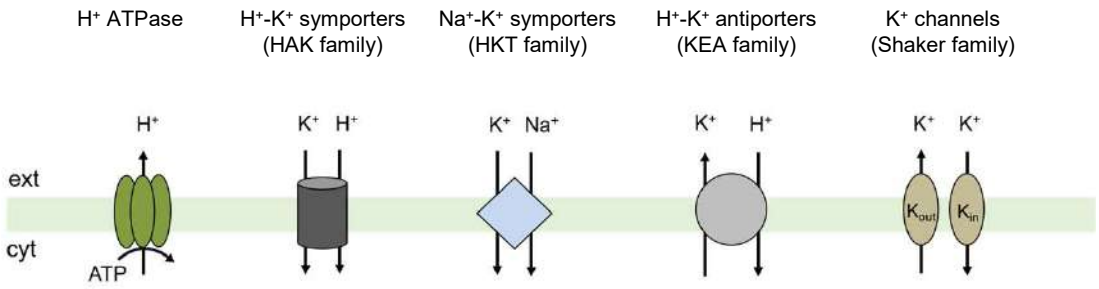

Figure I.1 Families of plant K^+ transport systems in plasma membrane.

I.1.2.4 Cell turgor-driven movements

As the most abundant inorganic solute in plant, K^+ plays an important role in building cell turgor. Accumulation of intracellular K^+ decreases the cell water potential leading to the water influx from external solution which creates turgor pressure. Cell turgor is required for cell expansion together with cell wall loosening in order to drive growth at the cell and whole plant levels. Also, guard cell as specialized cell type on leaf epidermis that controls stomatal movements, strongly uses K^+ associated with anions and organic solutes to adjust its turgor. K^+ entry into guard cells decreases the intracellular water potential which leads to water influx into guard cell, and as a consequence, the swelling of guard cells and stomatal opening. In contrast, the effluxes of K^+ and anion induce the outflow of water from guard cells which results in stomatal closure (Marschner, 2011; Nguyen et al., 2017; Nieves-Cordones, Al Shiblawi, & Sentenac, 2016; Ward, Mäser, & Schroeder, 2009).

I.2 Families of plant K^+ transport systems at the plasma membrane

Since the pioneering work on K^+ membrane transport by Epstein and collaborators which evidenced the dual mechanism of uptake in the root of barley, root K^+ uptake contribution by low affinity and high affinity transport systems, *i.e.*, K^+ channels and K^+ transporters can be separated (Epstein, 1976). Many K^+ transport systems have been identified in model plants (Mäser et al., 2001; Véry et al., 2014). They possess different properties in terms of ion selectivity, affinity and transport energetics (passive or active transports of K^+ fueled by energetic coupling with other ions, H^+ or Na^+). As shown in Figure I.1, these K^+ transport systems in plants form two families of K^+ channels, *i.e.*, Shaker and TPK, and three families of K^+ transporters, *i.e.*, HAK/KUP/KT, HKT and KEA/CPA (Véry et al., 2014). Shaker K^+ channel family mediates passive K^+ fluxes, that contribute to the major K^+ conductance at the plasma membrane in most tissues and cell types (Lebaudy, Véry, & Sentenac, 2007; Véry et al., 2014). Most K^+ channels in the TPK family are localized on the vacuolar membrane where they mediate instantaneously-activating K^+ currents with exception of TPK4 (at least in Arabidopsis; Becker et al., 2004), but this family is still not fully characterized (Dunkel et al., 2008). The HAK/KUP/KT family comprises H^+-K^+ symporters displaying high affinity K^+ uptake by the root (Grabov, 2007). The HKT family is comprised of K^+-permeable transporters likely functioning as Na^+-K^+ symporters, present in monocotyledonous plants

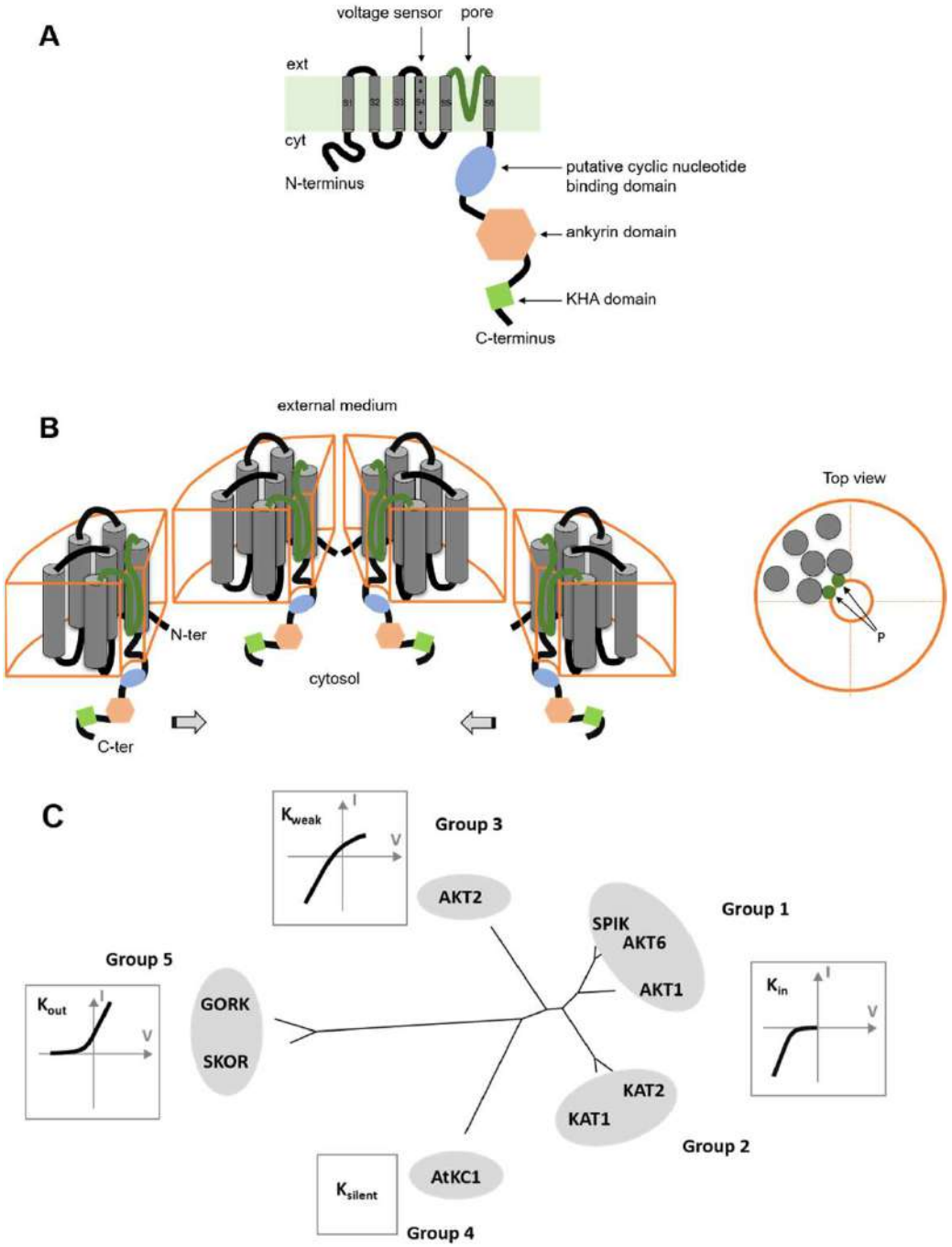

Figure I.2 Shaker K^+ channels in *Arabidopsis thaliana* (Véry et al., 2014). (A), Topology of a plant Shaker K^+ channel subunit. (B), Structure of Shaker K^+ channels. Functional Shaker K^+ channels are tetramers composed of four α-subunits. (C), Phylogenetic tree of Shaker K^+ channels and their functional types. In the model plant *Arabidopsis thaliana*, Shaker K^+ channels display five phylogenetic groups and four functional types. K_{in}, inwardly rectifying, K_{out}, outward rectifying, K_{weak}, weakly rectifying, $K_{silent,}$ does not form functional homomeric channels when expressed on its own, but associates with K_{in} types to form functional heteromeric channels.

only, and Na^+-selective transporters, in both monocotyledonous and dicotyledonous plants (Corratgé-Faillie et al., 2010). The KEA family is comprised of H^+/K^+ antiporters localized either at the plasma membrane or endomembranes (Mäser et al., 2001; Zheng et al., 2013). Below, I focus on plasma membrane K^+ transport systems in *Arabidopsis thaliana* and rice plants.

I.2.1 Shaker K^+ channels

In plants, Shaker K^+ channels constitute the most extensively characterized family mediating K^+ transport across the plasma membrane, particularly in the model plant *Arabidopsis thaliana*.

I.2.1.1 Shaker K^+ channel structure

Plant Shaker channels exhibit highly similar predicted structure to that of animal voltage-gated K^+ channels, forming the so-called Shaker family (Véry & Sentenac, 2003). Functional plant Shaker channels are tetrameric proteins composed of four α-subunits with the transmembrane core involved in K^+ permeation (Figure I.2 B). It is worth pointing out that the four subunits can be the products encoded by a single Shaker gene (homomeric channels) or by different Shaker genes (heteromeric channels). Each α-subunit contains six typical hydrophobic transmembrane segments (S1-S6), one pore domain between the fifth and sixth segment (P), and N- and C-terminus (Figure I.2 A). The fourth transmembrane segment S4 is rich in positively-charged amino acids (R, K and H) and acts as a voltage sensor, which can move within the membrane in response to changes in membrane potential leading to the opening and closure of the channel pore via conformational changes (Pilot, Pratelli, Gaymard, Meyer, & Sentenac, 2003). The P domain between S5 and S6 displays a highly conserved stretch of residues TxGYG (Thr-X-Gly-Tyr-Gly), which acts as a K^+ selectivity filter (Véry et al., 2014). The N- and C-termini are located in cytosol, and the N-terminal region is short. Interestingly, the C-terminus contains several regulatory elements, including the cyclic nucleotide binding domain (CNBD), the ankyrin repeat domain (Anky; not present in all channels), and the domain rich in hydrophobic and acidic residues (KHA). The Ankyrin domain can act as a site for the functional regulation of Shaker channels by interacting with regulatory partners (*e.g.*, kinases or phosphatases) (Véry et al., 2014).

I.2.1.2 Shaker K^+ channel functional properties in *Arabidopsis thaliana*

Phylogenetic analyses show that the nine members of the Shaker K^+ channel family in the model plant Arabidopsis can be sorted in five groups, which correspond to four functional types according to current characteristics in response to voltage, as shown in Figure I.2 C (Véry et al., 2014). Groups 1 and 2 in Arabidopsis are comprised of five inwardly rectifying (K_{in}) channels which include AKT1, AKT6, and SPIK from group 1, and KAT1 and KAT2 from group 2. K_{in} channels are voltage gated and can be activated by membrane hyperpolarization resulting in K^+ uptake into the cell (Hirsch, Lewis, Spalding, & Sussman, 1998; Mouline et al., 2002; Nakamura et al., 1995; Pilot et al., 2001). Group 3 is only comprised of AKT2, which is a weakly rectifying channel displaying two distinct gating models (Dreyer, Gomez-Porras, & Riedelsberger, 2017; Dreyer, Michard, Lacombe, & Thibaud, 2001). In the mode 1, AKT2 is a K_{in} channel activated by membrane hyperpolarization and which mediates K^+ influx. In the mode 2, AKT2 is non-rectifying ("open") channel allowing both K^+ influx and K^+ efflux. The group 4 also contains only a single member, AtKC1, which acts as a regulatory subunit. AtKC1 does not form functional homomeric channels when expressed on its own, but it displays ability to associate with K_{in} types from groups 1, 2, and 3 to form inwardly rectifying heteromeric channels (Duby et al., 2008; Jeanguenin et al., 2011). The group 5 is comprised of two outwardly rectifying (K_{out}) channels, SKOR and GORK. These two channels are voltage gated and open upon membrane depolarization and therefore mediate K^+ export from the cell (Ache et al., 2000; Gaymard et al., 1998; Hosy et al., 2003).

I.2.1.3 The physiological roles of Shaker K^+ channels in *Arabidopsis thaliana*

The physiological roles of the nine Shaker channels in the model plant *Arabidopsis thaliana* have been examined. The study of ion transport system functions in the plant classically includes combination of methodologies, such as heterologous expression (in different possible systems like *Xenopus laevis* oocytes, *Saccharomyces cerevisiae*, HEK293, COS, and Sf9 cells), reporter systems for localization studies at the tissue and subcellular levels (like GUS and GFP), as well as physiological experiments using mutant (knock-out and overexpressing) plants (Dreyer et al., 1999). The physiological roles of the family of Shaker channels in Arabidopsis which is the best characterized family of Shaker channels, are summarized

below.

In root peripheral layers, homotetrameric AKT1 and/or heterotetrameric AKT1/AtKC1 contribute to a large extent to K^+ uptake from external soil solution (Hirsch, Lewis, Spalding, & Sussman, 1998; Reintanz et al., 2002). In particular from as low as 10 μM of K^+ in the external medium, AKT1 turns out to contribute to root K^+ uptake owing to the strongly negative membrane potentials of cortical root cells (Lebaudy, Véry, & Sentenac, 2007; Nieves-Cordones, Martínez, Benito, & Rubio, 2016). At external K^+ concentration below 5 mM, it is worth mentioning that beside the AtAKT1 channel, the AtHAK5 transporter has also a significant to major role in root K^+ uptake in *Arabidopsis thaliana* (Nieves-Cordones, Martínez, Benito, & Rubio, 2016). Regarding the long distance transport of K^+, SKOR which is expressed in the root pericycle and xylem parenchyma cells, strongly contributes to K^+ secretion into xylem sap for translocation towards the shoot (Gaymard et al., 1998). AKT2, which is expressed in the phloem vascular tissues throughout the whole plant, plays important role in plant growth under energy-limiting conditions (Deeken et al., 2002; Gajdanowicz et al., 2011). It was proposed to be involved in loading K^+ into phloem sap in source tissues under sufficient chemical energy condition acting as K_{in} channel, but also to be able to energize the plasma membrane of phloem sieve tubes/companion cells through the transmembrane K^+-gradient when the channel is converted to open mode, for sucrose loading to phloem sap under energy limitation (Dreyer, Gomez-Porras, & Riedelsberger, 2017; Gajdanowicz et al., 2011). In guard cells, the Shaker K_{in} channel subunits (mainly KAT1 and KAT2) and K_{out} channel subunit GORK constitute the major K^+ conductances of the plasma membrane involved in K^+ uptake and, respectively, release, leading to stomatal movements (Lebaudy, Véry, & Sentenac, 2007; Roelfsema & Hedrich, 2005; Véry et al., 2014). Finally, SPIK and AKT6 are expressed in reproductive organs (Pilot et al., 2003). SPIK is the major K^+ inward conductance in pollen, and plays a crucial role in the turgor-dependent expansion of the pollen tube, and thereby pollen fertilization ability (Mouline et al., 2002).

I.2.2 K^+ transporters

I.2.2.1 HAK/KUP/KT transporters

Plant HAK/KUP/KT transporters constitutes a large family of K^+ transporters. The HAK/KUP/KT transporters were first identified in bacteria, and named KUP (Schleyer &

Bakker, 1993). The bacterial KUP transporters are described as responsible for the low-affinity transport of K^+ into these cells with the probable concomitant uptake of protons, *i.e.*, likely acting as H^+-K^+ symports (Trchounian & Kobayashi, 1999; Zakharyan & Trchounian, 2001), and are also able to transport cesium (Cs^+) (Bossemeyer, Schlösser, & Bakker, 1989). The first eukaryotic HAK/KUP/KT transporter gene, named *HAK1*, was cloned in the yeast *Schwanniomyces occidentalis* (Banuelos, Klein, Alexander-Bowman, & Rodríguez-Navarro, 1995). The yeast *S. occidentalis* HAK1 is able to take up K^+ from external solution in which K^+ concentration is as low as 0.03 μM. This means that SoHAK1 can transport K^+ actively, against an extremely high cell transmembrane gradient of K^+, higher than 10^6. When SoHAK1 was expressed in a mutant strain of *Saccharomyces cerevisiae* which was defective in K^+ uptake, similar high-affinity K^+ uptake to that by *S. occidentalis* were observed, in K^+-shortage growth condition (Banuelos, Klein, Alexander-Bowman, & Rodríguez-Navarro, 1995). Plant HAK/KUP/KT transporters were first cloned and identified from barley (HvHAK1) (Santa-María, Rubio, Dubcovsky, & Rodríguez-Navarro, 1997) and Arabidopsis (AtKT1 and AtKT2) (Quintero & Blatt, 1997). Some research studies have then used different acronyms, KUP, HAK or KT for these transporters in Arabidopsis (Fu & Luan, 1998; Kim, Kwak, Uozumi, & Schroeder, 1998). Plant HAK/KUP/KT transporters play important roles in in K^+ nutrition and regulation of plant development.

No crystal has been obtained for a HAK/KUP/KT transporter, so little is known about the structure of these transporters (Gierth & Mäser, 2007). Hydrophobicity analyses of HAK/KUP/KT transporters from Arabidopsis and rice suggest that they possess 10 to 14 transmembrane domains (TMs) and three cytosolic domains, *i.e.*, the N-, C- termini and the relatively large loop between the second and third TMs (Ragel, Raddatz, Leidi, Quintero, & Pardo, 2019). The protein folding pattern of a single polypeptide was proposed by modelling (Santa-María, Oliferuk, & Moriconi, 2018). However, whether functional HAK/KUP/KT transporters may have a multimeric structure is not fully excluded.

The HAK/KUP/KT transporter families display highly variable number of members in different plant species genomes. For instance, Arabidopsis contains 13 HAK/KUP/KT transporter genes, while there are 27 members of this family in rice genome (Bañuelos, Garciadeblás, Cubero, & Rodríguez-Navarro, 2002; Rubio, Santa-María, & Rodríguez-Navarro, 2000; Véry et al., 2014). The HAK/KUP/KT transporters in Arabidopsis

and rice are classified into four clusters according to their sequence homology. The members in cluster I have been the most studied so far. They exhibit high-affinity K^+ uptake in roots. For instance, *AtHAK5*, the only cluster I member in Arabidopsis, is transcriptionally activated by low external K^+ concentration, and is the main actor in K^+ uptake by the plant from the soil solution in K^+ shortage conditions (Gierth, Mäser, & Schroeder, 2005; Rubio, Santa-María, & Rodríguez-Navarro, 2000). In cluster II, the transport properties and physiological functions of the members are comparatively diverse, and their roles in K^+ nutrition are not well identified. In Arabidopsis, however, the members in Cluster II are probably involved in developmental processes dependent on, or resulting in cell expansion (Véry et al., 2014). Little information is available on Cluster III and Cluster IV transporters.

I.2.2.2 HKT transporters

Plant high-affinity K^+ transporters (HKT) are another type of membrane transport systems, which mediate K^+ and/or Na^+ transport. Plant HKTs are homologous to fungal and bacterial K^+ transporters from Trk and Ktr families (Corratgé-Faillie et al., 2010). Plant HKT family can be sorted into two subfamilies based on phylogenetic relationships and functional properties determined in heterologous expression systems. HKT subfamily 1 includes transporters only permeable to Na^+, and HKT subfamily 2 contains transporters permeable to both Na^+ and K^+ (Corratgé-Faillie et al., 2010). The HKT polypeptide is comprised of short N- and C- cytosolic termini and four "MPM" domains. A "MPM" domain is formed by the succession of one transmembrane segment, one pore loop, and one transmembrane segment. This "MPM" topology was initially proposed based on sequence analyses (Durell & Guy, 1999), then was further supported from biochemical analyses on AtHKT1 (Kato et al., 2001). According to the crystallization of bacterial Trk/Ktr homologues (Cao et al., 2011; Vieira-Pires, Szollosi, & Morais-Cabral, 2013), the four MPM domains assemble in a radially symmetric way such that the four pore loops are located at the center of the hydrophobic structure to form part of the permeation pathway.

HKT transporter families display variable number of members in different plant species genomes. For instance, rice contains 9 HKT members, whereas only one HKT member exists in *Arabidopsis thaliana*. Numerous studies have shown that the members from subfamily 1 are key determinants of plant salinity tolerance, since they are associated to QTLs of salt tolerance by controlling of Na^+ exclusion from leaf (*Cf.* also below § I.4.5) (Asins et al.,

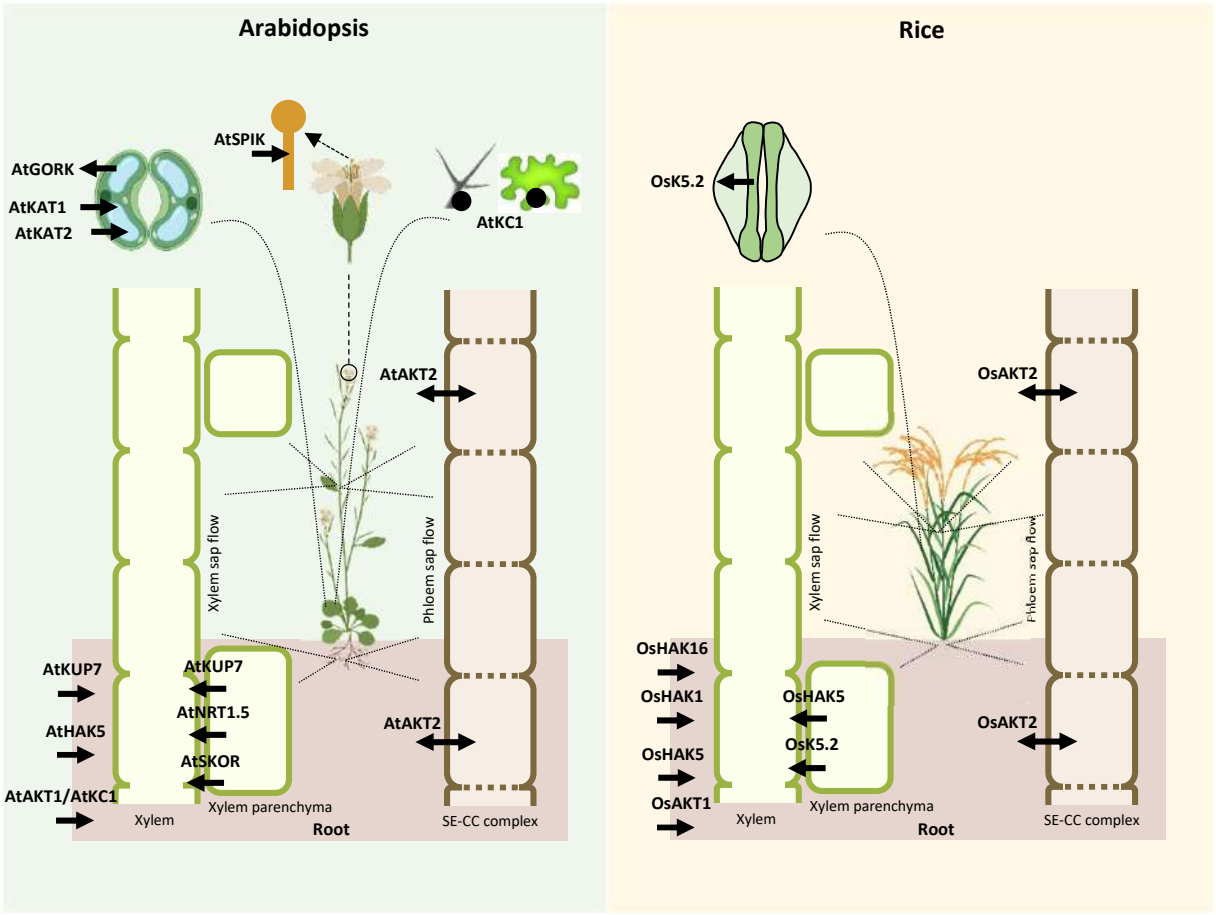

Figure I.3 Integrative model of plasma membrane K^+ transport system activity in *Arabidopsis* and rice

2013; Byrt et al., 2007; Ren et al., 2005). The main sequence feature that distinguishes subfamily 2 K^+-permeable transporters from subfamily 1 non-K^+-permeable ones is a glycine instead of a serine residue at the selectivity filter position in the first pore domain of the HKTs (Garciadeblás, Senn, Bañuelos, & Rodríguez-Navarro, 2003; Mäser et al., 2002).

I.2.2.3 KEA transporters

K^+ efflux antiporters (KEA) belong to the monovalent cation/proton antiporters (CPA) superfamily, which consists of two subfamilies. CPA1 subfamily comprises the $Na^+(K^+)/H^+$ exchangers (SOS1, NHX), and CPA2 subfamily includes KEA and cation/H^+ exchangers (CHX) (Gierth & Mäser, 2007; Mäser et al., 2001). KEA transporters have been extensively studied in bacteria. KefB and KefC-like proteins are characterized as glutathione-gated K^+ efflux systems in *Escherichia coli* (Booth, Epstein, Giffard, & Rowland, 1985). Arabidopsis contains 6 putative members of KEA family, named KEA1 to KEA6, whereas information about this family is largely unknown in other higher plants. Phylogenetic analyses have sorted the Arabidopsis KEA into two clades related to *E. coli* KefB and KefC-like proteins, *i.e.*, KEA1 to KEA3 in clade KEA-I and KEA4 to KEA6 in clade KEA-II (Chanroj et al., 2012). The functions of these transporters remain elusive although the studies on Arabidopsis KEA transporters have been increasingly reported (Aranda-Sicilia et al., 2016; Armbruster et al., 2014; Kunz et al., 2014; Stephan, Kunz, Yang, & Schroeder, 2016; Tsujii et al., 2019; C. Wang et al., 2017; Zhu et al., 2018).

I.3 Integration of K^+ transport in Arabidopsis and rice

I summarized below advances in the field of molecular transport of K^+ throughout the plant of *Arabidopsis thaliana* and rice (Figure I.3).

I.3.1 Root K^+ uptake from soil

Roots take up K^+ from the soil solution. Compared with high K^+ concentrations in plant cell cytoplasm, K^+ concentrations are low in the external soil solution, ranging generally from 0.1 mM to a few mM (Véry & Sentenac, 2003). As already mentioned above, both low-affinity (passive) and high-affinity (active) K^+ uptake systems are present in root peripheral layers for optimized absorption of this cation by the root with respect to external K^+ availability (Epstein, 1973; Epstein, Rains, & Elzam, 1963).

In Arabidopsis, the inward Shaker K^+ channel subunit AKT1 and the high-affinity K^+ transporter HAK5 have been shown to be the major players for root K^+ uptake from the external soil solution (Nieves-Cordones, Martínez, Benito, & Rubio, 2016). AKT1, which is present in root peripheral cell layers (Lagarde et al., 1996) mediates low-affinity K^+ uptake by the roots from the soil solution (Gaymard et al., 1996; Hirsch, Lewis, Spalding, & Sussman, 1998). In addition, AtKC1, which is expressed in root epidermis and cortex (Pilot et al., 2003) and interacts with AKT1 to form a functional heterotetrameric channel with slightly different transport properties, is regarded as a regulatory subunit that prevents K^+ leakage from the roots under low K^+ conditions (Geiger et al., 2009; Wang, He, Li, Xu, & Wu, 2010). Under low external K^+ conditions also, AKT1 is activated by a CIPK kinase-Calcineurin B-Like protein signaling, thereby increasing its possible contribution to root K^+ uptake (Xu et al., 2006; Wang & Wu, 2010). The Arabidopsis HAK5, expressed in root epidermis, is able to take up K^+ from micromolar concentrations and was shown through reverse genetics study to be the main system involved in root K^+ uptake below 200 μM (Gierth, Mäser, & Schroeder, 2005). Another KUP/HAK/KT transporter from clade III, AtKUP7 was shown to contribute to root K^+ uptake in K^+ shortage conditions (Han, Wu, Wu, & Wang, 2016).

In rice, the structure of the Shaker channel family is very similar to that in Arabidopsis (Pilot et al. 2003) and a clear orthologue of AKT1 based on phylogenetic considerations exists. In contrast, while HAK5 is a unique member of clade I in the KUP/HAK/KT family in Arabidopsis, 8 members are present in this clade in rice (Véry et al., 2014). However, the high-affinity K^+ transporters OsHAK1 along with the inward Shaker K^+ channel OsAKT1 are thought to be the main systems for rice root K^+ uptake from the external soil solution (Nieves-Cordones, Martínez, Benito, & Rubio, 2016). Regarding low-affinity K^+ uptake, OsAKT1, expressed in whole root tissues, *i.e.*, epidermis, root hairs, cortex, endodermis, and vascular bundles, substantially contribute to root K^+ uptake in a large range of external K^+ concentrations from about 50-100 μM to millimolar (Li et al., 2014). OsAKT1 activity, like that of its Arabidopsis homologue, is positively regulated in rice roots by the CBL1-CIPK23 complex (Li et al., 2014). *OsAKT1* loss of function affects, as a consequence of the reduced root K^+ uptake, the K^+ contents in rice root and leaf tissues, the plant growth and the grain yield and quality (Li et al., 2014). With respect to high-affinity K^+ uptake, OsHAK1, expressed in root epidermis and vascular tissues, is the major K^+ uptake system operating in the submillimolar range of external K^+ concentrations, accounting for almost all high-affinity

K^+ uptake under external K^+ conditions lower than 50 µM (Chen et al., 2015; Nieves-Cordones et al., 2017). Beside OsHAK1, another clade I HAK transporter from rice, OsHAK5, and an HAK from clade IV (a clade which does not exist in Arabidopsis), OsHAK16, were also shown to significantly contribute to root K^+ uptake, in the 0.1 to 1 mM external K^+ concentration, and to plant growth (Yang et al., 2014).

I.3.2 Long-distance transport of K^+ in xylem and phloem

I.3.2.1 Xylem K^+ transport

K^+ absorbed by the roots is loaded into the xylem, and then translocated to the shoots via the xylem vessels, fueled by the root pressure and the transpiration, to constitute the root-to-shoot K^+ transport. In Arabidopsis, the outward Shaker K^+ channel SKOR has been shown to play a major role in K^+ secretion into the xylem sap (Gaymard et al., 1998; Li et al., 2017). SKOR is expressed in the root pericycle and xylem parenchyma cells. The reverse genetics approach and electrophysiological characterization demonstrated that SKOR functions as an outwardly rectifying voltage-gated channel and contributes to about 50% of K^+ translocation toward the shoots (Gaymard et al., 1998). The molecular identity of the other systems controlling K^+ loading to the xylem sap is so far little determined. The Nitrate Transporter NRT1.5 which is expressed in root pericycle (Lin et al., 2008) was shown to slightly contribute to the K^+ concentration in xylem sap, along with the nitrate concentration, in plants grown under K^+-limited conditions (Li et al., 2017). In addition, AtKUP7, which is ubiquitously expressed, and takes part to root K^+ uptake, was reported to be possibly also directly involved in the control of xylem sap K^+ load in plants grown in low K^+ conditions (Han, Wu, Wu, & Wang, 2016).

In rice, the outward Shaker K^+ channel OsK5.2 and the high-affinity K^+ transporters OsHAK5 are considered to be involved in K^+ loading into xylem sap (Nguyen et al., 2017; Yang et al., 2014). OsK5.2 is expressed in root vascular tissues and stomata. The reverse genetics approach revealed that *OsK5.2* strongly contributes to K^+ translocation towards the shoots, like SKOR in Arabidopsis (Nguyen et al., 2017). The expression studies on *OsHAK5* showed in addition to a wide expression in root peripheral layers, expression in the vasculature, and enhancement upon K^+ starvation, which suggests that OsHAK5 can have physiological roles in roots in both K^+ uptake and K^+ translocation between roots and shoots,

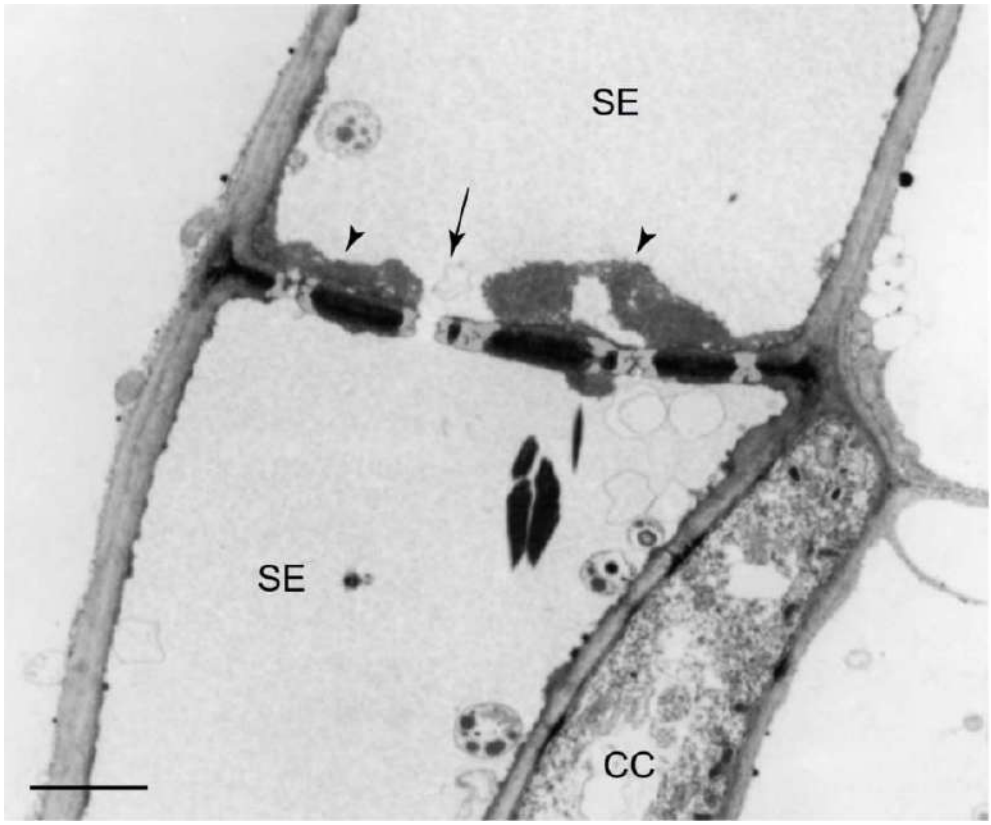

Figure I.4 Electron micrograph of the SE-CC complex in broad bean (Vicia faba) (van Bel, Ehlers, & Knoblauch, 2002).

especially in low external K^+ conditions (Yang et al., 2014). The reverse genetics approach showed decreased xylem sap K^+ concentration in loss of function mutant plants, specifically under K^+-deficient conditions (Yang et al., 2014). This could originate from the reduced uptake by the roots, but also may indicate a direct involvement of OsHAK5 in K^+ translocation from roots to shoots.

I.3.2.2 Phloem K^+ transport

I.3.2.2.1 Sugar loading mechanisms

The phloem vasculature is composed of living cells: sieve tube elements, which have degraded most of their organelles including nucleus, and tightly associate with companion cells connected through numerous plasmodesmata pores to form the so-called sieve tube element-companion cell (SE-CC) complex (Figure I.4) (Williams, Lemoine, & Sauer, 2000). Phloem can transport photosynthetic assimilates from the sites of synthesis in source organs (mature leaves) to the sites of utilization in sink organs (*e.g.*, root and shoots apices) (Patrick, 1997). Diverse compounds can be found in the phloem exudate such as carbohydrates, ions, proteins, nucleic acids, hormones, fatty acids, in particular as long-distance regulatory signals between source and sink (Lucas, Yoo, & Kragler, 2001).

It is recognized that the phloem sucrose loading can use 3 strategies: diffusion, polymer trapping, and apoplastic loading (Figure I.5) (Turgeon, 2010).

Diffusion is a passive mechanism. Photosynthetic assimilates can use a symplastic pathway to circulate from mesophyll cells to the SE-CC complex of minor vein through plasmodesmata. The plant species such as the woody plants willow and poplar, that utilize this diffusion strategy which is an energetically downhill process, usually contain high levels of sucrose in the mesophyll cells of leaves and numerous plasmodesmata connections between phloem parenchyma and CC (Figure I.5 A and D) (Eom, Choi, Ward, & Jeon, 2012; Rennie & Turgeon, 2009).

Polymer trapping is regarded as a specialization of the symplastic pathway. In this process, sucrose synthesized during photosynthesis in mesophyll cells is passively transported to the phloem parenchyma cells and then diffuses to the CC of minor vein through plasmodesmata. Sucrose is then converted to raffinose and stachyose in the CC of minor vein, in which these two oligosaccharides are supposed to be too large to diffuse back to phloem

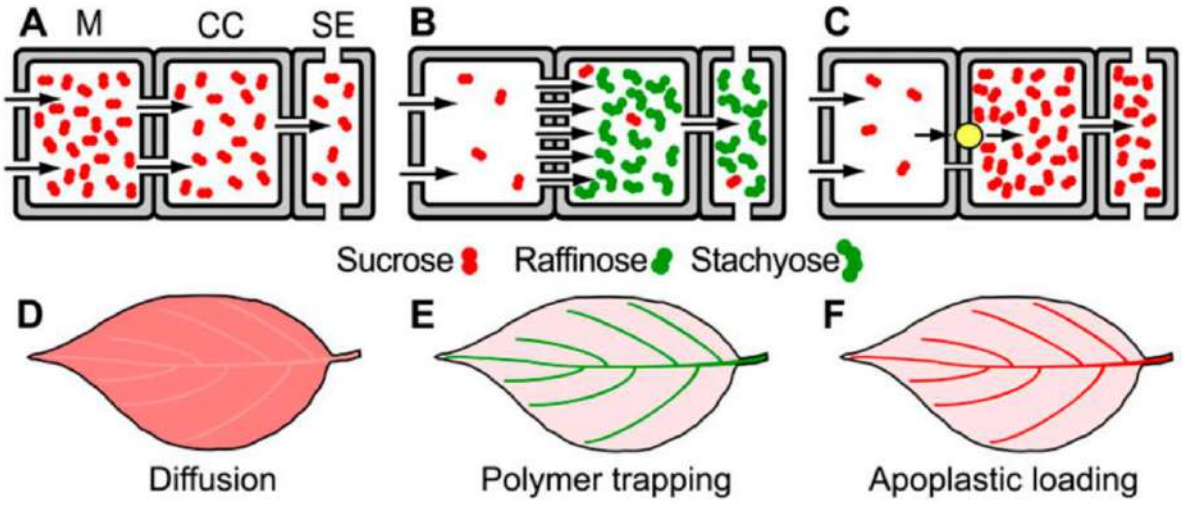

Figure I.5 Schematic diagrams of possible phloem sucrose loading strategies at the minor vein (A–C) and whole leaf (D–F) levels (Turgeon, 2010). Sucrose diffuses through plasmodesmata (gaps in walls) into the SE-CC of minor veins; Sucrose levels are higher in the mesophyll than in the SE-CC (Diffusion, A and D). Sucrose diffuses through plasmodesmata into the CC of minor vein, and then is converted to raffinose and stachyose, that increases the levels of these two oligosaccharides in the SE-CC of minor veins; this allows the mesophyll cells to maintain low sucrose levels (polymer trapping, B and E). Sucrose is transported from the apoplast into the CC of minor vein by SUT (yellow circle) (Apoplastic loading, C and F).

parenchyma cells through the plasmodesmata but can diffuse into wider plasmodesmata into SE of minor vein. Thus, plant species such as *Verbascum phoeniceum*, *Rehmannia glutinosa*, *Catalpa speciosa*, *Buddleja davidii*, *Citrullus lanatus*, *Coleus blumei*, that utilize this polymer trapping strategy, are able to maintain high levels of the oligosaccharides in the SE-CC complex of minor vein and low levels of sucrose in the mesophyll cells (Figure I.5 B and E) (Eom, Choi, Ward, & Jeon, 2012).

Apoplastic loading is an active process, in which sucrose must be transported from the apoplast across the plasma membrane of the CC and/or SE of minor vein by H^+-sucrose transporters (SUT). The proton motive force generated by H^+-ATPases is needed to drive sucrose into the phloem by SUT against a concentration gradient. The plant species, that utilize this apoplastic loading strategy such as several herbaceous plants, Arabidopsis, common plantain, sea plantain, celery, allow to maintain low levels of sucrose in the leaves, (Figure I.5 C and F) (Nadwodnik & Lohaus, 2008; Turgeon, 2010).

The sucrose loading mechanism used by rice is a matter of debate. The presence of numerous plasmodesmatal connections between parenchyma cells and CCs observed in rice and the relatively high sucrose concentrations in the leaf suggests utilization of a passive symplastic pathway to translocate sucrose through plasmodesmata into the phloem of the minor veins (Eom, Choi, Ward, & Jeon, 2012). In the framework of this hypothesis, the tonoplastic OsSUT2 transporter could control the mesophyll cytosolic concentration by functioning as a valve ("vacuolar trapping"), to regulate sucrose flux into the phloem (Eom, Choi, Ward, & Jeon, 2012). Some arguments supporting the use by rice of sucrose apolastic loading mechanism to the phloem, such as the presence of plasma membrane-localized proton pyrophosphatase and SUT transporters in the SE-CC complexes of source leaves, also exist (Regmi, Zhang, & Gaxiola, 2016; Wang et al., 2021).

I.3.2.2.2 AKT2 is required for electrical polarization of the phloem membrane

Little is known on the molecular mechanism of phloem K^+ transport in plants. K^+ is the major inorganic ion found in phloem sap (Deeken et al., 2008). The control of K^+ transport in phloem plays a role in building the osmotic gradient which drives the translocation of photosynthetic assimilates from the source organs (leaves) to the sink organs (root and shoots apices) (Patrick, 1997).

In Arabidopsis, AKT2, the sole K^+ Shaker channel characterized in the phloem, is

believed through its involvement in K^+ transport to play crucial role in the regulation of sucrose reloading into phloem (Deeken et al., 2002; Gajdanowicz et al., 2011; Lacombe et al., 2000). The weakly rectifying functional property of AKT2 allows this channel to mediate both K^+ influx and efflux, depending on the transmembrane K^+ electrochemical gradient, in sink and source phloem tissues where it is expressed (Lacombe et al., 2000). The activity of AKT2 channel is therefore expected to strongly contribute to the phloem cell membrane electrical polarization through a component linked to the transmembrane K^+ concentration gradient ("K^+-battery" component). The reverse genetics approach demonstrated that AKT2 is actually required for phloem membrane electrical polarization (in a K^+ dependent way) and to the sucrose loading to the phloem sap, likely through its control of the phloem membrane polarization (Deeken et al., 2002). In contrast, AKT2 activity turned out to have little impact on the control of K^+ concentrations in phloem sap (Deeken et al., 2002). Mathematical simulations, furthermore, indicated that the regulation of AKT2 that switches the channel activity from inwardly rectifying to non-rectifying plays a key role in building the "K^+ battery", which can compensate for the reduced pH gradient under carbohydrate energy limitation for H^+-ATPases and can thereby provide electrical energization "stored" in the K^+ gradient between the cytosol of SE-CC complex and the apoplast for membrane transport processes (Deeken et al., 2002; Gajdanowicz et al., 2011).

In rice, little is known on phloem K^+ transport. Recently, by the analysis of transgenic rice plants expressing the *OsAKT2* (*OsK3.1*) promoter::*GUS* construct, *OsAKT2*, as its Arabidopsis homolog *AKT2*, has been shown to be particularly expressed in the phloem vascular tissue of shoots (Shen et al., 2020). OsAKT2 functions as a weakly rectifying channel and phosphatidic acid can inhibit its activity (Shen et al., 2020). The physiological role of OsAKT2 in phloem K^+ transport in rice remains mostly unknown.

I.3.3 K^+ fluxes in guard cells and control of stomatal aperture

The control of stomatal aperture allows optimization of gas exchanges between the leaf inner tissues and the atmosphere, including CO_2 intake for photosynthesis and water loss by transpiration. Leaf transpiration is one of the parameters that modulate K^+ translocation towards the shoots.

Stomatal movements are permitted by turgor changes of the guard cells. These changes are mainly driven by transport of ions such as K^+, Cl^-, NO_3^-, and malate across cell

and vacuolar membranes (Roelfsema & Hedrich, 2005).

In Arabidopsis, the inward Shaker channels KAT1 and KAT2 are considered to be the major systems that mediate K^+ influx into guard cells during stomatal opening, while the outward Shaker channel GORK is the main one involved in K^+ efflux from these cells during stomatal closure (Hosy et al., 2003; Lebaudy, Vavasseur, et al., 2008b; Pilot et al., 2001). The reverse genetics approach showed that disruption of GORK activity resulted in impaired stomatal closure in response to darkness or ABA. Furthermore, absence of GORK activity caused increased transpirational water loss by the plant, by about 10-50% depending on the soil water availability (Hosy et al., 2003). Compared with the control of K^+ efflux during stomatal closure by the single channel GORK, the control of K^+ influx during stomatal opening by inward channels is more complex. Although KAT1 is a dominant K_{in} channel in guard cells, it is not essential for stomatal opening (Szyroki et al., 2001). In addition to *KAT1*, the K_{in} channel subunits *KAT2*, and to a lesser extent *AKT1*, *AKT2*, and *AtKC1* are also expressed in the guard cells, and they are able to form homomeric and/or heterotetrameric channels contributing to stomatal opening (Lebaudy et al., 2008a). Heterotetramerization can indeed occur between subunits of the same functional type (inward or outward), and C-terminus has been indicated to be involved in discrimination between outward and inward channel-forming subunits (Xicluna et al., 2007). The guard cell inward Shaker channel activity as a whole was found to be crucial for stomatal opening, and to improve the stomatal reactivity to internal and environmental signals (*e.g.*, light, CO_2, air relative humidity; Lebaudy et al., 2008b).

In rice, stomatal movements are regulated by the ion shuttle transport between guard cells and adjacent subsidiary cells, which form the stomatal complex (Mumm, Wolf, Fromm, Roelfsema, & Marten, 2011). To date, outward Shaker K^+ channel OsK5.2 was shown to play a role in K^+ release by guard cells for stomatal closure (Nguyen et al., 2017). The expression studies showed that *OsK5.2* is expressed in whole stomatal complex, *i.e.*, guard cells and subsidiary cells. The reverse genetics approach and electrophysiological characterization on intact guard cells demonstrated that disruption of OsK5.2 activity resulted in absence of the Shaker-type outward currents. Furthermore, disruption of OsK5.2 activity caused slower kinetics of stomatal closure and larger steady-state rates of transpirational water loss, by about 25% (Nguyen et al., 2017).

I.4 K^+ significance in plant tolerance to salinity stress

I.4.1 Soil salinization: a major restriction for agriculture

Global climate change induces land degradation. Soil salinization favored by climate change, as one of the major factors contributing to land degradation and desertification, significantly affects all major cereal crop production and quality worldwide. Inappropriate irrigation practices give rise to accumulation of water-soluble salts in fields which are often located in arid and semiarid zones. The damage to land due to salinity concerns more than 800 million hectares throughout the world, *i.e.*, at least 20% of the world's arable land and more than 40% of irrigated land. Saline soils usually contain a variety of soluble salts, such as the cations Na^+, Mg^{2+}, Ca^{2+}, and K^+, and the anions Cl^-, SO_4^{2-}, CO_3^{2-}, and HCO_3^-, but NaCl is most often the dominant soluble salt causing inhibition of plant growth and crop production (Flowers, Troke, & Yeo, 1977). As saline soils cause now growing concern on the potential resource of land with land scarcity worldwide, attempts to improve salt tolerance of crops are regarded as an important aspect of plant breeding for the future.

I.4.2 The alkali cation Na^+

I.4.2.1 K^+ replacement by Na^+ as vacuolar osmolyte

Although K^+ is an essential plant nutrient, its role in the vacuoles of plant cells is non-specific and K^+ can be replaced by Na^+ as an alternative osmolyte to maintain vacuolar turgor. In particular under low K^+ supply, K^+ can be replaced by Na^+ for non-specific functions like being used as osmolyte in vacuole to maintain the osmotic potential. Thus, a relatively limited amount of K^+ is used for specific functions in cytoplasm. Examples can be found in species such as sugar beet, rice and wheat (Horie et al., 2007; Krishnasamy, Bell, & Ma, 2014; Wakeel, Farooq, Qadir, & Schubert, 2011). In sugar beet, K^+ replacement by an equivalent amount of Na^+ in hydroponic solution can compensate for plant's K^+ requirement, showing no K^+-deficiency symptom, even facilitating plant's growth (Wakeel, Farooq, Qadir, & Schubert, 2011). In rice, loss of function mutant plants for the root Na^+ uptake transporter OsHKT2;1 exhibited less Na^+ accumulation and reduced growth under K^+ starvation and 0.5 mM Na^+ supply compared with corresponding wild-type plants (Horie et al., 2007). In conclusion, this

study indicated that Na^+ at low concentration can partially compensate K^+ demand and enhance rice growth under K^+ starvation condition (Horie et al., 2007).

I.4.2.2 A beneficial element in some plant species

In most cases, Na^+ is a not essential element for higher plants with the exception of some C_4 plants species, such as *Atriplex vesicaria* (Brownell & Wood, 1957), *Echinochloa utilis* (Japanese millet), and *Portulaca grandiflotra* (rose moss) (Brownell & Crossland, 1972). It is known that a trace amount of Na^+ is required to be involved in specific C_4 metabolism in several species by the Na^+-pyruvate cotransporter to facilitate the uptake of pyruvate into chloroplasts (Furumoto et al., 2011). Additionally, appropriate concentrations of Na^+ have beneficial effects on growth of dicotyledonous halophytes (Tester & Davenport, 2003). For instance, the growth of *Suaeda salsa* can be stimulated in the presence of 200 mM of NaCl (Song et al., 2009), *Chenopodium quinoa* displays optimal growth at 150 mM of NaCl (Shabala et al., 2012), and 100 mM of NaCl gives a maximal growth potentiality in *Cakile maritima* (Debez, Hamed, Grignon, & Abdelly, 2004). In these plants, Na^+ is preferentially used as an osmolyte for osmotic adjustment in the shoots. This happens because, in hydrated form, Na^+ and K^+ are chemically and structurally very similar.

I.4.2.3 A limiting factor in most species at high concentration

Restriction of plant growth in saline soils is primarily due to high levels of Na^+ and Cl^-. Only a small portion of plant species, the halophytes, do not display inhibition of growth at a moderate concentration of external Na^+. In contrast, glycophytes account for the majority of crops (Cheeseman, 2015). Massive entry of Na^+ and Cl^- ions gives rise to toxic effects on glycophytes as a consequence of physiological failures (James, Blake, Byrt, & Munns, 2011), but Na^+ and Cl^- differ in the inhibitory effect on plant growth. For some plant species, especially woody perennial crops and legumes, Cl^- accumulates more than Na^+ in leaves. High concentration of Cl^- reduces the photosynthetic capacity and quantum yield of PSII electron transport due to chlorophyll degradation (Flowers, 1988). However, for the majority of plants, Na^+ is considered to be the primary toxic ion under salt stress. Na^+-specific damages are often associated with K^+ deficiency and other ionic nutrient imbalances (Cramer, Lynch, Läuchli, & Epstein, 1987; Parida & Das, 2005).

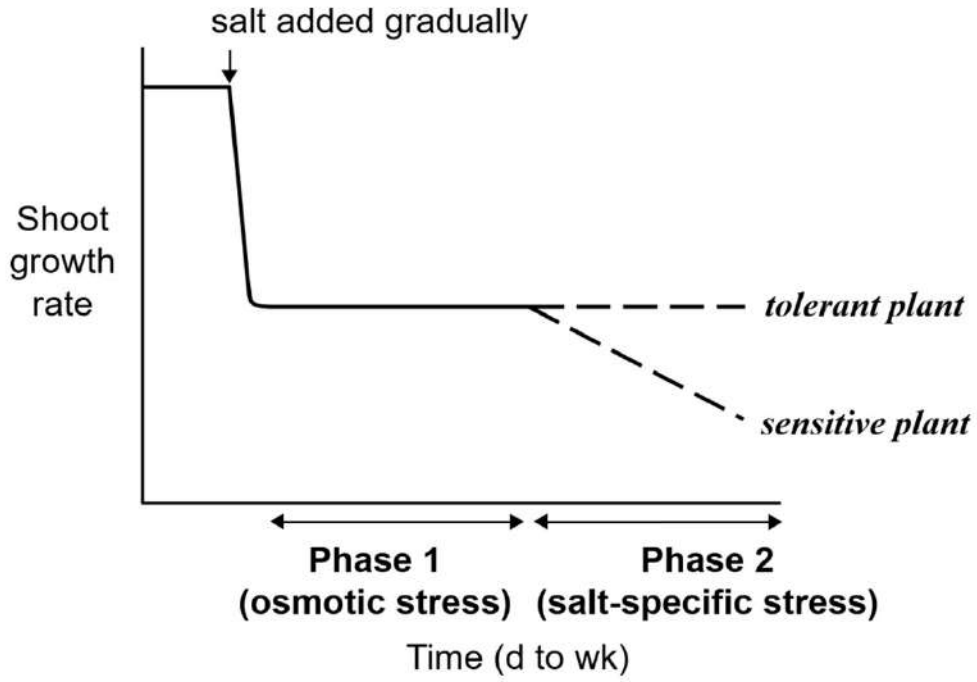

Figure I.6 Schematic illustration of the two-phase growth response to salinity for genotypes that differ in the rate at which salt reaches toxic levels in leaves (Munns, 2005). With annual species, the timescale is day (d) or week (wk), depending on species and salinity level. With perennial species, the timescale is month or year.

I.4.3 The components of salt stress (osmotic, ionic)

Soils are classified as saline when the electrical conductivity of soil solution exceeds 4 dS/m. A conductivity of 4 dS/m is approximately equivalent to 40 mM NaCl (Munns, 2005). That is, significant inhibition of plant growth and yield in crops occurs in a majority of species when the NaCl concentration of external soil solution is more than 40 mM. Salt stress inhibits plant growth for two main reasons, osmotic stress and ionic stress (Deinlein et al., 2014; Munns, 2005; Xiong, Schumaker, & Zhu, 2002).

In the short term, exposure of plants to salinity s lowers the water potential of soil solution. Roots, therefore, have difficulty to take up water from external soil leading to osmotic stress (Munns & Tester, 2008; van Zelm, Zhang, & Testerink, 2020). As shown in Figure I.6, this initial osmotic phase occurs rapidly after salt concentration increase to above-mentioned toxic level around the roots. The major symptoms commonly appear on new leaves, with growth rate reduction, root growth being impacted to a lesser extent (Munns, 1993). An adaptive response to cope with this salt shock is uptake by the root of salt from soil. Therefore, some salt-tolerant plant species, for instance halophytes, rapidly take up salt from saline soil and transport these ions towards aerial parts, thanks to efficient ion transport systems, to be accumulated into vacuoles (Nikalje & Suprasanna, 2018). However, for salt-sensitive plant species, massive uptake of salt triggers a second problem, ionic stress, essentially due to Na^+ toxicity at high concentration (*i.e.*, also known as Na^+-specific stress).

In the long term, exposure of plants to salinity, leads to a massive arrival of ions, in particular Na^+, at toxic level in cytoplasm of leaf cells via the transpiration stream (Munns, 2005; Munns & Tester, 2008). This later Na^+-specific effect generally appears on old leaves by inhibiting their photosynthetic capacity (van Zelm, Zhang, & Testerink, 2020). Since the rate of leaf death directly determines the survival of plants, if the old leaves die faster than the new developing leaves, this results in insufficient photosynthesizing leaves, and in turn, less photoassimilates available for plant growth and seed production (Munns, 2005). Besides, excess of Na^+ in the soil further causes deficiency to a certain to serious extent in uptake of K^+, Ca^{2+} and NO_3^- , which are essential ions for plant growth and development, and eventually may lead to plant death (James, Blake, Byrt, & Munns, 2011).

In spite of the fact that the early osmotic stress and later Na^+-specific stress are thought to display spatial and temporal separation, there is certainly a significant overlap

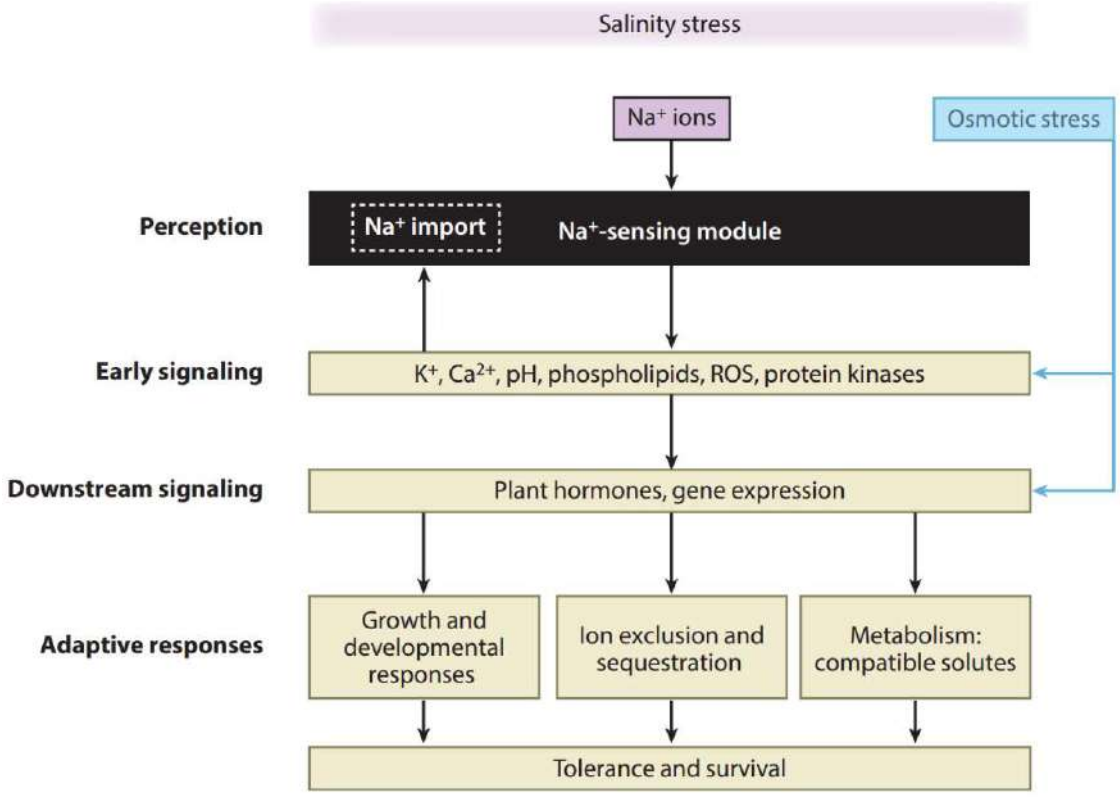

Figure I.7 Na^+ sensing and import are the black box of salt stress responses (van Zelm et al., 2020). There are part overlaps in early and downstream signaling responses to osmotic stress and Na^+-specific stress.

between osmotic stress and Na^+-specific stress in early and downstream signaling (van Zelm, Zhang, & Testerink, 2020). In response to salt stress, plants can activate complex mechanisms at physiological and molecular levels. As shown in Figure I.7, the cellular and molecular responses of plants to salt stress include a generic signal transduction pathway, after initial salt perception, composed of the early Na^+ signaling responses, downstream signaling phase, and final adaptive responses (van Zelm, Zhang, & Testerink, 2020). In the early Na^+ signaling phase, Na^+ sensing and Na^+ uptake initiate the salt signal transduction pathway, the Na^+ sensing mechanism by plants remaining little known. Salt signal perception may occur inside or outside the cell, before or after Na^+ uptake (van Zelm, Zhang, & Testerink, 2020). According to the recent study, there is significant advance in the nature of Na^+ sensor with identification of *MOCA1* ("*MONOCATION-INDUCED* $[Ca^{2+}]_i$ *INCREASES 1*"), which encodes a glucuronosyltransferase, likely functioning in extracellular sensing of salt, including but not restricted to Na^+ ions (Jiang et al., 2019). Na^+ entry into cells following the electrochemical gradient of Na^+ through the plasma membrane is mainly mediated by non-selective cation channels (NSCCs) in Arabidopsis at least, and evokes a depolarization of the cell membrane (Demidchik & Maathuis, 2007; Ward, Hirschi, & Sze, 2003). The changes in membrane voltage modifies the driving force for ion transport and can also significantly influence ion transport by regulating voltage-gated ion channels for K^+ and Ca^{2+} transport. As the earliest signal response, a Ca^{2+} signal is immediately generated by Na^+ through Ca^{2+} entry to the cells and/or Ca^{2+} release from intracellular stores, for instance vacuoles. Besides, Na^+ entry also results in the increase in 3',5'-cyclic guanosine monophosphate (cGMP) levels, and the production of reactive oxygen species (ROS). The increased cGMP reduces Na^+ influx promotes K^+ influx (Maathuis, 2006), and reduces K^+ efflux as well (Ordoñez et al., 2014). The salt-induced Ca^{2+} signal, in turn, activates the Na^+/H^+ exchanger SOS1 via CBL-CIPK complex activation and phosphorylation of SOS1 C-terminus, which leads to Na^+ efflux (Maathuis, Ahmad, & Patishtan, 2014; Shi, Ishitani, Kim, & Zhu, 2000). In the downstream Na^+ signaling phase, phytohormones and altered gene expressions are helpful in orchestrating plant responses to salt stress. The salt-induced signaling cascade finally results in adaptive responses, such as regulation of growth and development, Na^+ exclusion and sequestration, and production of compatible solutes to compensate for the Na^+-induced osmotic stress (van Zelm, Zhang, & Testerink, 2020).

At the physiological level, the multitude of effects of salt stress indicates the

importance of protecting the organism from damage by reactive oxygen species that inevitably increase upon water deficit and from impair photosynthesis induced by increased toxic ion uptake.

I.4.4 The K^+/Na^+ balance: a determinant of tolerance to salt stress

The most deleterious effects on plants under salt stress appear in the second phase due to disruption of ion homeostasis (Munns & Tester, 2008). Although Na^+ can be used as a cheap osmolyte for Na^+ sequestration into vacuoles, massive Na^+ entry via uptake by roots results in accumulation of Na^+ to a toxic level in the leaf blades of plants, carried by the transpiration stream. Since Na^+ and K^+ are very similar in their physicochemical properties (*i.e.*, ionic radius and ion hydration energy), they can compete for binding sites in proteins involved in key metabolic processes in the cytoplasm (Marschner, 1995). As an essential nutrient, K^+ is required for activation of more than 60 cytoplasmic enzymes, whereas Na^+ cannot substitute for K^+ in these specific functions (Evans & Sorger, 1966; Suelter, 1970). Hence, massive accumulation of Na^+ in cytoplasm can severely disrupt cellular metabolism by Na^+ competition with K^+. Furthermore, salt stress sensitivity is largely attributed to salt-induced K^+ deficiency, especially since K^+ concentration in soil is usually in the 100 micromolar range (Véry & Sentenac, 2003), several orders of magnitude lower than that of Na^+. As a consequence, in addition to the capacities of Na^+ exclusion from shoots, K^+ accumulation in shoots and maintaining a high cytosolic K^+/Na^+ ratio in leaves, are crucial for plant survival upon salinity stress (Hauser & Horie, 2010; Shabala & Cuin, 2008). Plant cell membranes contain a large number of transport systems that are responsible for the transport of K^+ and Na^+ across membranes. All these systems potentially contribute to K^+/Na^+ homeostasis and plant salt tolerance.

I.4.5 Ion transport systems involved in QTLs of K^+/Na^+ homeostasis under salt stress in Arabidopsis and rice

It is widely known that HKT transporters from the subfamily 1 are key contributors to salt tolerance in many plant species including rice and Arabidopsis (Hauser & Horie, 2010). Ion transport systems involved in QTLs of K^+/Na^+ homeostasis have almost all been identified so far in this family. In Arabidopsis, *AtHKT1;1*, single gene from this family in this species, was

found to control natural variation in leaf and flower Na^+ contents in saline conditions (Baxter et al., 2010; An et al., 2017). AtHKT1;1 functions as a Na^+-selective transporter when expressed in *Xenopus laevis* oocytes and yeast (Uozumi et al., 2000) and plays important roles in plant salinity tolerance by retrieving Na^+ from xylem sap to load it to xylem parenchyma cells and also by recirculating Na^+ from shoots to roots through loading Na^+ into phloem sap in shoots and then unloading it in roots, for massive Na^+ exclusion from shoots (Berthomieu et al., 2003; Sunarpi et al., 2005). In rice, among the four *HKT* genes in subfamily 1 encoding functional proteins (*OsHKT1;2* is a pseudogene in *Japonica* rice cv Nipponbare in which three stop codons appear in its ORF, and is currently considered non-functional (Garciadeblás, Senn, Bañuelos, & Rodríguez-Navarro, 2003; Platten et al., 2006), *OsHKT1;1* and *OsHKT1;5* have been identified to correspond to QTLs of salt tolerance. *OsHKT1;1* expressed in xylem and phloem in both roots and leaves regulates Na^+ exclusion from shoots by xylem sap desalinization and Na^+ recirculation in phloem sap, which favors root *versus* leaf Na^+ accumulation (Campbell et al., 2017; Wang et al., 2015). *OsHKT1;5* (*SKC1*) is a major QTL for maintaining K^+/Na^+ homeostasis in the salt-tolerant rice plant under salt stress (Ren et al., 2005). *OsHKT1;5* expressed in vascular tissues, mainly in root xylem parenchyma, plays a role in Na^+ retrieval from xylem sap upon salt stress (Kobayashi et al., 2017; Ren et al., 2005). *OsHKT1;4*, although not identified to correspond to QTLs of salt tolerance so far, has been shown through reverse genetics to contribute to rice salt tolerance. Expressed in xylem parenchyma in both roots and leaves, *OsHKT1;4* plays a role in rice leaf desalinization through the control of xylem sap Na^+ concentration (Oda et al., 2018; Suzuki et al., 2016; Khan et al., 2020).

Besides, variation in the abundance of the high affinity K^+ transporter gene *OsHAK1* was recently reported to underlie the differential salinity tolerance between *indica* and *japonica* rice cultivars (Chen et al., 2018). K^+/Na^+ variations in roots and leaves correlated with those in *OsHAK1* expression level. Several other K^+ transporters from the KUP/HAK/KT family in both Arabidopsis and rice (*e.g.*, AtHAK5, OsHAK5, OsHAK16, OsHAK21) were also shown through reverse genetics to contribute to tissue K^+/Na^+ homeostasis and plant salt tolerance (Nieves-Cordones, Alemán, Martínez, & Rubio, 2010; Chen et al., 2015; Shen et al., 2015; Feng et al. 2019).

I.5 Objectives of my thesis

It is of great agricultural importance in a staple food crop as rice to propose useful strategies for improving the plant mineral nutrition, and thus potentially, biomass and yield production and adaptation to environmental treats such as high soil salinity. Understanding the mechanisms mediated by K^+ transport systems, by which rice can absorb K^+ from the external soil solution and partition this ion via the vasculature within the whole-plant tissues for plant growth, and under saline stress for prevention of Na^+ toxicity, can contribute to achieve this goal. My focus at the molecular level was on two outward K^+ channels from rice, OsK5.1 and OsK5.2. Very little information was available on OsK5.1 (Kim et al., 2015), but OsK5.2 had been already partly characterized. OsK5.2 was shown to be expressed in both root vascular tissues and stomatal complex, and to be involved in xylem sap K^+ load and K^+ release by guard cells for stomatal closure and thereby in the control of leaf transpiration (Nguyen et al., 2017).

Since leaf transpiration is in addition to secretion to the xylem vessels one of the parameters that modulate ion translocation towards the shoots, this channel seemed like an interesting model to assess the level of contribution of these functions to the control of K^+ and Na^+ delivery to the shoots upon saline conditions and plant salt tolerance. This study, based on reverse genetics, is presented in Chapter III.

By further investigating the expression of *OsK5.2* in the vasculature, we localized *OsK5.2* expression in the whole-plant phloem tissues of rice plants. This new finding gave rise to the questions of how OsK5.2 controls the K^+ concentration in the xylem sap and of the role of this channel in the whole K^+ cycling throughout the plant. The study of the roles of OsK5.2 in K^+ cycling through xylem and phloem within the whole plant of rice, using reverse genetics, is reported in Chapter IV.

Our tissue expression studies indicated that OsK5.1 is a potential ortholog of the Arabidopsis SKOR K^+ channel, with expression mostly restricted to root pericycle and xylem parenchyma. The function of OsK5.1 was analyzed in rice using reverse genetics, and in heterologous contexts, through complementation of *atskor* knock-out mutant for phenotypical analyses and through transient expression in mammalian COS cells for insight on the channel functional properties. This work, which included comparison with OsK5.2, is reported in Chapter V.

Chapter II

Materials and methods

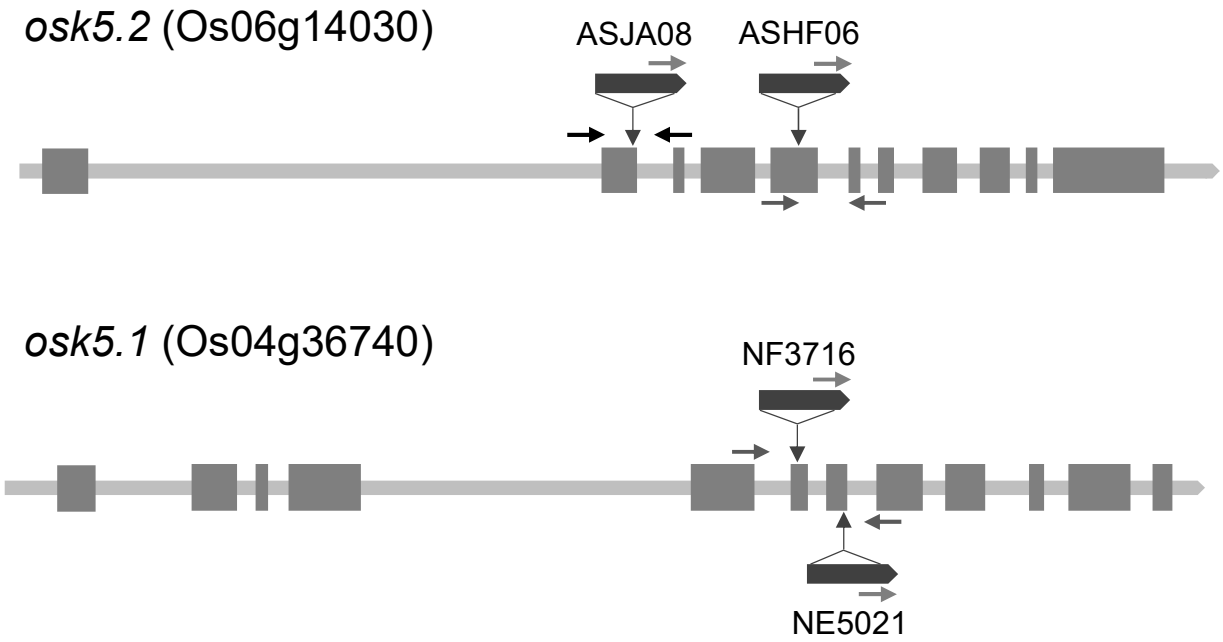

Figure II.1 Diagram of the *osk5.1* and *osk5.2* mutant lines used in this study and positions of *Tos17* insertions. Grey boxes represent exon size and position in *OsK5.1* and *OsK5.2* genes. Arrows indicate gene-specific primers used for genotyping (**Table II.1**).

II.1 Plant materials

The *osk5.2* knock-out mutant and corresponding wild-type (WT) plants in the background of rice cultivar Nipponbare (*Oryza sativa* L. japonica cv. Nipponbare) previously selected by Thanh Hao NGUYEN in the host group, originated from the ASJA08 and ASHF06 lines of the OTL (Oryza Tag Line, France) mutant library with insertion of *Tos17* retrotransposon in the second and fifth exons, respectively, of *OsK5.2* gene (Os06g14030) (Figure II.1).

The *osk5.1* knock-out mutant and corresponding WT plants in the background of rice cultivar Nipponbare previously selected by Thanh Hao NGUYEN originated from the NF3716 and NE5021 lines of the NIAS (National Institute for Agrobiological Sciences, Japan) mutant library, with the insertions of *Tos17* in the sixth and seventh exons, respectively, of *OsK5.1* gene (Os04g36740) (Figure II.1).

The Arabidopsis mutant *atskor* (Gaymard et al., 1998) in the *Arabidopsis thaliana* Wassilewskija (Ws) ecotype background was obtained from Hervé Sentenac in the BPMP laboratory.

II.2 Plant culture systems

Various rice culture systems are used in this study depending on the experimental purpose.

II.2.1 Rice culture on terrines

The rice seeds of mutant plants obtained by hybridization were sown on 50 x 37 x 11 cm plastic terrines for tissue sampling used for genotyping by PCR (Polymerase chain reaction) (Figure II.2 A). Terrines were filled with soil supplemented with fertilizer. Plants were grown under natural light, 60-70% of relative humidity, 27-29°C day/20-23°C night temperature regime in the greenhouse of CIRAD, Montpellier, France. The rice plants were sufficiently watered.

II.2.2 Rice culture on individual pots

Four-week-old plants selected by genotyping were then transferred from terrines to individual pots for grain production (Figure II.2 B). Five-liter plastic pots were filled with soil supplemented with fertilizer. The whole root systems of plants together with surrounding soil were transferred from terrines to individual pots. The plants were grown in the greenhouse

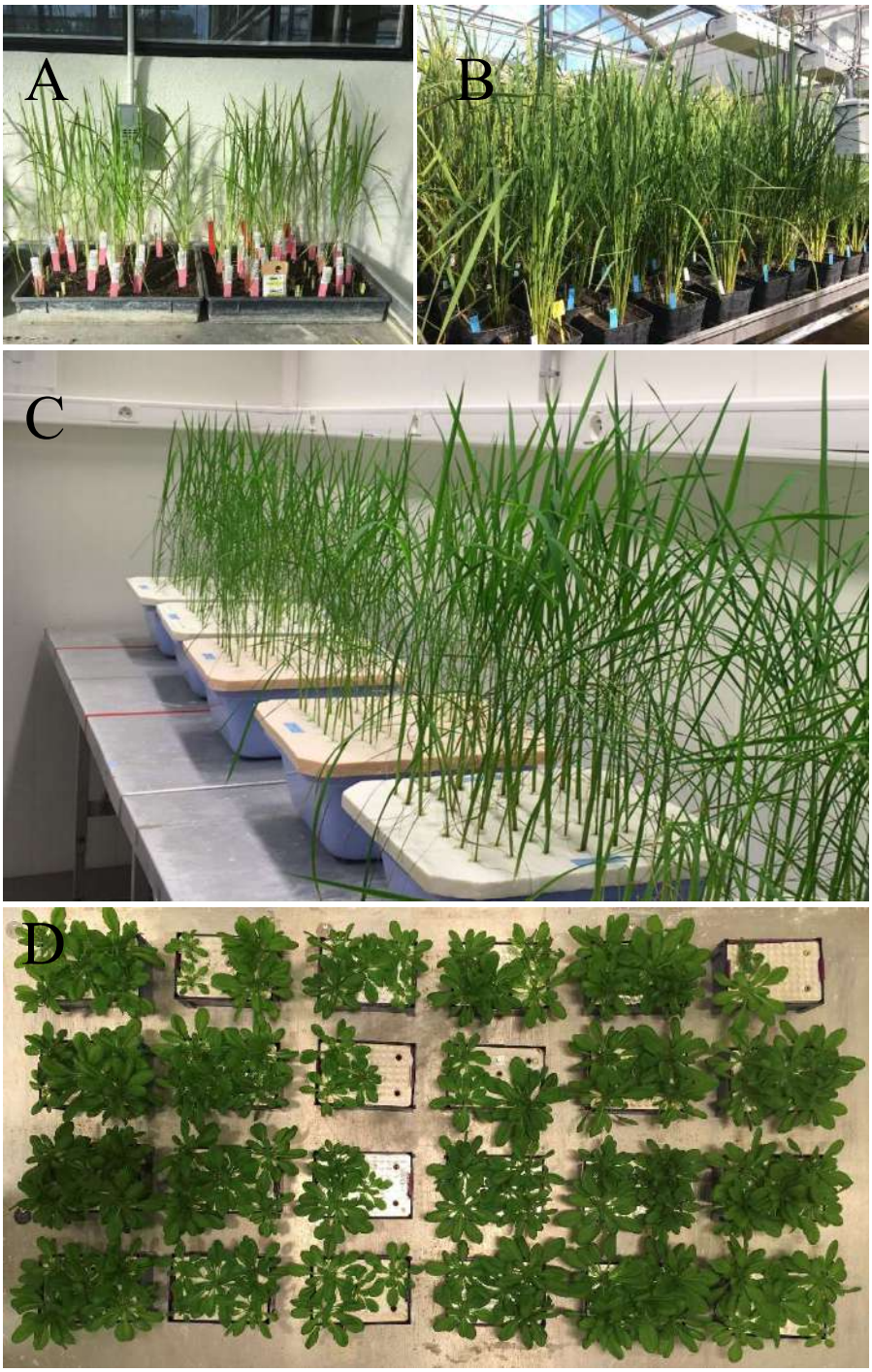

Figure II.2 Culture systems of rice cultivation. (A), rice growth on terrines in greenhouse. (B), rice growth on individual pots in greenhouse. (C), rice hydroponic cultivation system in growth chamber. (D), Arabidopsis hydroponic cultivation system in growth chamber

with the same conditions as indicated above. The rice plants were watered by submerging the bottom of pots in 3-4 cm of water. Water temperature was maintained at 20-23°C and water was renewed once a week. Plants were dried by removing pots from water when the grains were mature. Rice grains were dried as soon as possible after harvesting in a ventilated incubator at 37°C for 2 days and then were stored at 5°C with 30% relative humidity.

II.2.3 Rice hydroponic culture

The plants used for physiological analysis were hydroponically grown on media adapted from Yoshida medium (Figure II.2 C). Rice seeds were germinated on a raft floating on deionized water for one week. One-week-old rice seedlings were transferred on hydroponic cultivation system containing half of the complete concentrations of Yoshida medium for one week, followed by complete concentrations: 0.5 mM $(NH_4)_2SO_4$, 1.6 mM $MgSO_4$, 1.2 mM $Ca(NO_3)_2$, 0.7 mM KNO_3, 0.8 mM KH_2PO_4, 60 µM $Na_2FeEDTA$, 20 µM $MnSO_4$, 0.32 µM $(NH_4)_6Mo_7O_{24}$, 1.4 µM $ZnSO_4$, 1.6 µM $CuSO_4$, 45.2 µM H_3BO_3, and pH adjusted to 5.5 with H_2SO_4. In the low K^+ (0.2 mM K^+) medium, 0.7 mM KNO_3 and 0.8 mM KH_2PO_4 from Yoshida medium were substituted by 0.7 mM $Ca(NO_3)_2$, 0.6 mM NaH_2PO_4, and 0.2 mM KH_2PO_4. In the K^+-free medium, 0.7 mM $Ca(NO_3)_2$ and 0.8 mM NaH_2PO_4 substituted for KNO_3 and KH_2PO_4. Plants were grown in a growth chamber with a 12 h day/12 h night cycles and a 29°C/25°C temperature regime at 130 µmol protons m^{-2} s^{-1} light intensity under 70% relative humidity. To reduce plant transpiration, four-week-old plants grown on hydroponic Yoshida medium were then transferred and kept under high relative humidity (90% RH) in a phytotron for one week. For phenotypical analyses under short-day, plants were grown in a phytotron with a 8 h day/16 h night cycles. For salinity treatment, 5-week-old rice plants were transferred on hydroponic Yoshida medium supplemented with 50 mM or 100 mM NaCl.

II.2.4 Arabidopsis culture

The plants used for seed production were grown on individual pots in the greenhouse of BPMP laboratory, Montpellier, France. The plants used for physiological analysis were hydroponically grown on Hoagland medium in growth chamber (Figure II.2 D). For hydroponic culture, Arabidopsis seeds germinated on half-strength MS (Murashige & Skoog) agar medium, were then grown on Hoagland medium under short-day in a growth chamber (8 h day/16 h night cycles; 23°C/20°C temperature regime; 65% relative humidity; 150 μmol^{-1}

cm^{-2} s^{-1} light intensity) for four weeks. The long-day condition was applied on the four-week-old Arabidopsis plants which were transferred in a growth chamber (16 h day/8 h night cycles; 22°C/20°C temperature regime; 65% relative humidity; 150 μmol^{-1} cm^{-2} s^{-1} light intensity) for at least one week before physiological analysis experiment.

Hoagland medium contained as macroelements (mM), 1 KH_2PO_4, 5 KNO_3, 2 $MgSO_4$, 5 $Ca(NO)_2$, and as microelements (μM), 50 H_3BO_3, 0.05 $CoCl_2$, 0.2 $CuSO_4$, 1.2 $ZnSO_4$, 2.5 KI, 5 $MnSO_4$, 0.3 Na_2MoO_4, 25 Na-Fe-EDTA ($C_{10}H_{12}FeN_2NaO_8 \cdot 3H_2O$). The pH was adjusted to 5.5, and the nutrient medium was renewed weekly.

II.3 Generation of rice double mutants using cross-pollination

In the parental generation, single homozygous rice mutants *osk5.2* were used as the maternal parent and were cross-pollinated with single homozygous rice mutants *osk5.1* to generate hybrid double mutant plants with a *osk5.2* x *osk5.1* genotype. Anthers of *osk5.2* mutants were removed without harming the stigma using vacuum emasculators. Fully emasculated panicles of *osk5.2* mutant plants were then placed into a labeled glassine paper bag together with the panicles of an *osk5.1* mutant plant whose anthers were beginning to be extruded for better pollen shedding. Flicking the bag was carried out every half hour during midday (12h-14h) while the pollen was being shed. The bag was removed after 2 days of cross-pollination. F_1 seeds were harvested once ripened. F_1 plants were allowed to self-pollinate. The gene-specific primers and *Tos17* primers were used for genotyping by PCR to select the heterozygous plants successfully crossed from the knockout mutant plants in *OsK5.2* and *OsK5.1* genes. The double heterozygous mutants ♀ *osk5.2* (ASJA08) x ♂ *osk5.1* (NF3716) have been successfully obtained so far. F_2 plants were self-pollinated and F_2 seeds were harvested from the double heterozygous mutant plants. Double homozygous *osk5.2* x *osk5.1* mutant plants will be looked for in the offspring using the same set of primers.

II.4 Physiological analysis of mutant lines

II.4.1 Plant tissue collection and analysis of Na^+, K^+ and Rb^+ contents in rice and Arabidopsis

Five-week-old rice plants hydroponically grown on Yoshida medium and subsequently treated

(addition of NaCl, K^+ starvation and/or tracer Rb^+ addition) for varying times were used for tissue analysis. The root system was excised, and rinsed in deionized water. Roots and shoots were collected dried (60℃ for 3 days) and weighed. Ions were extracted from the tissues by immersing tissues in 0.1N HCl for 3 days and Na^+, K^+ and Rb^+ contents were determined by flame spectrophotometry (SpectrAA 220FS, Varian).

Five-week-old Arabidopsis plants hydroponically grown on Hoagland medium were used for tissue analysis. Roots and shoots were collected and K^+ contents were determined as explained in rice K^+ assay above.

II.4.2 Xylem sap collection and analysis of Na^+, K^+ and Rb^+ concentrations in rice and Arabidopsis

Five-week-old rice plants hydroponically grown on Yoshida medium and subsequently treated (addition of NaCl, K^+ starvation and/or tracer Rb^+ addition) for varying times were used for xylem sap analysis. Xylem sap was collected by de-topping plants 3 cm above root system through natural exudation in absence of high salinity treatment. Upon salt treatment, xylem sap was obtained through pressurization. The root system of the de-topped plants was so placed into a pressure chamber filled with hydroponic medium containing 50 mM NaCl, and sealed with a silicon dental paste (PRESIDENT Light Body, Coltene, Switzerland). The first few drops (2 µl) were discarded to avoid the contamination that results from injured cells by the cut. Twenty microliter samples were then collected, using a micro-pipette, in 0.2 ml Eppendorf tubes kept on ice, and diluted in 0.1N HCl. The concentrations of Na^+, K^+ and Rb^+ ions were determined using flame spectrophotometry (SpectrAA 220FS, Varian).

Five-week-old Arabidopsis plants hydroponically grown on Hoagland medium were used for xylem sap analysis. Xylem sap was collected by cutting the middle of the hypocotyl with a razor blade. The first few drops (2 µl) were discarded to avoid the contamination that results from injured cells by the cut. Twenty microliter samples were then collected. K^+ contents were determined as explained in rice K^+ assay above.

A

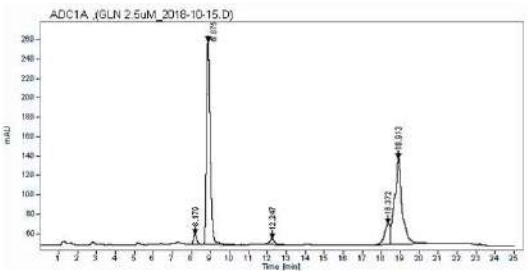

2.5 µM Gln

B

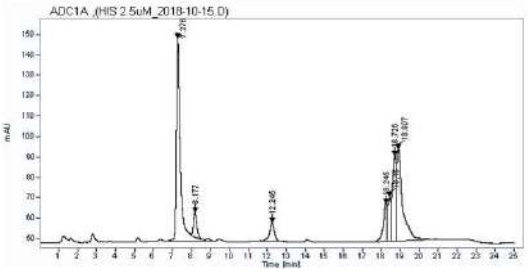

2.5 µM His

C

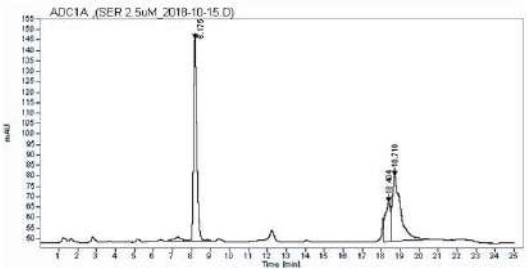

2.5 µM Ser

D

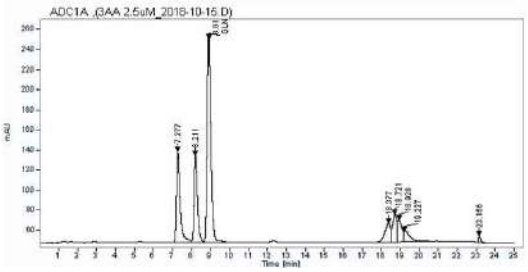

2.5 µM Gln, His, and Ser

E

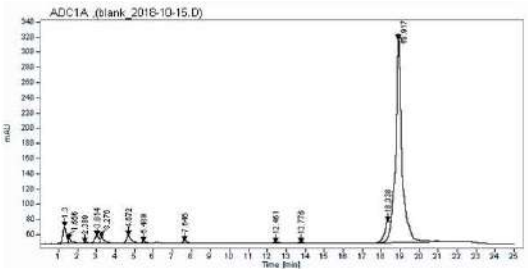

15 mM $(NH_4)_2EDTA$

F

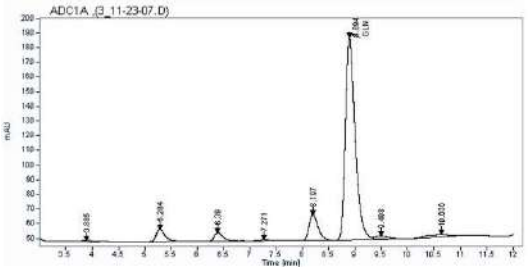

Phloem sap

Figure II.3 1220 Infinity II LC system analyses of phloem sap. (A) 2.5 µM standard glutamine (Gln); (B) 2.5 µM standard histidine (His); (C) 2.5 µM standard serine (Ser); (D) the mixture of 2.5 µM Gln, 2.5 µM His, and 2.5 µM Ser; (E) 15mM $(NH_4)_2EDTA$; (F) collected phloem sap from rice plant.

II.4.3 Phloem sap collection and analysis in rice

II.4.3.1 Phloem sap collection and analysis of Na^+, K^+ and Rb^+ concentrations

Five-week-old plants hydroponically grown on Yoshida medium and subsequently treated as desired were used for phloem sap analysis. Phloem sap was obtained by cutting the bottom of the mature leaf blades at the noon of day. The cut end of leaf blades was immediately transferred in dishes containing 15 mM $(NH_4)_2$EDTA solution (pH 7.5). In order to prevent sealing of sieve elements at the cut end parts, the leaf blades were recut about 1mm at the end-most parts under the same EDTA solution. The leaf blade ends were then immediately placed into reaction tubes containing 2 ml of the same EDTA solution and incubated in an illuminated growth chamber under water-saturated atmosphere for 5 hours. The EDTA solution containing phloem sap was immediately frozen at −80°C, and then lyophilized at −52°C (0.3 mbar) until extracts dried. The samples were resolubilized into an equal volume (100 µL) of deionized water. The quantities of Na^+, K^+ and Rb^+ in the phloem sap were determined using flame spectrophotometry. The concentration of glutamine in the phloem sap was analyzed using 1220 Infinity II LC System (Agilent Technologies)(*Cf.* § II.4.3.2 below). The concentrations of Na^+, K^+ and Rb^+ in phloem sap samples were presented normalized by the concentration of glutamine.

II.4.3.2 Glutamine analysis using HPLC system

Concentrations of amino acids were determined in phloem sap using the 1220 Infinity II LC System (Agilent Technologies) equipped with a ZORBAX eclipse Plus C18 column (3.0 x 150 mm, 3.5 µm particles; Part No. 959963-302, Agilent Technologies). Samples were injected in a volume of 10 µL with a mobile phase flow rate of 0.6 mL/min. Separation was achieved at room temperature by gradient elution using a mobile phase A consisting of 97:3 sodium acetate (25 mM, pH 5.85):tetrahydrofuran and a mobile phase B consisting of 96:4 methanol:tetrahydrofuran. The gradient profile started with 90% A (hold time 2 min) and continued with a linear change to 85% A until up to 12 min and then proceeded with 82% A until up to 12.5 min followed by a linear change to 90% B until up to 16.5 min and finally held until 17 min. Initial conditions were regained at 17 min followed by equilibration until 21 min. Peaks were identified by comparing the retention times with the standard amino acids.

Peak areas were determined automatically using Agilent OpenLAB CDS ChemStation Edition software (Agilent Technologies) (Figure II.3).

II.4.4 Measurement of rice leaf transpiration using multi-potometer

Five-week-old plants hydroponically grown on Yoshida medium and subsequently treated as desired were used for the measurement of leaf transpiration. Plants were transferred into a multi-potometer device one day before the experiments. The root system of the intact plants was inserted into a 50 mL syringe filled with hydroponic experimental medium through the rubber plunger, and sealed with a silicon dental paste. The syringe was connected with graduated 1 ml serological plastic pipettes via thin silicone tubes. The pipettes were refilled with the same medium in a proper interval of time in making sure no air bubble was present in the system. A camera was used to capture the water level in the pipettes by an interval of two minutes. Image capture was started after 2 h under light condition and maintained for 30 minutes. Plants were then exposed to darkness for 4 h upon continuous recording. The recorded decrease in the water level in the pipettes was used to calculate the transpiration rate of plants.

II.4.5 Sugar content assay in rice leaf tissues

Approximately 40 mg (Fresh weight) of leaf blades of 5-week-old rice plants was grinded and resuspended in 200 µL deionized water, then incubated at 90°C for 15 min. The insoluble fraction was removed by centrifugation at 13000 rpm for 2 min. The supernatant was transferred into a new tube. The grinded leaf contents were extracted by three times addition of 200 µL deionized water. The contents of sugars were determined in the soluble fractions using an enzymatic assay method in 96-well microplate as described previously (Gomez, Bancel, Rubio, Vercambre, & Agriculture, 2007). The contents of glucose, fructose, and sucrose were successively quantified by spectrophotometrically measuring the production of NADH at 340 nm.

II.5 Molecular biology techniques

II.5.1 Genotyping of *Tos17* and T-DNA insertion lines

The rice mutants *osk5.2* and *osk5.1* used in this study displayed insertions of *Tos17*

Table II.1 List of primers used for genotyping in rice and Arabidopsis.

Species	Gene	Insertion line	PCR purpose	Primer name	Sequence (5'-3')	Amplicon length(bp)
Rice	OsK5.2	ASJA08	PCR WT	Gt-OsK52-F3509	GGTGGTATCGGTTATGGACGA	506
				Gt-OsK52-R4014	GCATCCCACGGAAAACAACC	
			PCR mutant	Tos17tail2S	AGTCGCTGATTTCTTCACCAAGG	528
				Gt-OsK52-R4014	GCATCCCACGGAAAACAACC	
		ASHF06	PCR WT	Gt-OsK52-F4638	TTCTTGGAGCCTACCTCATTGG	609
				Gt-OsK52-R5246	GATCACCTGCCACATCAGAACAT	
			PCR mutant	Tos17tail2S	AGTCGCTGATTTCTTCACCAAGG	759
				Gt-OsK52-R5246	GATCACCTGCCACATCAGAACAT	
	OsK5.1	NF3716	PCR WT	Gt-OsK51-F2817	ACCTTAGCTCCGCCACTTAAAA	1475
				Gt-OsK51-R4291	GCAGCATTGTTTACTCCAAGGAC	
			PCR mutant	Tos17tail2S	AGTCGCTGATTTCTTCACCAAGG	1042
				Gt-OsK51-R4291	GCAGCATTGTTTACTCCAAGGAC	
		NE5021	PCR WT	Gt-OsK51-F2817	ACCTTAGCTCCGCCACTTAAAA	1475
				Gt-OsK51-R4291	GCAGCATTGTTTACTCCAAGGAC	
			PCR mutant	Tos17tail2S	AGTCGCTGATTTCTTCACCAAGG	814
				Gt-OsK51-R4291	GCAGCATTGTTTACTCCAAGGAC	
Arabidopsis	SKOR		PCR WT	Gt-AtSKOR-F594	GTTATTCATTCATTTCCCGCC	1150
				Gt-SKOR-R1743	AATGAAATGTAGACCATCGCG	
			PCR mutant	T-DNA-AtLB4	CGTGTGCCAGGTGCCCACGGAATAGT	600
				Gt-SKOR-R1743	AATGAAATGTAGACCATCGCG	

retrotransposon, while the Arabidopsis mutant *atskor* displayed T-DNA insertion.

II.5.1.1 Extraction of genomic DNA

Genomic DNA was extracted using CTAB (cetyltrimethylammonium bromide) method (Doyle, 1991), which allows to obtain high-quality genomic DNA. Fresh rice leaves (300-400 mg) were ground into fine powder. Three hundred microliters of CTAB extraction buffer (2% m/v CTAB, 1.4 M NaCl, 20 mM EDTA, and 100 mM Tris-HCl pH8.0) were added into the homogenized samples and incubated at 65°C for 15 minutes. Three hundred microliters of chloroform were then added to samples and vortexed. After centrifugation at 14000 x g for 10 minutes, the supernatant was transferred to new tubes and mixed with 300 µl of isopropanol to precipitate DNA. Samples were centrifuged at 14000 x g for 10 minutes. The DNA pellet was washed using 500 µl of 70% ethanol and air-dried. Fifty microliters of deionized water were added to resuspend the DNA pellet and the DNA solution was kept at −20°C.

II.5.1.2 Conventional PCR

PCR reaction allowed to amplify the sequence of gene of interest for different purposes, such as genotyping of *Tos17* insertions in the single and double mutants and gene cloning, etc. In the case of genotyping, PCR reactions were performed using GoTaq® DNA Polymerase (Promega) in a total volume of 25 µl, and a reaction mixture comprised of 5 µl of green GoTaq reaction buffer (5X), 0.5 µl of dNTPs (10 mM), 1 µl of forward primer (10 µM), 1 µl of reverse primer (10 µM), 0.1 µl GoTaq polymerase (5 units/µl), 1 µl of genomic DNA, and 16.4 µl deionized water. Annealing temperature and extension time for the thermal profile of PCR reactions were designed according to the used primers and the expected product size. The primers used for genotyping of *Tos17* insertions in the single and double mutants are provided in Table II.1. The Tos17tail2S primer that anneals to the 3'LTR (long terminal repeat) of *Tos17* was used to detect the existence of the *Tos17* insertion in the rice single and double mutant plants. The T-DNA-AtLB4 primer that anneals to the left border of T-DNA was used to detect the existence of the T-DNA insertion in the Arabidopsis *skor* mutant plants.

PCR reaction for cloning was performed with a Phusion™ high-fidelity DNA polymerase (Thermo Fisher Scientific) according to the manufacturer's instructions.

II.5.2 qRT-PCR analysis of gene expression

II.5.2.1 RNA isolation

Roots and leaves (20 mg) were collected from 5-week-old Nipponbare plants hydroponically grown on Yoshida medium and subsequently subjected to different experimental conditions. Total RNA extractions were performed using the RNeasy plus mini kit with gDNA eliminator (Qiagen, Germany), according to the manufacturer's protocol.

II.5.2.2 cDNA synthesis

First-strand cDNAs were synthesized using SuperScript III reverse transcriptase (Invitrogen, USA). About 3 µg of total RNA, 1 µl of 500 ng oligo(dT)$_{12\text{-}18}$, and 1 µl of 10 mM dNTPs were mixed and heated at 65°C for 5 minutes. After a quick chilling on ice, 4 µl of 5X first-strand buffer, 1 µl of 0.1 M DTT, 1 µl of RNaseOUT™ recombinant RNase inhibitor, and 1 µl of SuperScript™ III reverse transcriptase were added to the mixture and gently mixed by pipetting up and down. Then, the mixture was incubated at 50°C for 60 minutes. The reaction was inactivated by heating at 70°C for 15 minutes. The synthesized cDNA was kept at −20°C.

II.5.2.3 qRT-PCR

Rice cDNAs were used as a template for qRT-PCR experiments. qRT-PCR analyses were performed on the Lightcycler480 system (Roche diagnostics) using SYBR *Premix Ex Taq* (Takara) in a total volume of 10 µl which contained 2 µl cDNA (corresponding to 120 ng or total RNA), 3 µl forward and reverse primer mixture (1 µM), and 5 µl SYBR *Premix Ex Taq*. Reactions were performed in three independent biological replicates and three technical replicates per biological replicate. The following standard thermal profile was used in all qRT-PCR reactions: 95°C for 30 sec; 45 cycles of 95°C for 10 sec, 60°C for 10 sec, and 72°C for 15 sec; followed by a melt cycle from 60°C to 95°C. The target genes *OsK5.2* and *OsK5.1* and three rice housekeeping genes ubiquitin-like protein gene *SMT3* (LOC_Os01g68950) (Horie et al., 2007), type 2A-interacting protein-like protein gene *Tip41* (Os03g0760600) (Caldana, Scheible, Mueller-Roeber, & Ruzicic, 2007), and elongation factor gene *EF1beta* (LOC_Os07g42300) (Khan et al., 2020) were used in this study.

Table II.2 List of the primers used for qRT-PCR.

Gene	Primer name	Sequence (5'-3')	Amplicon length (bp)
OsK5.2	qPCR-OsK52-F358	TTTGGCTTCTTCAGGGGGCT	470 *
	qPCR-OsK52-R808	TCTCCCAACTGCAAGCTCCC	
	qPCR-OsK52-F467	CTGACACCTACCGCATGGTT	D-164
	qPCR-OsK52-R611	TCGTGTCAACCGAATCCACA	
OsK5.1	qPCR-OsK51-F74	TTGCGAGGGAGCTCAAGTCA	490 *
	qPCR-OsK51-R563	ATGTCCTTCTCCACCCGCTT	
	qPCR-OsK51-F129	GAGGCTGCCAAAGGATCTGT	D-125
	qPCR-OsK51-R253	TGAACTCGAACGGGGTGAAG	
SMT3	SMT3B303F	GGGAGGAGGACAAGAAGC	273 *
	SMT3B303R	CTCCAGTCTGGTGGAGCAT	
	QRT94SMT3-F	CCTCAAGGTCAAGGGACAGG	D-94
	QRT94SMT3-R	ACGGTCACAATAGGCGTTCA	
Tip41	Tip41B389F	TGGTTTTTGGGGAGAGTTTC	389 *
	Tip41B389R	TGAAATGCCATTATCGGCTA	
	QRT101Tip41-F	TGGGAGTGATGCTTTGGTTC	D-101
	QRT101Tip41-R	CAAGGTCAATCCGATCCTCA	
eEF-1-beta2	eEFB2Pcs	TGGTGAGGAGACTGAAGAGG	418 *
	eEFB2Pcas	CTTCCGGATTTTTCTTTTTATC	
	qPCR-eEF1b2-F413	TGGGAAGTCCTCAGTGTTGC	D-136
	qPCR-eEF1b2-R549	GTAACCAACCGGGACAAGCT	

"D", pair of primers for transcript level quantification, that anneal on cDNA fragments derived from two exons. "*" refers to big amplicons that were used as a template for the amplification of calibration standards.

To determine the transcript level (number of copies) of target gene in samples, an absolute quantification analysis was used in this study according to the C_T (cycle threshold) values in samples (Cuéllar et al., 2010). At first, two pairs of primers of each target and housekeeping gene were used to amplify the big amplicon, which was used as a template for the amplification of calibration standards, and which included the small amplicon used for qRT-PCR (Table II.2). In brief, serial dilutions of the big amplicons of target and housekeeping genes with predefined known concentrations were used to create standard curves of each target and housekeeping gene. The small amplicon of the target and housekeeping genes was then amplified by qRT-PCR. All amplification plots were analyzed using a threshold of 0.37 to obtain C_T values. The C_T values obtained from each housekeeping gene in each sample were then compared to the minimum C_T value of each housekeeping gene among all samples for normalization. $2^{-\Delta CT}$ values (ΔC_T= minimum C_T of each housekeeping gene among all samples − C_T of each housekeeping gene in each sample) were determined, and introduced into geNorm software (Vandesompele et al., 2002) to obtain the normalization factor to be used for the absolute quantification analysis. Finally, the absolute expression of target gene in each sample was determined as the mean copy number of target gene obtained in the qRT-PCR triplicate analysis divided by the normalization factor in each sample. The primers used for qRT-PCR experiments are provided in Table II.2.

II.5.3 Gene cloning

In this study, several constructs were prepared for different experimental purposes: (1) to test by complementation of the *atskor* mutant, the *in planta* function of OsK5.2 and OsK5.1, the sequences of p*SKOR*::*OsK5.2* and p*SKOR*::*OsK5.1* were cloned into pCambia1301 vector; (2) to test the functional properties of OsK5.2 and OsK5.1 in an heterologous animal system like COS cells, coding sequences (CDS) of *OsK5.2* and *OsK5.1* were cloned into pCI vector; (3) chimeric *AtGORK N-terminus::OsK5.2* and *AtGORK N-terminus::OsK5.1* constructs were also prepared in pCI, for functional analyses in transfected COS cells. The vectors pCambia1301 and pCI were obtained from the host Lab.

II.5.3.1 Cloning strategies

In the thesis, traditional cloning using restriction enzymes was used to construct pCambia1301-p*SKOR*::*OsK5.2*, pCambia1301-p*SKOR*::*OsK5.1*, pCI-*OsK5.2*, and

Table II.3 List of the primers used for In-fusion cloning.

Construct	fragment	Primer name	Sequence (5'-3')	Amplicon length (bp)
pCI-OsK5.2(N-ter GORK)	N-terminus of GORK	GORK-N ter for K5.2-F	CGTGGTACCTCTAGAATGGGACGTCTCCGGAGACGGC	225
		GORK-N ter for K5.2-R	CCTCGTCCATAACCGGTACCACCTGTTTTTGGGATGA	
	Linearized pCI-OsK5.2	pCI-OsK5.2-N-ter-remove-F	CGGTTATGGACGAGGTTCATAC	6285
		pCI-OsK5.2-N-ter-remove-R	TCTAGAGGTACCACGCGTGAAT	
pCI-OsK5.1(N-ter GORK)	N-terminus of GORK	GORK-N ter for K5.1-F	GGTACCCGGGGATCCATGGGACGTCTCCGGAGACGGC	225
		GORK-N ter for K5.1-R	GTTCGCCCAGATCCTGTACCACCTGTTTTTGGGATGA	
	Linearized pCI-OsK5.1	pCI-OsK5.1-N-ter-remove-F	AGGATCTGGGCGAACATGATGTTC	5979
		pCI-OsK5.1-N-ter-remove -R	GGATCCCCGGGTACCACGCGTG	

pCI-*OsK5.1*. In-fusion cloning was used to construct pCI-*OsK5.2*(*N-ter GORK*) and pCI-*OsK5.1*(*N-ter GORK*).

II.5.3.1.1 In-fusion cloning

With appropriate primer design (Table II.3), the insert N-terminus fragment of *GORK* can be recombined with the linearized vectors pCI-*OsK5.2* and pCI-*OsK5.1* using In-Fusion® HD Cloning Kit (Clontech® Laboratories, Inc.). The insert fragment and linearized vectors were amplified by PCR generating a 15 bp overlap at their 5' and 3' ends. After purification, In-fusion cloning reaction was set up in a total volume of 5 µl, which consisted of 1 µl 5X In-fusion HD enzyme premix, 100 ng PCR-generated linearized vector and 50 ng PCR-generated insert fragment, and water. Then, 1 µl of the In-fusion reaction mixture was transformed into 50 µl *E. coli* Stellar competent cells using heat shock method. Five hundred microliters of SOC medium were added and the cell suspension was incubated with shaking at 37°C for 1 h. Twenty-five to hundred microliters of the cell suspension were spread on LB agar plate containing 100 mg/L ampicillin and the plate was incubated at 37°C overnight. Positive colonies were screened by colony PCR and were sequenced.

II.5.3.1.2 Traditional cloning using restriction enzymes

Traditional clonings using restriction enzymes were used for promoter::cDNA fusion construction in plant expression vector and for the subcloning in mammalian expression vector for heterologous expression. Detail in restriction strategy used for each cloning is found below:

p*SKOR*::*OsK5.2* and p*SKOR*::*OsK5.1* fusions were constructed from *OsK5.2* and *OsK5.1* cDNAs and *SKOR* gene promoter sequence already available at the host Lab. First, the fusion between p*SKOR* and each of the rice cDNAs was obtained in pCambia2300. For the pCambia2300-p*SKOR*::*OsK5.2* construct, desired restriction sites were added in the PCR reactions using modified primers to amplify sequence of *SKOR* promoter with the SmaI (5') and XbaI (3') restriction enzymes and CDS of *OsK5.2* with the XbaI (5') and PmeI (3') restriction enzymes. For the pCambia2300-p*SKOR*::*OsK5.1* construct, desired restriction sites were added to amplify sequence of *SKOR* promoter with the KpnI (5') and BamHI (3') restriction enzymes and CDS of *OsK5.1* with the BamHI (5') and PmeI (3') restriction enzymes. The primers used for gene cloning are provided in Table II.4.

Table II.4 List of the primers used for traditional cloning using restriction enzymes.

Construct	Gene	Primer name	Sequence (5'-3')	Amplicon length (bp)
pCambia2300-pSKOR::OsK5.2	SKOR promoter	pAtSKOR-SmaI-k52F	TCCCCCGGGATCTGTACCCTGGT	1817
		pAtSKOR-XbaI-k52R	GCTCTAGATACACCTCCGAATCACG	
	OsK5.2 CDS	OsK52-XbaI-F	GCTCTAGAATGGGGAGGGGGATAG	2599
		OsK52-PmeI-R	AGCTTTGTTTAAACTCACTGCCTTGCCT	
pCambia2300-pSKOR::OsK5.1	SKOR promoter	pAtSKOR-KpnI-k51F	CGGGGTACCATCTGTACCCTGGT	1818
		pAtSKOR-BamHI-k51R	CGCGGATCCTACACCTCCGAATC	
	OsK5.1 CDS	OsK51-BamHI-F	CGCGGATCCATGGCTGAAGAGTAT	2183
		OsK51-PmeI-R	AGCTTTGTTTAAACTCAATTAGTCGCAAC	

The promoter::cDNA fusions in pCambia2300 were then transferred to pCambia1301 upstream of the Nopaline synthase (NOS) polyA terminator for obtaining final constructs. For the pCambia1301-p*SKOR*::*OsK5.2* construct, the p*SKOR*::*OsK5.2* fragment was obtained by the digestion with the SmaI (5') and AflII (3') restriction enzymes using the cloned pCambia2300-p*SKOR*::*OsK5.2* vector as template, then the digested p*SKOR*::*OsK5.2* fragment was ligated to pCambia1301 vector fragment digested by Eco53kI (5') and AflII (3') restriction enzymes. For the pCambia1301-p*SKOR*::*OsK5.1* construct, the p*SKOR*::*OsK5.1* fragment was obtained by the digestion with the KpnI (5') and AflII (3') restriction enzymes using the cloned pCambia2300-p*SKOR*::*OsK5.1* vector as template, then the digested p*SKOR*::*OsK5.1* fragment was ligated to pCambia1301 vector fragment digested by KpnI (5') and AflII (3') restriction enzymes. The strategy for cloning of pCambia1301-p*SKOR*::*OsK5.2* and pCambia1301-p*SKOR*::*OsK5.1* constructs is shown in Table II.5.

For the pCI-OsK5.2 construct, the CDS of *OsK5.2* was obtained by the digestion with the XbaI (5') and PmeI (3') restriction enzymes using the cloned pCambia2300-p*SKOR*::*OsK5.2* vector as template, then the digested *OsK5.2* fragment was ligated to pCI vector fragment digested by XbaI (5') and SmaI (3') restriction enzymes. For the pCI-OsK5.1 construct, the CDS of *OsK5.1* was obtained by the digestion with the KpnI (5') and PmeI (3') restriction enzymes using the cloned pCambia2300-p*SKOR*::*OsK5.1* vector as template, then the digested *OsK5.1* fragment was ligated to pCI vector fragment digested by KpnI (5') and SmaI (3') restriction enzymes. The strategy for cloning of pCI-OsK5.2 and pCI-OsK5.1 constructs is shown in Table II.5.

II.5.3.2 Amplification of CDS

To amplify complete coding sequence, PCR reactions were performed using Phusion™ high-fidelity DNA Polymerase (Thermo Fisher Scientific) in a total volume of 50 µl, following the manufacturer's protocol.

II.5.3.3 Restriction digestion

Restriction digestions were performed in accordance with the manufacturer's protocol. The restriction enzymes were used in this study from Thermo Scientific, or New England Biolabs (NEB), or Promega.

Table II.5 The strategy for cloning of pCambia1301-p*SKOR*::*OsK5.2*, pCambia1301-p*SKOR*::*OsK5.1*, pCI-OsK5.2, and pCI-OsK5.1 constructs.

Construct	Vector template	Restriction enzyme	Purpose
pCambia1301-pSKOR::OsK5.2	pCambia2300-pSKOR::OsK5.2	SmaI	Digested insert pSKOR::OsK5.2 fragment
		AflII	
	pCambia1301	Eco53kI	Digested vector pCambia1301 fragment
		AflII	
pCambia1301-pSKOR::OsK5.1	pCambia2300-pSKOR::OsK5.1	KpnI	Digested insert pSKOR::OsK5.1 fragment
		AflII	
	pCambia1301	KpnI	Digested vector pCambia1301 fragment
		AflII	
pCI-OsK5.2	pCambia2300-pSKOR::OsK5.2	XbaI	Digested insert OsK5.2 fragment
		PmeI	
	pCI	XbaI	Digested vector pCI fragment
		SmaI	
pCI-OsK5.1	pCambia2300-pSKOR::OsK5.1	KpnI	Digested insert OsK5.1 fragment
		PmeI	
	pCI	KpnI	Digested vector pCI fragment
		SmaI	

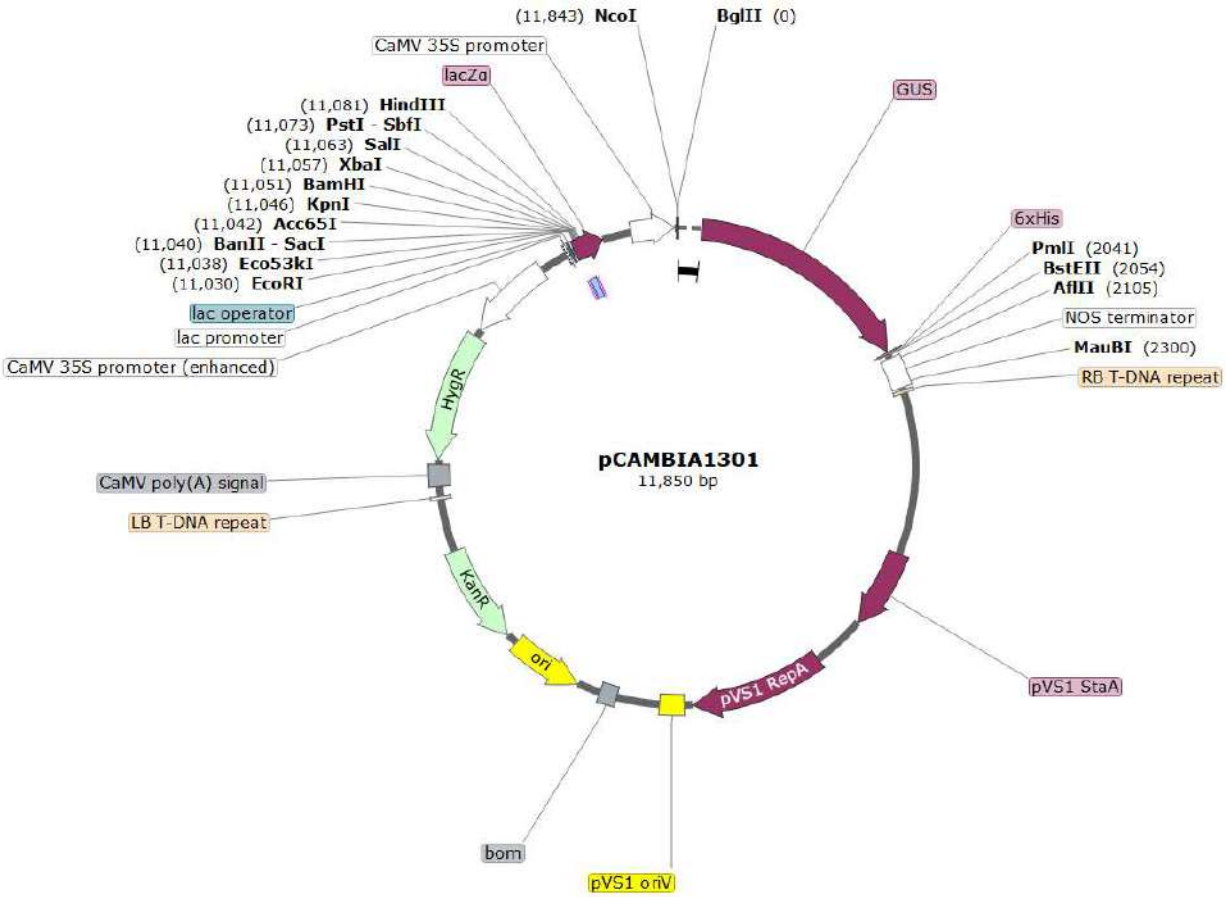

Figure II.4 Plant expression vector pCambia1301 map.

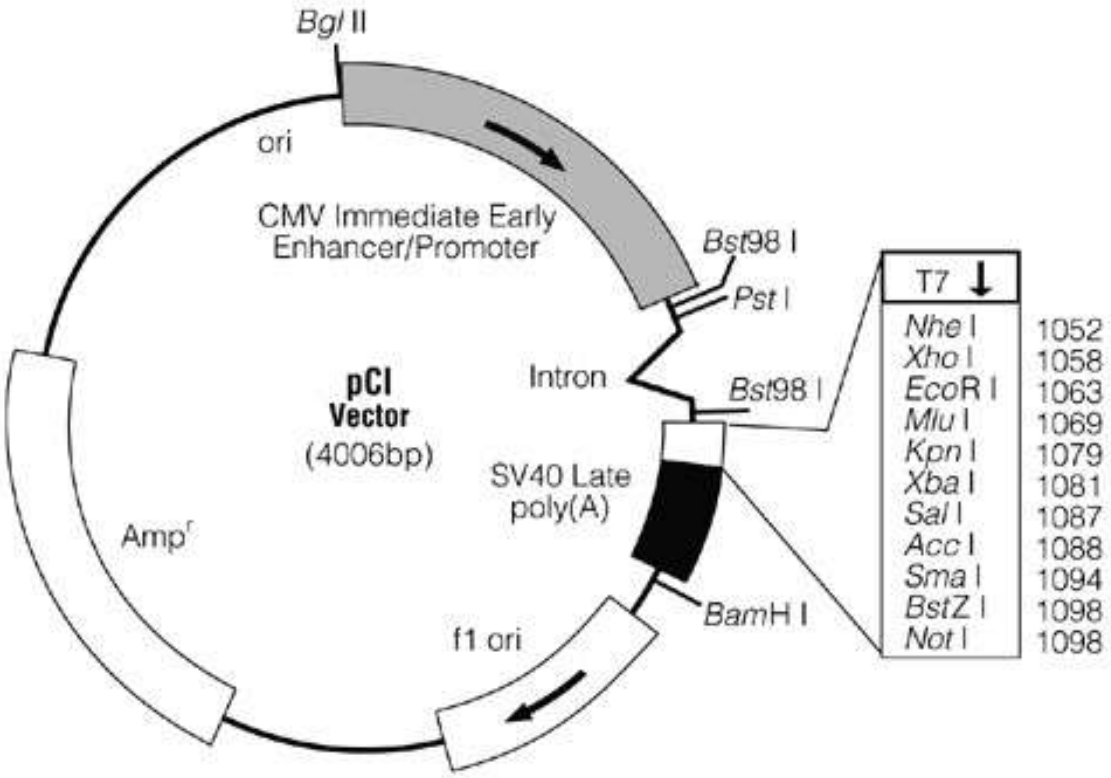

Figure II.5 Mammalian expression vector pCI map.

II.5.3.4 Purification of DNA fragment

The digested vector DNA mixtures were migrated in the gel electrophoresis for cleavage analysis. The linearized vector DNA was extracted from gel and purified using SmartPure Gel Kit (Eurogentec) according to the manufacturer's protocol. The digested insert DNA mixtures were directly purified using Wizard® Genomic DNA Purification Kit (Promega) according to the manufacturer's protocol. The concentrations of linearized vector DNA and insert DNA fragments were measured using the spectrophotometer (NanoDrop^{TM} 1000, Thermo Scientific) after purification.

II.5.3.5 Insertion of DNA fragment into a vector

The ligation was performed using T4 DNA ligase (Thermo Fisher Scientific) in a total volume of 10 µl, following the manufacturer's protocol. For preparing ligation mixture, an insert: vector molar ratio of 3:1 was used following the protocol for either sticky-end ligation or blunt-end ligation. After gently mixing by pipetting and brief centrifugation, the ligation mixture was incubated at 16°C overnight. The ligation mixture was then used in transformation of competent *Escherichia coli* cells.

In this thesis, purified insert DNA fragments were cloned into either the plant expression vector pCAMBIA1301 (Figure II.4) for agrobacterium-mediated Arabidopsis transformation or the mammalian expression vector pCI (Figure II.5) for heterologous expression of genes of interest in COS cells.

II.5.3.6 Transformation of competent *Escherichia coli* cells

The ligation mixture was transformed to DH5α competent *E. coli* cells (New England Biolab) using heat shock method. The transformed cells were grown in SOC medium following the High Efficiency Transformation Protocol (New England Biolab). Hundred to five-hundred microliters of transformed cells were spread on LB agar plate containing 50 mg/L kanamycin (pCambia vectors) or 100 mg/L ampicillin (pCI vectors) and incubated at 37°C overnight. Positive and negative control plates were prepared simultaneously. The positive control plate was done with bacteria transformed with a circular vector of known concentration and the negative control was done with bacteria transformed with a linearized vector of known concentration.

II.5.3.7 Colony PCR

Single colonies were picked by hardly touching and re-streaked on fresh LB agar plate containing desired antibiotic. Sterile micropipette tips (0.1-1 µl) were used to pick single colonies and were then dipped into PCR reaction mixture as a template DNA.

For instance for the cloning in pCambia vectors, colony PCR was performed using universal primer "lac operator-For" that anneals to the locus of lactose operator on pCambia vector series, as forward primer (5'-TGTGTGGAATTGTGAGCGGA-3'), and reverse primer of insert fragment (see Table II.4). The colony PCR products were then migrated in electrophoresis gel to verify exact band size.

II.5.3.8 Isolation of plasmid DNA

Colonies with successful ligation that were selected by colony PCR, were inoculated to fresh LB liquid medium containing desired antibiotic and grown under shaking in an incubator at 37°C overnight. NucleoSpin Plasmid EasyPure (Macherey-Nagel) was used to isolate plasmid DNA, according to manufacturer's protocol. For cell transfection, NucleoBond Xtra Midi Plus (Macherey-Nagel™ 740412.50) was used to purify transfection-grade plasmid DNA with high yield, according to manufacturer's protocol.

II.5.3.9 Diagnostic restriction digestion of plasmid and sequencing

To confirm successful ligation, diagnostic digestion was carried out on isolated plasmid DNA using desired restriction enzymes. Since the size of insert and empty vector fragments were known, the pattern of the fragments migrated in electrophoresis gel that showed bands corresponding to expected size of insert and empty vector, were confirmed to be a successful ligation. The isolated DNA vector with successful diagnostic digestion was then sequenced to confirm the sequence of the insert DNA.

II.6 Histochemical analysis of GUS activity in transgenic plants expressing *promoter::GUS* constructs

Transgenic rice plants expressing the *GUS* reporter gene under the control of *OsK5.2* promoter or *OsK5.1* promoter were obtained from previous work by Thanh Hao NGUYEN in the host group and were used to study histochemical analysis of GUS activity. Transgenic rice

plants were grown on Yoshida medium in growth chamber. Leaf and root samples from 3-week-old plants were collected and submerged in GUS staining solution containing 50 mM sodium phosphate buffer (pH7.0), 0.05% (v/v) Triton X-100, 1 mM X-Gluc (5-bromo-4-chloro-3-indolyl-β-D-glucuronide), 2.5 mM potassium ferricyanide, and 2.5 mM potassium ferrocyanide. Vacuum was then applied to facilitate the infiltration of GUS staining solution into samples for 30 minutes. The GUS staining was carried out at 37°C in the dark overnight. The chlorophyll was removed by extensive decoloration in 70% ethanol. The GUS-stained samples were observed under a BH2 microscope (Olympus).

To obtain the GUS-stained cross-sections of roots and leaves, the samples were fixed in fixation solution (50 mM sodium phosphate buffer (pH7.0), 1.6% paraformaldehyde, 0.5% glutaraldehyde) at 4 °C for 2 h under the hood. The chlorophyll was removed by successive decoloration with increasing concentration of ethanol (EtOH): 50% EtOH for 30 minutes, 70% EtOH for 30 minutes, 70% EtOH for 1 h, 95% EtOH for 30 minutes, 95% EtOH for 1 h, 100% EtOH for 90 minutes, 50% EtOH + 50% butanol for 4h, 100% butanol overnight. The GUS-stained samples were then embedded in the hydroxyethyl methacrylate resin (Technovit 7100, Heraus-Kulzer GmBH) at 4 °C overnight, following the protocol provided by the manufacturer. The 0.2 mL Eppendorf tubes and the Histoform mold were used as the molds for embedding roots and leaves respectively. Polymerization occurred at room temperature. The GUS-stained roots and leaves were sliced into semithin sections with microtome using a glass knife. The cut sections were transferred to a drop of water on a coverslip warmed at 40°C for 5 minutes and then observed under BH2 microscope (Olympus).

II.7 Agrobacterium tumefaciens-mediated transformation of *Arabidopsis thaliana*

II.7.1 Transformation of competent *A. tumefaciens* cells

A. tumefaciens strain GV3101 was transformed with the ligated plasmid by electroporation. Plasmid (0.2-1 µl) was mixed with 20 µl of electrocompetent *A. tumefaciens* cells. The plasmid/cell mixture was then transferred to a chilled electroporation cuvette and placed on the cuvette holder. The electroporation was performed with an electroporator (MicroPulser™ Electroporator, Bio-Rad). LB medium (1 ml) was added immediately to the electroporation cuvette. The resulting *A. tumefaciens* suspension was then transferred to an Eppendorf tube and incubated at 30°C for 1-3 h under agitation (200 rpm). Transformed cells (100-500 µl)

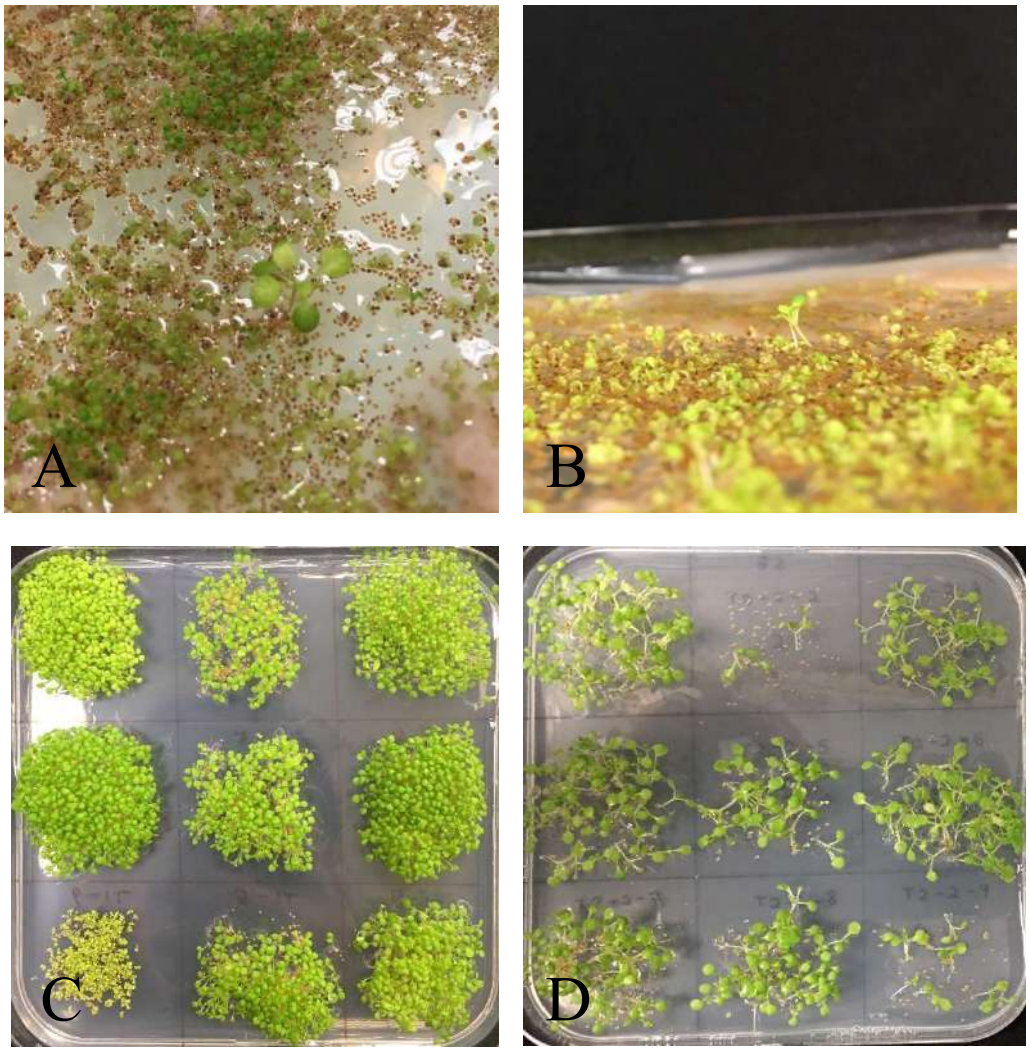

Figure II.6 Half-strength MS agar plate for the selection of transgenic Arabidopsis plants. T_1 (A and B), T_2 (C), and T_3 (D) transgenic seedlings grown on the presence of 50 mg/L hygromycin.

were spread on LB agar plate containing 50 mg/L kanamycin, 15 mg/L gentamycin, and 25 mg/L rifampicin and were incubated at 30°C for 2-3 days. Successfully transformed colonies were verified by colony PCR with gene-specific primers.

II.7.2 Arabidopsis transformation by floral dip method

About 6-7 week-old Arabidopsis plants were transformed using *A. tumefaciens*-mediated floral dip method. In brief, the verified colony containing the ligated plasmid was inoculated in 5 ml of LB medium containing 50 mg/L kanamycin, 15 mg/L gentamycin, and 25 mg/L rifampicin and was incubated at 30°C overnight with agitation (200 rpm). Two milliliters of the *A. tumefaciens* culture were then transferred from 5 ml of prepared culture to 50 ml of fresh LB medium containing the same antibiotics and incubated for 1 day in the same conditions as indicated above. The *A. tumefaciens* culture was centrifuged for 10 minutes at 5000 rpm for pellet collection. The pellet was then resuspended in 50 ml of half-strength MS (Murashige & Skoog) liquid medium containing 5% (w/v) sucrose and 0.025% (v/v) Silwet L-77. The flowers of Arabidopsis plants were immersed into the *A. tumefaciens* suspension for 30 seconds and then wrapped with transparent plastic bag to maintain moisture for 1 day. After removing the bag, the transformed Arabidopsis plants were grown in greenhouse with appropriate watering until the seeds were mature.

II.7.3 Selection of transgenic plant

Hygromycin was used for the selection of transgenic Arabidopsis plants. Non-transgenic plant displays a clear decrease in hypocotyl length and no root elongation, as compared to transgenic plant (Figure II.6). T_1 seeds were first surface-sterilized and sown on half-strength MS agar plate containing 50 mg/L hygromycin in growth chamber. The seedlings that were tolerant to hygromycin showing elongated hypocotyls, were kept and transferred on individual pot for seed production. T_2 segregation ratios were analyzed to obtain T_3 homozygous plants with a single insertion. T_2 transgenic seedlings on half strength MS agar plate containing 50 mg/L hygromycin that displayed a 3:1 segregation ratio of hygromycin resistance to sensitivity, were selected for seed production. Three T_2 lines were kept. The hygromycin resistance segregation was further examined in T_3 transgenic plants. For T_3 generation, homozygous transgenic plants were expected to be identified. T_3 transgenic seedlings that displayed no segregation of hygromycin resistance, in other words, that were all

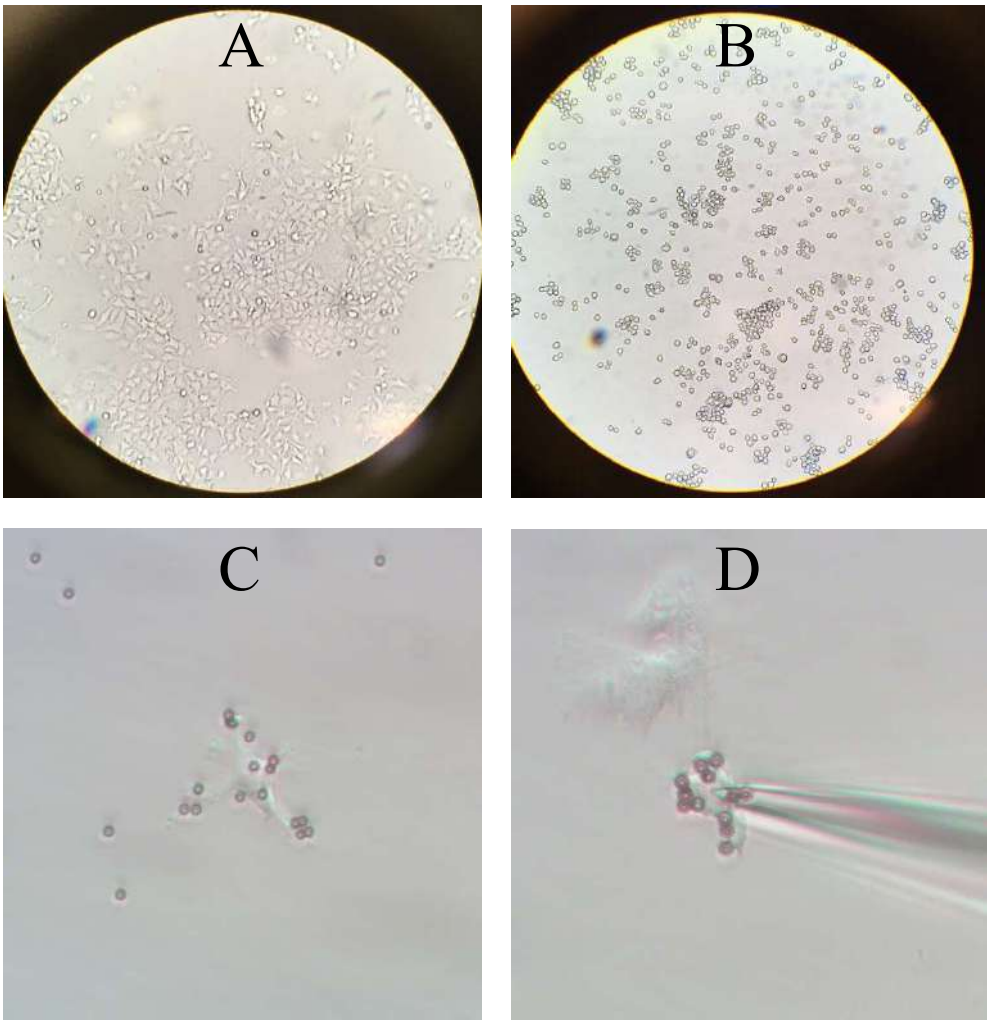

Figure II.7 COS-7 cells under microscope. (A), COS-7 cells grow adherently to glass and plastic surfaces and are fibroblastic-like. (B), COS-7 cells detach after trypsinization. (C), visual identification of transfected cells with beads coated with antibody against CD8 receptor marker for electrophysiology. (D), microelectrode sealed on a bead-coated transfected cell membrane.

tolerant to hygromycin, were homozygous transgenic plants. Homozygous lines were used in physiological experiments.

II.8 Heterologous expression in COS-7 cells and electrophysiology

II.8.1 COS-7 cell line

COS-7 cells were obtained from BPMP laboratory and were used to study functional properties of OsK5.2 and OsK5.1 in heterologous system. The COS-7 cell line was established from a CV-1 simian cell line derived from African green monkey (*Cercopithecus aethiops*) fibroblast cells through transformation with an origin-defective mutant of Simian Virus 40 (SV40) that codes for the wild-type T-antigen. COS-7 cells support the growth of recombinant SV40 viruses. Because of the combination of fibroblastic-like growth and SV40 susceptibility, COS-7 cell line is generally utilized as a transfection host.

II.8.2 COS-7 cell culture

In culture, COS-7 cell line grows adherently to glass and plastic surfaces (Figure II.7 A). All materials and reagents were obtained from Fisher Scientific (www.fishersci.fr). Freshly thawed COS-7 cells (Passage 24) from long-term storage in liquid nitrogen were maintained at 37°C, 5% CO_2 in Dulbecco's MEM (D-MEM) (Gibco^{TM} 61965026) supplemented with 10% (v/v) decomplemented FBS (fetal bovine serum) (Gibco™ A3160901) plus 50 mg/L penicillin-G and 65 mg/L streptomycin (referred to as 'complete' D-MEM). For the FBS decomplementation, heat-inactivation is a common treatment of FBS to inactivate complement proteins that are part of the immune response, by heating FBS at 56°C for 30 minutes in a water bath with occasional shaking. COS-7 cells were subcultured on a regular basis every 6 days from 95-100% confluent T25 flask to a new T25 flask with a subcultivation ratio of 1:5 to 1:7. In brief, cells were first rinsed with 10 ml of 1x sterile PBS (phosphate-buffered saline) (Gibco™ 14190094) solution to remove all traces of media containing FBS, and cell detachment was then achieved by treatment of the cell layer with 1 ml of 0.05% trypsin-EDTA solution (Gibco™ 25300054) at 37°C for 5-7 minutes (Figure II.7 B). If cells did not detach, the time of incubation was increased. During the procedure of cell detachment, agitation on cells was avoided since agitation encourages clustering. Five milliliters of complete D-MEM were added to T25 flask to neutralize the trypsin. An

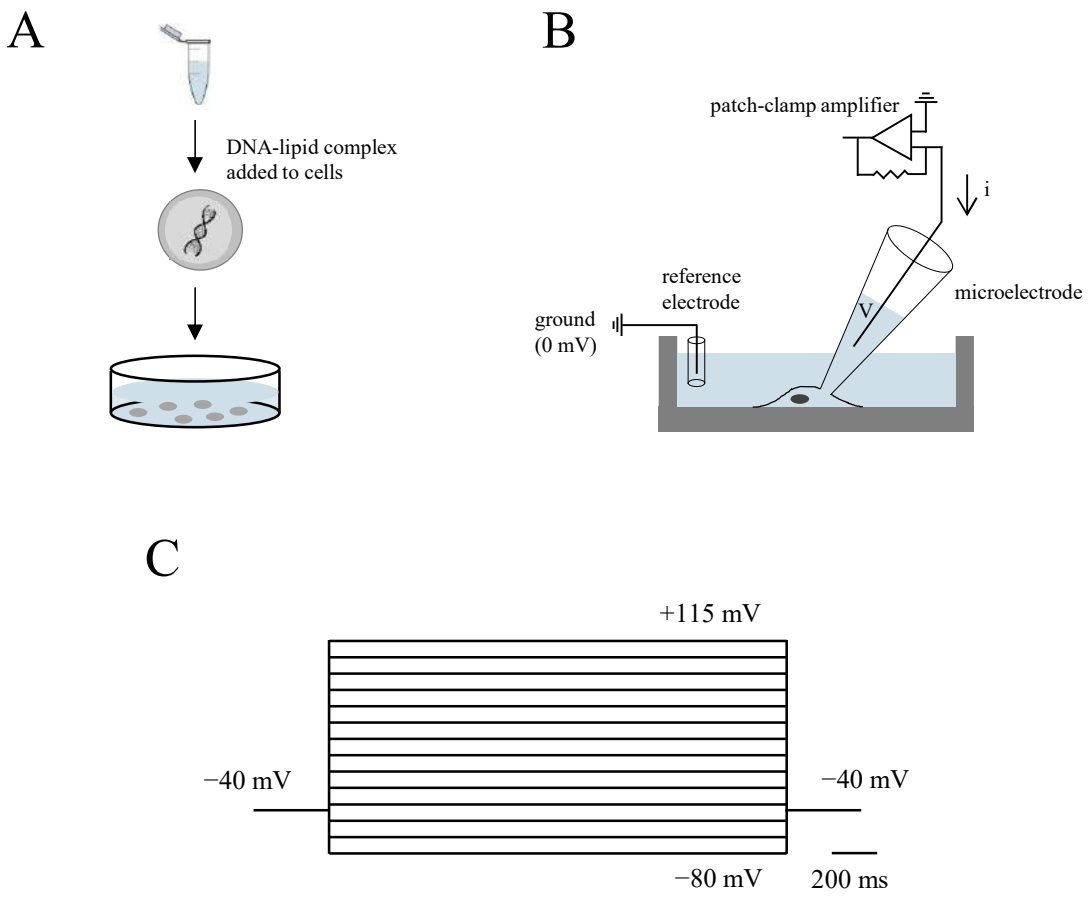

Figure II.8 COS-7 cell transfection and patch-clamp recording.

(A), lipid-based transfection of cDNAs in COS-7 cells.

(B), simplified scheme of a transfected COS-7 cell studied in whole-cell patch-clamp recording configuration. A glass microelectrode filled with electrolyte solution is tightly sealed onto the cell membrane (cell-attached configuration). By applying a brief but strong suction, the cell membrane is ruptured and the pipette gains access to the cytoplasm to obtain the whole-cell patch-clamp configuration. A reference electrode is placed extracellularly in the bath solution. A current is injected through the cell membrane via the patch-clamp microelectrode in order to change the cell membrane potential (Vm) to the desired value, and is recorded along with the applied Vm.

(C), voltage-clamp protocol for activation of outwardly rectifying K^+ channels: depolarization steps from −80 to +115 mV in 15 mV interval, from holding potential at −40 mV.

appropriate volume of the cell suspension (trypsinized cells) was added to a new culture system according to the need. For cell culture maintaining in T25 flask, 200 µl, 100 µl, and 40 µl of cell suspension were respectively seeded into a new T25 flask containing 10 ml of complete D-MEM with a subcultivation ratio of 1:5, 1:6, and 1:7 to a confluency of 95-100%. For cell transfection, 8 µl, 12 µl, 16 µl, 20 µl of cell suspension were respectively seeded into a 0.95 cm^2 48-well plate containing 250 µl of complete D-MEM to a confluency of 70-90% at the time of transfection.

II.8.3 Cell transfection

COS cell transfection was performed using lipofectamine LTX reagent with PLUS reagent (Invitrogen™ A12621), following the protocol provided by the manufacturer. In brief, (1) 2.4 µl of lipofectamine LTX reagent was diluted in 60 µl of serum-free D-MEM (no antibiotics) in an Eppendorf tube 1; (2) 500 ng of plasmid DNA (50 ng of pCI-CD8, the expression of the CD8 membrane receptor being used as transfection marker, and 450 ng of pCI-OsK5.2 or pCI-OsK5.1) was diluted in 62.5 µl of serum-free D-MEM (no antibiotics) in a new Eppendorf tube 2 supplemented with 1.25 µl of PLUS reagent; (3) 60 µl of diluted plasmid DNA in tube 2 was added and mixed into 60 µl of diluted lipofectamine LTX reagent in tube 1 (1:1 ratio). The DNA-lipid complex was incubated at room temperature for 5 minutes; (4) 40 µl of the DNA-lipid complex was added into each well, and the transfected cells were incubated at 37°C, 5% CO_2 for 1-3 days. Positive controls were obtained by cell transfection with the circular vectors of pCI-SPIK (for recording inward K^+ currents in COS-7 cells) and pCI-GORK (for recording outward K^+ currents in COS-7 cells) together with pCI-CD8. Negative controls were obtained by cell transfection with pCI-CD8 only.

II.8.4 Whole-cell patch-clamp

The COS-7 cells co-transfected with *CD8* and *OsK5.2* cDNAs or *CD8* and *OsK5.1* cDNAs in 1:10 ratio per well, were used for patch clamp assays from 1 day to 3 days after transfection. On the day of electrophysiological recordings, cells were trypsinized from each well and reseeded into 9.6 cm^2 culture dishes containing 2 ml of complete D-MEM. Cells were then incubated at 37°C, 5% CO_2 to let them adherently grow to dish surfaces before starting recordings. Transfected cells can be identified with the anti-CD8 antibody-coated bead method (Figure II.7 C, D) (Jurman, Boland, Liu, & Yellen, 1994). Cells were rinsed with 2 ml

Table II.6 Pipette and bath solutions used to record K^+ currents.

Pipette solution	Bath solution			
	K50 pH7.5	K50 pH5.0	K10 pH7.5	K10 pH5.0
150 mM KCl	50 mM KCl	50 mM KCl	10 mM KCl	10 mM KCl
2 mM $MgCl_2$	2 mM $MgCl_2$	2 mM $MgCl_2$	2 mM $MgCl_2$	2 mM $MgCl_2$
5 mM EGTA	1 mM $CaCl_2$	1 mM $CaCl_2$	1 mM $CaCl_2$	1 mM $CaCl_2$
10 mM Hepes	10 mM Hepes	-	10 mM Hepes	-
5 mM Mg-ATP	-	10 mM MES	-	10 mM MES
50 mM D-Mannitol	210 mM D-Mannitol	210 mM D-Mannitol	270 mM D-Mannitol	270 mM D-Mannitol
Tris to pH7.8	Tris to pH7.5	Tris to pH5.0	Tris to pH7.5	Tris to pH5.0

of PBS solution and were then immersed into desired bath solution. CD8 Dynabeads (0.5 µl; Invitrogen™ 11147D) were added to bath solution with gently shaking for 5 minutes, in order that transfected cells are coated with beads, and can be selected in patch clamp experiments.

The whole-cell patch-clamp configuration was used to record K^+ currents (Figure II.8), using a pipette and different bath solutions which are given in Table II.6. All experiments were performed at room temperature. Patch-clamp pipettes with resistance measured between 1-4 MΩ were routinely pulled from Borosilicate Glass (Part No. 34500-99, Kimble Chase) using a P-97 Flaming/Brown Micropipette Puller (Sutter Instrument Company). A reference half-cell component (Ag/AgCl reference electrode wire) and a sensing half-cell component (AgCl coated silver wire) were jointly used for a complete circuit. An Axopatch 200B patch-clamp amplifier (Axon Instruments, Molecular Devices) was used for current recordings, which were digitized at 1 kHz, using a Digidata 1322A 16-bit data acquisition system (Axon Instruments, Molecular Devices) connected to a computer. Currents passing through the cell membrane were measured at least 5 min after seal formation and whole-cell configuration achievement, in order to allow the pipette solution to diffuse and control the ionic composition of the cell cytosol. Cells were held at a potential of −40 mV (V_H) where the holding current was less than −500 pA. When the outward Shaker K^+ channel types were examined, a voltage-clamp activation protocol from command voltages of −80 to +115 mV in 15 mV increment was used. The Clampex module of the pClamp9 software (Axon Instruments, Molecular Devices) was used to define voltage-clamp protocol and data acquisition. Data analysis was performed using the Clampfit module of pClamp10 and SigmaPlot 13 (Systat Software Inc., USA).

II.9 Statistical methods

Student's *t*-test (two tailed, two sample equal variance) were performed using Microsoft Excel. Variation between batches was determined to be statistically significant when $p<0.05$.

Chapter III

The outward Shaker channel OsK5.2 is beneficial to the plant salt tolerance through its role in K^+ translocation and its control of leaf transpiration

doi: https://doi.org/10.1101/2021.05.28.446164

The outward Shaker channel OsK5.2 is beneficial to the plant salt tolerance through its role in K^+ translocation and its control of leaf transpiration

Running head: OsK5.2 K^+ channel contribution to salt tolerance

Jing Zhou, Thanh Hao Nguyen[1], Doan Trung Luu, Hervé Sentenac, Anne-Aliénor Véry*

BPMP, Univ Montpellier, CNRS, INRAE, Institut Agro, Montpellier, France
[1]Present address: University of Glasgow, Institute of Molecular Cell & System Biology, Bower Building, Glasgow G12 8QQ, UK

*For correspondence. E-mail anne-alienor.very@cnrs.fr

Funding
This work was supported in part by a grant from the China Scholarship Council (to J.Z.), by a doctoral fellowship from the French Embassy in Vietnam (to T.H.N.), and by an ANR-DFG grant (ANR-20-CE92-0005 to A.A.V.).

Acknowledgments
We are grateful to Emmanuel Guiderdoni, Christian Chaine, Eve Lorenzini, Christophe Périn and Remy Michel for the rice mutant line amplification.

Abstract
High soil salinity constitutes a major environmental constraint to crop production worldwide, and the identification of genetic determinants of plant salt tolerance is awaited by breeders. While the leaf K^+ to Na^+ homeostasis is considered as key parameter of plant salt tolerance, the underlying mechanisms are not fully identified. Especially, the contribution of K^+ channels to this homeostasis has been scarcely examined. Here, we show, using a reverse genetics approach, that the outwardly-rectifying K^+ channel OsK5.2, involved in K^+ translocation to the shoot and K^+ release by guard cells for stomatal closure, is a strong

determinant of rice salt tolerance. Upon saline treatment, OsK5.2 function in xylem sap K^+ load was maintained, and even transiently increased, in roots. OsK5.2 selectively handled K^+ in roots and was not involved in xylem sap Na^+ load. In shoots, OsK5.2 expression was up-regulated from the onset of the saline treatment, enabling fast reduction of stomatal aperture, decreased transpirational water flow and therefore decreased trans-plant Na^+ flux and reduced leaf Na^+ accumulation. Thus, the OsK5.2 functions allowed shoot K^+ nutrition while minimizing arrival of Na^+, and appeared highly beneficial to the leaf K^+ to Na^+ homeostasis, the avoidance of salt toxicity and plant growth maintaining.

Keywords (5-10)

Outward K^+ channel, Shaker channel, salt tolerance, rice, K^+/Na^+ homeostasis, transpirational flux, xylem sap, root-to-shoot translocation, *Tos17* insertion mutants

1 | INTRODUCTION

High soil salinity is a widespread environmental constraint over the world that causes substantial restrictions in production and quality of a majority of crops, including cereals. Understanding how plants cope with high salinity in the environment is thus an issue of great agricultural importance. Rice is rated as a salt-sensitive cereal (Munns & Tester, 2008; Zeng & Shannon, 2000), and salinity levels have increased in rice fields, in particular owing to the climate changes and sea level rise, which strongly challenge rice culture in coastal regions.

The adverse effects of high soil salinity on plant growth are mainly related to the decrease in osmotic potential of the soil and to ionic toxicity of Na^+ in leaves (Munns & Tester, 2008). Studies on the latter phenomenon have revealed that genes encoding Na^+ transport systems correspond to major quantitative trait loci (QTLs) of salt tolerance (Hauser & Horie, 2010). In return, such findings have spurred research efforts in this domain of membrane transport biology, highlighting also that Na^+ detrimental effects are counteracted by the plant's ability to take up the essential macronutrient K^+ and control its K^+ nutritional status in presence of high external Na^+ concentrations (Maathuis & Amtmann, 1999). K^+ is involved in vital functions such as enzyme activation, the cytoplasmic pH homeostasis, control of cell membrane potential and cell turgor-driven movements (Marschner, 2011; Nieves-Cordones, Al Shiblawi & Sentenac, 2016). Upon salt stress, the massive influx of

positively charged Na^+ ions causes cell membrane depolarization, which reduces the driving force for K^+ uptake and even in some cases leads to channel-mediated root K^+ losses (Jayakannan, Bose, Babourina, Rengel, & Shabala, 2013; Rubio, Nieves-Cordones, Horie, & Shabala, 2020). Thus, plant exposure to high salinity is inevitably accompanied by chronic K^+ deficiency, which affects the leaf K^+ to Na^+ content ratio, whose maintenance to a high value is a key determinant of salt tolerance (Hauser & Horie, 2010; Maathuis & Amtmann, 1999).

K^+ and Na^+ ions taken up by root cells can migrate to stelar tissues and be translocated to leaves by the upward flow of sap in the xylem vessels. Control of the ionic composition of xylem sap, involving membrane ion transport processes in parenchyma cells along the sap ascent pathway, is thus a major determinant of salt tolerance, together with control of the flux of xylem sap, which is driven by leaf transpiration and hence dependent on the level of stomatal aperture, or driven by the so-called root pressure, resulting from increased osmotic pressure in the xylem vessels due to increased solute concentration in the sap in absence of significant plant transpiration (Jeschke, 1984; Marschner, 2011). Therefore, transport systems contributing to Na^+ or K^+ secretion/retrieval into/from the xylem sap or to regulation of stomatal aperture can contribute to processes that play crucial roles in salt tolerance.

In various plant species, Na^+ transporters from the HKT family have been shown to contribute to Na^+ retrieval from the xylem sap and loading into the xylem parenchyma cells bordering the vessels, *i.e.* to the so-called "sap desalinization" process (Hauser & Horie, 2010). In rice, the *HKT* transporter genes identified as involved in this process are *OsHKT1;5*, which is mainly expressed in root xylem parenchyma cells and corresponds to the major salt-tolerance QTL *SKC1* (Ren et al., 2005), *OsHKT1;4*, expressed in both root and basal leaf xylem tissues (Suzuki et al., 2016; Khan et al., 2020), and *OsHKT1;1* expressed in both xylem and phloem and thereby additionally involved in Na^+ recirculation from leaves to roots within the phloem sap, favoring root *versus* leaf Na^+ accumulation (Campbell et al., 2017; Wang et al., 2015).

Compared with the large number of studies focused on the Na^+ transporters controlling Na^+ translocation to leaves and thereby contributing to maintain the ratio of leaf K^+ to Na^+ contents to a high value, less attention has been paid to the K^+ transport mechanisms that operate under saline conditions and ensure efficient K^+ supply to leaves. Current knowledge in this domain essentially concerns K^+ transport systems involved in root

K^+ uptake, and mainly high-affinity K^+ transporters from the HAK/KUP/KT family, AtHAK5 in Arabidopsis and OsHAK1, OsHAK5, OsHAK16 and OsHAK21 in rice (Chen et al., 2015; Feng et al., 2019; Nieves-Cordones, Alemán, Martínez & Rubio, 2010; Shen et al., 2015; Yang et al., 2014).

In rice, the outwardly rectifying Shaker K^+ channel OsK5.2 is involved both in K^+ translocation into the xylem sap toward the shoots and in control of stomatal aperture and leaf transpiration by driving K^+ efflux from guard cells for stomatal closure (Nguyen et al., 2017). This channel thus emerged as a good model to assess the level of contribution of these functions to the control of Na^+ and K^+ delivery to shoots upon saline conditions and salt tolerance. This has been achieved in the present study by phenotyping *osk5.2* knock-out (KO) mutant plants subjected to saline conditions. We found that the lack of functional *OsK5.2* expression does result in increased plant sensitivity to salt stress and analyzed the bases of the salt sensitive phenotype.

2 | MATERIALS AND METHODS

2.1 | Plant growth and salt treatment

The selection from *Tos17*-insertion lines of *osk5.2* mutant and corresponding wild-type (WT) plants in the background of rice Nipponbare cultivar (*Oryza sativa* L. ssp. japonica cv. Nipponbare) has been previously described (Nguyen et al., 2017). Rice seeds were germinated on a raft floating on deionized water for one week. The seedlings were then hydroponically grown on half-strength Yoshida medium for one week, and thereafter on Yoshida medium (0.5 mM $(NH_4)_2SO_4$, 1.6 mM $MgSO_4$, 1.2 mM $Ca(NO_3)_2$, 0.7 mM KNO_3, 0.8 mM KH_2PO_4, 60 µM $Na_2FeEDTA$, 20 µM $MnSO_4$, 0.32 µM $(NH_4)_6Mo_7O_{24}$, 1.4 µM $ZnSO_4$, 1.6 µM $CuSO_4$, 45.2 µM H_3BO_3, and pH adjusted to 5.5 with H_2SO_4). Five-week-old rice plants were subjected to salt treatment by supplementing the hydroponic Yoshida medium with NaCl. The rice plants were grown in a growth chamber (70% relative humidity, light intensity 130 photon $\mu mol.m^{-2}.s^{-1}$, 29°C/25°C 12 h/12 h day/night).

2.2 | RNA extraction and quantitative real time PCR experiments

Five-week-old Nipponbare plants grown on Yoshida medium were either supplemented with 50 mM NaCl for 14 days and then transferred back to standard Yoshida medium for three days, or further grown during this period on Yoshida medium (control batch). Total RNAs

were extracted from samples collected at same times from salt-treated or control plant batches using the RNeasy plus mini kit with gDNA eliminator (Qiagen, Germany). First-strand cDNAs were synthesized from 3 µg of RNAs using SuperScript III reverse transcriptase (Invitrogen) and used as template for qRT-PCR experiments. qRT-PCR analyses were performed using the Lightcycler480 system (Roche diagnostics) and SYBR *Premix Ex Taq* (Takara) in a total volume of 10 µl, which contained 2 µl of cDNA, 3 µl of forward and reverse primer mixture (1 µM), and 5 µl of SYBR *Premix Ex Taq*. Reactions were performed with three independent biological replicates, each one with three technical replicates (PCR program: 95°C for 30 sec; 45 cycles of 95°C for 10 sec, 60°C for 10 sec, and 72°C for 15 sec; followed by a melt cycle from 60°C to 95°C). C_T (cycle threshold) values were obtained from amplification data using a threshold of 0.37. The *OsK5.2* absolute number of copies was calculated according to standard curves obtained by successive dilutions with known quantities of *OsK5.2*, and then normalization using the C_T values of three housekeeping genes (ubiquitin-like protein gene *SMT3*, PP2A-interactor gene *Tip41* and elongation factor gene *EF1beta*) as described in Khan et al. (2020). The sequences of the primers used for qRT-PCR experiments are provided in Table II.2.

2.3 | Na^+ and K^+ assays in tissues and xylem sap

Five-week-old plants hydroponically grown as described above were supplemented or not with 50 mM NaCl for 14 days. Excised root systems and shoots were periodically collected during the salt treatment, both from salt treated and control plants. The roots (rinsed in deionized water) and shoots were dried (60°C for 3 days) and weighed. Ions were extracted from the tissues in 0.1 N HCl for 3 days and assayed by flame spectrophotometry (SpectrAA 220FS, Varian).

Xylem sap was collected through natural exudation under control condition from de-topped plants (3 cm above the root system). Upon salt treatment, xylem sap was obtained through pressurization. The root system of the de-topped plants was placed into a pressure chamber (Boursiac *et al*., 2005) filled with hydroponic medium containing 50 mM NaCl, and sealed with a silicon dental paste (PRESIDENT Light Body, Coltene, Switzerland). The first few drops (2 µl) were discarded to avoid the contamination that results from injured cells. Twenty µl of sap samples were then collected using a micro-pipette, transferred into 0.2 ml Eppendorf tubes kept on ice, and diluted in 0.1 N HCl for Na^+ and K^+ assay (flame

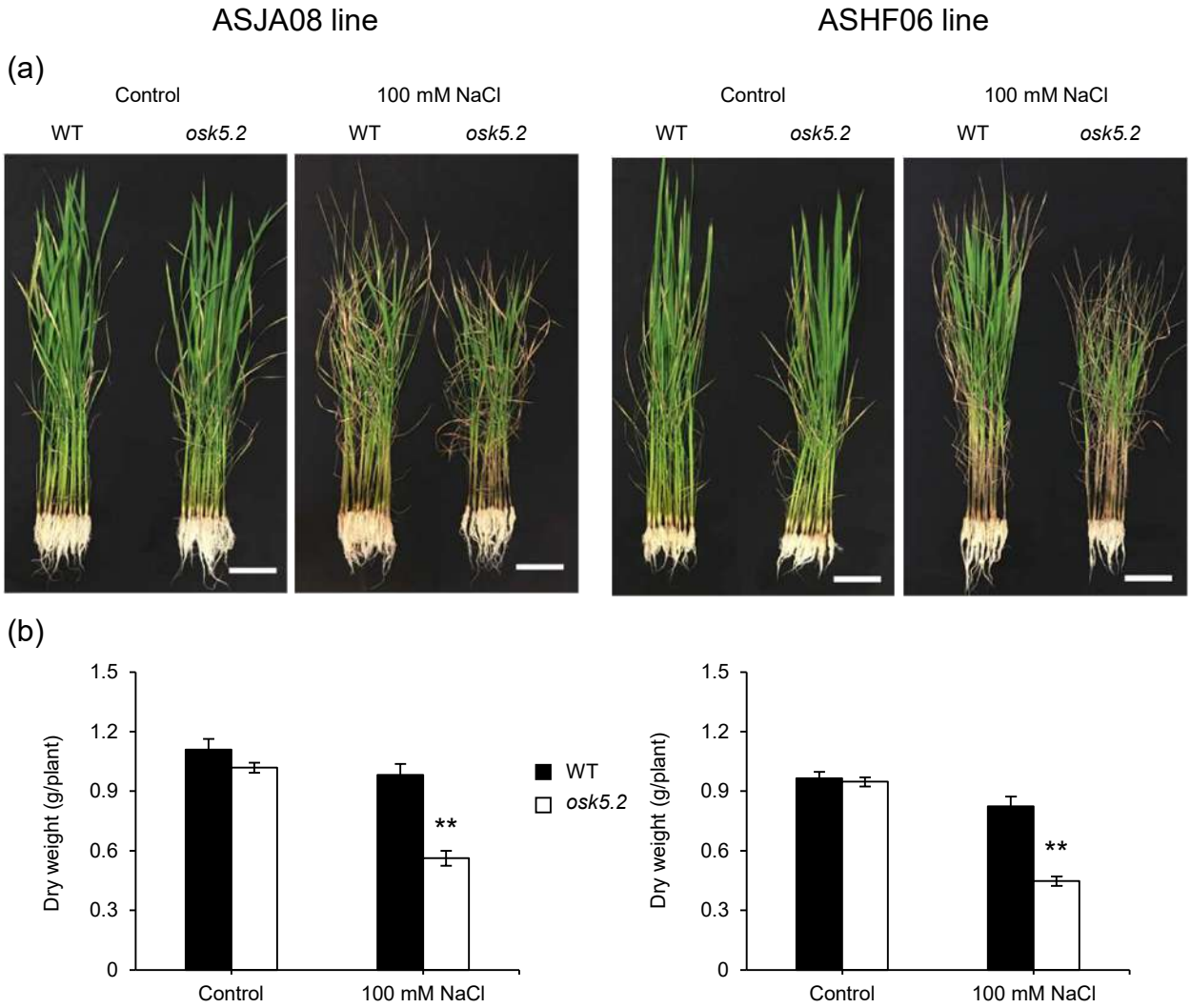

FIGURE 1 Effect of *OsK5.2* loss of function on rice plant phenotype in control and salt stress conditions. Comparison of growth phenotype (a) and dry weight (b) between corresponding wild-type and *osk5.2* mutant plants (black and white bars, respectively) issued from ASJA08 or ASHF06 lines (left and right panels, respectively) under control and salt treatment. Six-week-old plants grown on hydroponic Yoshida medium were supplemented or not during the last 7 days with 100 mM NaCl. Scale bars = 10 cm in (a). Means ± SE, n = 10. Double stars above the bars denote statistically significant differences between wild-type and *osk5.2* mutant plants (Student's t test, $P \leq 0.01$).

spectrophotometry).

2.4 | Leaf transpiration

Intact plants were transferred into a multipotometer device (Nguyen et al., 2017) one day before transpiration rate measurement. The root system of each intact plant was inserted into a 50 ml syringe filled with hydroponic medium through the rubber plunger, and sealed with a silicon dental paste. Each syringe was connected to a graduated 1-ml serological plastic pipette via a thin silicone tube. The pipettes were refilled with the same medium with proper time intervals, making sure that no air bubble was present in the system. A camera took photographs of the set of pipettes every two minutes in order to record the changes in water level in the pipettes. Image capture was started after 3 h under light condition and maintained for 30 minutes. Plants were then exposed to darkness for 5 h under continuous recording. The rate of decrease in the water volume in the pipettes was used to calculate the mean transpiration rate of plants.

3 | RESULTS

3.1 | *osk5.2* mutant plants exhibit increased sensitivity to salinity

The two *osk5.2* KO mutant lines ASJA08 and ASHF06 (Nguyen et al., 2017) and the corresponding wild type (WT) plants displayed a very similar development and phenotype when growth occurred in absence of salt stress (Figure 1). This was no longer the case when the plants were subjected to saline conditions (6-week-old plants subjected to 100 mM NaCl for 7 days). The mutant plants then displayed a severe reduction in biomass, by about 45-50% when compared with the biomass of plants from the same mutant lines but grown in control conditions, while the corresponding reduction observed for the WT plants appeared weak (less than 10-15%) and not statistically significant (Figure 1b). Furthermore, under this saline treatment, the mutant plants displayed a greater extent of stunted leaf growth and a larger number of dried leaves than the WT plants (Figure 1a). Thus, the lack of *OsK5.2* functional expression resulted in reduced tolerance to saline conditions.

3.2 | *OsK5.2* transcript accumulation under salt stress

Real-time qRT-PCR analyses revealed that *OsK5.2* was expressed in both roots and leaves (Figure 2). In plants grown in control condition, *OsK5.2* transcripts were 4 folds more

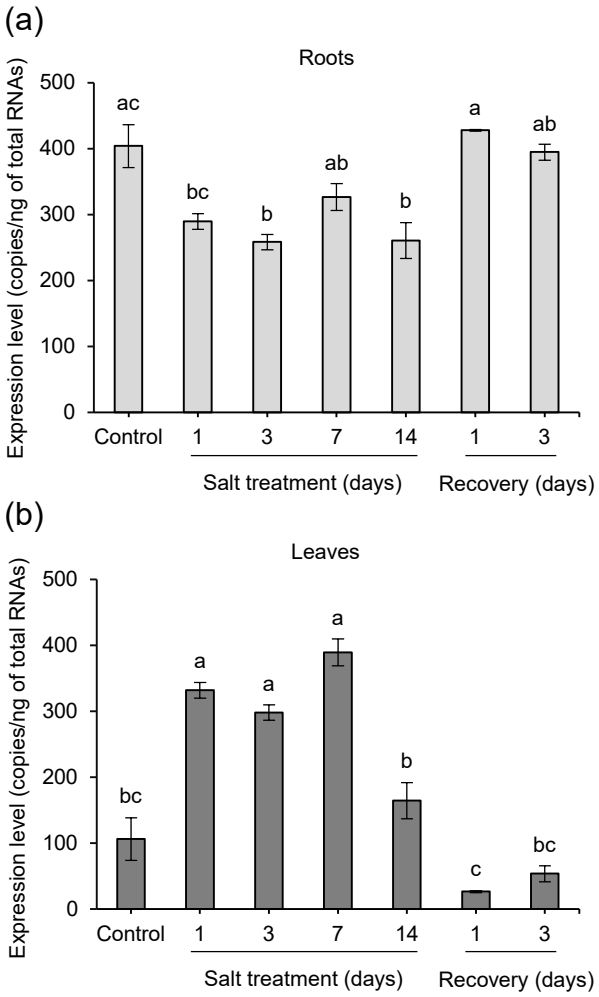

FIGURE 2 Effect of saline conditions on *OsK5.2* transcript levels in roots and leaves. Five-week-old rice plants cv Nipponbare hydroponically grown on Yoshida medium were supplemented or not with 50 mM NaCl for 14 days. Salt-treated plants were thereafter allowed to recover for 3 days on standard Yoshida medium. Expression data in roots (a) and leaves (b) were determined by real-time quantitative RT-PCR. Means ± SE (n = 3 biological replicates under salt treatment after 1, 3, 7 and 14 days and recovery, and n = 4 under control treatment sampled at each time of salt treatment). Different letters indicate statistically significant differences (Student's t test, $P \leq 0.05$).

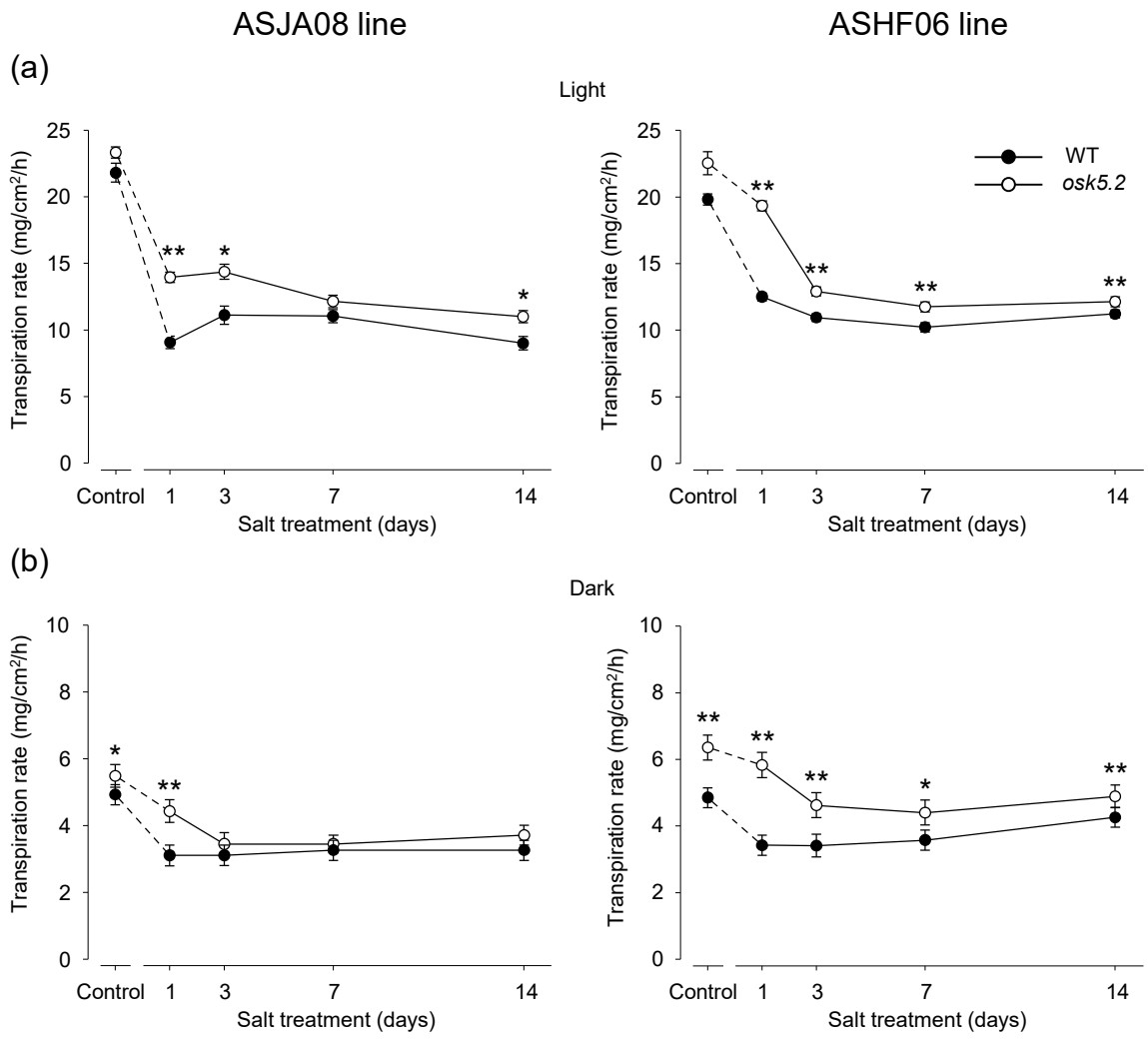

FIGURE 3 Steady-state transpiration rates in wild-type and *osk5.2* mutant plants under control and salt treatment conditions. Five-week-old plants hydroponically grown on Yoshida medium were supplemented or not with 50 mM NaCl for 14 days. Left and right panels: *osk5.2* mutant plants (○) issued from ASJA08 or ASHF06 lines, respectively, and the corresponding wild-type plants (●). Transpiration was measured after 1, 3, 7 and 14 days of salt treatment (and at the same times for the plants maintained in control conditions). (a) and (b): steady-state transpiration rates in light (panel a; ~3 h after light was switched on) and in dark (panel b; ~5 h after light was switched off) conditions. Steady-state transpiration rate was determined by dividing the average plant rate of water loss at steady-state (means of 3 values) by the total surface of the plant aerial parts. Means ± SE; n = 9 under salt treatment after 1, 3, 7, 14 days, and n = 12 under control conditions. Single and double stars denote statistically significant differences between wild-type and *osk5.2* mutant plants (Student's t test, $P \leq 0.05$ and $P \leq 0.01$, respectively).

abundant in roots than in leaves. When the plants were subjected to saline conditions (50 mM NaCl), a change in the relative expression of *OsK5.2* between roots and shoots was observed leading to balanced expression in the plant. In leaves, the accumulation of *OsK5.2* transcripts was rapidly (from one day after salt treatment) up-regulated by about 3 folds, and remained high during 7 days (Figure 2b). The leaf level of *OsK5.2* transcripts appeared to decrease with longer exposure to the saline conditions but, after 14 days of salt treatment, it was still about 1.5-fold that observed in control conditions (Figure 2b). Recovery from salt stress for 1 to 3 days further decreased the leaf level of *OsK5.2* transcripts, down to that observed in leaves from control plants. In roots, as compared with leaves, the accumulation of *OsK5.2* transcripts showed more reduced variations in response to the saline treatment and tended to slightly decrease, a down-regulation by about 25% observed at days 3 and 14 of the salt treatment being statistically significant (Figure 2a). After 1 day of recovery from salt stress, the root level of *OsK5.2* transcripts recovered to same expression level of control plants and then remained stable for at least 2 days.

3.3 | *osk5.2* mutant plants display larger transpirational water loss than WT plants under salt stress

To investigate the role of *OsK5.2* in control of leaf transpiration under salt stress, 50 mM NaCl was added into the hydroponics solution of 5-week-old *osk5.2* mutant and WT plants, and the steady-state rates of plant water loss were measured periodically for 14 days (on days 1, 3, 7 and 14 of the salt treatment) both under light and in dark conditions using a multipotometer (Figure 3). The data obtained with the 2 *osk5.2* mutant lines ASJA08 and ASHF06 led to the same conclusions. The salt treatment strongly decreased the rate of transpirational water loss, in the *osk5.2* mutant and the corresponding WT plants, by up to 50 to 55 % in the light and 30 to 40% in the dark conditions (Figure 3). The kinetics of reduction of transpiration rate upon NaCl exposure was clearly slower in *osk5.2* mutant compared with WT plants both in light and dark conditions. During the two weeks of salt treatment, a higher rate of transpirational water loss was consistently observed in *osk5.2* mutant as compared with WT plants in light and dark conditions, and the difference was highly significant in most of the analyzed time points (Figure 3). The greatest difference in transpiration rate between WT and *osk5.2* mutant plants occurred after one day of treatment owing to the slower response to NaCl exposure in *osk5.2* mutant plants.

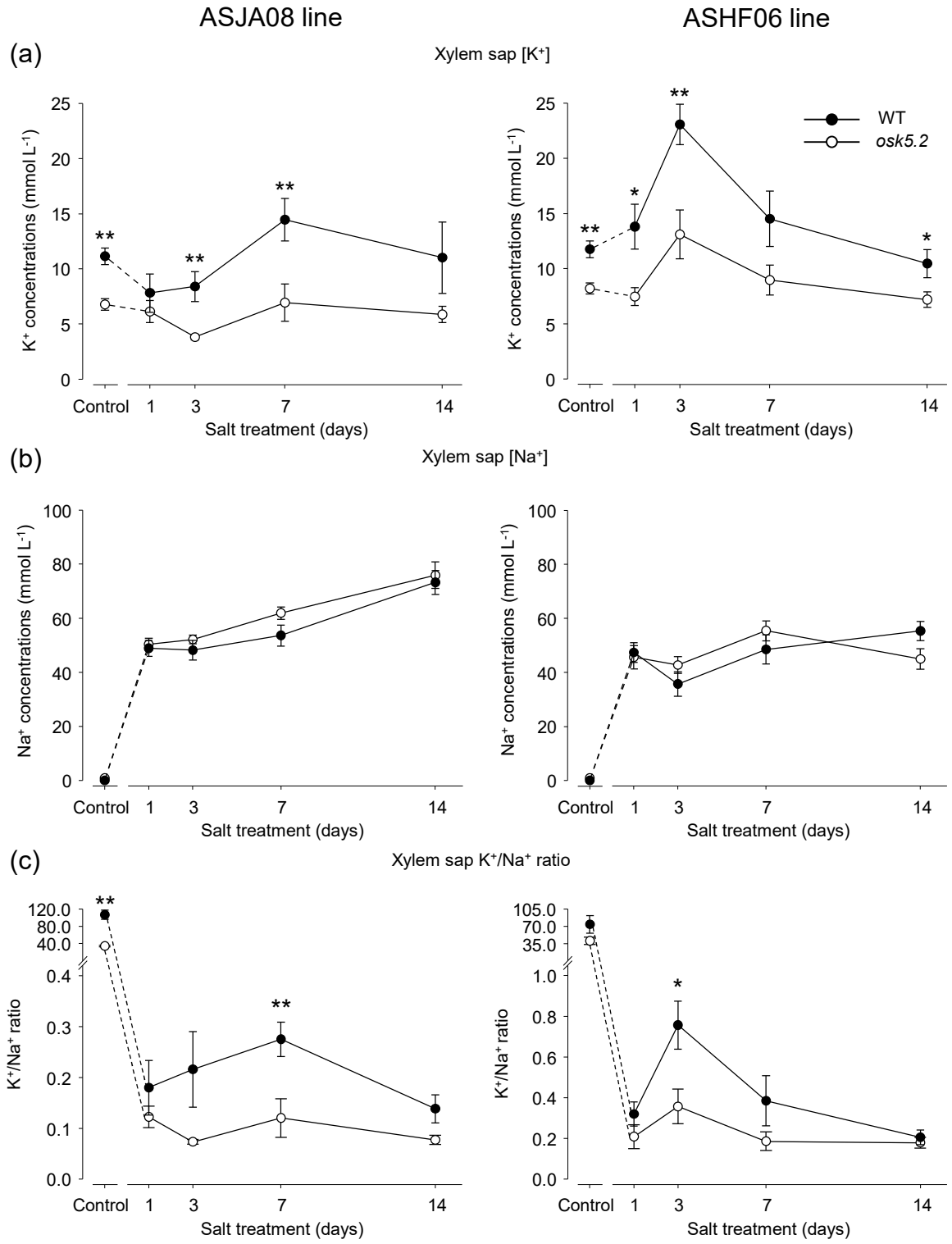

FIGURE 4 Xylem sap K^+ and Na^+ concentrations in wild-type and *osk5.2* mutant plants under control and salt treatment conditions. Five-week-old plants hydroponically grown on Yoshida medium were supplemented or not with 50 mM NaCl for 14 days. Left and right panels: *osk5.2* mutant plants (○) issued from ASJA08 or ASHF06 lines, respectively, and the corresponding wild-type plants (●). Xylem sap exudates were collected after 1, 3, 7 and 14 days of salt treatment (and at the same times for the plants maintained in control conditions). (a) and (b): K^+ (a) and Na^+ (b) concentrations assayed in the collected xylem sap samples. (c) K^+/Na^+ concentration ratios deduced from (a) and (b). Means ± SE; n = 9 under salt treatment after 1, 3, 7, 14 days, and n = 12 under control conditions. Single and double stars denote statistically significant differences between wild-type and *osk5.2* mutant plants (Student's t test, $P \leq 0.05$ and $P \leq 0.01$, respectively).

3.4 | Na^+ and K^+ concentrations in xylem sap under salt stress and translocation fluxes towards the shoots

Xylem sap samples were collected from de-topped plants subjected to the same protocol of salt treatment as that that used in the experiment described by Figure 3: 2 weeks in 50 mM NaCl hydroponics solution applied to 5-week-old plants previously grown under control conditions. The concentrations of K^+ and Na^+ determined in sap samples (Figure 4) and the transpiration rates recorded under the same experimental conditions (Figure 3) were used to estimate the transpiration-driven fluxes of K^+ and Na^+ (Figure S1) arriving in shoots under such conditions.

Under control condition, K^+ concentrations measured in xylem sap were close to 11 mM (7-folds the K^+ concentration in the hydroponic medium) in WT plants, and were 30 to 40% lower in the two *osk5.2* mutant lines (as previously reported; Nguyen et al., 2017). The xylem sap K^+ concentration in both WT and *osk5.2* mutant plants displayed transient variations upon exposure to the saline conditions (Figure 4a). The concentrations observed in the *osk5.2* mutant plants remained lower than those displayed by the corresponding WT plants by about 40% to 50% over the entire duration of the salt treatment (Figure 4a). With respect to Na^+, the concentration of this cation in the xylem sap was extremely low, in the submillimolar range, in the absence of salt treatment (Figure 4b). Exposure to 50 mM NaCl led to the loading of a large amount of Na^+ to the xylem sap with no significant difference between WT and *osk5.2* mutant plants (Figure 4b). The Na^+ concentrations measured in the xylem sap of the two types of plants were close to that of the hydroponic medium (50 mM) after one day of NaCl supplementation, and remained fairly stable during the two weeks of salt treatment. Altogether, these results indicated that the lack of *OsK5.2* functional expression constitutively resulted in a large reduction in xylem sap K^+ concentration, by *ca.* 40-50%, but did not affect xylem sap Na^+ concentration. As a result, the K^+/Na^+ xylem sap concentration ratios, computed from the data provided by Figure 4a and 4b, appear consistently higher in WT than in *osk5.2* mutant plants (Figure 4c).

The estimated K^+ flux arriving in shoots during the light period in these experimental conditions, obtained by integrating the data from Figure 3a and 4a (Figure S1a), is decreased by the salt treatment in both the *osk5.2* mutant and WT plants. It is lower in both *osk5.2* mutant lines than in the corresponding WT plants, except at day 1 of the salt treatment due to

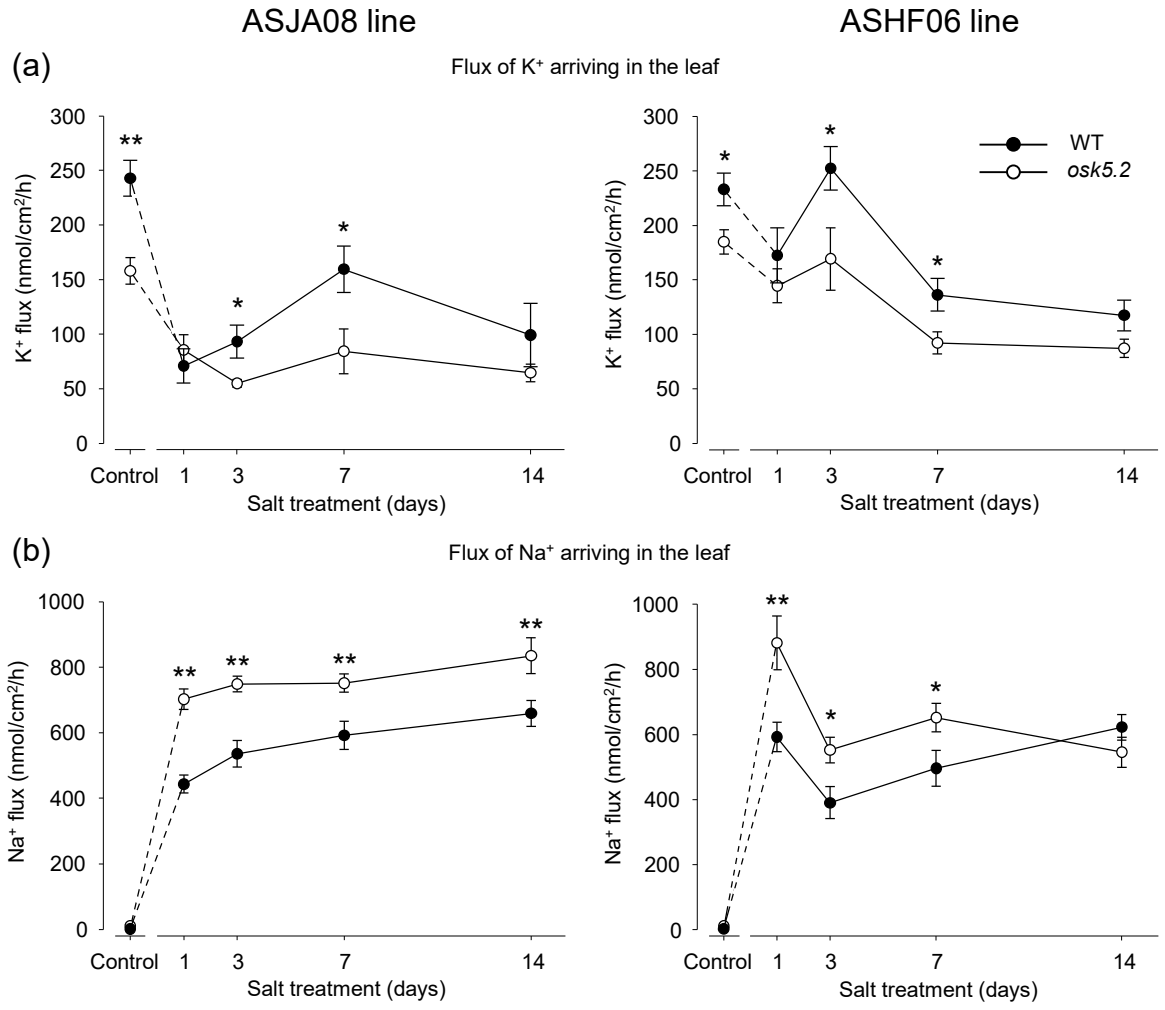

Figure S1 K^+ and Na^+ fluxes arriving at light in leaves of wild-type and *osk5.2* mutant plants under control and salt treatment conditions. (a) and (b): normalized values (expressed per leaf surface) of K^+ (a) and Na^+ (b) fluxes assessed by multiplying the mean transpiration rates (data from Figure 3) by the corresponding K^+ or Na^+ concentrations in xylem sap (data of Figure 4). Left and right panels: *osk5.2* mutant plants (○) and corresponding wild-type plants (●) issued from ASJA08 (left) or ASHF06 (right) lines. Means ± SE; $n = 9$ under salt treatment after 1, 3, 7 and 14 days, and $n = 12$ under control conditions. See legends to Figures 3 and 4. Single and double stars denote statistically significant differences between the wild-type and *osk5.2* mutant plants (Student's *t* test, $P \leq 0.05$ and $P \leq 0.01$, respectively).

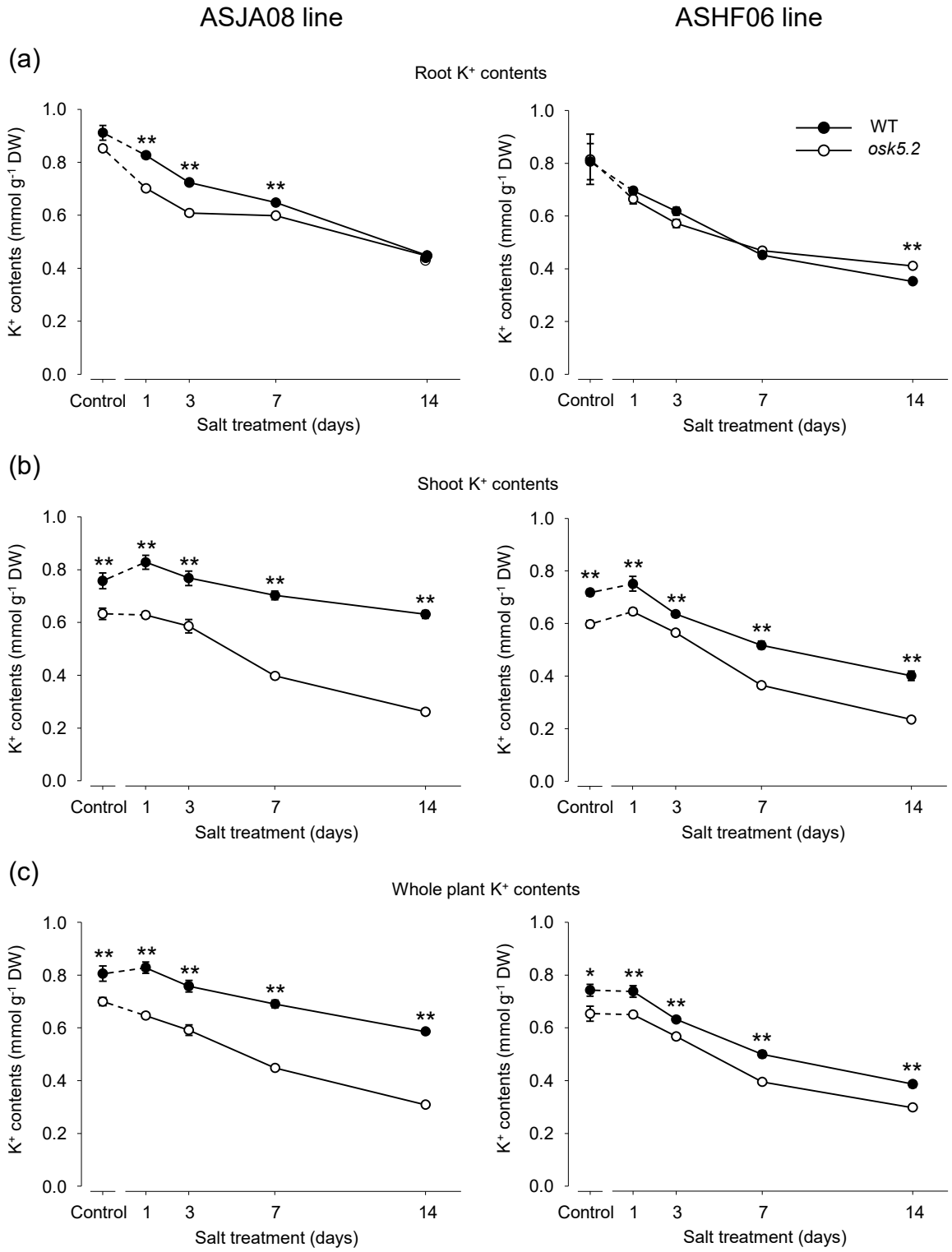

FIGURE 5 Root and Shoot K^+ contents in wild-type and *osk5.2* mutant plants under control and salt treatment conditions. Five-week-old plants hydroponically grown on Yoshida medium were supplemented or not with 50 mM NaCl for 14 days. Left and right panels: *osk5.2* mutant plants (○) and the corresponding wild-type plants (●) issued from ASJA08 (left) or ASHF06 (right) lines. Roots and shoots were sampled after 1, 3, 7 and 14 days of salt treatment (and at the same times for the plants maintained in control conditions). (a), (b) and (c): K^+ contents in roots, shoots and whole plant, respectively. Means ± SE; n = 9 under salt treatment after 1, 3, 7 and 14 days, and n = 12 under control conditions. Single and double stars denote statistically significant differences between the wild-type and *osk5.2* mutant plants (Student's t test, $P \leq 0.05$ and $P \leq 0.01$, respectively).

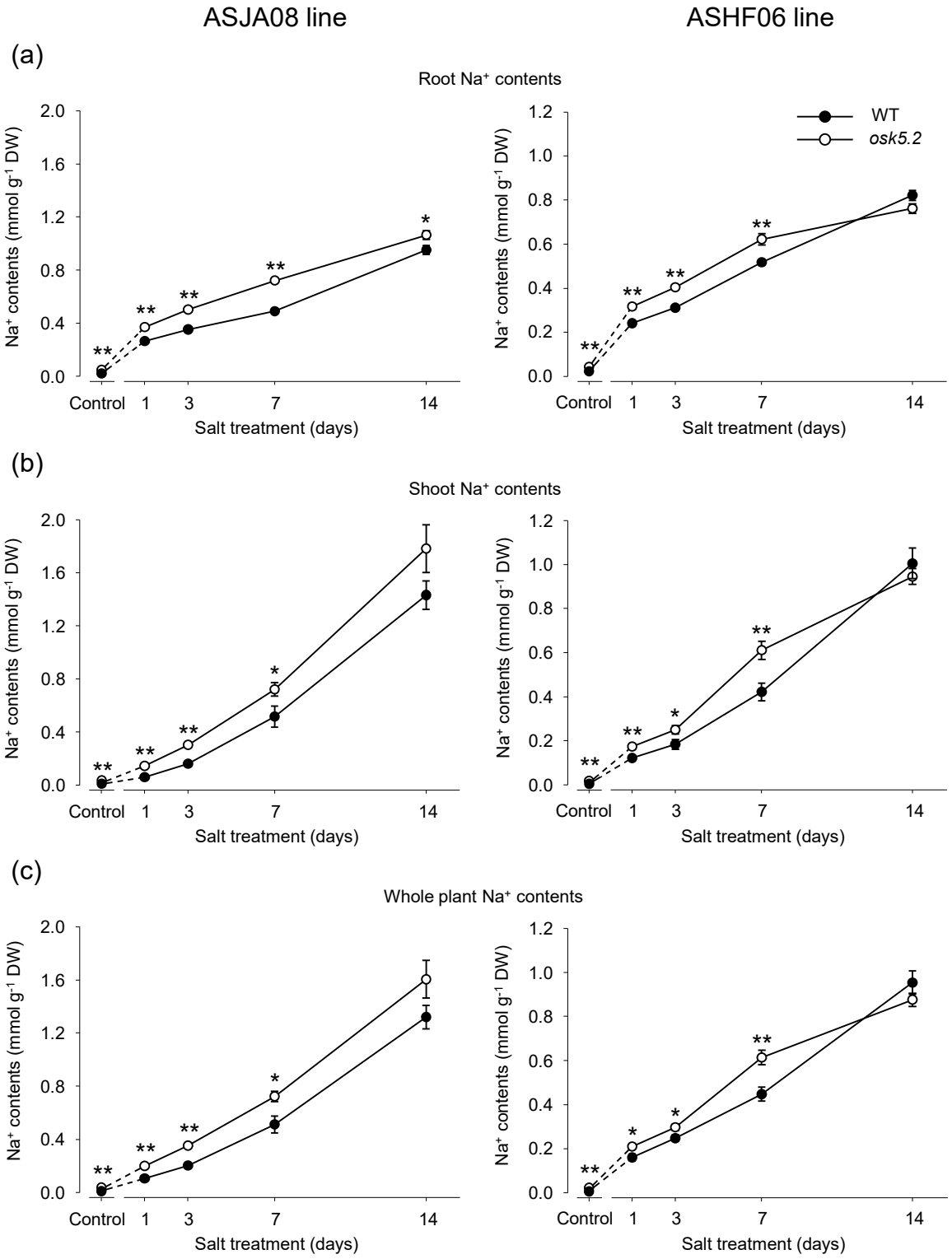

Figure 6 Root and Shoot Na^+ contents in wild-type and *osk5.2* mutant plants under control and salt treatment conditions. Same plants as in Figure 5. (a), (b) and (c): Na^+ contents in roots, shoots and whole plant, respectively. Means ± SE; n = 9 under salt treatment after 1, 3, 7 and 14 days, and n = 12 under control conditions. Single and double stars denote statistically significant differences between the wild-type and *osk5.2* mutant plants (Student's t test, $P \leq 0.05$ and $P \leq 0.01$, respectively).

the sharp decrease in transpiration rate displayed by WT plants at this time point. The differences between the WT and mutant plants under salt treatment are in the 30 to 50% range from days 3 of the salt treatment, *i.e.*, similar to those observed between the two types of plants in control conditions (Figure S1a).

The estimated flux of Na^+ arriving in the shoots of WT and *osk5.2* mutant plants is very low under control conditions (this cation being then present as trace contaminant in the hydroponics solution). A marked increase in Na^+ flux is observed in all genotypes from the first day of exposure to NaCl (Figure S1b). The flux is larger in *osk5.2* mutant than in WT plants, by ca. 20 to 40% during the first week of the salt treatment, which essentially reflects the difference in transpiration rate between the two types of plants during this period (see Figure 3).

3.5 | *osk5.2* mutant plants accumulate less K^+ and more Na^+ under salt stress

K^+ and Na^+ contents were determined in roots and shoots of *osk5.2* and WT plants subjected to the same salt treatment protocol as that previously used.

In all genotypes, root and shoot K^+ contents, and thus whole plant K^+ contents, decreased with the duration of the salt treatment (Figure 5a, b, respectively). In shoots, the decrease was clearly more pronounced in the *osk5.2* mutant lines, when compared with the corresponding WT plants, and the relative difference in shoot K^+ contents between the mutant and WT plants increased with the duration of the salt treatment (Figure 5b): the difference was in the range of 10-20% at the beginning of the treatment (in the absence of NaCl addition and at day 1 of the salt treatment), and reached 40-60% after two weeks of treatment (Figure 5b). In roots, the impact of lack of *OsK5.2* functional expression on K^+ contents appeared much weaker than that observed in shoots (Figure 5a).

Regarding Na^+, the contents of this cation were very low in all plants, whatever their genotype, in the absence of salt treatment (Figure 6). The salt treatment increased both the root and shoot (and thus the whole plant) contents of this cation, from the first day of treatment and over the two weeks of treatment, in all plant genotypes (Figure 6). Under all conditions except the longest duration of the salt treatment (in other words, under control conditions and during the first week of salt exposure), significantly higher Na^+ contents were found in the *osk5.2* mutants than in the corresponding WT plants, for both mutant lines, by more than 20% in roots and 35% in shoots (Figure 6b). The relative differences between the

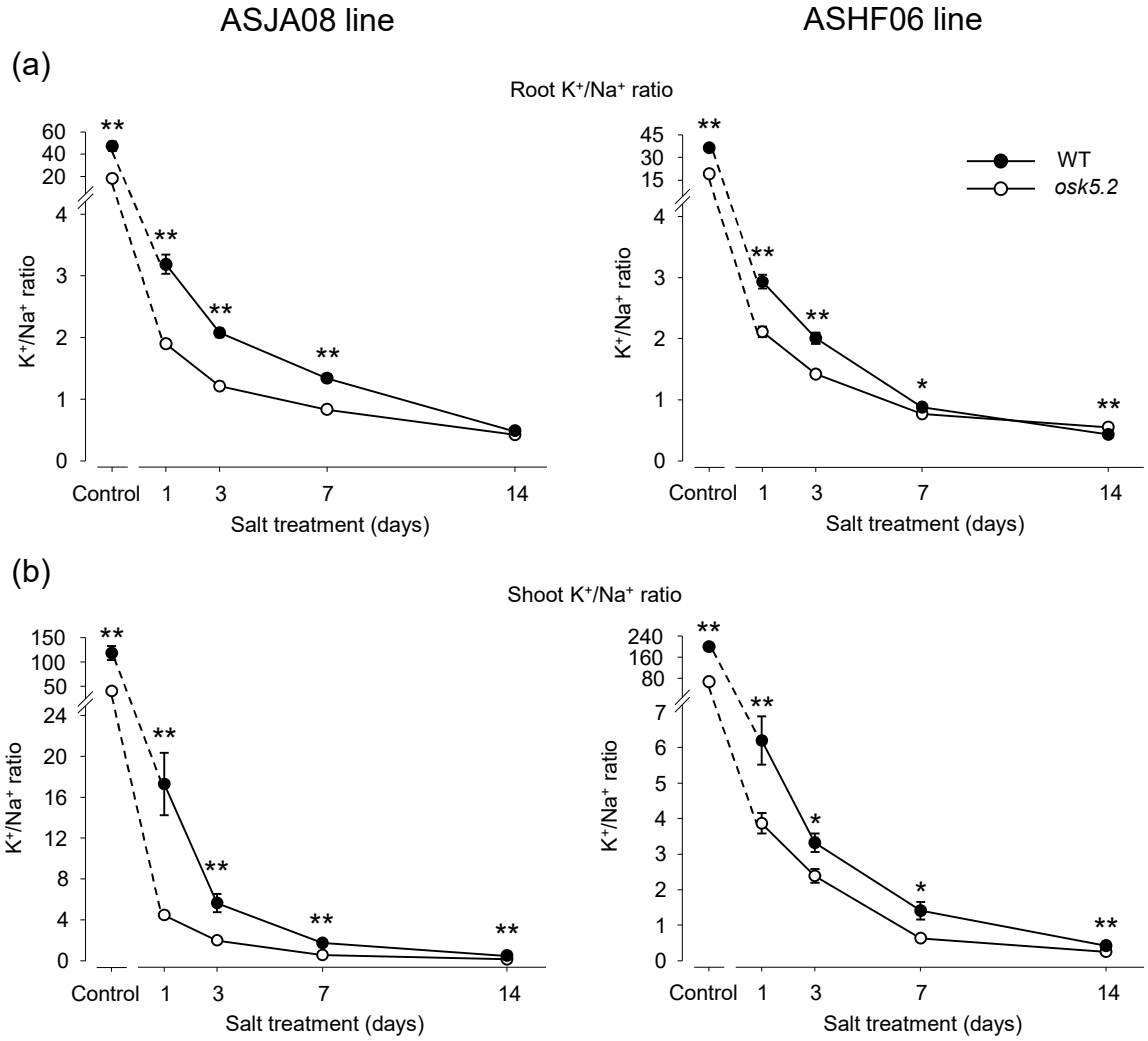

FIGURE 7 Root and shoot K^+/Na^+ content ratio in wild-type and *osk5.2* mutant plants under control and salt treatment conditions. Same experiment as in Figures 5 and 6. K^+/Na^+ content ratio: K^+ content from Figure 5 divided by the corresponding Na^+ content from Figure 6. (a) and (b): K^+/Na^+ content ratio in roots and shoots. Left and right panels: *osk5.2* mutant plants (○) and corresponding wild-type plants (●) issued from ASJA08 (left) or ASHF06 (right) lines. Means ± SE; n = 9 under salt treatment after 1, 3, 7 and 14 days, and n = 12 under control conditions. Single and double stars denote statistically significant differences between the wild-type and *osk5.2* mutant plants (Student's t test, $P \leq 0.05$ and $P \leq 0.01$, respectively).

mutant and WT plants were weaker at the last time point of salt treatment (after 14 days), and the differences were no longer statistically significant (except for the roots of one mutant line). At this time, Na^+ levels in shoots exceeded those in roots in all genotypes (Figure 6a, b). Thus, Na^+ accumulation was higher in *osk5.2* mutant plants than in the corresponding WT plants until the late stage of Na^+ plant invasion, when the level of Na^+ in shoots had become higher than that in roots.

K^+/Na^+ content ratios were calculated from the data displayed by Figures 5 and 6. The ratios were significantly lower in *osk5.2* mutant plants than in WT plants both in shoots and roots under all conditions except in roots of one mutant line at the last time point of salt treatment (Figure 7). In salt-stressed leaves, the relative reduction in K^+/Na^+ content ratios observed in the *osk5.2* mutant plants as compared with the corresponding WT plants, was in the range of 35-70% (Figure 7). Thus, *OsK5.2* lack of functional expression strongly impaired K^+/Na^+ homeostasis in leaves under salt stress.

4 | DISCUSSION

4.1 | OsK5.2, a model for analyzing K^+ channel-mediated control of K^+ and Na^+ translocation to the shoots under salt stress

Mechanisms that control long distance transport of Na^+ and K^+ in the plant vasculature contribute to maintaining the shoot K^+/Na^+ content ratio at a high value, which is a key determinant of salt tolerance (Munns and Tester, 2008; Maathuis, Ahmad and Patishtan, 2014; Ismail and Horie, 2017; Wu, Zhang, Giraldo and Shabala, 2018). In rice, as well as in Arabidopsis and various other species, clear evidence has been obtained that Na^+ transporters belonging to the HKT family are involved in desalinization of the ascending xylem sap (Hauser & Horie, 2010). The H^+/Na^+ antiport system SOS1 has been suggested to also contribute to this function when the concentration of Na^+ in the xylem sap reaches very high values (Maathuis et al., 2014). Regarding the mechanisms controlling K^+ translocation to shoots, outwardly rectifying channels belonging to the Shaker family, among which SKOR in Arabidopsis and OsK5.2 in rice, have been shown to mediate K^+ secretion into the xylem sap under normal conditions (Gaymard et al., 1998; Nguyen et al., 2017) but their contribution to this function under salt stress remains poorly documented. It should be noted that K^+ secretion into the xylem sap may have to be active, under some environmental conditions (Wu, Zhang, Giraldo and Shabala, 2018), which would exclude channel-mediated (passive) contribution to

this function in such conditions. Active H^+-coupled K^+ transports mediated by HAK/KUP/KT transporters (see below) or involving a NRT1/PTR family member, NRT1;5 (Li et al., 2017), have been shown to contribute to K^+ translocation towards the shoots. In rice, OsHAK1 and OsHAK5, which are thought to be endowed with H^+-K^+ symport activity (Véry et al., 2014), have been shown to play a role in K^+ translocation towards the shoots under saline conditions (Chen et al., 2015; Yang et al., 2014). The mechanisms that underlie these contributions remain however to be specified. H^+-K^+ symport activity in parenchyma cells bordering the xylem vessels would result in K^+ retrieval from the xylem sap since the pH gradient between the sap and the cytoplasm is inwardly directed and thus favors K^+ influx into the cells. It has thus been hypothesized that such H^+-K^+ symporters may allow K^+ acquisition within the stele by parenchyma cells, and that this would result in a higher concentration of K^+ in xylem-adjacent cells, and thus in an outwardly-directed K^+ electrochemical gradient that would allow SKOR-like K^+ channels to release K^+ into the sap (Yang et al., 2014). At the leaf surface, control of stomatal aperture provides another type of contribution to salt tolerance. Exposure to saline conditions rapidly results in stomatal closure, which limits the flux of xylem sap, and thus the rate of Na^+ translocation to shoots (Fricke et al., 2006; Huang et al., 2009; Hedrich and Shabala, 2018). Such a control is however likely to also affect the rate of K^+ translocation to shoots, and thus its contribution to shoot K^+/Na^+ homeostasis should benefit from mechanisms allowing to counteract the depressive effect of the reduction in volumetric flow of xylem sap on K^+ translocation.

OsK5.2, which belongs to Shaker channel subfamily 5 (outwardly rectifying Shaker channels) like its two counterparts in Arabidopsis SKOR and GORK (Véry et al., 2014), is expressed in both stomata and vascular tissues (Nguyen et al., 2017). Previous analyses have shown that OsK5.2 is involved both in xylem sap K^+ loading, as SKOR in Arabidopsis (Gaymard et al., 1998), and in guard cell K^+ release-mediated stomatal closure, as GORK (Hosy et al., 2003). The roles of SKOR and GORK in Arabidopsis salt tolerance remain poorly documented. The expression level of *OsK5.2* is fairly maintained in roots under saline conditions, and even increased in shoots in these conditions (Figure 2). This channel has thus been used as a model in the present report to investigate xylem sap K^+ loading under salt stress, *i.e.*, whether it can be channel mediated or requires active transport systems, and the involvement of stomatal aperture control in salt tolerance.

4.2 | K^+ Secretion into the xylem sap under salt stress

Saline conditions weakly affected the expression level of *OsK5.2* in roots (Figure 2a), as shown for its counterpart *SKOR* in Arabidopsis roots (Pilot et al., 2003). In line with this rather stable expression, the contribution of OsK5.2 to K^+ secretion into the xylem sap (estimated from the difference in sap concentration between the WT and *osk5.2* mutant plants; Figure 4a) did not appear to be much modified by the salt treatment. This contribution even tended to slightly increase during the first week of the treatment, which may be due to increased driving force for K^+ secretion under conditions of salt-induced membrane depolarization (Jayakannan et al., 2013; Mian et al., 2011).

Reliable measurements of both the membrane potential and the apoplastic K^+ concentration of stelar cells are difficult to obtain. However, the fact that OsK5.2 can contribute to K^+ secretion under salt stress provides definitive evidence that passive (since channel-mediated) secretion of K^+ can occur in stelar cells of rice plants facing saline conditions. This conclusion, which does not exclude a contribution of active K^+ transport mechanisms to K^+ secretion under saline conditions, also means that other channels besides OsK5.2, either K^+-selective and belonging to the Shaker family (Véry et al., 2014) or poorly K^+-selective like NSCC channels identified in stelar cells by patch clamp experiments (Wegner & de Boer, 1997), could also contribute to K^+ secretion into xylem sap under such conditions.

4.3 | Reduction of the volumetric flux of xylem sap under salt stress

Exposure to saline conditions is known to rapidly result in reduced stomatal aperture and plant transpiration (Fricke et al., 2006; Hedrich & Shabala, 2018; Robinson, Véry, Sanders, & Mansfield, 1997). In the present study, the transpiration rate was similarly reduced in WT and *osk5.2* mutant plants at the end of the salt treatment, by about 50% under light conditions and 30% under dark conditions (Figure 3). The kinetics of the reduction in transpiration rate was however more rapid in WT than in *osk5.2* mutant plants.

Upon an increase in external medium salinity, abscisic acid (ABA) produced in response to the resulting osmotic stress is rapidly directed to guard cells, where it is expected to activate the PYR/PYL/RCAR-ABI1 PP2C phosphatase-OST1 SnRK kinase signaling pathway, leading to guard cell anion channel activation and stomatal closure (Hedrich & Shabala, 2018). The actual contribution of guard cell anion channels to the triggering of

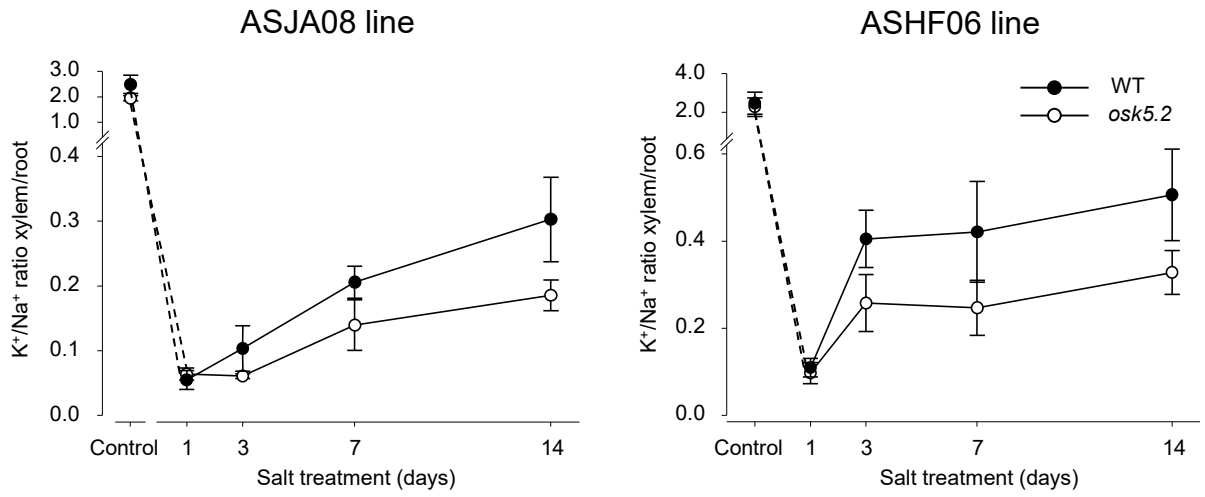

Figure S2 The ionic composition of the xylem sap does not reflect the K^+ and Na^+ relative contents of the roots. Plants were subjected to a saline treatments (50 mM NaCl for 2 weeks; x axis). Y axis: xylem sap K^+/Na^+ concentration ratio (data from Figure 4c) reported to the root K^+/Na^+ content ratio (data from Figure 7a). Left and right panels: *osk5.2* mutant plants (○) and corresponding wild-type plants (●) issued from ASJA08 (left) or ASHF06 (right) lines. Means ± SE; n = 9 under salt treatment after 1, 3, 7 and 14 days, and n = 12 under control conditions. See legends to Figures 4 and 7.

stomatal closure upon salt stress has however been little investigated so far. Likewise, the role in stomatal closure upon salt stress of the K^+ outward channels acting as downstream effectors (Pandey et al., 2007; Schroeder et al., 2001) was still poorly documented. Indeed, although extensive analyses have concerned the integrated involvement of transport systems in regulation of guard cell turgor (Jezek & Blatt, 2017), little information is related to high salinity conditions (Lebaudy et al., 2008; Thiel & Blatt, 1991; Véry, Robinson, Mansfield, & Sanders, 1998). Here, our data reveal the important role of outward K^+ channel activity in control of stomatal aperture upon salt stress. The whole plant transpiration data (Figure 3) indeed indicate that OsK5.2 activity in stomata contributed to the reduction in stomatal aperture observed over the entire duration of the salt treatment. Furthermore, our data indicate that this activity is of particular importance at the onset of salt stress by allowing a more rapid reduction of stomatal aperture (Figure 3).

4.4 | Na^+ and K^+ translocation to shoots by the xylem sap and K^+/Na^+ shoot homeostasis

An apoplastic pathway strongly contributing to Na^+ entry into the root and radial migration to the root vasculature (the so-called bypass flow across the root to the xylem) has been evidenced in rice in the presence of high Na^+ concentrations (Faiyue, Al-Azzawi, & Flowers, 2012; Flam-Shephered et al., 2018; Yeo, 1998). In our experimental conditions, the concentration of Na^+ in the xylem sap in both WT and *osk5.2* mutant plants was quite similar to that in the hydroponic medium (50 mM) (Figure 4). Also, the xylem sap K^+/Na^+ concentration ratio decreased very rapidly down to values lower than 0.1 after one day of salt treatment, and was then more than 10 times lower than the K^+/Na^+ root content ratio (Figure S2). This indicates that the former ratio (in the xylem sap) was not likely to reflect the corresponding ratio in the root symplasm. Altogether, these results support the hypothesis that the bypass flow of Na^+ was the major determinant of the migration of this cation towards the xylem vasculature. In such conditions, the flux of Na^+ translocated to the shoot becomes proportional to the volumetric flow of xylem sap. Since the Na^+ concentration of the xylem sap was similar in the mutant and WT plants, the larger rate of transpiration under salt stress in the mutant plants due to impaired control of stomatal aperture (Figure 3) is the major determinant of the difference in Na^+ translocation rate between the two types of plants (Figure S1b). Thus, OsK5.2-dependent control of stomatal aperture results in a reduction of Na^+ translocation towards the shoots.

A reduction in the volumetric flow of xylem sap is however likely to impact the rate of K^+ translocation to shoots (Figure S1a). Because OsK5.2 contributes to K^+ secretion into the xylem sap, besides its involvement in stomatal aperture control, the reduction in the rate of K^+ translocation to shoots induced by the salt treatment is more reduced in WT than in osk5.2 mutant plants. In other words, although OsK5.2 activity in stomata has a negative effect on K^+ translocation to shoots by decreasing the transpiration rate (Figure 3), the contribution of OsK5.2 to K^+ loading into the xylem sap (Figure 4a) outperforms the "negative" effect resulting from reduced xylem volumetric flow (Figure S1a). This conclusion supports the hypothesis that the beneficial effect, in terms of control of Na^+ translocation to shoots and tolerance to salinity, of the reduction in stomatal aperture upon salt stress is likely to integrate the plant ability to increase, or at least maintain, the rate of K^+ secretion into the xylem sap.

Due to the beneficial effects of the overall OsK5.2 activity, the ratio of the K^+ to Na^+ translocation rates towards the shoots (identical to the xylem sap K^+/Na^+ concentration ratio; Figure 4c) is larger in WT than in *osk5.2* mutant plants. This is probably the main reason why the kinetics of the decrease in shoot K^+/Na^+ content ratio is slower in WT than in mutant plants (Figure 7b), and why the overall activity of OsK5.2 contributes to salt tolerance (Figure 1).

4.5 | Contribution of a K^+ channel to plant salt tolerance

Salt stress, not only strongly increasing shoot Na^+ content, but generally also leads to severe K^+ deficiency (Hauser & Horie, 2010; Marschner, 2011). Since ensuring efficient root K^+ uptake from soil appears as the primary way to ensure shoot K^+ feeding, most studies aiming at identifying salt tolerance determinants among K^+ transport systems have focused on root uptake systems. Exposure to high salinity can substantially depolarize root periphery cells and make passive K^+ uptake through inwardly rectifying K^+ channels thermodynamically impossible (Rubio et al., 2020). High-affinity HAK/KUP/KT transporters, expected to rely on pH gradients created by the H^+-ATPase pump to energize inward K^+ fluxes through H^+-K^+ symport mechanism, are therefore considered as the main K^+ transport systems taking part in root K^+ uptake under high saline conditions. Several HAK transporters have been shown to be involved in root K^+ uptake and thereby to contribute to plant salt tolerance: AtHAK5 in Arabidopsis (Nieves-Cordones et al., 2010), and OsHAK1, OsHAK5, OsHAK16 and OsHAK21 in rice (Chen et al., 2015; Feng et al., 2019; Shen et al., 2015; Yang et al., 2014).

KO mutations in these different genes have been shown to result in reduced K^+ uptake and root K^+ content, and probably as a consequence, also in reduced K^+ translocation to shoots and often reduced shoot K^+ contents. Such defects could be observed upon salt stress but also in absence of saline treatment, and resulted in reduced plant growth in all conditions (Chen et al., 2015; Feng et al., 2019; Nieves-Cordones et al., 2010; Shen et al., 2015; Yang et al., 2014), Increased plant Na^+ uptake was noted in some mutants (Shen et al., 2015), which could originate from higher root cell polarization (Nieves-Cordones et al., 2017). Also supporting the importance of HAK-mediated plant K^+ uptake in salt tolerance, transcript level variations in the *OsHAK1* gene between rice subspecies have been found to underlie the difference in their salt tolerance (Chen et al., 2015).

It is also well known that transport systems from the H^+/cation antiporter families, involved in K^+ and Na^+ intracellular compartmentalization, are major contributors to salt tolerance (van Zelm et al., 2020) through their roles in Na^+ compartmentalization and turgor regulation, but also through indirect contributions to K^+ homeostasis. For instance, increased activity (due to overexpression in transgenic plants) of the antiporter AtNHX1 from Arabidopsis or LeNHX2 from tomato has been shown to result in improved root K^+ uptake and higher K^+ contents in all tissues. Such effects, which are beneficial to salt tolerance, have been proposed to result from a decrease in cytosolic K^+ concentration that these transport systems would generate, by compartmentalizing K^+, which would lead to increased expression and/or activity of high affinity K^+ transporters involved in root K^+ uptake (Leidi et al., 2010; Huertas et al., 2013). Altogether, these studies provide evidence of strong interactions between K^+ uptake, compartmentalization and translocation to shoots.

Other K^+ transport-mediated mechanisms of plant salt tolerance and in particular mechanisms involving K^+ channels, were reported but have not yet been deciphered. Transcriptional regulation of a few K^+ channel genes, especially the strong up-regulation of the inward Shaker regulatory subunit *AtKC1* in leaves (Pilot et al., 2003), suggests a role of inward K^+ channels in salt tolerance, which has not been determined so far. Here, we showed that KO mutation in the outward Shaker K^+ channel gene *OsK5.2* leads to increased salt sensitivity. Lack of *OsK5.2* functional expression was found to result in impaired growth in plants subjected to saline conditions but not in plants grown in standard conditions (Figure 1), in contrast to what has been reported in KO mutant plants impaired in root K^+ uptake, which mostly showed growth defects even in absence of salt stress (see above). OsK5.2 is involved

in control of stomatal aperture and in K^+ secretion into the xylem sap, and these two functions together underlie its contribution to salt tolerance. It is also worth to note that lack of OsK5.2 activity results also in impaired root K^+ uptake under saline conditions since plant growth and root and shoot K^+ contents were lower in *osk5.2* mutant plants compared with the corresponding WT plants (Figure 1 and Figure 5). Together with the defects in K^+ translocation to shoots under salt stress that have been reported in mutant plants impaired in root K^+ uptake or in K^+ intracellular compartmentalization (see above), the reduction in K^+ uptake resulting from lack of OsK5.2 channel activity provides evidence that the three functions, uptake, compartmentalization and translocation, are especially intensively coordinated under saline conditions. In conclusion, the present results highlight K^+-channel-mediated mechanisms of salt tolerance, and provide a new possible target for plant breeders towards the improvement of tolerance to salt stress in rice.

CONFLICT OF INTEREST

The authors declare no competing interests

AUTHOR CONTRIBUTIONS

A.-A.V., H.S., T.H.N. and J.Z. conceived the original research plans; A.-A.V., and D.T.L. supervised the experiments; T.H.N. and J.Z. performed the experiments. A.-A.V., H.S., T.H.N. and J.Z. analyzed the data; A.-A.V., H.S. and J.Z. wrote the first draft of the manuscript. All authors contributed to the article and approved the submitted version.

Chapter IV

K^+ unloading from phloem sap mediated by the OsK5.2 outward K^+ channel strongly determines shoot K^+ nutrition

IV.1 Introduction

Breeding high yield and quality rice largely relies on the supply of N, P, and K (Dobermann & White, 1999). Developing leaves and roots, flowers, and seeds, serve as sink organs for carbohydrates and mineral nutrients for their growth. K^+, the most abundant mineral cation in plants, after its acquisition by roots, uses the whole-plant vasculature, ascending xylem and phloem saps for long distance transport to feed developing tissues. Xylem basically transports K^+ from roots to shoots, while K^+ transport in phloem, in addition to feeding sinks with K^+, plays a role in building the osmotic gradient which drives the translocation of photoassimilates from the sites of synthesis in leaves to the sites of utilization in sink organs (Lang, 1983; Mengel & Haeder, 1977; Patrick, 1997). Big amounts of K^+ recirculate from mature or senescent leaves to sink organs via the phloem. During reproductive stage, this is an important function of senescence in relation to seed quality and crop productivity (Wolf, Munns, Tonnet, & Jeschke, 1991; Yu, Lo, & Ho, 2015).

While the molecular mechanisms of K^+ uptake by the roots have been extensively characterized (Epstein, 1976; Nieves-Cordones, Alemán, Martínez, & Rubio, 2014), less is known concerning those controlling long-distance K^+ transport. Xylem vascular tissue is formed by thick-walled dead cells surrounded by xylem parenchyma and pericycle. K^+ loading to the xylem sap requires a step of secretion through cell membrane within the root stele. The activity of different types of transport systems has been shown through reverse genetics to contribute to the control of K^+ concentration in the xylem sap and K^+ feeding of the shoots (Gaymard et al., 1998; Yang et al., 2014; Han et al., 2016; Li et al., 2017). The precise mechanism by which these systems contribute to these functions was in most cases, not determined. However, reverse genetics analyses coupled to root pericycle and xylem parenchyma cell localization for the outward K^+ channel SKOR in Arabidopsis, allowed to highlight the important contribution of this channel to secretion function from these tissues for loading the xylem sap with K^+ (Gaymard et al., 1998). In xylem parenchyma cells, activity of other K^+-permeable outward channel type has been described at the plasma membrane (Wegner & de Boer, 1997), but its contribution to K^+ transport in the xylem was not quantified by reverse genetics. In addition to the secretion from pericycle and xylem parenchyma, unloading from the phloem sap is also known to feed the xylem sap with K^+. The mechanism of K^+ unloading from the phloem for recirculation in the xylem has been little

addressed at the molecular level. Phloem vascular tissue is composed of living cells (sieve elements) which lacks most of their organelles including nucleus, in tight association with companion cells connected through plasmodesmata to form the so-called sieve element-companion cell (SE-CC) complex (Williams, Lemoine, & Sauer, 2000). Membrane transport mechanisms are required for both loading K^+ to the phloem sap and unloading K^+. The Shaker channel AKT2, owing to the weak rectification of the currents that it mediates, was hypothesized to contribute to both phloem sap K^+ loading and release (Lacombe et al., 2000). AKT2-mediated inward and outward K^+ fluxes were evidenced through reverse genetics analyses to control the phloem cell membrane electric polarization and through this, sugar loading to the phloem sap, but were not involved in the control of phloem sap K^+ concentration (Deeken et al., 2002; Gajdanowicz et al., 2011). Thus, AKT2 was not likely the major contributor to the phloem sap K^+ loading and unloading for source to sink K^+ transfer. Basically, K^+ transport mechanisms in phloem are still poorly understood, although their uncovering is considered to be an important issue for achieving the sustainability of crop production. At last, beside direct sap K^+ loading and unloading mechanisms to control K^+ transport through the vasculature, the level of transpiration also impacts the translocation of K^+ in the xylem and beyond, the rate of the whole K^+ circulation. Therefore, guard cell inward and outward K^+ channels involved in the control of stomatal movements (Roelfsema & Hedrich, 2005; Lebaudy et al., 2008b) can also be considered to indirectly contribute to the long-distance K^+ transport.

Activities of SKOR-like outwardly rectifying channels from varying plant species at the root stele cell membrane or in the *Xenopus* oocyte expression system, have been characterized (Roberts & Tester, 1995; Wegner & de Boer, 1997; Véry et al., 2014; Huang et al., 2018; Villette, Cuéllar, Zimmermann, Verdeil, & Gaillard, 2019). At the physiological level, little information was obtained on these SKOR homologues. The rice OsK5.2 channel was shown, like SKOR, to strongly contribute to K^+ secretion to the xylem sap and K^+ feeding of the shoots (Nguyen et al., 2017; Chapter 3), but the cellular mechanism by which it controls the xylem sap K^+ loading was not precisely analyzed. The fact that OsK5.2 is also active in the stomatal complex (conversely to SKOR) suggested that the contribution of OsK5.2 to long-distance K^+ transport was not fully that of SKOR, and this prompted us to further analyze OsK5.2 role in the whole plant K^+ transport. In this chapter, a more precise tissue localization of *OsK5.2* expression within the vasculature was performed. This new

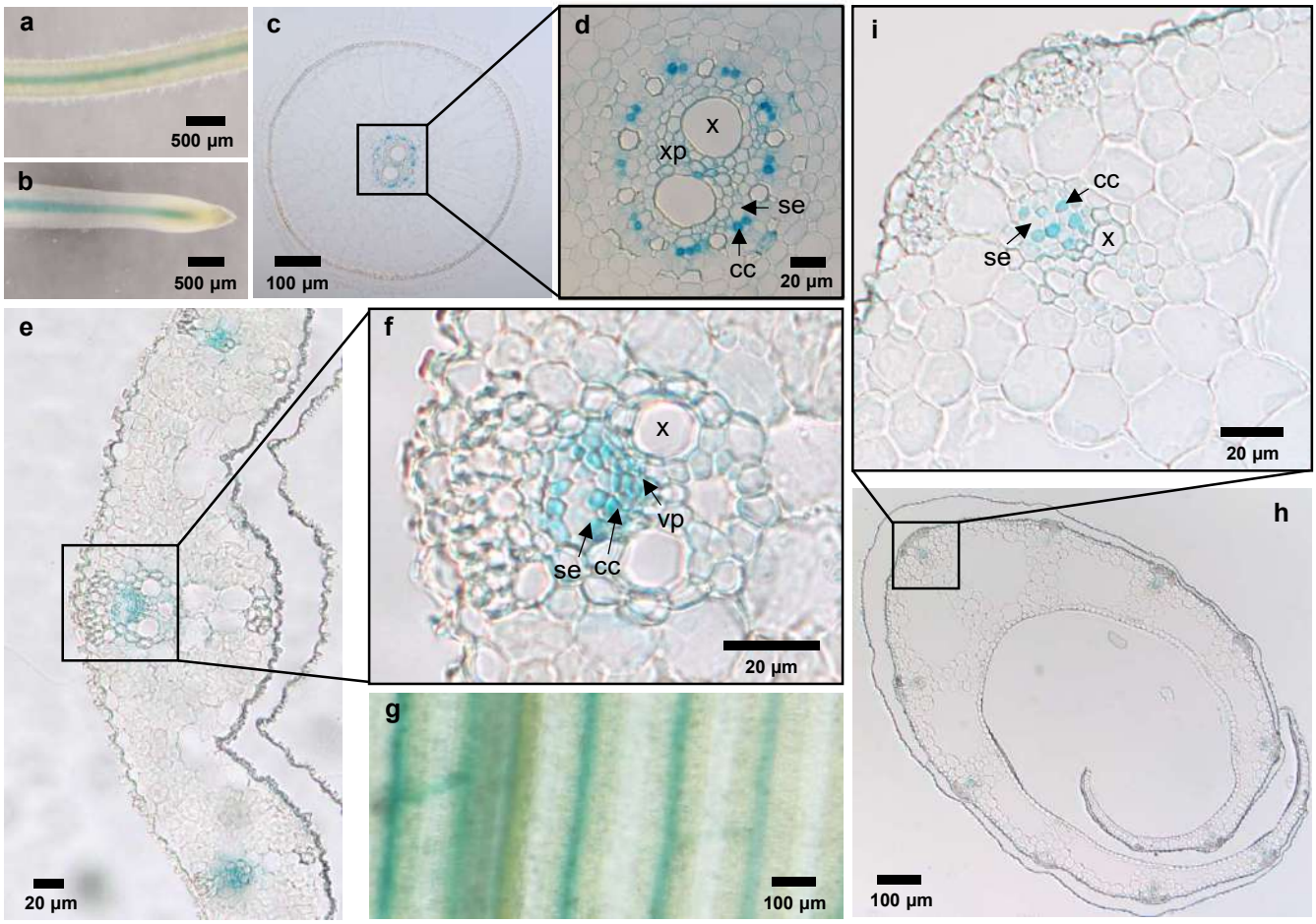

Figure IV.1 Localization of *OsK5.2* promoter activity in 3-week-old transgenic rice plants expressing *pOsK5.2*::*GUS*. GUS activity was detected in root (a, crown root; b, root tip) and leaf (g) of rice hydroponically grown in standard Yoshida medium. (c), cross-section of root. (d), enlarged stele of root. (e), cross-section of leaf blade. (f), enlarged vascular bundle of leaf blade. (h), cross-section of leaf sheath. (i), enlarged vascular bundle of leaf sheath. cc, companion cells; se, sieve elements; x, xylem; xp, xylem parenchyma; vp, vascular parenchyma.

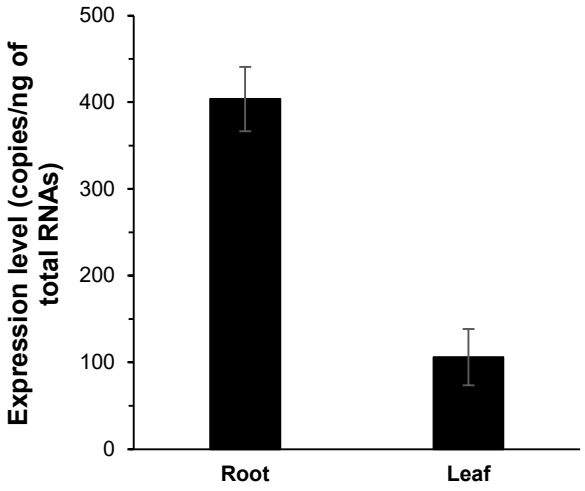

Figure IV.2 Expression level of *OsK5.2* in root and leaf of 5-week-old Nipponbare plants by real-time quantitative PCR on total RNAs. Data are presented as means ± SE of $n = 4$ biological replicates.

information was coupled with experiments aiming at distinguishing in the K^+ secreted into xylem sap, that originating from the K^+ taken up by the roots and that originating from the K^+ unloaded from the phloem sap in the roots, and at determining the possible contribution of OsK5.2 to both secretion mechanisms, using Rb^+ as a tracer of K^+ circulation in the whole plant. Different regimes of plant transpiration were applied.

IV.2 Results

IV.2.1 *OsK5.2* is particularly expressed in phloem tissues of sink organs

GUS activity analysis in transgenic rice plants expressing the *OsK5.2* promoter::*GUS* construct (*pOsK5.2*::*GUS*) had localized *OsK5.2* expression in particular in vascular tissues of both roots and leaves (Nguyen et al., 2017). We further completed the expression pattern of *OsK5.2* in vascular tissues of roots, leaves, and leaf sheaths. GUS staining of cross-sections of roots, leaves, and leaf sheaths revealed the localization of *OsK5.2* promoter activity especially in the phloem tissues (Figure IV.1). In roots, GUS activity was absent at the root tip and present in vasculature (Figure IV.1 a, b). In the cross-section of roots, GUS activity was detected in phloem companion cells and xylem parenchyma (Figure IV.1 c, d). In leaves, GUS activity in the vasculature was detected in all main veins and commissural veins (Figure IV.1 g). Leaf cross-sectional analysis detected GUS activity in phloem companion cells and vascular parenchyma (Figure IV.1 e, f). In cross-sections of leaf sheaths, GUS activity was specifically detected in phloem companion cells (Figure IV.1 i, h).

qRT-PCR analysis showed that the expression of *OsK5.2* was detected in both root and leaf, but that the transcripts of *OsK5.2* were more abundant in root than in leaf of 5-week-old plants, by 4-fold, at vegetative stage (Figure IV.2). Similarly, a previous report indicates that the expression of *OsK5.2* (*Os06g14030*, named *OsGORK*) was about 1.7-fold higher in roots than in shoots of 2-week-old rice seedings (Kim et al., 2015). Furthermore, the expression of *OsK5.2* at reproductive stage was mentioned to be high in flower, and relatively low in leaf blade, leaf sheath, node, tiller, and root (Kim et al., 2015). The results of GUS staining and qRT-PCR analysis thus suggest that *OsK5.2* is particularly expressed in phloem tissues of sink organs in the life cycle of rice plants.

IV.2.2 Reduced K^+ concentration in the phloem sap of *osk5.2* plants in addition to that in

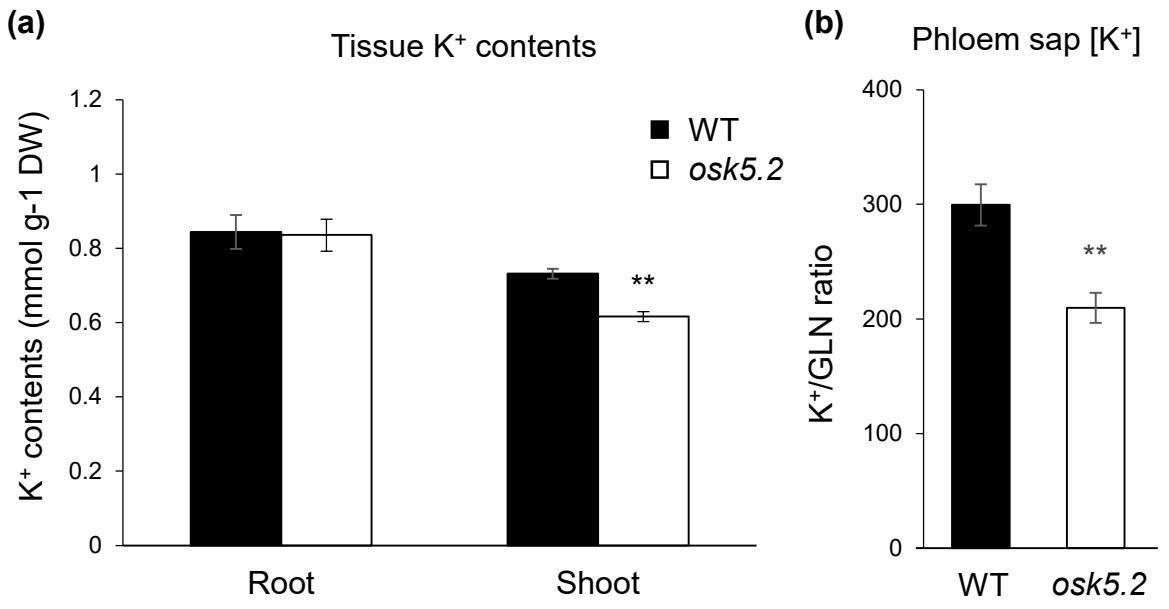

Figure IV.3 Tissue K^+ contents (a) and phloem sap K^+ concentrations (b) in wild-type and *osk5.2* mutant plants. Assayed roots, shoots and phloem sap samples were collected from 5-week-old wild-type and *osk5.2* mutant plants hydroponically grown in standard Yoshida medium. Black bars, wild-type plants; white bars, *osk5.2* plants. Data are presented as means ± SE (n = 48 biological replicates for phloem sap [K^+], and n = 22 biological replicates for tissue K^+ contents, merged from ASJA08 and ASHF06 lines for both wild type and *osk5.2* plants). Single and double stars denote statistically significant differences between the wild-type and *osk5.2* mutant plants at $P \leq 0.05$ and $P \leq 0.01$, respectively (Student's t test).

the xylem sap and leaf tissues

Following observation that *OsK5.2* is expressed in phloem tissues, the role of OsK5.2 in the phloem was first investigated by analyzing the phloem sap in WT and *osk5.2* mutant plants. Mature leaf blades were used, and in order to prevent sealing of the phloem sieve tubes by the cut, EDTA solution was applied to facilitate continued phloem sap flow (King & Zeevaart, 1974). K^+ concentrations (presented as the relative K^+ to glutamine ratio) (Berthomieu et al., 2003; Ren et al., 2005) were assayed in phloem sap of 5-week-old plants hydroponically grown on standard Yoshida medium. The amounts of glutamine in the EDTA solution varied from 0.4 to 3.6 µmol (mean value 1.3 ± 0.1 µmol, *n*=48) for WT plants, and from 0.4 to 7 µmol (mean value 1.3 ± 0.2 µmol, *n*=48) for *osk5.2* mutant plants. K^+ concentrations were significantly reduced in the phloem sap of *osk5.2* mutant plants as compared with that of WT plants, by about 30% in both ASJA08 and ASHF06 lines (Figure IV.3 b). We confirmed in this batch of plants the previously observed lower K^+ content of leaf tissues (Figure IV.3 a; Nguyen et al., 2017; Chapter 3). Thus, *OsK5.2* loss-of-function was identified to lead to both a defect in xylem sap K^+ concentration (Chapter 3; Nguyen et al., 2017), a defect in leaf K^+ content, and a defect in phloem sap K^+ concentration. Therefore, the K^+ defect in *osk5.2* mutant plants appeared to concern the whole loop of K^+ circulation between roots and shoots, and it became not so clear what was the precise role of OsK5.2 channel and the origin of the defect. Indeed, the reduced K^+ concentrations in phloem sap could be ascribed to the involvement of OsK5.2 in phloem K^+ transport but also caused by the decreased K^+ contents in shoots itself due to the decrease in xylem sap K^+ concentration. Also, the decrease in xylem sap K^+ concentration may be due to the lower phloem sap K^+ concentration, and thereby a reduced unloading of K^+ from phloem for recirculation in the xylem.

IV.2.3 Using Rb^+ to trace K^+ circulation in the plant and assess OsK5.2 functions

Since *OsK5.2* is mostly expressed in the root, we first focused on this organ to complete the analysis of OsK5.2 functions. *OsK5.2* being expressed in both xylem parenchyma and phloem companion cells in root, it could play a role in xylem sap K^+ loading in two distinct ways: (1) be involved in “direct” secretion to the xylem sap of K^+ arriving symplastically to xylem parenchyma cells from the root uptake flow, and (2) be involved in K^+ unloading from the

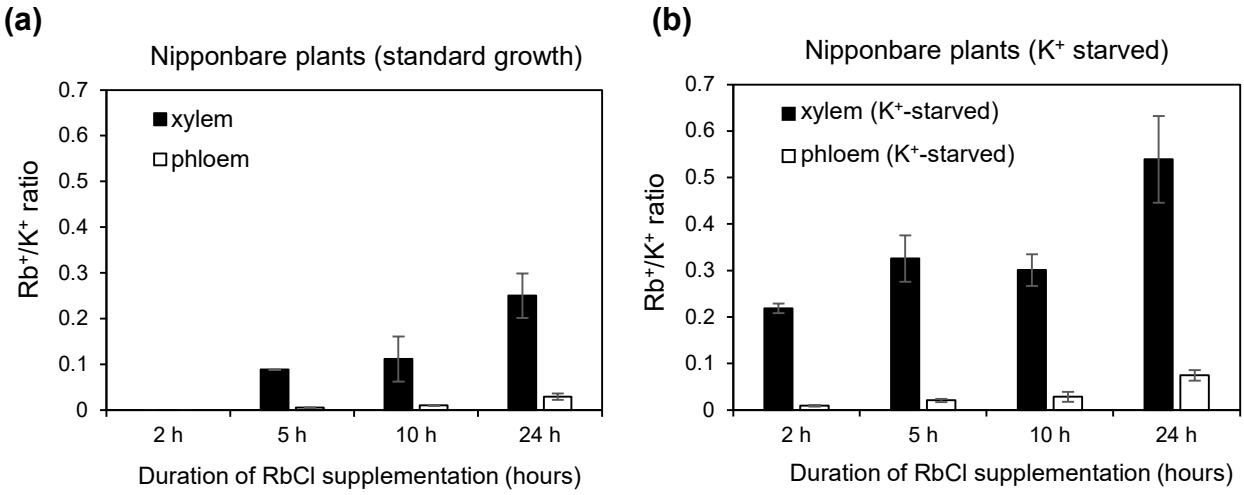

Figure IV.4 Rb^+/K^+ ratio in xylem and phloem saps of Nipponbare plants at varying times after 1.5 mM RbCl supplementation. Nipponbare plants were hydroponically grown in complete Yoshida medium containing 1.5 mM K^+ under standard growth condition for 5 weeks. (a) 5-week-old Nipponbare plants were transferred in K^+-free Yoshida medium supplemented with 1.5 mM RbCl for 2 to 24 hours. (b) 5-week-old Nipponbare plants were treated with K^+-starved Yoshida medium containing 0.2 mM K^+ for 4 days, then transferred in K^+-free Yoshida medium supplemented with 1.5 mM RbCl for 2 to 24 hours. Data are presented as means (± SE) of 4 biological replicates. Black bars, Rb^+/K^+ ratio in xylem sap; white bars, Rb^+/K^+ ratio in phloem sap.

phloem sap, this released K^+ being able to recirculate in the xylem (Wegner & de Boer, 1997). In order to discriminate these two roles, we opted for setting up a series of K^+ tracer experiments using the K^+ analog Rb^+.

At first, kinetics of Rb^+ arrival to xylem and phloem saps after RbCl supplementation in the plant growth medium were carried out, in order to identify appropriate times for our experiments: *i.e.* (1) Rb^+ substantially arrived to the xylem sap to be able to be reliably detected, but not significantly arrived to the phloem sap, in order to analyze secretion from root uptake flow only; (2) Rb^+ sufficiently arrived to the phloem sap for reliable assay. These preliminary experiments were performed on wild type rice cv Nipponbare plants. Rb^+ and K^+ concentrations in the xylem and phloem saps were determined at different time-points ranging from 2 h to 24 h after RbCl supplementation. Rb^+ to K^+ ratios in both xylem and phloem saps provided a mean to estimate to which extent Rb^+ was secreted to the sap and had recirculated within the plant. The experiments were performed on plants grown in two different conditions: one analysis concerned 5-week-old plants grown in standard conditions; the other one concerned plants of the same age, initially grown in standard condition, but transferred for their last 4 days of growth in low K^+ conditions (K^+ concentration in the growth medium reduced to 0.2 mM), K^+-starved conditions being expected to stimulate root Rb^+ uptake through HAK transporters known to weakly discriminate between K^+ and Rb^+ (Véry et al., 2014). In both standard and low K^+-treated plants, 1.5 mM Rb^+ replaced K^+ in the growth medium at start of the K^+ tracer experiment.

In plants grown in standard conditions, Rb^+ was not detected in the xylem sap 2 hours after its addition to the external medium. It started to be detected from 5 hours after its addition (Figure IV.4 a). At that time, Rb^+ concentration in the xylem sap represented 9% of K^+ one. In the phloem sap, Rb^+ was also detected at that time, but its concentration represented only 0.5% of K^+ one (Figure IV.4 a). Thus, at 5 hours after Rb^+ addition to the external medium, Rb^+ in the xylem sap would originate mostly from the external flow (*i.e.* at least at 94%) and very little from recirculation from the phloem (*i.e.* at most at 6%). It should be noted that the value of 94% of Rb^+ in the xylem sap from external flow origin is a low estimate determined with the hypothesis that 100% of Rb^+ in phloem sap recirculated in the xylem. After longer plant exposure to Rb^+, Rb^+/K^+ in xylem sap and phloem sap gradually increased as expected. At 24 hours after Rb^+ addition to the external medium, Rb^+ concentration had reached 25% of K^+ one in the xylem sap, and 3% of K^+ one in the phloem

sap (Figure IV.4 a). Although the proportion of Rb^+ which could recirculate in the xylem sap had increased, this remained quite low, with at least 88% of Rb^+ in the xylem sap still originating from direct secretion from external flow.

In plants in K^+ shortage prior to Rb^+ addition, Rb^+ arrival to the xylem sap and phloem sap were detected at earlier time as expected. At 2 hours after Rb^+ addition to the external medium, Rb^+ concentration represented already 22% of K^+ one in the xylem sap, and 1% of K^+ one in the phloem sap (Figure IV.4 b). Calculation indicated that Rb^+ in the xylem sap that originated from the external flow was at least of 96%. At 5 hours after Rb^+ addition, Rb^+ in the xylem sap that originated from the external flow had only slightly decreased to 94%, and at 24 hours, to 86 % (Figure IV.4 b).

Finally, these results suggested that sampling at 5 hours after RbCl supplementation would be appropriate for obtaining xylem sap Rb^+ concentrations almost exclusively originating from the external ion flow, for plants grown both in standard conditions or K^+ shortage. This duration of RbCl treatment was fixed for subsequent xylem sap analyses. In addition, these experiments indicated that even after 24 hours of Rb^+ addition, due to the high K^+ concentration in the phloem sap, the amount of Rb^+ that recirculated in the xylem from the phloem was still low. Thus, analysis of Rb^+ contents in plant tissues, even at this longer time would mostly reflect Rb^+ arrived from the external ion flow. The time for assaying Rb^+ in the tissues and phloem sap to complete the analysis of OsK5.2 functions was then set at 48 h after supplementation. Below, only K^+-replete plants were further considered.

IV.2.4 OsK5.2 contributes to xylem sap K^+ loading in the roots via both direct secretion in the stele and K^+ unloading from the phloem sap, its role in phloem being predominant in standard plant growth conditions

The *osk5.2* mutant and WT plants grown under standard conditions were subjected to short-term (5 hours) or longer-term (2 days) RbCl supplementation. Either 70% RH or 90% RH condition was applied during the period of the RbCl supplementation, in order to examine possible differences in Rb^+ transport between transpiring and “non”-transpiring plants.

In the case of short-term RbCl supplementation under 90% RH, Rb^+ concentration in the xylem sap of *osk5.2* mutant plants was significantly decreased as compared to that of WT

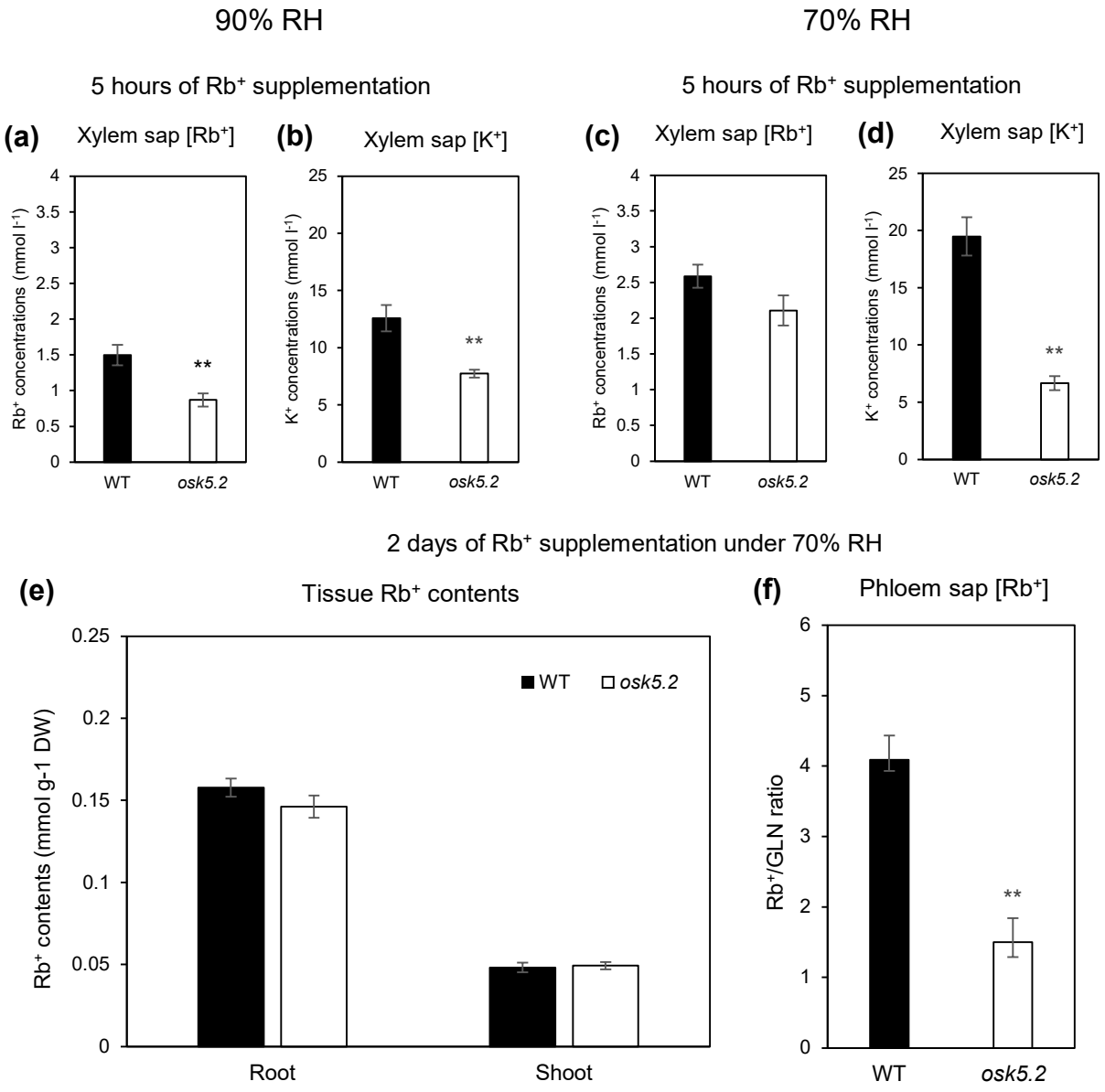

Figure IV.5 $Rb^+(K^+)$ loading into xylem sap, arrival to the leaf tissues, and recirculation in the phloem sap in wild-type and *osk5.2* mutant plants. The wild-type and *osk5.2* mutant plants were hydroponically grown in complete Yoshida medium containing 1.5 mM K^+ under standard growth condition for 5 weeks. (a to d) 5-week-old wild-type and *osk5.2* mutant plants were transferred in K^+-free Yoshida medium supplemented with 1.5 mM RbCl for 5 hours. (a, b) The plants were placed under 90% RH condition during the RbCl treatment. (c, d) The plants remained under 70% RH condition during the RbCl treatment. (e, f) 5-week-old wild-type and *osk5.2* mutant plants were transferred in K^+-free Yoshida medium supplemented with 1.5 mM RbCl under 70% RH condition for 2 days. Black bars, wild-type plants; white bars, *osk5.2 plants*. Data are presented as means ± SE (n = 12 biological replicates, merged from ASJA08 and ASHF06 lines for both wild type and *osk5.2* plants). Single and double stars denote statistically significant differences between the wild-type and *osk5.2* mutant plants at $P \leq 0.05$ and $P \leq 0.01$, respectively (Student's t test).

In 90% RH condition

- No transpiration
- Low K^+ cycling
- OsK5.2 contribution to xylem sap K^+ loading: higher from external K^+ flow than re-cycling from phloem

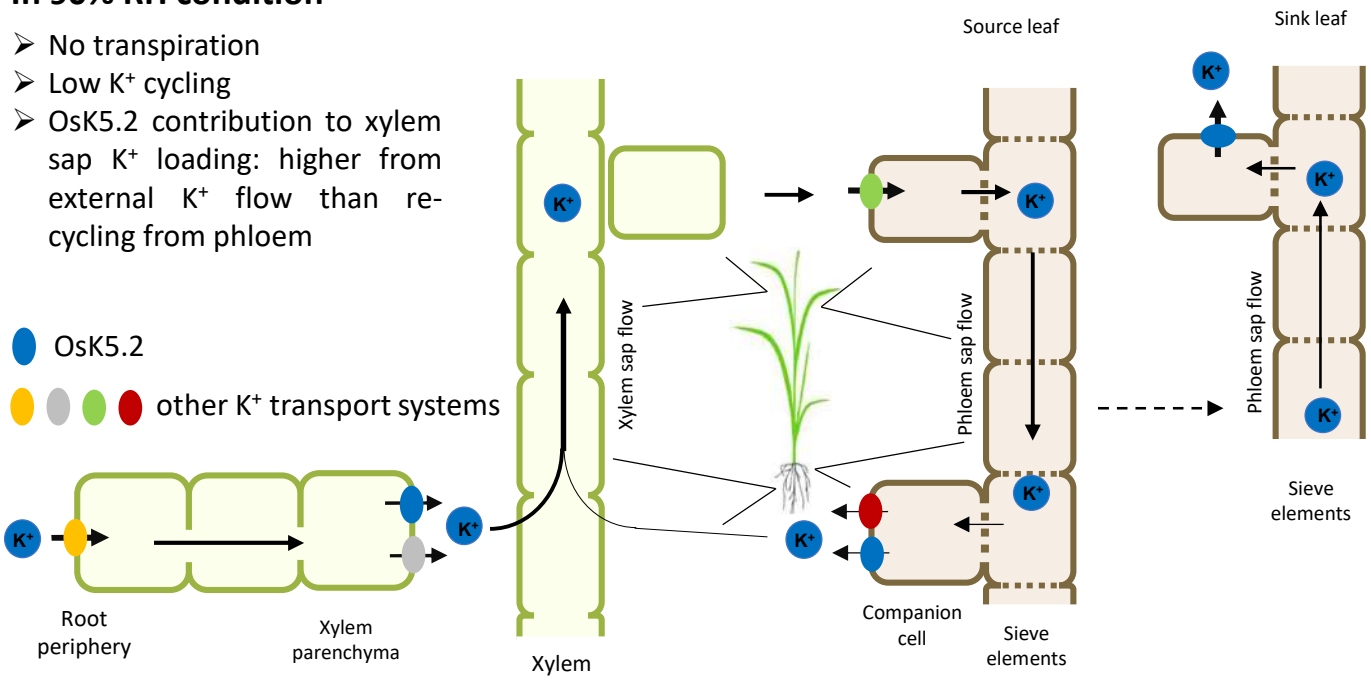

In 70% RH condition

- Transpiration
- High K^+ cycling
- OsK5.2 contribution to xylem sap K^+ loading: lower from external K^+ flow than re-cycling from phloem

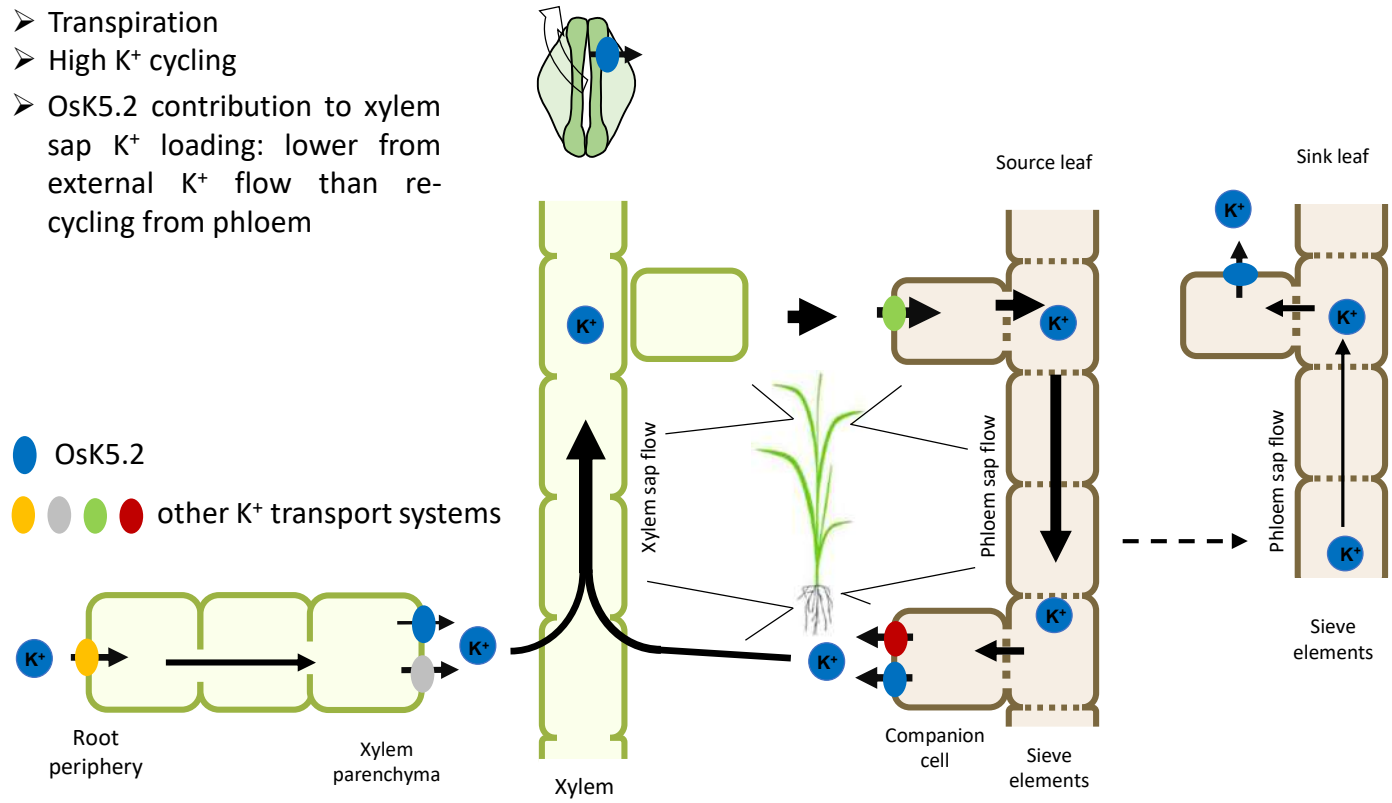

Figure IV.6 Integrative model of OsK5.2 function in non transpiring (top) and transpiring (bottom) rice plants.

plants (Figure IV.5 a). This corresponded to a mean reduction in Rb^+ concentration of 0.6 mM. The percentage of decrease in *osk5.2* mutant plants was by about 40%. This indicated that in "non"-transpiring plants, OsK5.2 strongly contributes to direct secretion of K^+ to the xylem sap from the uptake flow (Figure IV.6 top). For the K^+ concentration measured in same samples of xylem sap, a similar percentage of decrease between *osk5.2* mutant and WT plants was determined (Figure IV.5 b). The similar ratios of concentrations between *osk5.2* mutant and WT plants observed for Rb^+ and K^+ suggested that OsK5.2 did not significantly contribute to recirculation of K^+ from phloem to xylem in the "non"-transpiring plants (Figure IV.6 top).

Under 70% RH, the Rb^+ and K^+ concentrations in the xylem sap of WT plants were clearly increased, both by about 66% (Figure IV.5 c), which suggested that the rate of K^+ secretion to the xylem sap was increased in transpiring plants. In *osk5.2* mutant plants, the mean Rb^+ concentration in the xylem sap upon short-term RbCl supplementation, was only reduced by about 20% as compared to that of WT plants, the difference being not statistically significant (Figure IV.5 c). It is worth noting that the difference in the mean xylem sap Rb^+ concentration between WT and *osk5.2* plants was of about 0.5 mM, *i.e.*, a value quite close to that under 90% RH. Since the flux of Rb^+ in the xylem rather than the concentration should be considered to compare Rb^+ secretion to the xylem sap under 90% RH and 70% RH, and a higher flux was expected at 70% RH due to plant transpiration, the determination of just slightly lower concentration difference between WT and mutant plants under 70% RH as compared to 90% RH, suggested that the rate of OsK5.2 direct secretion of Rb^+ (and K^+) to the xylem sap was likely not decreased under 70% RH. However, under 70% RH as compared to 90% RH, the contribution of other K^+ transport systems to direct K^+ secretion to the xylem sap was strongly increased, and the relative contribution of OsK5.2 became minor (decreased by 50%; Figure IV.5 a, c) (Figure IV.6 bottom). K^+ concentrations measured in same samples of xylem sap were under 70% RH, in sharp contrast with those of Rb^+, strongly lower in the mutant plants, by about 65% (Figure IV.5 d), consistently with previous reports (Nguyen et al., 2017; Chapter 3). This indicates that a major part of the K^+ concentration in the xylem sap at steady state in transpiring plants originated from downstream recirculation of K^+ unloaded from the phloem, dependent on OsK5.2 activity in this tissue (Figure IV.6 bottom). Since *OsK5.2* was well-expressed in companion cells of sieve tubes in the root, we could hypothesize that OsK5.2 at the membrane of the companion cells was involved in unloading

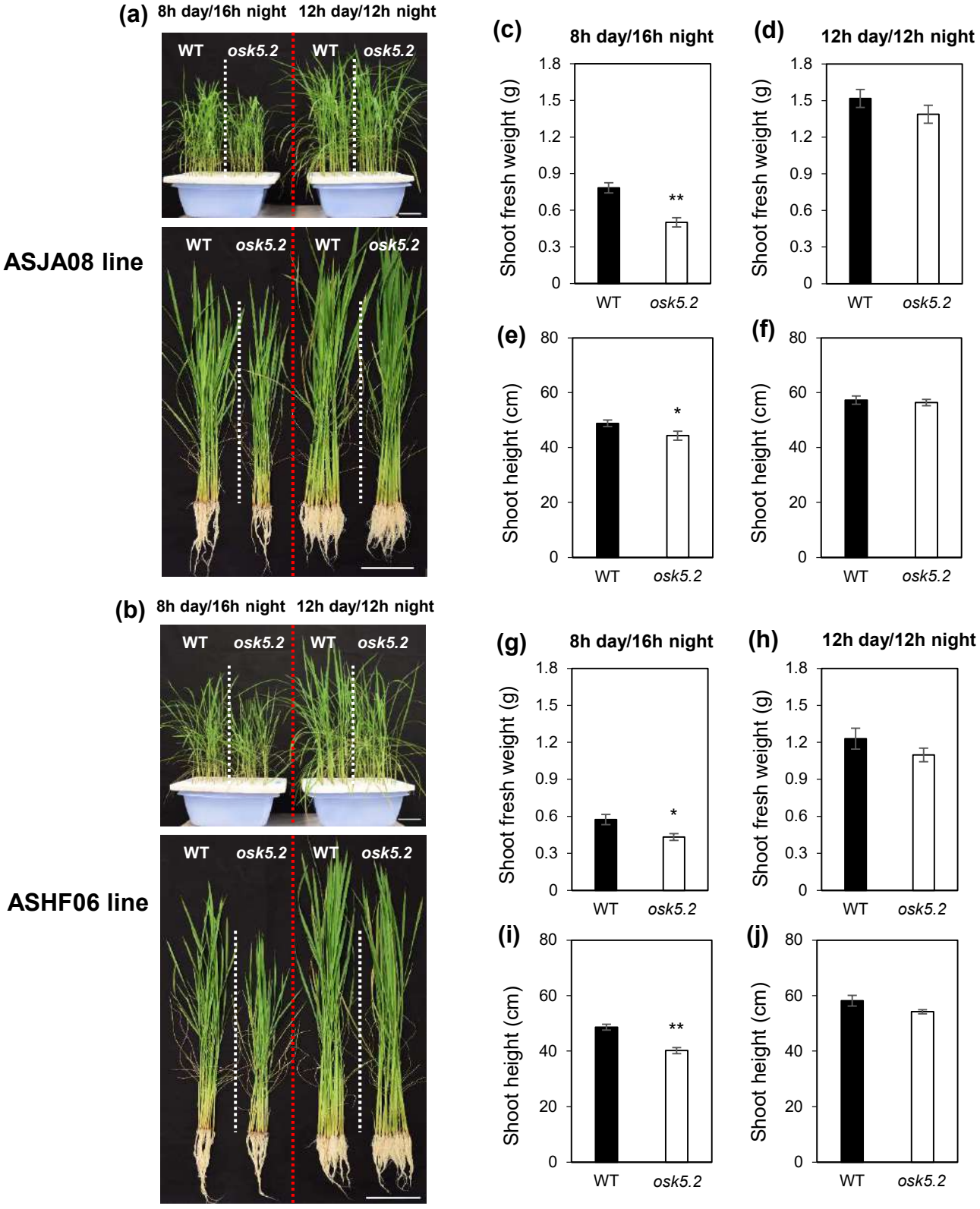

Figure IV.7 Day length-dependent phenotype of *osk5.2* mutant plants. Phenotypic analysis of wild-type and *osk5.2* mutant plants from ASJA08 (a, c to f) and ASHF06 (b, g to j) lines, hydroponically grown in standard Yoshida medium under two different photoperiod regimes: 8 h day/16 h night (short-day) and 12 h day/12 h night (normal day length). (a, b) Photos were taken with 5-week-old plants. Scale bars = 10 cm. Shoot fresh weight (c, d, g, h) and shoot height (e, f, i, j) of 5-week-old wild-type (WT) and *osk5.2* mutant plants are presented as means (± SE) of $n = 10$ biological replicates. Black and white bars, WT and *osk5.2* plants, respectively. Single and double stars denote statistically significant differences between the WT and *osk5.2* plants at $P \leq 0.05$ and $P \leq 0.01$, respectively (Student's *t* test).

K^+ from the phloem sap (see also the discussion section below).

Rb^+ contents in the shoots and roots of *osk5.2* mutant plants were not different to those in WT plants when assayed 2 days after RbCl supplementation under 70% RH (Figure IV.5 e). This was likely explained by the following facts: after 2 days of RbCl addition, Rb^+ concentration in the xylem sap was very likely still mostly originating from direct secretion (Figure IV.4 a); therefore, during the 2 days of RbCl treatment, Rb^+ concentration in the xylem sap was likely only slightly less in *osk5.2* mutant plants than in WT plants (as observed after 5 hours; Figure IV.5 c); in the meantime, the steady state transpiration rate, due to the role of OsK5.2 in stomatal closure, was slightly higher in the mutant plants (Chapter 3); overall, the transpirational flux of Rb^+ in the xylem, arriving to the leaves was likely quite similar in WT and *osk5.2* mutant plants during the RbCl treatment.

In these conditions where no difference in Rb^+ concentration existed in the leaves between WT and mutant plants, *OsK5.2* mutation still resulted in significant reduction of Rb^+ concentration in phloem sap, by 60% (Figure IV.5 f). Thus, this reflected a severe impairment of Rb^+ loading into the phloem sap, due to lack of OsK5.2 activity, as that of K^+ loading into the phloem sap (Figure IV.3 b).

IV.2.5 Reduced growth of *osk5.2* plant under short-day condition

No phenotypic difference in term of plant growth between 5-week-old WT and *osk5.2* mutant plants, for both ASJA08 and ASHF06 lines, has been previously reported with plants grown in K^+-replete standard conditions (Chapter 3). Since connections exist between K^+ transport and photoassimilate transport in the phloem, we examined the effect of a reduction in the daylight duration on growth phenotype of *osk5.2* mutant and WT plants hydroponically grown on standard Yoshida medium. Under short-day (8 h light/16 h night cycle) condition, *osk5.2* mutant plants and WT plants of both ASJA08 and ASHF06 lines displayed clear phenotypic growth differences (Figure IV.7 a, b, left). Reduced development in *osk5.2* mutant plants concerned both roots and shoots of the 5-week-old plants. In the shoots, the depressive effect of *OsK5.2* KO mutation was observed for the height and especially the fresh weight which was significantly reduced by 25% in ASHF06 plants and 35% in ASJA08 plants (Figure IV.7 c, e, g, i). Under longer day length (12 h light/12 h night cycle, standard growth condition in our experiments) in the same growth chamber, no growth phenotype between *osk5.2* mutant and WT plants were any longer observed with plants hydroponically grown by the same

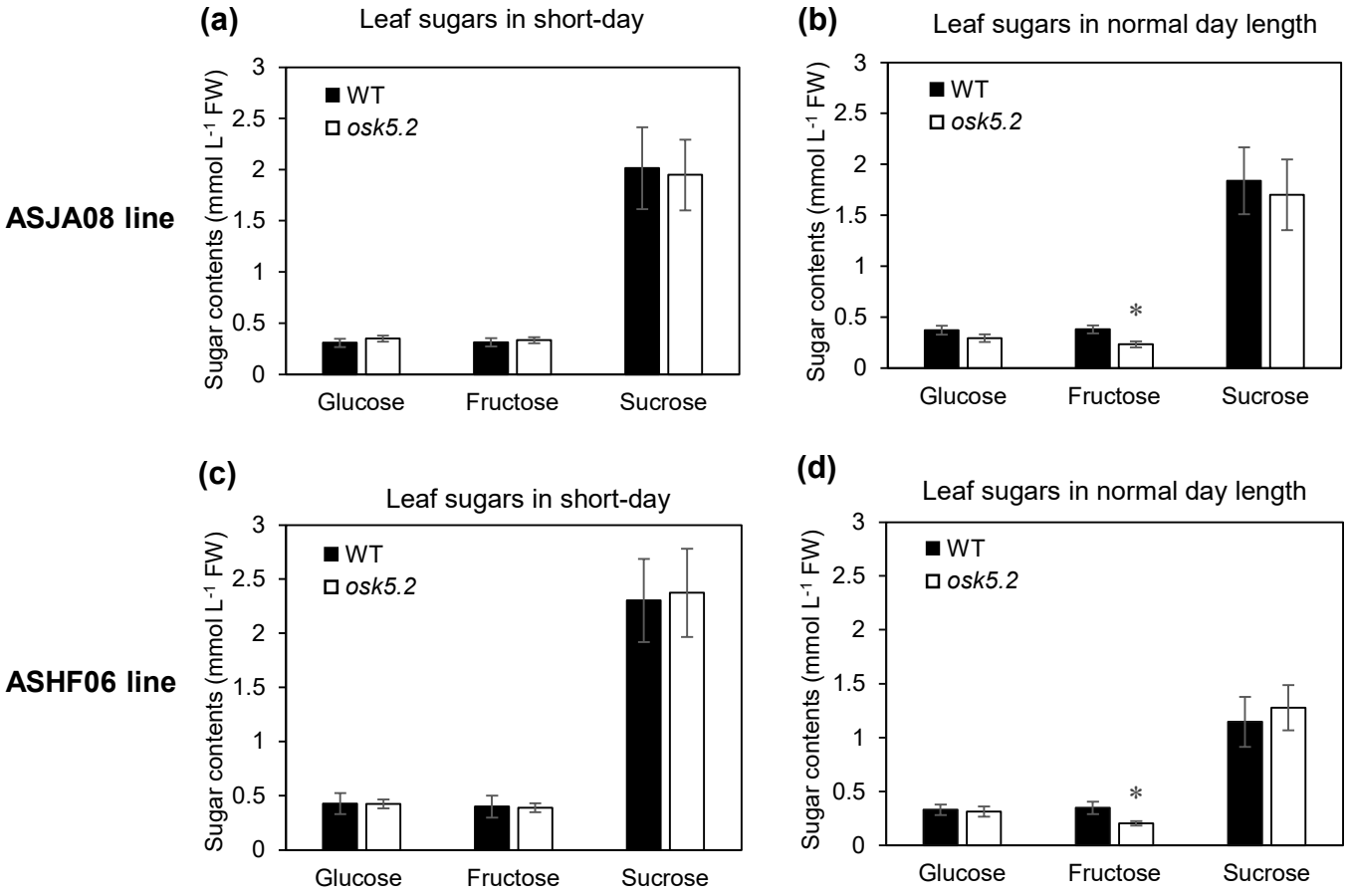

Figure IV.8 Contents in glucose, fructose and sucrose in total leaf extracts of wild-type and *osk5.2* mutant plants under short-day (a, c) and normal day length (b, d) conditions. Data are presented as means ± SE of $n = 6$ biological replicates. Black bars, wild-type plants; white bars, *osk5.2* plants. Single and double stars denote statistically significant differences between the wild-type and *osk5.2* mutant plants at $P \leq 0.05$ and $P \leq 0.01$, respectively (Student's *t* test).

during 5 weeks on standard Yoshida medium (Figure IV.7 d, f, h, j), consistently with previous reports in similar conditions. As expected, the plants were bigger as compared to those grown with 8 hours of light per day, the shoot biomass being increased by 50% in WT plants (Figure IV.7).

IV.2.6 Reduced fructose content in the leaves of *osk5.2* plants under normal day length

To assess whether the levels of soluble sugars were affected in the *osk5.2* mutant plants, we determined the contents of glucose, fructose, and sucrose in the leaves of 5-week-old mutant and WT plants grown under short day or standard day lengths. In plants grown under short-day condition, the levels of glucose, fructose, and sucrose did not differ in the analyzed leaves between mutant and WT plants (Figure IV.8 a, c). In plants grown under normal day length condition, on the other hand, while the contents of glucose and sucrose were similar in the analyzed leaves of mutant and WT plants, the content of fructose was significantly decreased in the analyzed leaves of mutant plants compared with WT ones, by 35% in ASJA08 and 40% in ASHF06 lines (Figure IV.8 b, d). It is well known that the export of carbohydrates from photosynthesizing source organs provides the substrate for the maintenance of non-photosynthetic organs and growth of sink organs, and phloem acts as vehicle for the delivery of carbohydrates from source to sink organs (Ainsworth & Bush, 2011). The reduced shoot fresh weight and height as well as root development of *osk5.2* mutant plants reflect the stunted growth of sink organs. Next step in our study of possible connections between OsK5.2 activity in the phloem and carbohydrate transport, would be to analyze the translocation of soluble sugars to sink organs in the phloem sap of 5-week-old WT and *osk5.2* mutant plants.

IV.3 Discussion

K^+ is known to be highly mobile in plants through vascular tissues, xylem and phloem. As already mentioned, this transport has a number of functions and is tightly regulated. In the xylem sap, K^+ is thought to originate in part from direct secretion after root absorption from the soil, but especially from reloading following recirculation via the phloem sap (Armstrong & Kirkby, 1979; Jeschke & Pate, 1991; Pate & Jeschke, 1995). The shoot-to-root K^+ flux recirculating via the phloem sap which contains a high K^+ concentration (*e.g.*, reported in the range from 50 to 110 mM by Fromm and Eschrish (1989) in barley) can be greater than the

flux of root uptake from the soil (Touraine, Grignon, & Grignon, 1988; Wolf, Munns, Tonnet, & Jeschke, 1991). The amount of K^+ that is recirculated via the phloem sap is also believed to serve as a signal to adjust the shoot K^+ delivery (Touraine, Grignon, & Grignon, 1988; Wegner & De Boer, 1997; White, 1997). However, little is still known on how K^+ transport systems manage these integrated long-distance transports (Ragel et al., 2019). Here, OsK5.2, already known to control the upward K^+ fluxes by its involvements in xylem sap K^+ loading and rate of transpiration control, was shown to additionally strongly control the phloem sap K^+ concentration (Figure IV.3 b), and thus to regulate the whole K^+ cycling between roots and shoots. Tracer experiments of K^+ circulation within the plant using Rb^+ and detailed tissue expression analyses allowed us to propose a mechanistic model of OsK5.2 function (Figure IV.6). The following main conclusions were drawn:

(1) OsK5.2 plays only a minor role in direct K^+ secretion to the xylem sap from root uptake flow in well K^+-fed plants under transpiring conditions (70% RH). Conversely, OsK5.2 is strongly involved in reloading xylem sap with K^+ unloaded from the phloem sap. This latter role of OsK5.2 deduced from our short-term tracer experiments is consistent with the previous studies indicating a substantial percentage of K^+ in the xylem sap originating from recirculation from the phloem, *e.g.*, 20% in tomato and French dwarf bean plants (Armstrong & Kirkby, 1979; Breteler & Cate, 1978). Since OsK5.2 has been previously shown to function as K^+ efflux channel (Nguyen et al., 2017) and we localized *OsK5.2* expression in particular in root phloem companion cells (Figure IV.1), we propose that OsK5.2 controls xylem sap K^+ concentration in well K^+-fed plants under transpiring conditions essentially through its function of K^+ secretion out of the phloem from root phloem companion cells (Figure IV.6 bottom).

(2) In well K^+-fed plants in which xylem sap flow relies on root pressure (under 90% RH), *OsK5.2* plays an important role in direct K^+ secretion to the xylem sap, very likely from the root xylem parenchyma cells where its expression has been detected (Figure IV.1). In these environmental conditions, OsK5.2 role in xylem sap K^+ loading is very similar to that of SKOR in Arabidopsis (Gaymard et al., 1998). It is likely that in these conditions where plants do not substantially transpire, the rate of K^+ recycling from phloem to xylem, as that of K^+ upward transport in the xylem, are much slower than in plant transpiring conditions (Figure IV.6 top), which could explain the lack of substantial contribution of OsK5.2 to xylem sap K^+ loading from recycling from root phloem in these conditions. Under “non”-transpiring

conditions, the relative contribution of OsK5.2 to overall loading of K^+ to xylem sap was lower than that under transpiring conditions (38% *vs* 65%; Figure IV.5 b, d).

How transpiration rate changes may affect the concentration of ions in the xylem sap has been debated in the literature (Else, Hall, Arnold, Davies, & Jackson, 1995; Jackson, 1993). Here, K^+ and Rb^+ concentrations in the xylem sap were higher at higher transpiration rate (70% RH) (Figure IV.5 a, b, c, d), which cannot be explained by a dilution mechanism and rather indicates higher secretion to the xylem sap at higher transpiration rate. The large contribution of recirculating K^+ to xylem sap K^+ loading in transpiring plants in contrast to "non"-transpiring ones may lead to higher overall xylem sap K^+ loading. Schurr and Schulze (Schurr & Schulze, 1995) in castor bean plants observed that ion concentrations in the xylem sap strongly vary according to the transpiration rate and the ion, with the concentration of some ions being inversely proportional to the transpiration rate, that of some other ions showing no relation to the transpiration rate and that of some other ones varying in proportion to the transpiration rate. K^+ appeared to follow the latter pattern, with K^+ concentration showing remarkable increase with that of the transpiration rate (Schurr & Schulze, 1995).

OsK5.2 was evidenced here to control not only the xylem sap K^+ concentration, but also the phloem one, its disruption leading to a decrease in the phloem sap concentration (this was shown with transpiring plants but was true also under 90% RH; not shown). How could this be interpreted? Could OsK5.2 be directly involved in phloem sap loading in the leaves? OsK5.2 is expressed in the leaves in the phloem tissue, as shown by our *pOsK5.2::GUS* plant analyses (Figure IV.1), although 4-fold less expressed in leaves than in roots, and not only expressed in the phloem in the leaves (also expressed in the stomate; Nguyen et al., 2017). However, since OsK5.2 is a K^+ efflux channel, it is unlikely directly involved in phloem sap loading in the leaves. It should be noted that the leaves that were analyzed in the GUS staining assays were still growing, indicating that they were both source and sink or mostly sink for phloem transport. We propose that OsK5.2 is involved in K^+ unloading from the phloem in sink leaves, in addition to roots (Figure IV.6). This role however, does not explain the lower phloem sap K^+ concentration in KO mutant plants. Xylem and phloem are interconnected through parenchyma cells along the whole-plant vascular tissues, implying a linkage function (Van Bel, 1990). Direct xylem-to-phloem transfer of K^+ in the stem tissues is thought to play important role in the partitioning of K^+ within the plant (Jeschke & Pate, 1991; Jeschke, Pate, & Atkins, 1987; Pate & Jeschke, 1995). In this study, a reduction of K^+

concentration in the phloem sap in *osk5.2* mutant plants was observed jointly with a reduction of K^+ concentrations in the xylem sap. While symplastic connections exist between xylem parenchyma and phloem tissues, there is no symplastic continuity between xylem sap and phloem sap. Ions from xylem sap have to enter a cell of xylem parenchyma or phloem tissue by crossing a cell membrane to recirculate in the phloem sap. We could hypothesize that lower K^+ concentration in the xylem sap would decrease the conductance of an inward channel (such as OsAKT2; Shen et al., 2020) in the parenchyma tissue, leading to decreased K^+ loading to the phloem sap. In our experiments with Rb^+, however, a strong decrease in the phloem sap concentration in *osk5.2* mutant plants was observed while no significant difference of concentration existed in the xylem sap between *osk5.2* and WT plants (Figure IV.5 c, f). Furthermore, Rb^+/K^+ ratio in the xylem sap was higher in *osk5.2* mutant plants than in WT plants (Figure IV.5 c, d). So, this indicated that Rb^+ concentration in the phloem sap was not simply correlated to that in the xylem sap. It is worth noting, however, that while the xylem sap Rb^+ concentration, in the short-term Rb^+ application experiments, was not significantly different in WT and *osk5.2* mutant plants, that of K^+ (7-fold higher than that of Rb^+) was, at the same time, strongly lower in *osk5.2* mutant plants (Figure IV.5 c, d). Rb^+ transport was likely dependent on K^++Rb^+ concentration gradients rather than Rb^+ ones only, which may explain the observed absence of correlation between xylem sap and phloem sap Rb^+ concentrations. In the parenchyma tissue, also, exchanges between cytosol and organelles (especially vacuoles) may take place.

Thus, we propose that the concentration of K^+ in the phloem sap may be strongly determined by that in the xylem sap in a OsK5.2 independent manner (although further investigations would be clearly needed to confirm this hypothesis), and that the K^+ unloading activity of OsK5.2 in the root phloem would be the main mechanism by which this channel takes part to the control of the xylem sap K^+ concentration in well K^+-fed transpiring plants.

In conclusion, together with the previous studies (Kim et al., 2015; Nguyen et al., 2017), data that are now available provide a quite complete view of the functions of OsK5.2, and in particular its role in K^+ cycling throughout the plant. OsK5.2 was known to be involved in the xylem sap loading with K^+, like SKOR. Except in the particular case of "non"-transpiring plants, OsK5.2 appeared to achieve this xylem sap K^+ loading in a different way to SKOR. An important physiological contribution of OsK5.2 to K^+ unloading from the phloem in roots was

evidenced. This constitutes a newly evidenced function for an outward K^+ channel. The observation of growth phenotype in *osk5.2* mutant plants in short-day condition suggests furthermore an important role of OsK5.2 in phloem sap (and in particular photoassimilate?) transport, which will need to be further investigated in future. The present study however already extends our understanding of the underlying mechanisms of K^+ cycling and especially of phloem K^+ transport in rice plant.

Chapter V

Study of K^+ transport by OsK5.1 and OsK5.2 in heterologous systems and in *planta*

V.1 Introduction

The Shaker K^+ channel family has been extensively characterized in the model plant Arabidopsis, which constitutes a paradigm of channel-mediated K^+ transport across the plasma membrane in varying plant tissues. The Shaker family structure is well conserved among plant species (Véry et al., 2014). However, whether homologous channels in other plants have the same physiological functions as in Arabidopsis has not yet been much examined so far, especially for K^+ Shaker channels from cereal crops. Phylogenetic tree shows that the nine Shaker K^+ channels in Arabidopsis are sorted into five groups, the group 5 being comprised of two K^+ export systems, *i.e.*, the Stelar K^+ Outward Rectifier (SKOR) and the Guard cell Outward Rectifying K^+ channel (GORK) (Ache et al., 2000; Gaymard et al., 1998; Lebaudy, Véry, & Sentenac, 2007). SKOR is specifically expressed in root pericycle and xylem parenchyma cells and contributes to about 50% of K^+ translocation toward the shoots (Gaymard et al., 1998). GORK is highly expressed in guard cells (Becker et al., 2003) and is involved in K^+ efflux during stomatal closure (Hosy et al., 2003). In rice, two K^+ export channels OsK5.1 and OsK5.2 are classified into the group 5 of the Shaker K^+ channel family (Véry et al., 2014) and are regarded as the homologs of Arabidopsis SKOR and GORK. However, *OsK5.2*, as previously reported (Nguyen et al., 2017; Chapter 4), in addition to displaying similar role as GORK in guard cells, also shares with SKOR involvement in K^+ loading to the xylem sap for translocation towards the shoots, although the xylem sap K^+ loading mechanism of OsK5.2 seems partly different to that of SKOR (Gaymard et al., 1998; Chapter 4). In a previous work by Thanh Hao NGUYEN in the host group (2016, PhD thesis), the other K^+ export channel gene *OsK5.1* from group 5 was shown to be expressed in the vascular tissues of both leaves and roots, root tips, root cortex, anther filament, and only slightly in the stomatal complex, by *GUS* reporter gene approach. Similarly, a previous study showed that *OsK5.1* (named *OsSKOR* in this study) was highly expressed in the root vascular tissue of rice seedling and also expressed in the flower and seed at reproductive stage, by *GUS* reporter gene approach and qRT-PCR analysis (Kim et al., 2015). However, the physiological role of OsK5.1 in rice has not been reported so far.

The plant Shaker K^+ channels resemble the animal voltage-gated K^+ channels (K_v): they are tetrameric proteins composed of four subunits, in which each subunit consists of N- and C-termini present in cytosol, six transmembrane segments (S1-S6), and one K^+-selective

pore domain between the S5 and S6 (P domain). Cytosolic domains allow tetramerization, clustering and through interaction with protein partners, *e.g.*, anchoring in the membrane or regulation of activity, in particular through control of the phosphorylation status (Luan, 2008; Véry & Sentenac, 2003; Wang & Wu, 2013). In plant Shaker channels, the C-terminus has been reported to be involved in these interactions/regulations. In animal Shaker channels, inactivation processes characterized by the fact that some K^+ channels terminate K^+ flow through their K^+-selective pores when the opening stimulus is still present, have been characterized. Inactivation of K^+ channels mostly occurs by "N-type" and/or "C-type" mechanisms (MacKinnon, 2003). N-type inactivation operates by a 'ball-and-chain' mechanism by which the cytoplasmic N-terminal peptide so-called 'ball' domain is tethered to a flexible chain (Hoshi, Zagotta, & Aldrich, 1990). In the "ball and chain" inactivation model, the 'ball' domain brings the structure to the open state pore domain, thereby obstructing the flow of K^+ ions (Hoshi, Zagotta, & Aldrich, 1990). The N-terminus structure of "ball and chain" inactivation consists of about first 10 hydrophobic amino acids ("ball"), followed by about 10 positively charged hydrophilic amino acids and T1-S1 linker (connecting cytoplasmic domain T1 to the first membrane-spanning segment S1) (Gulbis, Zhou, Mann, & MacKinnon, 2000). Electrostatic interactions between positively charged residues from hydrophilic region and negatively charged residues from T1-S1 linker have been characterized to facilitate entry of the "ball" into the K^+-selective pore domain, thereby blocking the K^+ flow (Gulbis, Zhou, Mann, & MacKinnon, 2000; Long, Campbell, & MacKinnon, 2005).

In a previous work by Thanh Hao NGUYEN in the host group, OsK5.1 and OsK5.2 were attempted to be expressed in *Xenopus laevis* oocytes, but no exogenous current in the oocytes was detected using the classical two-electrode voltage-clamp technique. In this chapter, my goal was to get insight into the function of OsK5.1 in the root and compare it with that of SKOR in Arabidopsis and that of OsK5.2 in rice. This was performed by a combination of approaches: (1) further expression studies and reverse genetics in rice, (2) complementation of the *skor* mutant with the rice *OsK5.1* or *OsK5.2* genes under control of *skor* promoter sequence, (3) attempt to express *OsK5.1* and *OsK5.2* in COS-7 cells to study their functional properties using the patch-clamp technique.

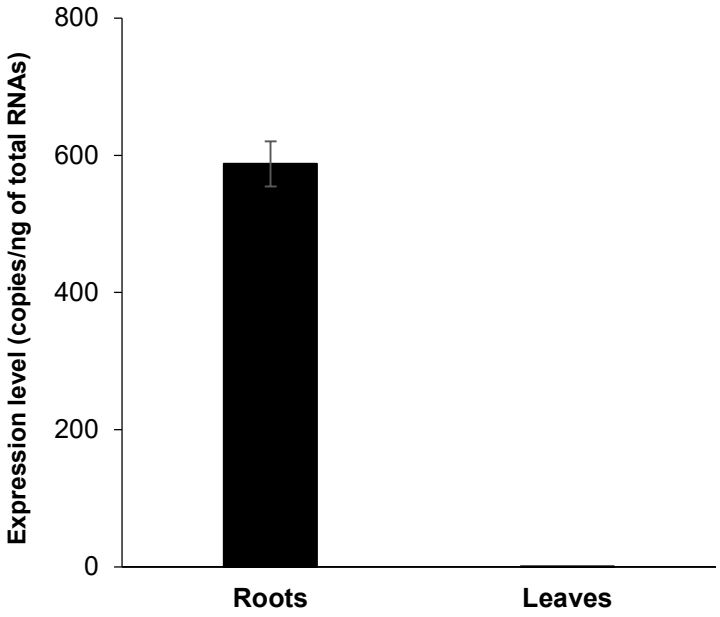

Figure V.1 The transcript level of *OsK5.1* in rice roots and leaves. Five-week-old rice plants cv Nipponbare were grown on hydroponic Yoshida medium. Expression data determined by real-time quantitative RT-PCR are presented as means ± SE (n = 4 biological replicates).

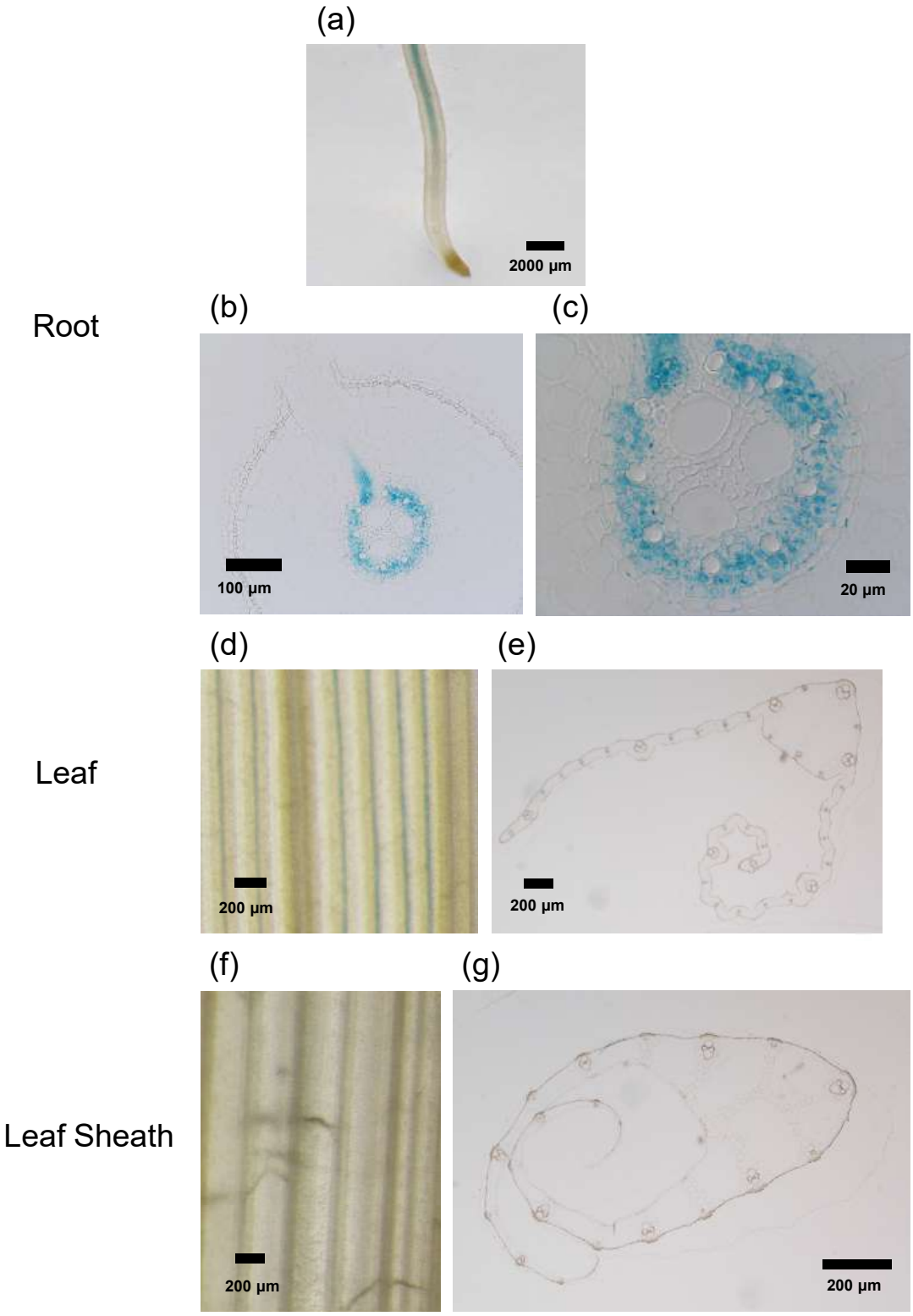

Figure V.2 GUS staining of transgenic rice plants expressing p*OsK5.1*::*GUS* construct. Three-week-old plants were grown on hydroponic Yoshida medium. (a) root tip, (b) cross-section of root, (c) enlarged stele of root, (d) leaf blade, (e) cross-section of leaf blade, (f) leaf sheath, (g) cross-section of leaf sheath.

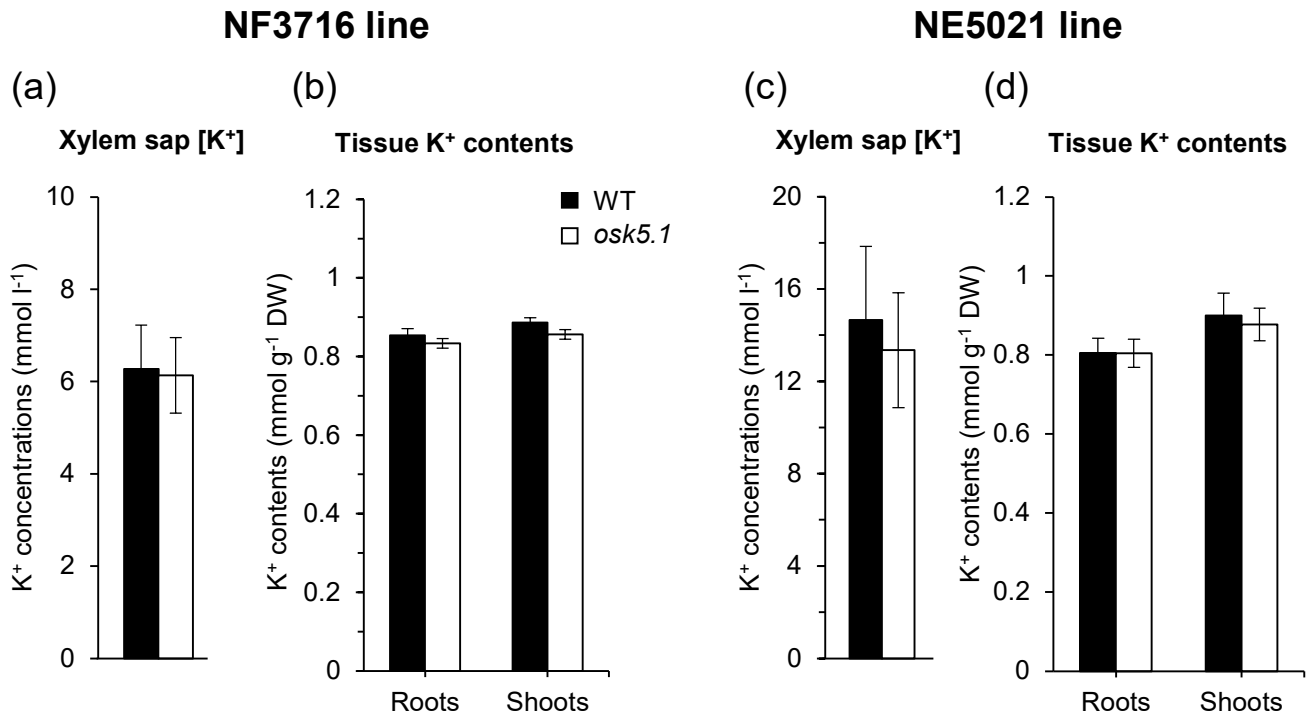

Figure V.3 Xylem sap K^+ concentrations and tissue K^+ contents in wild-type (black bars) and *osk5.1* mutant plants (white bars) issued from the rice NF3716 (a and b) or NE5021 (c and d) lines. Roots, shoots, and xylem sap exudates were collected from five-week-old wild-type and *osk5.1* mutant plants hydroponically grown on complete Yoshida medium. Data are presented as means ± SE (n = 9 biological replicates). Absence of star above white bars denotes absence of statistically significant differences between wild-type and *osk5.1* mutant plants (Student's t test, $P \leq 0.05$).

V.2 Results

V.2.1 *OsK5.1* expression pattern

The expression pattern of *OsK5.1* was investigated by qRT-PCR on total RNAs extracted from roots and leaves of 5-week-old rice plants cv Nipponbare. Our results showed that *OsK5.1* transcripts were hardly detected in leaves but abundant in roots (Figure V.1).

In order to identify the localization of *OsK5.1* expression at the tissue level, transgenic plants expressing *GUS* reporter under the control of *OsK5.1* promoter were analyzed. GUS activity localized *OsK5.1* expression in vascular tissues of both roots and leaves of transgenic rice plants expressing the p*OsK5.1*::*GUS* construct (Thanh Hao NGUYEN, 2016, PhD thesis). I further examined the cell-specific expression of *OsK5.1* in vascular tissues of roots, leaf blades, and leaf sheaths. In Figure V.2, GUS activity was hardly present in leaf blades and leaf sheaths but strongly detected in roots, in agreement with qRT-PCR data. Cross-sections of GUS-stained roots showed that GUS activity was mainly detected in root pericycle, early metaxylem parenchyma, and phloem. No GUS activity was detected in central late metaxylem parenchyma.

V.2.2 Analysis of tissue K^+ contents and xylem sap K^+ concentrations in wild-type and *osk5.1* mutant plants

K^+ was assayed in roots and shoots of 5-week-old plants hydroponically grown on standard Yoshida medium. The K^+ concentrations in the xylem sap did not differ between wild-type and *osk5.1* mutant plants issued from two different lines (Figure V.3 a and c). Moreover, comparison of *osk5.1* mutant plants with the corresponding wild-type plants revealed that the disruption of *OsK5.1* functional expression did not affect K^+ accumulation in roots and shoots (Figure V.3 b and d). Thus, these results, surprisingly, suggested that *OsK5.1* does not significantly contribute to K^+ translocation from roots to shoots in WT rice plant.

V.2.3 Production of *atskor* complemented lines expressing p*AtSKOR::OsK5.1* or p*AtSKOR::OsK5.2* constructs

OsK5.1 is thought to be the rice homolog of AtSKOR which controls xylem sap K^+ loading. While the expression pattern of *OsK5.1* is compatible with this function and *OsK5.1* is quite

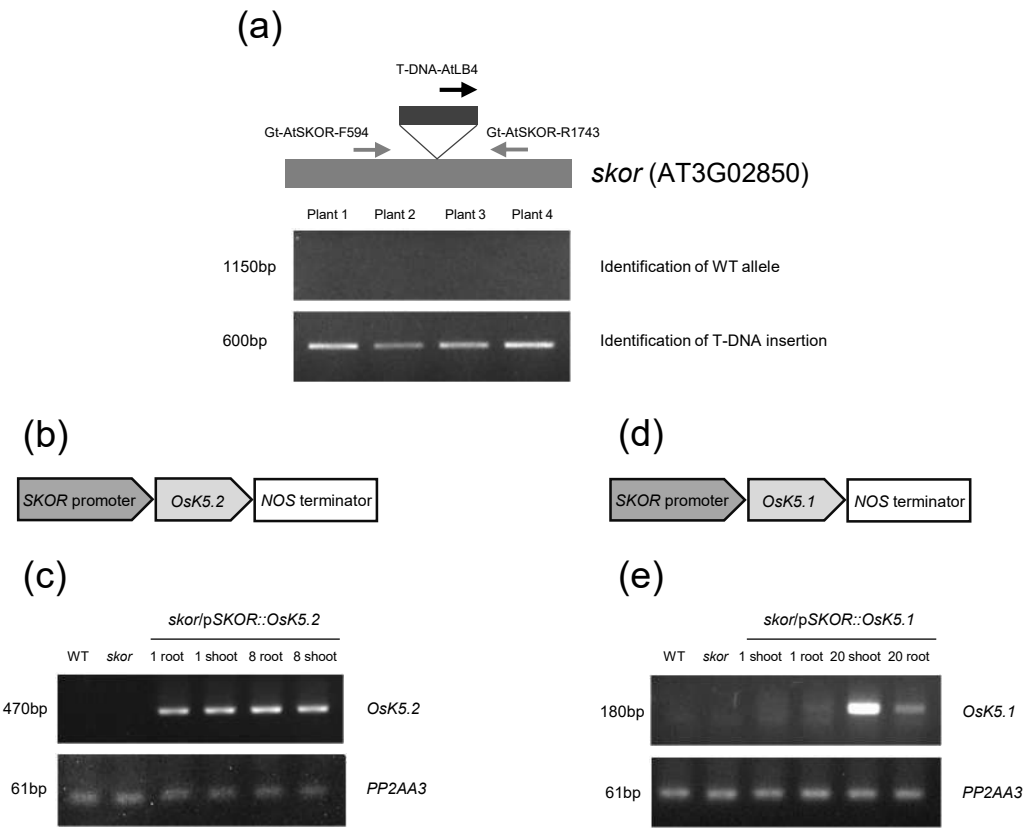

Figure V.4 Detection of *OsK5.2* and *OsK5.1* transcripts in Arabidopsis *atskor* complemented lines.

(a) Genotyping of homozygous *atskor* mutant plants. The gene-specific primers and primer hybridizing on the T-DNA were used for the genotyping by PCR (see Table II.1)

(b) *AtSKOR* promoter*::OsK5.2* coding sequence construct.

(c) RT-PCR analysis of *OsK5.2* transcripts in 5 week-old wild-type plants (Ws ecotype), *atskor* mutant plants, and T_3 homozygous *atskor* complemented lines expressing p*AtSKOR::OsK5.2*. The primers "qPCR-OsK52-F358 and qPCR-OsK52-R808" were used for the amplification of *OsK5.2* (see Table II.2). The primers "PP2AA3-Forward 5'-TAACGTGGCCAAAATGATGC-3' and PP2AA3-Reverse 5'-GTTCTCCACAACCGCTTGGT-3' " were used for the amplification of *PP2AA3* (*Arabidopsis* housekeeping gene, NCBI Gene ID: 837892; *protein phosphatase 2A subunit A3* gene).

(d) *AtSKOR* promoter*::OsK5.1* coding sequence construct.

(e) RT-PCR analysis of *OsK5.1* transcripts in 5 week-old wild-type plants (Ws ecotype), *atskor* mutant plants, and T_3 homozygous *atskor* complemented lines with p*AtSKOR::OsK5.1*. The primers "qPCR-OsK51-F74" and "qPCR-OsK51-R563" were used for the amplification of *OsK5.1* (see Table II.2).

highly expressed in roots, no xylem sap K^+ loading phenotype has been detected, and another channel gene, *OsK5.2*, has been identified to contribute to K^+ secretion into the xylem sap (Nguyen et al., 2017). One possible explanation could be that *OsK5.1* has a redundant function in controlling also xylem K^+ loading. To test the K^+ secretion function of OsK5.1, I opted for taking advantage of the fact that in Arabidopsis, the *SKOR* gene is the only *Shaker* gene involved in xylem sap K^+ loading. Therefore, I produced complemented lines of the Arabidopsis *atskor* loss-of-function mutant (Gaymard et al., 1998), which expressed p*AtSKOR::OsK5.1* construct. Complemented lines expressing p*AtSKOR::OsK5.2* construct were also produced for parallel phenotyping.

To check the presence of *OsK5.1* and *OsK5.2* transcripts in *atskor*/p*AtSKOR::OsK5.1* and *atskor*/p*AtSKOR::OsK5.2* complemented lines, total RNAs were extracted from the roots and leaves of two homozygous complemented lines and first-strand cDNAs were synthesized. The cDNAs were then used as the templates in a RT-PCR analysis to detect the existence of *OsK5.1* and *OsK5.2* transcripts in the respective complemented lines. RT-PCR analysis revealed that *OsK5.1* and *OsK5.2* transcripts were absent in Arabidopsis wild-type (Ws ecotype) and *atskor* mutant plants, as expected, but were present in both roots and shoots of *atskor*/p*AtSKOR::OsK5.1* (line 20) plants and *atskor*/p*AtSKOR::OsK5.2* (lines 1 and 8) plants (Figure V.4). Thus, one successful *atskor*/p*AtSKOR::OsK5.1* complemented line (line 20) and two independent *atskor*/p*AtSKOR::OsK5.2* complemented lines (lines 1 and 8) were identified among the produced lines.

V.2.4 Analysis of K^+ translocation towards the shoots in *atskor*/p*AtSKOR::OsK5.1* or *atskor*/p*AtSKOR::OsK5.2* complemented lines

With the aim to assess the contribution to K^+ translocation to shoots of OsK5.2 and OsK5.1 in Arabidopsis complemented lines, K^+ concentration or content was assayed in these lines in xylem sap, and root and shoot tissues. Arabidopsis plants (the complemented lines, the *atskor* mutant line and Ws ecotype) were grown in parallel on hydroponic Hoagland medium containing 6 mM K^+ for four weeks under short-day condition (8 h day/16 h night cycles), then for one further week under long-day condition (16 h day/8 h night cycles).

The xylem sap concentration of the *atskor* mutant plants was found to be ca. 50% lower than that of WT Arabidopsis plants, in line with previous reports (Gaymard et al., 1998).

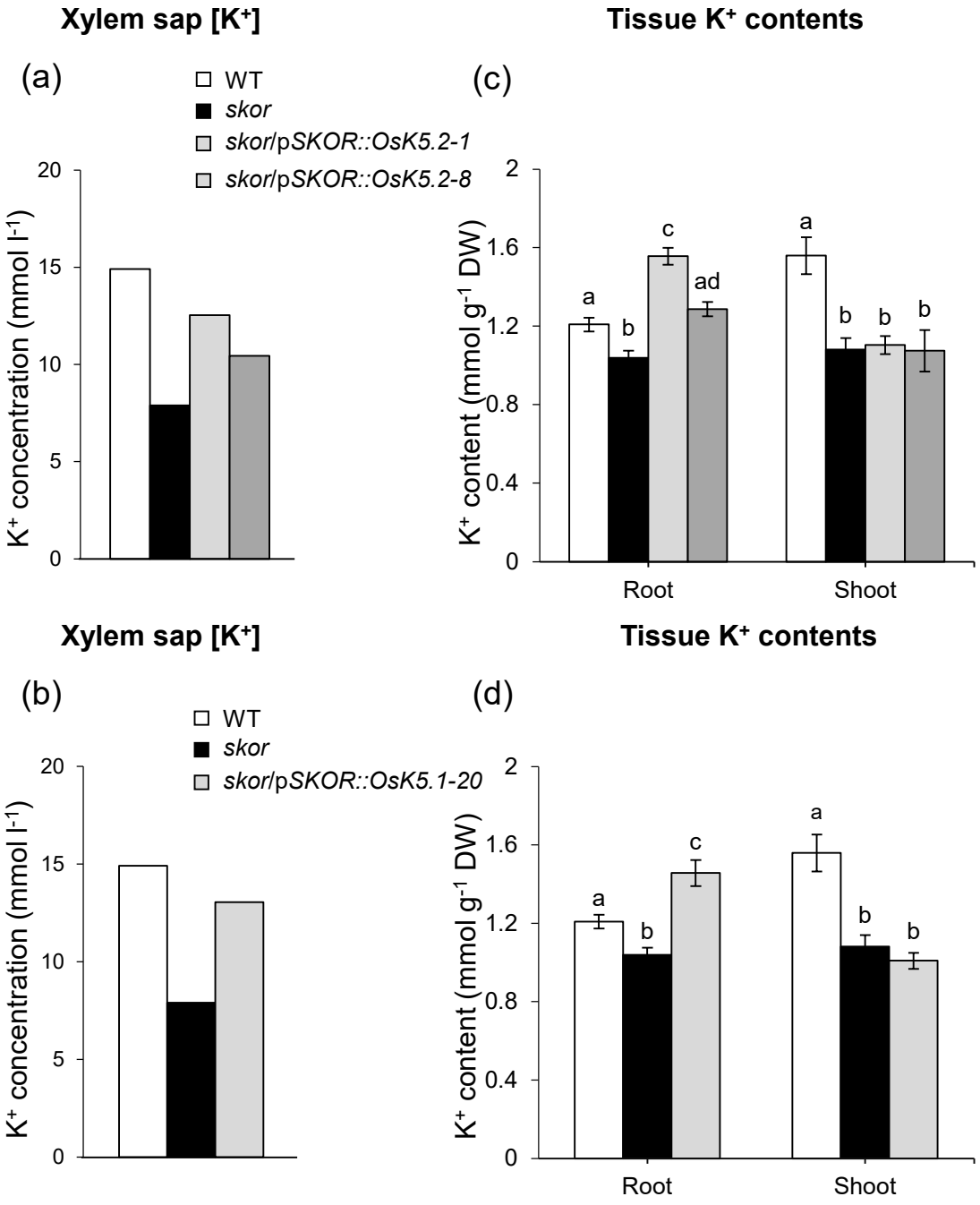

Figure V.5 Xylem sap, and root and shoot K^+ contents in wild-type, *atskor* mutant, *atskor*/p*AtSKOR::OsK5.2*, and *atskor*/p*AtSKOR::OsK5.1* complemented plants. (a and c) Xylem sap K^+ concentration and tissue K^+ contents in Arabidopsis wild-type plants (Ws ecotype) (white bars)**,** *atskor* mutant plants (black bars), and two *atskor*/p*AtSKOR::OsK5.2* complemented lines (line 1 and line 8) (light grey bars and dark grey bars). (b and d) Xylem sap K^+ concentration and tissue K^+ contents in Arabidopsis wild-type plants (Ws ecotype) (white bars)**,** *atskor* mutant plants (black bars), and *atskor*/p*AtSKOR::OsK5.1* complemented line (line 20) (light grey bars). Roots, shoots, and xylem sap exudates were collected from five-week-old wild-type plants, *atskor* mutant plant, and *atskor*/p*AtSKOR::OsK5.2*, and *atskor*/p*AtSKOR::OsK5.1* complemented lines hydroponically grown on complete Hoagland medium. Tissue K^+ contents are presented as means $\pm$ SE (n = 10 biological replicates). Xylem sap K^+ concentrations are presented as mean of mixed collection from the ten same plants. Different letters indicate statistically significant differences (Student's t test, $P \leq 0.05$).

On the other hand, in agreement with the known cellular function of K^+ secretion of OsK5.2 (Nguyen et al., 2017), expression of *OsK5.2* driven by *AtSKOR* promoter sequence restored (at least in part) K^+ concentration in the root xylem sap of the Arabidopsis *atskor*/p*AtSKOR::OsK5.2* lines (Figure V.5 a). Restoration of the K^+ concentration in the root xylem sap at a similar value to that in WT Arabidopsis plants was also observed in *atskor*/p*AtSKOR::OsK5.1* (line 20) plants (Figure V.5 b). This indicated that *OsK5.2* and *OsK5.1* were both functionally expressed in Arabidopsis complemented lines, and that the encoded channels were both endowed with K^+ secretion ability.

K^+ content assays in the roots and shoots of the *atskor* mutant plants indicated significant lower accumulation than in the WT plants, especially in the shoots (decreased accumulation by ca. 30%; Figure V.5 c and d), in line with previous findings (Gaymard et al., 1998). Interestingly, assays of tissue K^+ contents in the *atskor*/p*AtSKOR::OsK5.2* (lines 1 and 8) plants and *atskor*/p*AtSKOR::OsK5.1* (line 20) plants revealed an absence of complementation of the phenotype of reduction in shoot K^+ content observed in *atskor* mutant plants (Figure V.5 c and d). In the roots, K^+ contents in plants from one of the two complemented lines with *OsK5.2* (lines 1) and those in plants from the complemented line with *OsK5.1* exceeded those in WT plants (Figure V.5 c and d).

V.2.5 Electrophysiological characterization of OsK5.1 and OsK5.2 in COS-7 cells

Two-electrode voltage-clamp experiments were previously performed on intact guard cells of WT and *osk5.2* mutant plants. Comparison of the K^+ currents across the guard cell membrane between WT and mutant plants revealed that OsK5.2 encodes a slowly activating, outwardly rectifying K^+ channel in rice guard cells (Nguyen et al., 2017). With the aim to characterize the functional properties of OsK5.1, and to get more insights into those of OsK5.2, since none of the two genes could be functionally expressed in *Xenopus laevis* oocytes, I attempted to express *OsK5.1* and *OsK5.2* in COS-7 cells to study their functional properties using whole-cell patch-clamp technique.

In non-transfected COS-7 cells or cells solely transfected with the CD8 transfection marker (negative control COS-7 cells), very small currents were recorded for a large range of applied voltages (+ 65 to −195 mV; Figure V.6 a to c, f) using external and internal solutions comprising K^+ and Cl^- as main mobile ions. COS-7 cells co-transfected with *CD8* and *GORK* cDNAs or *CD8* and *SPIK* cDNAs were used as positive controls of channels mediating

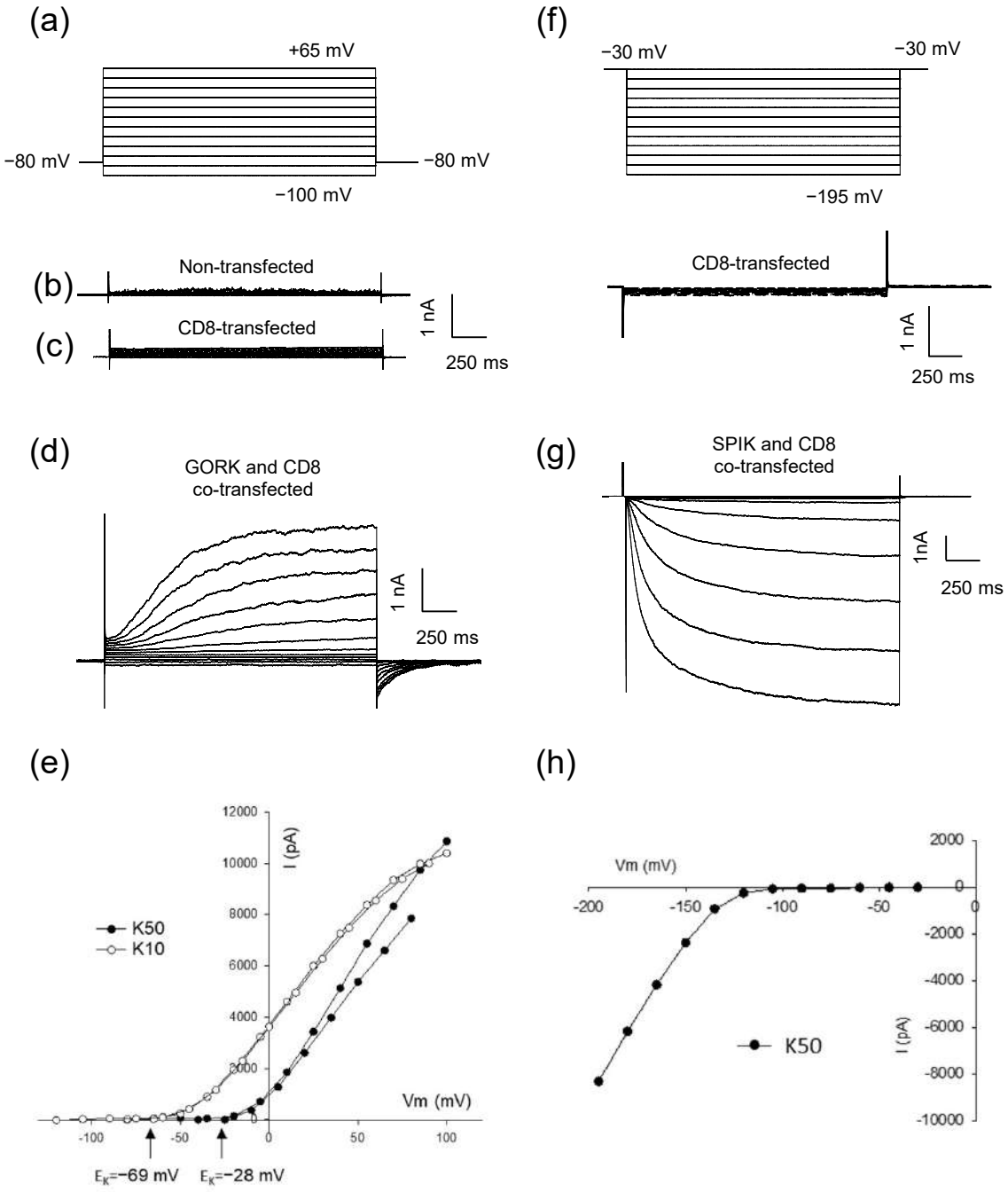

Figure V.6 Electrophysiological characterization of the outward Shaker channel GORK and the inward Shaker channel SPIK expressed in COS-7 cells.

Whole-cell patch-clamp experiments were performed. The pipette solution contained 150 mM KCl, 2 mM $MgCl_2$, 5 mM EGTA, 5 mM Mg-ATP, 10 mM Hepes/Tris (pH 7 for SPIK and pH 7.8 for GORK), and D-Mannitol for osmolarity adjustment to 350 mOsmol/l. The bath solution consisted of 50 mM KCl, 2 mM $MgCl_2$, 1 mM $CaCl_2$, 10 mM Hepes/Tris (pH7.5), and D-Mannitol for osmolarity adjustment to 330 mOsmol/l.

(a and f) Voltage-clamp protocols. Outward K^+ currents were recorded applying depolarization steps from −100 to +65 mV in +15 mV interval, from holding potential at −80 mV (a). Inward K^+ currents were recorded applying hyperpolarization steps from −30 to −195 mV in -15 mV interval, from holding potential at −30 mV (f).
(b and c) Current traces from control COS-7 cells: non-transfected (b) and CD8-transfected (c) cells. (at left and right, respectively with the protocol described in (a) and that in (f)). Currents were recorded in the bath solution containing 50 mM K^+.
(d and g) Representative K^+ current traces from COS-7 cells expressing the outward Shaker channel GORK (d) or the inward Shaker channel SPIK (g).
(e) GORK current-voltage relationships at different external K^+ concentrations: 10 and 50 mM (from a different example of transfected cell as in (d)).
(h) SPIK current-voltage relationships in the bath solution containing 50 mM K^+.

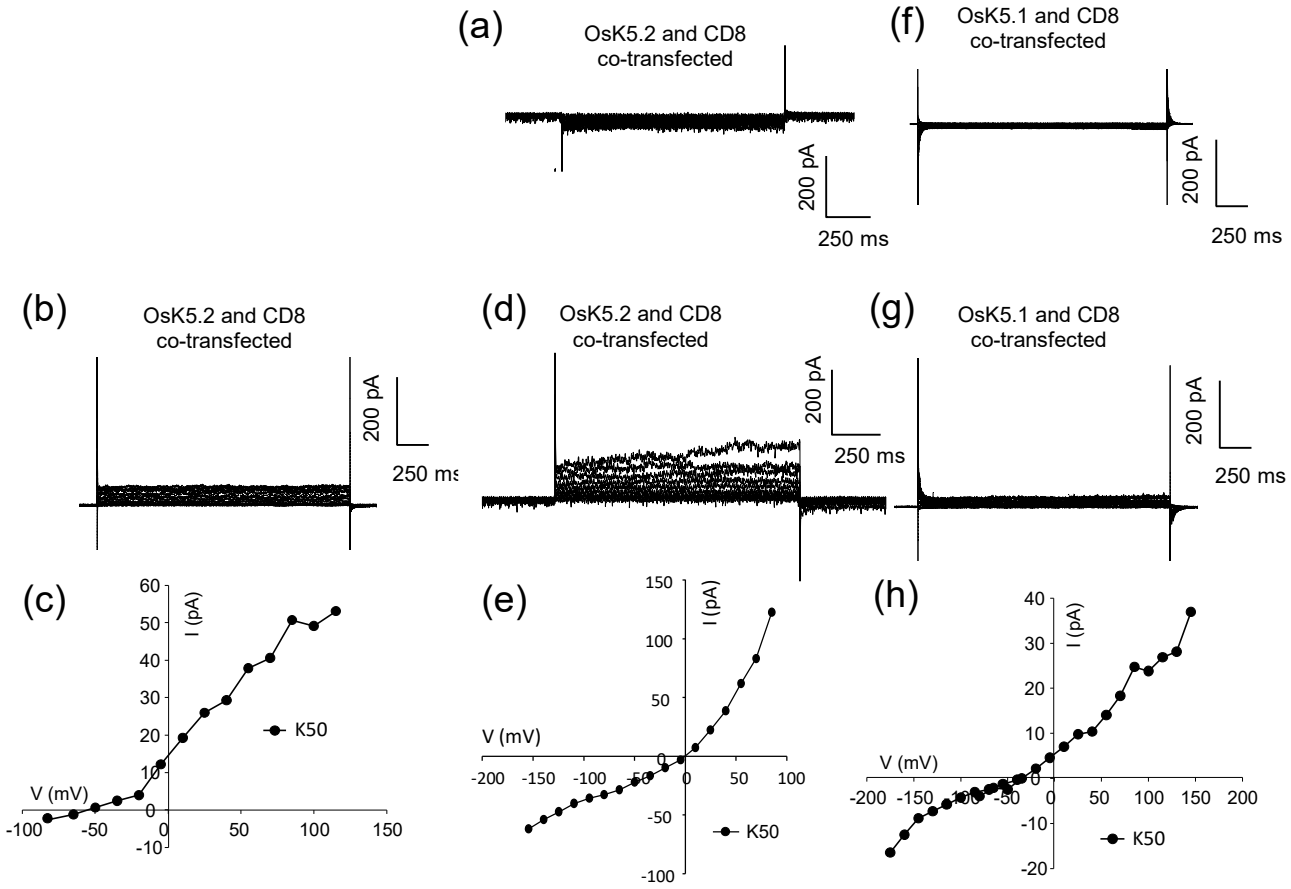

Figure V.7 Whole-cell patch-clamp experiments in COS-7 cells expressing OsK5.2 and OsK5.1.

Pipette and bath solutions used to record K^+ currents are given in the legend to Figure V.6.
(a, b, d) Examples of current traces recorded in OsK5.2 and CD8 co-transfected COS cells. (a) hyperpolarization steps were applied from −30 to −150 mV in -15 mV interval, from a holding potential at −30 mV; (b and d) depolarization steps were applied from −80 to +115 mV in 15 mV interval, from a holding potential at −60 mV. The bath solution contained 50 mM K^+.
(c) current-voltage (I-V) relationships from current traces shown in (a) and (b); (e) I-V relationships from current traces shown in (d).
(f and g) Examples of current traces recorded in OsK5.1 and CD8 co-transfected COS cells. (f) hyperpolarization steps were applied from −40 to −175 mV in -15 mV interval, from a holding potential at −60 mV; (g) depolarization steps were applied from −80 to +145 mV in 15 mV interval, from a holding potential at −60 mV. The bath solution contained 50 mM K^+.
(h) current-voltage relationships from current traces shown in (f) and (g).

outwardly-rectifying and, respectively, inwardly-rectifying currents. As expected, depolarization of the membrane from a holding voltage at −80 mV elicited activation of outward currents in COS-7 cells co-transfected with *GORK* and *CD8* (Figure V.6 d) with features similar to those obtained in *X. laevis* oocytes and Arabidopsis guard cells (Ache et al., 2000; Hosy et al., 2003). A typical slow kinetics of outward current activation during the voltage activation steps was observed (Figure V.6 d). Steady-state current-voltage (I-V) curves displayed a strong outward rectification (Figure V.6 e). Comparison of the I–V curves obtained in the presence of 10 or 50 mM K^+ in the external solution revealed that decreasing the concentration resulted in a negative shift of the activation potential of the outward currents, typically following that of the K^+ equilibrium potential (−69 mV and −28 mV, respectively with 10 mM and 50 mM K^+ in these experiments) (Figure V.6 e; Ache et al., 2000). In *SPIK* and *CD8* co-transfected COS-7 cells, activation of inward current elicited by hyperpolarization of the membrane (Figure V.6 g) resembled those previously reported in this expression system (Mouline et al., 2002). The steady-state I-V curve displayed a strong inward rectification (Figure V.6 h).

When we co-expressed *OsK5.2* and *CD8* or *OsK5.1* and *CD8* in COS-7 cells, however, only very small positive and negative currents, of similar amplitudes to those in control cells, were observed upon depolarization or hyperpolarization of the membrane, in the presence of 50 mM external K^+ (Figure V.7). In a few cells, an outwardly rectifying current that activated at voltage threshold close to the K^+ equilibrium potential (as for typical outwardly rectifying channels from the Shaker family, as mentioned above) could be observed upon cell transfection with *OsK5.2* (Figure V.7 b and c). The level of current was however in the range of that commonly observed in control cells, and the kinetics of current activation during voltage activation steps (instantaneous activation; Figure V.7 b) was not corresponding to that so far recorded through outward Shaker channels.

Absence of cytosolic interacting partner can be the reason for lack of functional expression of plant Shaker channels in heterologous expression systems (Xu et al., 2006; Li et al., 2014). Comparison of cytosolic domains of OsK5.1 and OsK5.2 with those of SKOR and GORK indicated that the N-terminal domain of OsK5.2 was quite different from that of its Arabidopsis homologues (Figure V.8). Indeed, two stretches of successions of positively charged residues adjacent to negatively charged ones were apparent, suggesting particular secondary structure, possibly dependent on interacting partner(s).

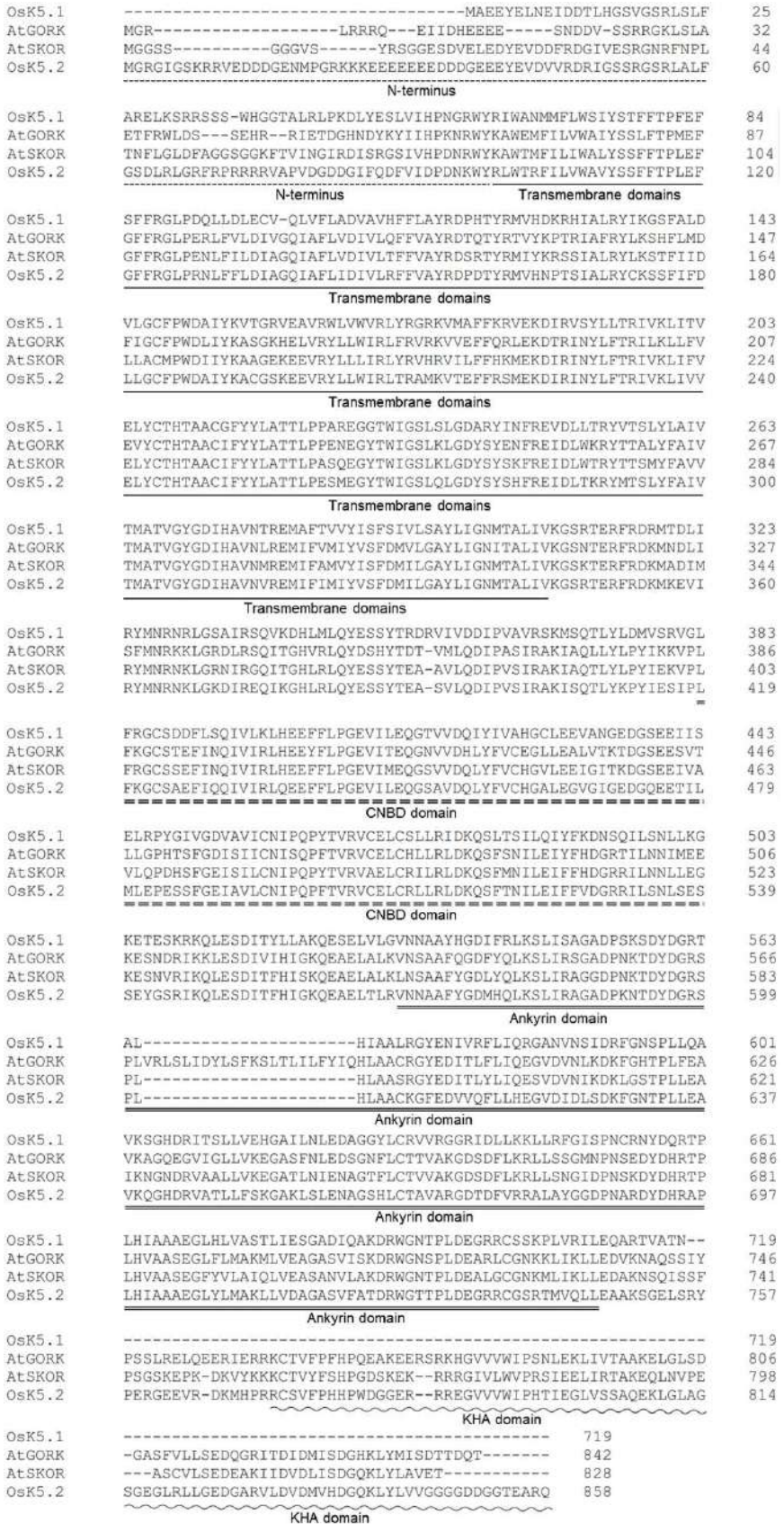

Figure V.8 Amino acid sequence alignment of OsK5.2 (XP_015644419.1), OsK5.1 (XP_015636107.1), SKOR (NP_186934.1), and GORK (NP_001332118.1) polypeptides. The regions corresponding to N-terminus (dashed single line), transmembrane domains (S1-S6) (solid single line), cyclic nucleotide-binding domain (CNBD domain) (dashed double line), ankyrin domain (solid double line), and KHA domain (wavy line) are indicated below the aligned sequences.

In order to get information on the functional properties of OsK5.2, I investigated whether the N-terminus of OsK5.2 caused its electrophysiological silence in COS-7 cells. I therefore replaced the N-terminus sequence of the rice *OsK5.2* cDNA by the N-terminus sequence of the Arabidopsis *GORK* cDNA, and thus constructed a chimeric Arabidopsis-rice K^+ channel. Interestingly, when co-transfection of the *CD8* marker and the chimeric *NterGORK-OsK5.2* construct in COS-7 cells was carried out, significant activation of outward K^+ currents upon depolarization of the membrane was elicited in whole-cell voltage-clamp experiments (Figure V.9 b), while very small negative currents not different from those in control cells were observed (Figure V.9 a). Although the level of current was smaller than that obtained upon expression of GORK in COS-7 cells, the kinetics of the outward current activation during voltage activation steps strongly resembled that of GORK (Figure V.6 d) or other outward Shaker channels. In addition, the I-V curve analysis indicated that the voltage threshold of outward current activation was close to −28 mV (the K^+ equilibrium potential in the presence of 50 mM K^+ in the external solution), as in the cells expressing GORK (Figure V.6 e and V.9 c). At last, since the Cl^- equilibrium potential was +28 mV in our conditions, positive currents at voltages more negative than +28 mV (Figure V.9 c) were undoubtedly carried by K^+. Taken together, these results strongly suggested that the chimeric NterGORK-OsK5.2 channel was functionally expressed in COS-7 cells as outwardly rectifying K^+ channel.

V.3 Discussion

The rice *OsK5.1* gene which belongs to the group #5 outward Shaker channel genes is annotated as *SKOR* orthologue in the rice genome. *AtSKOR* transcript has been shown to be present essentially in roots and pollen (Gaymard et al., 1998; Mouline et al., 2002; Arabidopsis eFP Browser at bar.utoronto.ca). Analysis of transgenic Arabidopsis plants expressing p*AtSKOR::GUS* also indicated that *AtSKOR* is mainly expressed in the roots, in pericycle and xylem parenchyma cells (Gaymard et al., 1998). Real-time RT-PCR analyses of *OsK5.1* transcript level and analyses of transgenic rice plants expressing p*OsK5.1::GUS* showed expression similarities between *AtSKOR* and the rice *OsK5.1*: expression essentially restricted to the roots (Figure V.1; Kim et al., 2015), and at the tissue level, in root pericycle and xylem parenchyma (Figure V.2). In addition, in contrast to *SKOR*, *OsK5.1* was well expressed in the root phloem (Figure V.2). Overall, the observed expression pattern of *OsK5.1*

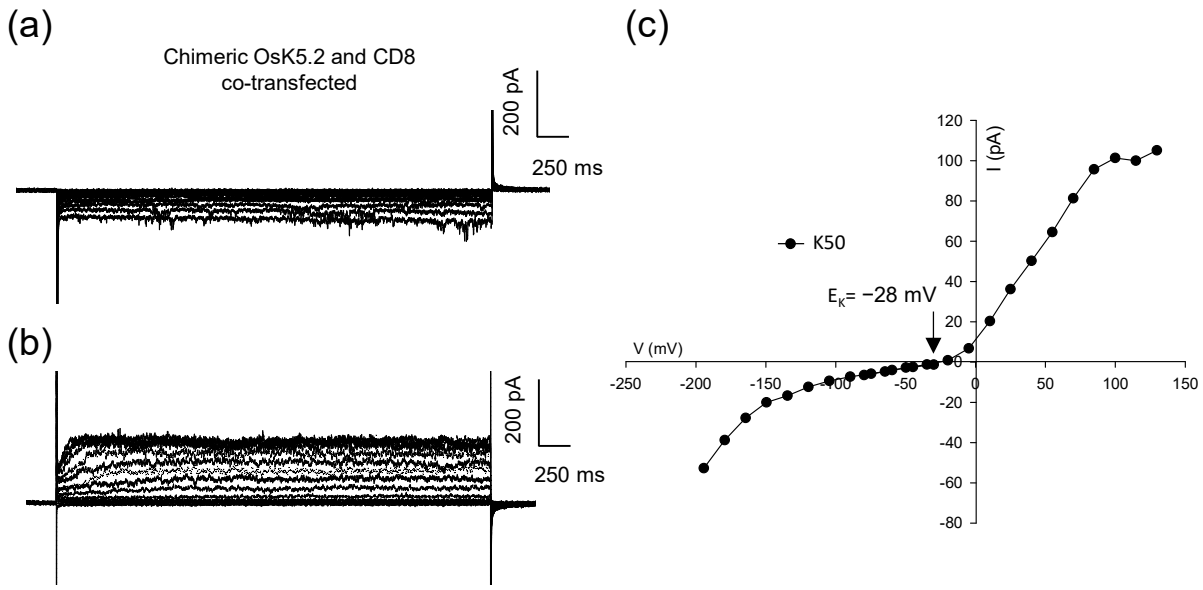

Figure V.9 Whole-cell patch clamp analysis of the chimeric OsK5.2 channel expressed in COS cells.

Pipette and bath solutions used to record K^+ currents as given in the legend to Figure V.6. K^+ concentration in the bath solution was 50 mM.

(a and b) Example of current traces recorded in a COS cell co-transfected with the chimeric *OsK5.2* channel and the *CD8* receptor. (a) hyperpolarization steps were applied from −30 to −195 mV in -15 mV interval, from a holding potential at −30 mV; (b) depolarization steps were applied from −80 to +130 mV in 15 mV interval, from a holding potential at −60 mV.

(c) Current-voltage relationships corresponding to the traces shown in (a) and (b).

rather supported the hypothesis that *OsK5.1* would be an *AtSKOR* orthologue, and *OsK5.1* could therefore be predicted to share similar functions to *AtSKOR* in translocation of K^+ from the roots to the shoots. Surprisingly, two *osk5.1* KO lines did not display any K^+ translocation phenotype (Figure V.3). Since in rice, in contrast to Arabidopsis, another Shaker channel, OsK5.2, was revealed to contribute to root-to-shoot K^+ translocation, we hypothesized that the absence of phenotype in *osk5.1* mutant plants may be due to redundant function between the two genes. An increase in *OsK5.2* transcript level may occur in *OsK5.1* KO lines, a point that should be examined in future analyses. Another hypothesis would be that despite the similarities between *OsK5.1* and *AtSKOR* with respect to gene expression patterns, the two encoded channels have quite different functional properties (*i.e.*, that OsK5.1 may not be a K^+ outward rectifier). Unfortunately, OsK5.1 was electrically silent in COS-7 cells, using whole-cell patch-clamp technique (Figure V.7), so did not appear to be functionally expressed in this expression system. The complementation of Arabidopsis *skor* mutant line with p*AtSKOR::OsK5.1*, however, restored K^+ concentration in the xylem sap (Figure V.5 b), which indicated that OsK5.1, like SKOR, displayed ability to secrete K^+ in the xylem sap when brought in the tissues where *SKOR* is expressed in Arabidopsis root. This supported the hypothesis that OsK5.1 is a SKOR-like K^+ outward rectifier.

While the complementation of the Arabidopsis *skor* mutant line with p*AtSKOR::OsK5.1* restored the K^+ concentration in the xylem sap, it did not restore K^+ contents in the shoots (Figure V.5 d). It could be hypothesized that the function of the rice channel OsK5.1 is not completely reminiscent of that of SKOR. However, it is worth noting that the plants from the two *atskor* lines complemented, instead, with p*AtSKOR::OsK5.2*, displayed the same phenotype as those expressing the p*AtSKOR::OsK5.1* construct (Figure V.5 a and c): complementation of the *atskor* K^+ concentration defect in the xylem sap, absence of complementation of the *atskor* K^+ content defect in the shoots. OsK5.2 was previously found to function as K^+ outward rectifier in rice guard cells (Nguyen et al., 2017), and we obtained here also indications of this type of feature for this channel upon expression of the chimeric NterGORK-OsK5.2 construct in COS-7 cells (Figure V.9). Therefore, we propose that both OsK5.1 and OsK5.2 channels are endowed with K^+ outward rectification property, and that the absence of complementation of the *atskor* K^+ content defect in the shoots is not primarily related to functional differences between AtSKOR and the homologous rice channels.

In Arabidopsis, *SKOR* transcript accumulation is restricted to the roots and the analysis of *AtSKOR* promoter activity in the transgenic plants expressing the *GUS* reporter also indicates root specificity (Gaymard et al., 1998). However, in the *skor* complemented lines expressing p*AtSKOR::OsK5.1* (line 20) or p*AtSKOR::OsK5.2* (lines 1 and 8), the *OsK5.1* and *OsK5.2* transcripts were detected not only in the roots but also in the shoots, in RT-PCR experiments (Figure V.4). We hypothesize that the expression of *OsK5.1* and *OsK5.2* in the roots of the complemented lines should be reminiscent of that of *AtSKOR*, in root pericycle and xylem parenchyma. Besides, it would be interesting to know the localization of cell-specific expression of *OsK5.1* and *OsK5.2* in the shoots of the complemented lines to infer the role that the two rice genes could play there. Due to time constraints, the expression levels of *OsK5.1* and *OsK5.2* in roots and shoots were not checked yet in all the produced complemented lines, though it would be worthwhile to examine whether the unexpected profile observed in the three analyzed lines (line 20 expressing *OsK5.1* and lines 1 and 8 expressing *OsK5.2*) was constantly detected in the transgenic lines. The unexpected expression profiles of *OsK5.1* and *OsK5.2* in corresponding complemented lines were not likely due to particular growth conditions since same expression results were obtained with plants fully grown in short-day condition (data not shown). One possible explanation for *OsK5.1* and *OsK5.2* transcripts found in leaves may be the presence of sequences in their cDNAs which influence the *SKOR* promoter activity. Whatever the explanation of the unexpected expression of *OsK5.1* and *OsK5.2* in leaves of Arabidopsis complemented lines, it is tempting to speculate that this probably contributes to explain the absence of restoration of K^+ contents in the shoots observed in the complemented lines, and that the contributions of *OsK5.1* and *OsK5.2* to xylem sap K^+ loading phenotype should be considered as a result of integration of K^+ transports in the whole plant.

Although the COS cell expression system could be used as an alternative expression system to the *X. laevis* oocytes for functional expression of the plant inward Shaker channel SPIK not functional in oocytes (Mouline et al., 2002; Figure V.6), here, we did not succeed to uncover the functional properties of OsK5.1 or those of the wild type OsK5.2 in this expression system (Figure V.7). Since the outward rectifying GORK channel appeared to be functional in COS cells (Figure V.6), we attempted a GORK-OsK5.2 chimera strategy to obtain functional expression. Cytosolic regions are believed in particular to be involved in channel activity regulation through phosphorylation processes and other mechanisms

involving interacting partners. As a first try, the N-terminal region of OsK5.2 was exchanged with that of GORK, this region in OsK5.2 appearing quite different from that of Arabidopsis outward Shaker, with successions of positively charged and negatively charged stretches (Figure V.8).

In Animal Shaker channels, a stretch of positively charged residues at the extremity of the N-terminus has been shown to produce a 'ball-and-chain' mechanism of inactivation (often referred to as the N-type inactivation): this sequence of amino acids (the inactivation domain) at the N-terminus of the channel occludes the cytoplasmic entrance of the channel pore and prevents ion permeation (Jan and Jan, 1992). It has been reported that the 'ball-and-chain' inactivation is abolished by a deletion of the inactivation domain at its N-terminus (Murrell-Lagnado & Aldrich, 1993; Zagotta, Hoshi, & Aldrich, 1990). The GORK outward K^+ channel in native Arabidopsis guard cells and root hairs displays inactivation of outward currents upon prolonged membrane depolarizing pulses (Ivashikina et al., 2001; Pei, Baizabal-Aguirre, Allen, & Schroeder, 1998). GORK polypeptide displays at the extremity of its N-terminus three positively charged residues followed by several negatively charged ones (Figure V.8), a pattern which is also found in OsK5.2 N-terminus in addition to other charged stretches. In our study, the construction of the chimeric OsK5.2 sequence, by replacing the N-terminus of the rice channel OsK5.2 by the N-terminus of the Arabidopsis outward channel GORK, allowed to examine the hypothesis that the repetitive stretches of charged residues in the N-terminus of OsK5.2 may result in strong (immediate) inactivation of the channel in COS-7 cells through a kind of 'ball-and-chain' mechanism, in absence of regulatory partner masking these charges. Upon co-expression of *CD8* and chimeric *Osk5.2* clones in COS-7 cells, an outward K^+ current strongly reminiscent of that mediated by Shaker outward rectifiers was recorded using the patch-clamp technique in whole-cell configuration (Figure V.9). Whether the chimeric channel displayed, like GORK in native Arabidopsis cells, inactivation upon prolonged depolarizing steps of voltage at lower external K^+ concentration and cytosolic pH conditions (Ivashikina et al., 2001; Pei et al., 1998) was not investigated yet. Finally, the chimera experiment result strongly supports the hypothesis that the N-terminus region of OsK5.2 contributes to prevent the functionality of the channel when heterologously expressed (at least in COS-7 cells but likely also in *Xenopus* oocytes), through a mechanism that remains to be elucidated, and which may involve a pore plugging by a 'ball-and-chain'. Recently, Fan *et al* (2020) conducted an interesting study on the gating of the MthK channel

from *Methanobacterium thermoautotrophicum*, an inward channel that lacks a voltage sensor, using structural and functional approaches. Normally, MthK channel was activated rapidly (within 1 millisecond) and was inactivated after a few seconds in the presence of Ca^{2+}. However, when the "ball" domain was deleted, MthK channel was still activated rapidly (within milliseconds) but then remained conductive during few seconds without pore plug, indicating that the N-terminal peptide is responsible for the inactivation of MthK channel by a 'ball-and-chain' mechanism (Fan et al., 2020). Thus, further interesting work will be needed in future for fully deciphering the mechanisms (and underlying sequences) which allow functional expression of the rice outward K^+ channels and obtaining detailed characterization of their functional properties.

Chapeter VI

Conclusion and perspectives

The aim of my thesis work was to study K^+ transport systems that might be responsible for long-distance K^+ transport within the plant, in a major crop, rice. My ultimate aim was that the information gained by this thesis work might be helpful to plant breeders for future development of more productive crop plants, especially under saline environments.

In my thesis work, one of the genes studied, *OsK5.2*, which is an outward Shaker K^+ channel gene, appeared to play a major role in plant growth in two limiting/adverse environmental conditions, short daylight cycle and saline soils. This gene therefore appears as a potentially interesting target for breeders. It would be interesting to further analyze impact of *osk5.2* loss of function on plant growth and yield in field conditions, in particular under salinity constraints. Also, assessment of ecotypic variability in expression level of this genes, in particular under saline conditions, would be useful to further evaluate the potential of this gene in future breeding programs.

The mechanisms of maintenance of K^+/Na^+ homeostasis in shoots have been extensively studied as this homeostasis is a key parameter of plant adaptation to saline conditions. However, the possible contribution of K^+ channels to this homeostasis had been very little assessed *in planta* previously. It was not clear whether the cellular context in saline conditions (*e.g.*, increased cytosolic Na^+ concentration, cell membrane polarization) would allow the maintaining of activity of K^+ channels (Thiel & Blatt, 1991; Nieves-Cordones et al., 2010). The present analyses, through reverse genetics, of OsK5.2 contribution to rice salt tolerance indicated that outward K^+ channels can still play major roles in saline conditions in outward K^+ fluxes in the plant, at least in the root stele for xylem sap K^+ loading and in guard cells for stomatal closure. The mechanistic analysis of OsK5.2 beneficial contribution to salt tolerance indicated that both functions of this channel, i.e., K^+ secretion to the xylem sap and the attenuation of leaf transpiration through its activity in stomatal guard cells, are important for salt tolerance, since their combination ensures a reduced flux of Na^+ translocated to the shoots and higher ratio of K^+ to Na^+ translocated. The contribution of OsK5.2 homologs in Arabidopsis, AtSKOR and AtGORK, to plant salt tolerance has not been analyzed so far. Since OsK5.2 cumulates the functions of AtSKOR (xylem sap K^+ loading) and of AtGORK (attenuation of leaf transpiration through stomatal closure), analyzing the contributions of AtSKOR and AtGORK to plant salt tolerance would enable to assess the contribution of the two physiological functions (xylem sap K^+ loading and the control of the transpiration stream) to plant tolerance to this stress, separately. On the other hand, it is interesting to note that in

legume plants (at least in *Medicago truncatula* and *Lotus japonicus*), a single outward Shaker channel gene exists in the genome, expressed in the root vasculature and the stomate (Drain et al., 2020). It can be therefore predicted that in these legume plants, the outward Shaker K^+ channel has a strong contribution to the plant salt tolerance, possibly even higher than in rice where another outward Shaker gene, *OsK5.1*, is expressed in the root stele and may contribute along with OsK5.2 to K^+ translocation to the shoots upon salt stress.

Comparatively to the molecular mechanisms involved in root K^+ uptake or stomatal movements, those controlling long-distance K^+ transport have been less studied. Here, the detailed expression pattern of *OsK5.2* in the rice vasculature coupled to reverse genetics analyses allowed us to take a step forward in the identification of possible roles of K^+ channels in long-distance K^+ transport. *OsK5.2* was shown to be expressed, through *promoter::GUS* fusion strategies, in phloem tissue in addition to xylem parenchyma. The availability of KO mutant lines for this gene provided us opportunity to start investigating the role of an outward K^+ channel in the phloem through reverse genetics. The fact that a growth phenotype was observed in *osk5.2* KO lines under conditions of limitation of daylight period, supported the hypothesis that OsK5.2 activity in the phloem was important for phloem sap transport to the sinks. The K^+ concentration in the phloem sap was lower in the *osk5.2* mutant plants than in WT plants, which may contribute to the reduced growth phenotype in mutant plants. Lower anion concentrations, in particular of carbohydrates from photosynthesis, may be associated to the lower K^+ concentration in *osk5.*2 plant phloem sap, which could also contribute to the growth phenotype. In order to better understand the *osk5.*2 plant growth phenotype under limitation of daylight period, it will be important to further investigate the content of the phloem sap, in sugars in particular. Although these analyses have to be completed, it already appears from the results I have obtained that the function of OsK5.2 in the phloem is different from that of the AKT2 channel, the only K^+ channel whose role was determined in this tissue. Although the activity of both channels in the phloem is important for plant growth under limitation of daylight period (Deeken et al., 2002; Shen et al., 2020), AKT2 was shown to affect indirectly the sucrose sap concentration (but not the sap K^+ concentration) by controlling the phloem cell membrane electric polarization, and hence the sucrose loading to the sap (Gajdanowicz et al., 2011), whereas OsK5.2 was shown to control the sap K^+ concentration, and maybe indirectly that of accompanying sucrose.

How OsK5.2 controls the K^+ concentration of the phloem sap has remained elusive at

the end of my PhD thesis work. I identified *OsK5.2* expression in leaf phloem, but it would be useful to determine whether *OsK5.2* is expressed in source leaves in the phloem or only in sink organs. In other words, whether OsK5.2 can play a role in K^+ unloading from the phloem in source leaves, or only in sinks.

While the mechanism by which OsK5.2 controlled the K^+ concentration in the phloem sap has still to be elucidated, my PhD thesis work revealed that OsK5.2 activity in the phloem has a major role in re-feeding the xylem sap with K^+ to maintain the whole-plant K^+ circulation. Since OsK5.2 is expressed in root companion cells, the simplest hypothesis was that the channel achieves this function by secreting K^+ to the apoplasm from root companion cells. Large amounts of K^+ are known to cycle throughout the plant, at least in standard growth conditions, so it could be expected that a channel-mediated K^+ secretion from the phloem sap plays crucial role in feeding the ascending part of the K^+ loop. The channel mediating orthologous function in Arabidopsis has not been evidenced yet. The weakly rectifying AKT2 channel has been initially hypothesized to be able to fulfil this function in root phloem (Lacombe et al., 2000), but this was not confirmed then.

OsK5.2 was shown additionally to be involved in initial secretion of K^+ to the stele, likely from xylem parenchyma (following root uptake), for xylem sap loading, like SKOR in Arabidopsis. My experiments with different transpiration regimes indicated that the relative contributions of OsK5.2 to xylem sap K^+ loading by initial secretion or recirculation, could strongly vary with environmental conditions. This revealed higher level of complexity in the role played by OsK5.2 in rice than in that played by SKOR in Arabidopsis in the control of xylem sap K^+ concentration. It would be interesting to explore additional environmental conditions (*e.g.*, K^+ deficiency, light limitation) to better understand how OsK5.2 activity is shared between initial K^+ supply to the loop and re-supply, depending on physiological needs. As a whole, my PhD thesis work on OsK5.2 channel thus provided interesting new findings and questions on K^+ channel-mediated regulation of K^+ cycling in the whole plant.

In rice, another putative K^+ efflux Shaker channel, OsK5.1, is present in the root stele, and could be hypothesized from its tissue expression pattern to fulfill the same function as SKOR in direct K^+ secretion to the xylem sap. Absence of any defect in K^+ concentration in the xylem sap in *osk5.1* KO plants in my analyses, was a bit surprising. It should however be noted that our experiments on OsK5.2 indicated that in standard growth conditions, K^+ in the xylem sap strongly originates from recirculation. So, the contribution from direct K^+ supply

was not major in these conditions, and knowing that OsK5.2 also contributes to the direct K^+ supply to the xylem sap, the contribution of OsK5.1 might be difficult to be detected. The role of OsK5.1 should also be examined in other environmental conditions such as 90% RH where the direct secretion of K^+ to the xylem sap was shown to be in contrast to standard conditions, higher than K^+ recirculation. The strategy of *atskor* mutant complementation by *OsK5.1* in Arabidopsis root (controlled by *AtSKOR* promoter), enabled us to confirm ability of OsK5.1 channel to secrete K^+ to the xylem sap, which supported the hypothesis that OsK5.1 actually fulfills this role in rice.

In a previous work by Thanh Hao NGUYEN in the host group, OsK5.2 and OsK5.1 were attempted to be expressed in *Xenopus laevis* oocytes, but no exogenous current in the oocytes was detected using the classical two-electrode voltage-clamp technique (Thanh Hao NGUYEN, thesis 2016). I therefore attempted to express OsK5.2 and OsK5.1 in COS-7 cells to study the functional properties using whole-cell patch-clamp technique, but no Shaker-like exogenous current was observed. This raises the question of the origin of these failures. The most likely explanation is the lack of information on how these two channels are regulated. It has been shown that three main kinase families can regulate the activity of K^+ membrane transport systems, including the SnRK2 family (SNF1-realted protein kinase 2), the SnRK3 family (SNF1-related protein kinase 3 or CIPK; calcineurin B-like-interacting protein kinase), and the CDPK/CPK family (calcium-dependent protein kinase) (Chérel & Gaillard, 2019). Several attempts were made to examine whether OsK5.2 and OsK5.1 can be activated in oocytes by co-expression with a number of the above-mentioned kinases, but none of them was successful (Thanh Hao NGUYEN, thesis 2016). Interestingly, failure of expression of an outward Shaker channel from plants in animal expression systems was not previously reported to my knowledge, suggesting existence of particular regulation in the rice (monocot?) outward Shaker channels. Our hypothesis then was that such regulation takes place in the cytosolic domains of the channel. The presence of highly charged (positively and negatively) stretches of sequences in the N-terminal domain of OsK5.2 suggested putative regulatory domain, possibly responsible for a kind of ball-and-chain mechanism of prevention of K^+ transport (MacKinnon, 2003). Interestingly, the replacement of the N-terminal domain of OsK5.2 by that of the Arabidopsis outward channel GORK allowed to confer functional expression with recording of typical Shaker outward K^+ currents. This result strongly supports the hypothesis that a sequence of amino acids in the N-terminus of OsK5.2 regulates the

channel activity. Thus, the next step would be to decipher the precise amino acids that result in the wild type channel lack of activity. This question could be examined by mutagenesis and electrophysiological experiments. Also, it would be very interesting to identify the regulation in plant cells which allows the channel activity (likely involving interacting partner(s)). My complementation experiments in Arabidopsis root indicated that OsK5.2 was also active in Arabidopsis, so that the regulation enabling the channel function was not specific to rice.

I could not achieve functional characterization of OsK5.1 in COS-7 cells in the framework of my PhD thesis. Similar strategy of replacement of cytosolic regions may turn out to be successful in future. Furthermore, as for OsK5.2, I obtained through complementation experiments in Arabidopsis evidence that this rice channel was functionally expressed in Arabidopsis (at least in the root stele), suggesting that Arabidopsis could eventually be used as an expression system for the electrophysiological characterization of OsK5.1, as well as OsK5.2 channels.

Thus, my initial attempts of heterologous expression of OsK5.2 and OsK5.1 channels suggest occurrence of particular post-translational regulations in these outward rice Shaker channels which will be worth further investigating in future.

References

Ache, P., Becker, D., Ivashikina, N., Dietrich, P., Roelfsema, M. R. G., & Hedrich, R. (2000). GORK, a delayed outward rectifier expressed in guard cells of Arabidopsis thaliana, is a K^+-selective, K^+-sensing ion channel. *FEBS Letters, 486*(2), 93-98.

Ainsworth, E. A., & Bush, D. R. (2011). Carbohydrate export from the leaf: a highly regulated process and target to enhance photosynthesis and productivity. *Plant Physiology, 155*(1), 64-69.

An, D., Chen, J. G., Gao, Y. Q., Li, X., Chao, Z. F., Chen, Z. R., ... & Chao, D. Y. (2017). AtHKT1 drives adaptation of Arabidopsis thaliana to salinity by reducing floral sodium content. *PLoS genetics, 13*(10), e1007086.

Aranda-Sicilia, M. N., Aboukila, A., Armbruster, U., Cagnac, O., Schumann, T., Kunz, H.-H., . . . Venema, K. (2016). Envelope K^+/H^+ antiporters AtKEA1 and AtKEA2 function in plastid development. *Plant Physiology, 172*(1), 441-449.

Armbruster, U., Carrillo, L. R., Venema, K., Pavlovic, L., Schmidtmann, E., Kornfeld, A., . . . Jonikas, M. C. (2014). Ion antiport accelerates photosynthetic acclimation in fluctuating light environments. *Nature communications, 5*(1), 1-8.

Armstrong, M. J., & Kirkby, E. A. (1979). Estimation of potassium recirculation in tomato plants by comparison of the rates of potassium and calcium accumulation in the tops with their fluxes in the xylem stream. *Plant Physiology, 63*(6), 1143-1148.

Asins, M. J., Villalta, I., Aly, M. M., Olias, R., Álvarez De Morales, P. A. Z., Huertas, R., ... & Belver, A. (2013). Two closely linked tomato HKT coding genes are positional candidates for the major tomato QTL involved in Na^+/K^+ homeostasis. *Plant, cell & environment, 36*(6), 1171-1191.

Atwell, B., & Steer, B. (1990). The effect of oxygen deficiency on uptake and distribution of nutrients in maize plants. *Plant and soil, 122*(1), 1-8.

Banuelos, M., Klein, R., Alexander-Bowman, S., & Rodríguez-Navarro, A. (1995). A potassium transporter of the yeast Schwanniomyces occidentalis homologous to the Kup system of Escherichia coli has a high concentrative capacity. *The EMBO journal, 14*(13), 3021-3027.

Banuelos, M. A., Garciadeblas, B., Cubero, B., & Rodrıguez-Navarro, A. (2002). Inventory and functional characterization of the HAK potassium transporters of rice. *Plant physiology, 130*(2), 784-795.

Barragán, V., Leidi, E. O., Andrés, Z., Rubio, L., De Luca, A., Fernández, J. A., . . . Pardo, J. M. (2012). Ion exchangers NHX1 and NHX2 mediate active potassium uptake into vacuoles to regulate cell turgor and stomatal function in Arabidopsis. *The Plant Cell, 24*(3), 1127-1142.

Baxter, I., Brazelton, J. N., Yu, D., Huang, Y. S., Lahner, B., Yakubova, E., ... & Salt, D. E. (2010). A coastal cline in sodium accumulation in Arabidopsis thaliana is driven by natural variation of the sodium transporter AtHKT1; 1. *PLoS Genet, 6*(11), e1001193.

Becker, D., Geiger, D., Dunkel, M., Roller, A., Bertl, A., Latz, A., ... & Hedrich, R. (2004). AtTPK4, an Arabidopsis tandem-pore K^+ channel, poised to control the pollen membrane voltage in a pH-and Ca^{2+}-dependent manner. *Proceedings of the National Academy of Sciences, 101*(44), 15621-15626.

Becker, D., Hoth, S., Ache, P., Wenkel, S., Roelfsema, M. R. G., Meyerhoff, O., ... & Hedrich, R. (2003). Regulation of the ABA-sensitive Arabidopsis potassium channel gene GORK in response to water stress. *FEBS letters, 554*(1-2), 119-126.

Berthomieu, P., Conéjéro, G., Nublat, A., Brackenbury, W. J., Lambert, C., Savio, C., ... & Casse, F. (2003). Functional analysis of AtHKT1 in Arabidopsis shows that Na^+ recirculation by the phloem is crucial for salt tolerance. *The EMBO journal, 22*(9), 2004-2014.

Booth, I. R., Epstein, W., Giffard, P. M., & Rowland, G. C. (1985). Roles of the trkB and trkC gene products of Escherichia coli in K^+ transport. *Biochimie, 67*(1), 83-89.

Bossemeyer, D., Schlösser, A., & Bakker, E. P. (1989). Specific cesium transport via the Escherichia coli Kup (TrkD) K^+ uptake system. *Journal of bacteriology, 171*(4), 2219-2221.

Boyer, P. D., Lardy, H. A., & Phillips, P. H. (1943). Further studies on the role of potassium and other ions in the phosphorylation of the adenylic system. *Journal of Biological Chemistry, 149*(2), 529-541.

Breteler, H., & Cate, C. H. H. T. (1978). Ionic balance of root-shoot nitrate transfer in dwarf bean. *Physiologia Plantarum, 42*(1), 53-56.

Brownell, P., & Crossland, C. (1972). The requirement for sodium as a micronutrient by species having the C4 dicarboxylic photosynthetic pathway. *Plant physiology, 49*(5), 794-797.

Brownell, P., & Wood, J. (1957). Sodium as an essential micronutrient element for Atriplex vesicaria, Heward. *Nature, 179*(4560), 635-636.

Byrt, C. S., Platten, J. D., Spielmeyer, W., James, R. A., Lagudah, E. S., Dennis, E. S., . . . Munns, R. (2007). HKT1;5-like cation transporters linked to Na^+ exclusion loci in wheat, Nax2 and Kna1. *Plant physiology, 143*(4), 1918-1928.

Caldana, C., Scheible, W.-R., Mueller-Roeber, B., & Ruzicic, S. (2007). A quantitative RT-PCR platform for high-throughput expression profiling of 2500 rice transcription factors. *Plant Methods, 3*(1), 7.

Campbell, M. T., Bandillo, N., Al Shiblawi, F. R. A., Sharma, S., Liu, K., Du, Q., . . . Lorenz, A. J. (2017). Allelic variants of OsHKT1; 1 underlie the divergence between indica and japonica subspecies of rice (Oryza sativa) for root sodium content. *PLoS genetics, 13*(6), e1006823.

Cao, Y., Jin, X., Huang, H., Derebe, M. G., Levin, E. J., Kabaleeswaran, V., . . . Weng, J. (2011). Crystal structure of a potassium ion transporter, TrkH. *Nature, 471*(7338), 336-340.

Chanroj, S., Wang, G., Venema, K., Zhang, M. W., Delwiche, C. F., & Sze, H. (2012). Conserved and diversified gene families of monovalent cation/H^+ antiporters from algae to flowering plants. *Frontiers in plant science, 3*, 25.

Cheeseman, J. M. (2015). The evolution of halophytes, glycophytes and crops, and its implications for food security under saline conditions. *New Phytologist, 206*(2), 557-570.

Chen, G., Hu, Q., Luo, L., Yang, T., Zhang, S., Hu, Y., . . . Xu, G. (2015). Rice potassium transporter O s HAK1 is essential for maintaining potassium-mediated growth and functions in salt tolerance over low and high potassium concentration ranges. *Plant, cell & environment, 38*(12), 2747-2765.

Chen, G., Liu, C., Gao, Z., Zhang, Y., Zhang, A., Zhu, L., ... & Qian, Q. (2018). Variation in the abundance of OsHAK1 transcript underlies the differential salinity tolerance of an indica and a japonica rice cultivar. *Frontiers in plant science, 8*, 2216.

Clarkson, D. T., & Hanson, J. B. (1980). The mineral nutrition of higher plants. *Annual review of plant physiology, 31*(1), 239-298.

Corratgé-Faillie, C., Jabnoune, M., Zimmermann, S., Véry, A.-A., Fizames, C., & Sentenac, H. (2010). Potassium and sodium transport in non-animal cells: the Trk/Ktr/HKT transporter family. *Cellular and Molecular Life Sciences, 67*(15), 2511-2532.

Chérel, I., & Gaillard, I. (2019). The complex fine-tuning of K^+ fluxes in plants in relation to osmotic and ionic abiotic stresses. *International journal of molecular sciences, 20*(3), 715.

Cramer, G. R., Lynch, J., Läuchli, A., & Epstein, E. (1987). Influx of Na^+, K^+, and Ca^{2+} into roots of salt-stressed cotton seedlings: effects of supplemental Ca^{2+}. *Plant physiology, 83*(3), 510-516.

Cuéllar, T., Pascaud, F., Verdeil, J. L., Torregrosa, L., Adam-Blondon, A. F., Thibaud, J. B., . . . Gaillard, I. (2010). A grapevine Shaker inward K^+ channel activated by the calcineurin B-like calcium sensor 1–protein kinase CIPK23 network is expressed in grape berries under drought stress conditions. *The Plant Journal, 61*(1), 58-69.

Debez, A., Hamed, K. B., Grignon, C., & Abdelly, C. (2004). Salinity effects on germination, growth, and seed production of the halophyte Cakile maritima. *Plant and soil, 262*(1-2), 179-189.

Deeken, R., Ache, P., Kajahn, I., Klinkenberg, J., Bringmann, G., & Hedrich, R. (2008). Identification of Arabidopsis thaliana phloem RNAs provides a search criterion for phloem-based transcripts hidden in complex datasets of microarray experiments. *The Plant Journal, 55*(5), 746-759.

Deeken, R., Geiger, D., Fromm, J., Koroleva, O., Ache, P., Langenfeld-Heyser, R., . . . Hedrich, R. (2002). Loss of the AKT2/3 potassium channel affects sugar loading into the phloem of Arabidopsis. *Planta, 216*(2), 334-344.

Deinlein, U., Stephan, A. B., Horie, T., Luo, W., Xu, G., & Schroeder, J. I. (2014). Plant salt-tolerance mechanisms. *Trends in plant science, 19*(6), 371-379.

Demidchik, V., & Maathuis, F. J. (2007). Physiological roles of nonselective cation channels in plants: from salt stress to signalling and development. *New Phytologist, 175*(3), 387-404.

Dobermann, A., & White, P. (1999). Strategies for nutrient management in irrigated and rainfed lowland rice systems. *In Resource management in rice systems: nutrients* (pp. 1-26): Springer.

Doyle, J. (1991). DNA protocols for plants. *In Molecular techniques in taxonomy* (pp. 283-293): Springer.

Drain, A., Thouin, J., Wang, L., Boeglin, M., Pauly, N., Nieves-Cordones, M., Gaillard, I., Véry, A.-A., & Sentenac, H. (2020). Functional characterization and physiological roles of the single Shaker outward K^+ channel in *Medicago truncatula*. *The Plant Journal, 102*(6), 1249-1265.

Dreyer, I., Gomez-Porras, J. L., & Riedelsberger, J. (2017). The potassium battery: a mobile energy source for transport processes in plant vascular tissues. *New Phytologist, 216*(4), 1049-1053.

Dreyer, I., Horeau, C., Lemaillet, G., Zimmermann, S., Bush, D. R., Rodríguez-Navarro, A., . . . Gaber, R. F. (1999). Identification and characterization of plant transporters using heterologous expression systems. *Journal of experimental botany*, 1073-1087.

Dreyer, I., Michard, E., Lacombe, B. t., & Thibaud, J.-B. (2001). A plant Shaker-like K^+ channel switches between two distinct gating modes resulting in either inward-rectifying or 'leak'current. *FEBS letters, 505*(2), 233-239.

Duby, G., Hosy, E., Fizames, C., Alcon, C., Costa, A., Sentenac, H., & Thibaud, J. B. (2008).

AtKC1, a conditionally targeted Shaker-type subunit, regulates the activity of plant K^+ channels. *The Plant Journal, 53*(1), 115-123.

Dunkel, M., Latz, A., Schumacher, K., Müller, T., Becker, D., & Hedrich, R. (2008). Targeting of vacuolar membrane localized members of the TPK channel family. *Molecular Plant, 1*(6), 938-949.

Durell, S. R., & Guy, H. R. (1999). Structural models of the KtrB, TrkH, and Trk1, 2 symporters based on the structure of the KcsA K^+ channel. *Biophysical Journal, 77*(2), 789-807.

Else, M. A., Hall, K. C., Arnold, G. M., Davies, W. J., & Jackson, M. B. (1995). Export of abscisic acid, 1-aminocyclopropane-1-carboxylic acid, phosphate, and nitrate from roots to shoots of flooded tomato plants (accounting for effects of xylem sap flow rate on concentration and delivery). *Plant Physiology, 107*(2), 377-384.

Eom, J.-S., Choi, S.-B., Ward, J. M., & Jeon, J.-S. (2012). The mechanism of phloem loading in rice (Oryza sativa). *Molecules and cells, 33*(5), 431-438.

Epstein, E. (1973). Mechanisms of ion transport through plant cell membranes. *International Review of Cytology, 34*, 123-168.

Epstein, E. (1976). Kinetics of ion transport and the carrier concept. Transport in Plants, II. Part B; Tissues and Organs (*Encyclopedia of Plant Physiology, New Series, volume 2B*), 70-94.

Epstein, E., Rains, D., & Elzam, O. (1963). Resolution of dual mechanisms of potassium absorption by barley roots. *Proceedings of the National Academy of Sciences of the United States of America*, 49(5), 684.

Evans, H. J., & Sorger, G. J. (1966). Role of mineral elements with emphasis on the univalent cations. *Annual review of plant physiology, 17*(1), 47-76.

Faiyue, B., Al-Azzawi, M. J., & Flowers, T. J. (2012). A new screening technique for salinity resistance in rice (Oryza sativa L.) seedlings using bypass flow. *Plant, Cell & Environment, 35*(6), 1099-1108.

Fan, C., Sukomon, N., Flood, E., Rheinberger, J., Allen, T. W., & Nimigean, C. M. (2020). Ball-and-chain inactivation in a calcium-gated potassium channel. *Nature, 580*(7802), 288-293.

Feng, H., Tang, Q., Cai, J., Xu, B., Xu, G., & Yu, L. (2019). Rice OsHAK16 functions in potassium uptake and translocation in shoot, maintaining potassium homeostasis and salt tolerance. *Planta, 250*(2), 549-561.

Flam-Shepherd, R,,.Huynh, W. Q,, Coskun, D., Hamam, A. M., Britto, D. T. & Kronzucker, H. J. (2018). Membrane fluxes, bypass flows, and sodium stress in rice: the influence of silicon. *Journal of Experimental Botany, 69*(7), 1679–1692.

Fricke, W., Akhiyarova, G., Wei, W., Alexandersson, E., Miller, A., Kjellbom, P. O., . . . Volkov, V. (2006). The short-term growth response to salt of the developing barley leaf. *Journal of Experimental Botany, 57*(5), 1079-1095.

Flowers, T. (1988). Chloride as a nutrient and as an osmoticum. *Advances in plant nutrition (USA)*.

Flowers, T., Troke, P., & Yeo, A. (1977). The mechanism of salt tolerance in halophytes. *Annual review of plant physiology, 28*(1), 89-121.

Fromm, J., & Eschrich, N. (1989). Correlation of ionic movements with phloem unloading and loading in barley leaves. *Plant Physiology and Biochemistry* (France).

Fu, H.-H., & Luan, S. (1998). AtKUP1: a dual-affinity K^+ transporter from Arabidopsis. *The Plant Cell, 10*(1), 63-73.

Furumoto, T., Yamaguchi, T., Ohshima-Ichie, Y., Nakamura, M., Tsuchida-Iwata, Y., Shimamura, M., . . . Westhoff, P. (2011). A plastidial sodium-dependent pyruvate transporter. *Nature, 476*(7361), 472-475.

Gajdanowicz, P., Michard, E., Sandmann, M., Rocha, M., Corrêa, L. G. G., Ramírez-Aguilar, S. J., . . . van Dongen, J. T. (2011). Potassium (K^+) gradients serve as a mobile energy source in plant vascular tissues. *Proceedings of the National Academy of Sciences, 108*(2), 864-869.

Garciadeblás, B., Senn, M. E., Bañuelos, M. A., & Rodríguez-Navarro, A. (2003). Sodium transport and HKT transporters: the rice model. *The Plant Journal, 34*(6), 788-801.

Gaymard, F., Cerutti, M., Horeau, C., Lemaillet, G., Urbach, S., Ravallec, M., . . . Thibaud, J.-B. (1996). The baculovirus/insect cell system as an alternative to Xenopus oocytes: First characterization of the AKT1 K^+ channel from Arabidopsis thaliana. *Journal of Biological Chemistry, 271*(37), 22863-22870.

Gaymard, F., Pilot, G., Lacombe, B., Bouchez, D., Bruneau, D., Boucherez, J., . . . Sentenac, H. (1998). Identification and disruption of a plant shaker-like outward channel involved in K^+ release into the xylem sap. *Cell, 94*(5), 647-655.

Geiger, D., Becker, D., Vosloh, D., Gambale, F., Palme, K., Rehers, M., . . . Hedrich, R. (2009). Heteromeric AtKC1· AKT1 channels in Arabidopsis roots facilitate growth under K^+-limiting conditions. *Journal of Biological Chemistry, 284*(32), 21288-21295.

Gierth, M., & Mäser, P. (2007). Potassium transporters in plants–involvement in K^+ acquisition, redistribution and homeostasis. *FEBS letters, 581*(12), 2348-2356.

Gierth, M., Mäser, P., & Schroeder, J. I. (2005). The potassium transporter AtHAK5 functions in K^+ deprivation-induced high-affinity K^+ uptake and AKT1 K^+ channel contribution to K^+ uptake kinetics in Arabidopsis roots. *Plant Physiology, 137*(3), 1105-1114.

Gomez, L., Bancel, D., Rubio, E., & Vercambre, G. (2007). The microplate reader: an efficient tool for the separate enzymatic analysis of sugars in plant tissues—validation of a micro-method. *Journal of the Science of Food and Agriculture, 87*(10), 1893-1905.

Grabov, A. (2007). Plant KT/KUP/HAK potassium transporters: single family–multiple functions. *Annals of botany, 99*(6), 1035-1041.

Gulbis, J. M., Zhou, M., Mann, S., & MacKinnon, R. (2000). Structure of the Cytoplasmic β Subunit-T1 Assembly of Voltage-Dependent K^+ Channels. *Science, 289*(5476), 123-127.

Han, M., Wu, W., Wu, W. H., & Wang, Y. (2016). Potassium transporter KUP7 is involved in K^+ acquisition and translocation in Arabidopsis root under K^+-limited conditions. *Molecular plant, 9*(3), 437-446.

Hauser, F., & Horie, T. (2010). A conserved primary salt tolerance mechanism mediated by HKT transporters: a mechanism for sodium exclusion and maintenance of high K^+/Na^+ ratio in leaves during salinity stress. *Plant, Cell & Environment, 33*(4), 552-565.

Hedrich, R., & Shabala, S. (2018). Stomata in a saline world. *Current opinion in plant biology, 46*, 87-95.

Hirsch, R. E., Lewis, B. D., Spalding, E. P., & Sussman, M. R. (1998). A role for the AKT1 potassium channel in plant nutrition. *Science, 280*(5365), 918-921.

Horie, T., Costa, A., Kim, T. H., Han, M. J., Horie, R., Leung, H. Y., . . . Schroeder, J. I.

(2007). Rice OsHKT2;1 transporter mediates large Na^+ influx component into K^+-starved roots for growth. *The EMBO journal, 26*(12), 3003-3014.

Hoshi, T., Zagotta, W. N., & Aldrich, R. W. (1990). Biophysical and molecular mechanisms of Shaker potassium channel inactivation. *Science, 250*(4980), 533-538.

Hosy, E., Vavasseur, A., Mouline, K., Dreyer, I., Gaymard, F., Porée, F., . . . Véry, A.-A. (2003). The Arabidopsis outward K^+ channel GORK is involved in regulation of stomatal movements and plant transpiration. *Proceedings of the National Academy of Sciences, 100*(9), 5549-5554.

Huang, X.-Y., Chao, D.-Y., Gao, J.-P., Zhu, M.-Z., Shi, M., & Lin, H.-X. (2009). A previously unknown zinc finger protein, DST, regulates drought and salt tolerance in rice via stomatal aperture control. *Genes & Development 23*, 1805–1817.

Huertas, R., Rubio, L., Cagnac, O., García-Sánchez, M. J., Alché, J. de D, Venema, K., … Rodríguez-Rosales, M. P. (2013). The K^+/H^+ antiporter LeNHX2 increases salt tolerance by improving K^+ homeostasis in transgenic tomato. *Plant, Cell and Environment, 36*, 2135–2149.

Long-Tang, H., Li-Na, Z., Li-Wei, G., Anne-Aliénor, V., Hervé, S., & Yi-Dong, Z. (2018). Constitutive expression of CmSKOR, an outward K^+ channel gene from melon, in Arabidopsis thaliana involved in saline tolerance. *Plant Science, 274*, 492-502.

Ismail, A. M., & Horie, T. (2017). Genomics, physiology, and molecular breeding approaches for improving salt tolerance. *Annual Review of Plant Biology, 68*, 405-434.

Ivashikina, N., Becker, D., Ache, P., Meyerhoff, O., Felle, H. H., & Hedrich, R. (2001). K^+ channel profile and electrical properties of Arabidopsis root hairs. *FEBS Letters, 508*(3), 463-469.

Jackson, M. (1993). Are plant hormones involved in root to shoot communication? *Advances in botanical research, 19*, 103-187.

James, R. A., Blake, C., Byrt, C. S., & Munns, R. (2011). Major genes for Na^+ exclusion, Nax1 and Nax2 (wheat HKT1;4 and HKT1;5), decrease Na^+ accumulation in bread wheat leaves under saline and waterlogged conditions. *Journal of experimental botany, 62*(8), 2939-2947.

Jan, L. Y., & Jan, Y. N. (1992). Structural elements involved in specific K^+ channel functions. *Annual review of physiology, 54*(1), 537-555.

Jayakannan, M., Bose, J., Babourina, O., Rengel, Z., & Shabala, S. (2013). Salicylic acid improves salinity tolerance in Arabidopsis by restoring membrane potential and preventing salt-induced K^+ loss via a GORK channel. *Journal of Experimental Botany, 64*(8), 2255-2268.

Jeanguenin, L., Alcon, C., Duby, G., Boeglin, M., Chérel, I., Gaillard, I., . . . Véry, A. A. (2011). AtKC1 is a general modulator of Arabidopsis inward Shaker channel activity. *The Plant Journal, 67*(4), 570-582.

Jeschke, W. D. (1984). Effects of transpiration on potassium and sodium fluxes in root cells and the regulation of ion distribution between roots and shoots of barley seedlings. *Journal of plant physiology, 117*(3), 267-285.

Jeschke, W. D., & Pate, J. S. (1991). Cation and chloride partitioning through xylem and phloem within the whole plant of Ricinus communis L. under conditions of salt stress. *Journal of Experimental Botany, 42*(9), 1105-1116.

Jeschke, W. D., Pate, J. S., & Atkins, C. A. (1987). Partitioning of K^+, Na^+, Mg^{++}, and Ca^{++} through xylem and phloem to component organs of nodulated white lupin under mild salinity. *Journal of plant physiology, 128*(1-2), 77-93.

Jezek, M., & Blatt, M. R. (2017). The membrane transport system of the guard cell and its integration for stomatal dynamics. *Plant Physiology, 174*(2), 487-519.

Jiang, Z., Zhou, X., Tao, M., Yuan, F., Liu, L., Wu, F., . . . Liu, F. (2019). Plant cell-surface GIPC sphingolipids sense salt to trigger Ca^{2+} influx. *Nature, 572*(7769), 341-346.

Jurman, M. E., Boland, L. M., Liu, Y., & Yellen, G. (1994). Visual identification of individual transfected cells for electrophysiology using antibody-coated beads. *Biotechniques, 17*(5), 876-881.

Kato, Y., Sakaguchi, M., Mori, Y., Saito, K., Nakamura, T., Bakker, E. P., . . . Uozumi, N. (2001). Evidence in support of a four transmembrane-pore-transmembrane topology model for the Arabidopsis thaliana Na^+/K^+ translocating AtHKT1 protein, a member of the superfamily of K^+ transporters. *Proceedings of the National Academy of Sciences, 98*(11), 6488-6493.

Khan, I., Mohamed, S., Regnault, T., Mieulet, D., Guiderdoni, E., Sentenac, H., & Véry, A.-A. (2020). Constitutive contribution by the rice OsHKT1;4 Na^+ transporter to xylem sap desalinization and low Na^+ accumulation in young leaves under low as high external Na^+ conditions. *Frontiers in plant science, 11*, 1130.

Kim, H. Y., Choi, E. H., Min, M. K., Hwang, H., Moon, S. J., Yoon, I., ... & Kim, B. G. (2015). Differential gene expression of two outward-rectifying shaker-like potassium channels OsSKOR and OsGORK in rice. *Journal of plant biology, 58*(4), 230-235.

Kim, E. J., Kwak, J. M., Uozumi, N., & Schroeder, J. I. (1998). AtKUP1: an Arabidopsis gene encoding high-affinity potassium transport activity. *The Plant Cell, 10*(1), 51-62.

King, R., & Zeevaart, J. (1974). Enhancement of phloem exudation from cut petioles by chelating agents. *Plant Physiology, 53*(1), 96-103.

Kobayashi, N. I., Yamaji, N., Yamamoto, H., Okubo, K., Ueno, H., Costa, A., ... & Horie, T. (2017). OsHKT1;5 mediates Na^+ exclusion in the vasculature to protect leaf blades and reproductive tissues from salt toxicity in rice. *The Plant Journal, 91*(4), 657-670.

Krishnasamy, K., Bell, R., & Ma, Q. (2014). Wheat responses to sodium vary with potassium use efficiency of cultivars. *Frontiers in Plant Science, 5*, 631.

Kunz, H.-H., Gierth, M., Herdean, A., Satoh-Cruz, M., Kramer, D. M., Spetea, C., & Schroeder, J. I. (2014). Plastidial transporters KEA1,-2, and-3 are essential for chloroplast osmoregulation, integrity, and pH regulation in Arabidopsis. *Proceedings of the National Academy of Sciences, 111*(20), 7480-7485.

Lacombe, B., Pilot, G., Michard, E., Gaymard, F., Sentenac, H., & Thibaud, J.-B. (2000). A shaker-like K^+ channel with weak rectification is expressed in both source and sink phloem tissues of Arabidopsis. *The Plant Cell, 12*(6), 837-851.

Lagarde, D., Basset, M., Lepetit, M., Conejero, G., Gaymard, F., Astruc, S., & Grignon, C. (1996). Tissue-specific expression of Arabidopsis AKT1 gene is consistent with a role in K^+ nutrition. *The Plant Journal, 9*(2), 195-203.

Lang, A. (1983). Turgor-regulated translocation. *Plant, cell & environment, 6*(9), 683-689.

Lea, P. J., & Morot-Gaudry, J. F. (Eds.). (2001). *Plant nitrogen*. Springer Science & Business Media.

Lebaudy, A., Hosy, E., Simonneau, T., Sentenac, H., Thibaud, J. B., & Dreyer, I. (2008a). Heteromeric K^+ channels in plants. *The Plant Journal, 54*(6), 1076-1082.

Lebaudy, A., Vavasseur, A., Hosy, E., Dreyer, I., Leonhardt, N., Thibaud, J.-B., . . . Sentenac, H. (2008b). Plant adaptation to fluctuating environment and biomass production are

strongly dependent on guard cell potassium channels. *Proceedings of the National Academy of Sciences, 105*(13), 5271-5276.

Lebaudy, A., Véry, A.-A., & Sentenac, H. (2007). K^+ channel activity in plants: genes, regulations and functions. *FEBS letters, 581*(12), 2357-2366.

Leidi, E. O., Barragán, V., Rubio, L., El-Hamdaoui, A., Ruiz, M. T., Cubero, B., ... & Pardo, J. M. (2010). The AtNHX1 exchanger mediates potassium compartmentation in vacuoles of transgenic tomato. *The Plant Journal, 61*(3), 495-506.

Li, H., Yu, M., Du, X.-Q., Wang, Z.-F., Wu, W.-H., Quintero, F. J., . . . Wang, Y. (2017). NRT1. 5/NPF7. 3 functions as a proton-coupled H^+/K^+ antiporter for K^+ loading into the xylem in Arabidopsis. *The Plant Cell, 29*(8), 2016-2026.

Li, J., Long, Y., Qi, G.-N., Li, J., Xu, Z.-J., Wu, W.-H., & Wang, Y. (2014). The Os-AKT1 channel is critical for K^+ uptake in rice roots and is modulated by the rice CBL1-CIPK23 complex. *The Plant Cell, 26*(8), 3387-3402.

Lin, S.-H., Kuo, H.-F., Canivenc, G., Lin, C.-S., Lepetit, M., Hsu, P.-K., . . . Tsai, C.-B. (2008). Mutation of the Arabidopsis NRT1. 5 nitrate transporter causes defective root-to-shoot nitrate transport. *The Plant Cell, 20*(9), 2514-2528.

Long, S. B., Campbell, E. B., & MacKinnon, R. (2005). Crystal structure of a mammalian voltage-dependent Shaker family K^+ channel. *Science, 309*(5736), 897-903.

Luan, S. (2009). The CBL–CIPK network in plant calcium signaling. *Trends in plant science, 14*(1), 37-42.

Lucas, W. J., Yoo, B.-C., & Kragler, F. (2001). RNA as a long-distance information macromolecule in plants. *Nature Reviews Molecular Cell Biology, 2*(11), 849-857.

Maathuis, F., & Sanders, D. (1994). Mechanism of high-affinity potassium uptake in roots of Arabidopsis thaliana. *Proceedings of the National Academy of Sciences, 91*(20), 9272-9276.

Maathuis, F. J. (2006). cGMP modulates gene transcription and cation transport in Arabidopsis roots. *The Plant Journal, 45*(5), 700-711.

Maathuis, F. J., Ahmad, I., & Patishtan, J. (2014). Regulation of Na^+ fluxes in plants. *Frontiers in Plant Science, 5*, 467.

Maathuis, F. J., & Amtmann, A. (1999). K^+ nutrition and Na^+ toxicity: the basis of cellular K^+/Na^+ ratios. *Annals of Botany, 84*(2), 123-133.

MacKinnon, R. (2003). Potassium channels. *FEBS letters, 555*(1), 62-65.

Marschner, H. (1995). *Mineral nutrition of higher plants*. 2nd. Edn. Academic Pres.

Marschner, H. (2011). *Marschner's mineral nutrition of higher plants*. Academic press.

Mäser, P., Hosoo, Y., Goshima, S., Horie, T., Eckelman, B., Yamada, K., . . . Oiki, S. (2002). Glycine residues in potassium channel-like selectivity filters determine potassium selectivity in four-loop-per-subunit HKT transporters from plants. *Proceedings of the National Academy of Sciences, 99*(9), 6428-6433.

Mäser, P., Thomine, S., Schroeder, J. I., Ward, J. M., Hirschi, K., Sze, H., . . . Sanders, D. (2001). Phylogenetic relationships within cation transporter families of Arabidopsis. *Plant Physiology, 126*(4), 1646-1667.

Mengel, K., & Haeder, H.-E. (1977). Effect of potassium supply on the rate of phloem sap exudation and the composition of phloem sap of Ricinus communis. *Plant Physiology, 59*(2), 282-284.

Mian, A., Oomen, R. J. F. J., Isayenkov, S., Sentenac, H., Maathuis, F. J. M., & Véry, A.-A. (2011) Over-expression of an Na^+- and K^+-permeable HKT transporter in barley improves salt tolerance. *The Plant Journal, 68*, 468–479.

Michelet, B., & Boutry, M. (1995). The plasma membrane H^+-ATPase (A highly regulated enzyme with multiple physiological functions). *Plant physiology, 108*(1), 1.
Mouline, K., Véry, A.-A., Gaymard, F., Boucherez, J., Pilot, G., Devic, M., . . . Sentenac, H. (2002). Pollen tube development and competitive ability are impaired by disruption of a Shaker K^+ channel in Arabidopsis. *Genes & development, 16*(3), 339-350.
Mumm, P., Wolf, T., Fromm, J., Roelfsema, M. R. G., & Marten, I. (2011). Cell type-specific regulation of ion channels within the maize stomatal complex. *Plant and Cell Physiology, 52*(8), 1365-1375.
Munns, R. (1993). Physiological processes limiting plant growth in saline soils: some dogmas and hypotheses. *Plant, Cell & Environment, 16*(1), 15-24.
Munns, R. (2005). Genes and salt tolerance: bringing them together. *New Phytologist, 167*(3), 645-663.
Munns, R., & Tester, M. (2008). Mechanisms of salinity tolerance. *Annu. Rev. Plant Biol., 59*, 651-681.
Murrell-Lagnado, R. D., & Aldrich, R. W. (1993). Interactions of amino terminal domains of Shaker K channels with a pore blocking site studied with synthetic peptides. *The Journal of general physiology, 102*(6), 949-975.
Nadwodnik, J., & Lohaus, G. (2008). Subcellular concentrations of sugar alcohols and sugars in relation to phloem translocation in Plantago major, Plantago maritima, Prunus persica, and Apium graveolens. *Planta, 227*(5), 1079-1089.
Nakamura, R. L., McKendree Jr, W. L., Hirsch, R. E., Sedbrook, J. C., Gaber, R. F., & Sussman, M. R. (1995). Expression of an Arabidopsis potassium channel gene in guard cells. *Plant physiology, 109*(2), 371-374.
Nguyen, T. H., Huang, S., Meynard, D., Chaine, C., Michel, R., Roelfsema, M. R. G., ... & Véry, A. A. (2017). A dual role for the OsK5. 2 ion channel in stomatal movements and K^+ loading into xylem sap. *Plant physiology, 174*(4), 2409-2418.
Nieves-Cordones, M., Alemán, F., Martínez, V., & Rubio, F. (2010). The Arabidopsis thaliana HAK5 K^+ transporter is required for plant growth and K^+ acquisition from low K^+ solutions under saline conditions. *Molecular plant, 3*(2), 326-333.
Nieves-Cordones, M., Alemán, F., Martínez, V., & Rubio, F. (2014). K^+ uptake in plant roots. The systems involved, their regulation and parallels in other organisms. *Journal of Plant physiology, 171*(9), 688-695.
Nieves-Cordones, M., Al Shiblawi, F. R., & Sentenac, H. (2016). Roles and transport of sodium and potassium in plants. *In The alkali metal ions: Their role for life* (pp. 291-324): Springer.
Nieves-Cordones, M., Martínez, V., Benito, B., & Rubio, F. (2016). Comparison between Arabidopsis and rice for main pathways of K^+ and Na^+ uptake by roots. *Frontiers in Plant Science, 7*, 992.
Nieves-Cordones, M., Mohamed, S., Tanoi, K., Kobayashi, N. I., Takagi, K., Vernet, A., . . . Véry, A. A. (2017). Production of low-Cs^+ rice plants by inactivation of the K^+ transporter OsHAK 1 with the CRISPR-Cas system. *The Plant Journal, 92*(1), 43-56.
Nikalje, G. C., & Suprasanna, P. (2018). Coping with metal toxicity–cues from halophytes. *Frontiers in Plant Science, 9*, 777.
Oda, Y., Kobayashi, N. I., Tanoi, K., Ma, J. F., Itou, Y., Katsuhara, M., . . . Horie, T. (2018). T-DNA tagging-based gain-of-function of OsHKT1; 4 reinforces Na exclusion from leaves and stems but triggers Na toxicity in roots of rice under salt stress.

International journal of molecular sciences, 19(1), 235.
Ordoñez, N. M., Marondedze, C., Thomas, L., Pasqualini, S., Shabala, L., Shabala, S., & Gehring, C. (2014). Cyclic mononucleotides modulate potassium and calcium flux responses to H2O2 in Arabidopsis roots. *FEBS letters, 588*(6), 1008-1015.
Pandey, S., Zhang, W., & Assmann, S. M. (2007). Roles of ion channels and transporters in guard cell signal transduction. *FEBS letters, 581*(12), 2325-2336.
Parida, A. K., & Das, A. B. (2005). Salt tolerance and salinity effects on plants: a review. *Ecotoxicology and environmental safety, 60*(3), 324-349.
Pate, J. S., & Jeschke, W. D. (1995). Role of stems in transport, storage, and circulation of ions and metabolites by the whole plant. *In Plant Stems* (pp. 177-I): Elsevier.
Patrick, J. (1997). Phloem unloading: sieve element unloading and post-sieve element transport. *Annual review of plant biology, 48*(1), 191-222.
Pei, Z. M., Baizabal-Aguirre, V. M., Allen, G. J., & Schroeder, J. I. (1998). A transient outward-rectifying K^+ channel current down-regulated by cytosolic Ca^{2+} in Arabidopsis thaliana guard cells. *Proceedings of the National Academy of Sciences, 95*(11), 6548-6553.
Pilot, G., Gaymard, F., Mouline, K., Chérel, I., & Sentenac, H. (2003). Regulated expression of Arabidopsis Shaker K^+ channel genes involved in K^+ uptake and distribution in the plant. *Plant Molecular Biology, 51*, 773–787.
Pilot, G., Lacombe, B. t., Gaymard, F., Chérel, I., Boucherez, J., Thibaud, J.-B., & Sentenac, H. (2001). Guard Cell Inward K^+ Channel Activity inArabidopsis Involves Expression of the Twin Channel Subunits KAT1 and KAT2. *Journal of Biological Chemistry, 276*(5), 3215-3221.
Pilot, G., Pratelli, R., Gaymard, F., Meyer, Y., & Sentenac, H. (2003). Five-group distribution of the Shaker-like K^+ channel family in higher plants. *Journal of Molecular Evolution, 56*(4), 418-434.
Platten, J. D., Cotsaftis, O., Berthomieu, P., Bohnert, H., Davenport, R. J., Fairbairn, D. J., . . . Luan, S. (2006). Nomenclature for HKT transporters, key determinants of plant salinity tolerance. *Trends in plant science, 11*(8), 372-374.
Proe, M., Midwood, A., & Craig, J. (2000). Use of stable isotopes to quantify nitrogen, potassium and magnesium dynamics in young Scots pine (Pinus sylvestris). *The New Phytologist, 146*(3), 461-469.
Quintero, F. J., & Blatt, M. R. (1997). A new family of K^+ transporters from Arabidopsis that are conserved across phyla. *FEBS letters, 415*(2), 206-211.
Ragel, P., Raddatz, N., Leidi, E. O., Quintero, F. J., & Pardo, J. M. (2019). Regulation of K^+ nutrition in plants. *Frontiers in Plant Science, 10*, 281.
Regmi, K. C., Zhang, S., & Gaxiola, R. A. (2016). Apoplasmic loading in the rice phloem supported by the presence of sucrose synthase and plasma membrane-localized proton pyrophosphatase. *Annals of botany, 117*(2), 257-268.
Reintanz, B., Szyroki, A., Ivashikina, N., Ache, P., Godde, M., Becker, D., . . . Hedrich, R. (2002). AtKC1, a silent Arabidopsis potassium channel α-subunit modulates root hair K^+ influx. *Proceedings of the National Academy of Sciences, 99*(6), 4079-4084.
Ren, Z.-H., Gao, J.-P., Li, L.-G., Cai, X.-L., Huang, W., Chao, D.-Y., . . . Lin, H.-X. (2005). A rice quantitative trait locus for salt tolerance encodes a sodium transporter. *Nature genetics, 37*(10), 1141-1146.
Rennie, E. A., & Turgeon, R. (2009). A comprehensive picture of phloem loading strategies. *Proceedings of the National Academy of Sciences, 106*(33), 14162-14167.

Roberts SK, Tester M (1995) Inward and outward K^+-selective currents in the plasma membrane of protoplasts from maize root cortex and stele. *The Plant Journal, 8*, 811-825.

Robinson, M. F., Véry, A.-A., Sanders, D., & Mansfield, T. A. (1997). How can stomata contribute to salt tolerance? *Annals of botany, 80*(4), 387-393.

Roelfsema, M. R. G., & Hedrich, R. (2005). In the light of stomatal opening: new insights into 'the Watergate'. *New Phytologist, 167*(3), 665-691.

Rubio, F., Nieves-Cordones, M., Horie, T., & Shabala, S. (2020). Doing 'business as usual' comes with a cost: evaluating energy cost of maintaining plant intracellular K^+ homeostasis under saline conditions. *New Phytologist, 225*(3), 1097-1104.

Rubio, F., Santa-María, G. E., & Rodríguez-Navarro, A. (2000). Cloning of Arabidopsis and barley cDNAs encoding HAK potassium transporters in root and shoot cells. *Physiologia Plantarum, 109*(1), 34-43.

Santa-María, G. E., Oliferuk, S., & Moriconi, J. I. (2018). KT-HAK-KUP transporters in major terrestrial photosynthetic organisms: A twenty years tale. *Journal of plant physiology, 226*, 77-90.

Santa-María, G. E., Rubio, F., Dubcovsky, J., & Rodríguez-Navarro, A. (1997). The HAK1 gene of barley is a member of a large gene family and encodes a high-affinity potassium transporter. *The Plant Cell, 9*(12), 2281-2289.

Schleyer, M., & Bakker, E. P. (1993). Nucleotide sequence and 3'-end deletion studies indicate that the K(+)-uptake protein kup from Escherichia coli is composed of a hydrophobic core linked to a large and partially essential hydrophilic C terminus. *Journal of bacteriology, 175*(21), 6925-6931.

Schroeder, J. I., Allen, G. J., Hugouvieux, V., Kwak, J. M., & Waner, D. (2001). Guard cell signal transduction. *Annual review of plant biology, 52*(1), 627-658.

Schurr, U., & Schulze, E. D. (1995). The concentration of xylem sap constituents in root exudate, and in sap from intact, transpiring castor bean plants (Ricinus communis L.). *Plant, cell & environment, 18*(4), 409-420.

Shabala, L., Mackay, A., Tian, Y., Jacobsen, S. E., Zhou, D., & Shabala, S. (2012). Oxidative stress protection and stomatal patterning as components of salinity tolerance mechanism in quinoa (Chenopodium quinoa). *Physiologia Plantarum, 146*(1), 26-38.

Shabala, S., & Cuin, T. A. (2008). Potassium transport and plant salt tolerance. *Physiologia Plantarum, 133*(4), 651-669.

Shen, Y., Shen, L., Shen, Z., Jing, W., Ge, H., Zhao, J., & Zhang, W. (2015). The potassium transporter OsHAK21 functions in the maintenance of ion homeostasis and tolerance to salt stress in rice. *Plant, cell & environment, 38*(12), 2766-2779.

Shen, L., Tian, Q., Yang, L., Zhang, H., Shi, Y., Shen, Y., . . . Zhang, W. (2020). Phosphatidic acid directly binds with rice potassium channel OsAKT2 to inhibit its activity. *The Plant Journal, 102*(4), 649-665.

Shi, H., Ishitani, M., Kim, C., & Zhu, J.-K. (2000). The Arabidopsis thaliana salt tolerance gene SOS1 encodes a putative Na^+/H^+ antiporter. *Proceedings of the National Academy of Sciences, 97*(12), 6896-6901.

Song, J., Chen, M., Feng, G., Jia, Y., Wang, B., & Zhang, F. (2009). Effect of salinity on growth, ion accumulation and the roles of ions in osmotic adjustment of two populations of Suaeda salsa. *Plant and soil, 314*(1-2), 133-141.

Stephan, A. B., Kunz, H.-H., Yang, E., & Schroeder, J. I. (2016). Rapid hyperosmotic-induced

Ca^{2+} responses in Arabidopsis thaliana exhibit sensory potentiation and involvement of plastidial KEA transporters. *Proceedings of the National Academy of Sciences, 113*(35), E5242-E5249.

Suelter, C. (1970). Enzymes activated by monovalent cations. *Science, 168*(3933), 789-795.

Sunarpi, Horie, T., Motoda, J., Kubo, M., Yang, H., Yoda, K., Horie, R., ... & Uozumi, N. (2005). Enhanced salt tolerance mediated by AtHKT1 transporter-induced Na^+ unloading from xylem vessels to xylem parenchyma cells. *The Plant Journal, 44*(6), 928-938.

Suzuki, K., Yamaji, N., Costa, A., Okuma, E., Kobayashi, N. I., Kashiwagi, T., . . . Murata, Y. (2016). OsHKT1;4-mediated Na^+ transport in stems contributes to Na^+ exclusion from leaf blades of rice at the reproductive growth stage upon salt stress. *BMC plant biology, 16*(1), 1-15.

Szyroki, A., Ivashikina, N., Dietrich, P., Roelfsema, M. R. G., Ache, P., Reintanz, B., . . . Steinmeyer, R. (2001). KAT1 is not essential for stomatal opening. *Proceedings of the National Academy of Sciences, 98*(5), 2917-2921.

Tester, M., & Davenport, R. (2003). Na^+ tolerance and Na^+ transport in higher plants. *Annals of botany, 91*(5), 503-527.

Thiel, G. & Blatt, M. R. (1991). The mechanism of ion permeation through K^+ channels of stomatal guard cells: voltage-dependent block by Na^+. *Journal of Plant Physiology 138*, 326–334.

Touraine, B., Grignon, N., & Grignon, C. (1988). Charge balance in NO_3^--fed soybean: estimation of K^+ and carboxylate recirculation. *Plant Physiology, 88*(3), 605-612.

Touraine, B., Muller, B., & Grignon, C. (1992). Effect of phloem-translocated malate on NO_3^- uptake by roots of intact soybean plants. *Plant Physiology, 99*(3), 1118-1123.

Trchounian, A., & Kobayashi, H. (1999). Kup is the major K^+ uptake system in Escherichia coli upon hyper-osmotic stress at a low pH. *FEBS letters, 447*(2-3), 144-148.

Tsujii, M., Kera, K., Hamamoto, S., Kuromori, T., Shikanai, T., & Uozumi, N. (2019). Evidence for potassium transport activity of Arabidopsis KEA1-KEA6. *Scientific reports, 9*(1), 1-13.

Turgeon, R. (2010). The role of phloem loading reconsidered. *Plant Physiology, 152*(4), 1817-1823.

Uozumi, N., Kim, E. J., Rubio, F., Yamaguchi, T., Muto, S., Tsuboi, A., . . . Schroeder, J. I. (2000). The Arabidopsis HKT1 gene homolog mediates inward Na^+ currents in Xenopus laevis oocytes and Na^+ uptake in Saccharomyces cerevisiae. *Plant physiology, 122*(4), 1249-1260.

Van Bel, A. J. E. (1990). Xylem-phloem exchange via the rays: the undervalued route of transport. *Journal of Experimental Botany, 41*(6), 631-644.

van Beusichem, M. L., Baas, R., Kirkby, E. A., & Nelemans, J. A. (1985). Intracellular pH regulation during NO_3^- assimilation in shoot and roots of Ricinus communis. *Plant Physiology, 78*(4), 768-773.

Vandesompele, J., De Preter, K., Pattyn, F., Poppe, B., Van Roy, N., De Paepe, A., & Speleman, F. (2002). Accurate normalization of real-time quantitative RT-PCR data by geometric averaging of multiple internal control genes. *Genome biology, 3*(7), 1-12.

van Zelm, E., Zhang, Y., & Testerink, C. (2020). Salt tolerance mechanisms of plants. *Annual Review of Plant Biology, 71*, 403-433.

Véry, A.-A., Nieves-Cordones, M., Daly, M., Khan, I., Fizames, C., & Sentenac, H. (2014).

Molecular biology of K^+ transport across the plant cell membrane: what do we learn from comparison between plant species? *Journal of plant physiology, 171*(9), 748-769.

Véry, A. A., Robinson, M. F., Mansfield, T. A., & Sanders, D. (1998). Guard cell cation channels are involved in Na^+–induced stomatal closure in a halophyte. *The Plant Journal, 14*(5), 509-521.

Véry, A.-A., & Sentenac, H. (2003). Molecular mechanisms and regulation of K^+ transport in higher plants. *Annual Review of Plant Biology, 54*(1), 575-603.

Vieira-Pires, R. S., Szollosi, A., & Morais-Cabral, J. H. (2013). The structure of the KtrAB potassium transporter. *Nature, 496*(7445), 323-328.

Villette, J., Cuéllar, T., Zimmermann, S. D., Verdeil, J.-L., & Gaillard, I. (2019). Unique features of the grapevine VvK5.1 channel support novel functions for outward K^+ channels in plants. *Journal of Experimental Botany, 70*(21), 6181-6193.

Wakeel, A., Farooq, M., Qadir, M., & Schubert, S. (2011). Potassium substitution by sodium in plants. *Critical reviews in plant sciences, 30*(4), 401-413.

Wang, Y., He, L., Li, H.-D., Xu, J., & Wu, W.-H. (2010). Potassium channel α-subunit AtKC1 negatively regulates AKT1-mediated K^+ uptake in Arabidopsis roots under low-K^+ stress. *Cell research, 20*(7), 826-837.

Wang, R., Jing, W., Xiao, L., Jin, Y., Shen, L., & Zhang, W. (2015). The rice high-affinity potassium transporter1;1 is involved in salt tolerance and regulated by an MYB-type transcription factor. *Plant Physiology, 168*(3), 1076-1090.

Wang, Y., & Wu, W. H. (2010). Plant sensing and signaling in response to K^+-deficiency. *Molecular plant, 3*(2), 280-287.

Wang, Y., & Wu, W. H. (2013). Potassium transport and signaling in higher plants. *Annual review of plant biology, 64*, 451-476.

Wang, G., Wu, Y., Ma, L., Lin, Y., Hu, Y., Li, M., ... & Chen, L. (2021). Phloem loading in rice leaves depends strongly on the apoplastic pathway. *Journal of Experimental Botany, 72*(10), 3723-3738.

Wang, C., Yamamoto, H., Narumiya, F., Munekage, Y. N., Finazzi, G., Szabo, I., & Shikanai, T. (2017). Fine-tuned regulation of the K^+/H^+ antiporter KEA3 is required to optimize photosynthesis during induction. *The Plant Journal, 89*(3), 540-553.

Ward, J. M., Hirschi, K. D., & Sze, H. (2003). Plants pass the salt. *Trends in plant science, 8*(5), 200-201.

Ward, J. M., Mäser, P., & Schroeder, J. I. (2009). Plant ion channels: gene families, physiology, and functional genomics analyses. *Annual review of physiology, 71*, 59-82.

Wegner, L. H., & De Boer, A. H. (1997). Properties of two outward-rectifying channels in root xylem parenchyma cells suggest a role in K^+ homeostasis and long-distance signaling. *Plant Physiology, 115*(4), 1707-1719.

White, P. J. (1997). The regulation of K+ influx into roots of rye (Secale cereale L.) seedlings by negative feedback via the K^+ flux from shoot to root in the phloem. *Journal of Experimental Botany, 48*(12), 2063-2073.

Williams, L. E., Lemoine, R., & Sauer, N. (2000). Sugar transporters in higher plants–a diversity of roles and complex regulation. *Trends in plant science, 5*(7), 283-290.

Wolf, O., Munns, R., Tonnet, M., & Jeschke, W. (1991). The role of the stem in the partitioning of Na^+ and K^+ in salt-treated barley. *Journal of Experimental Botany, 42*(6), 697-704.

Wu, H., Zhang, X., Giraldo, J. P., & Shabala, S. (2018). It is not all about sodium: revealing tissue specificity and signalling roles of potassium in plant responses to salt stress. *Plant and soil, 431*(1), 1-17.

Xicluna, J., Lacombe, B., Dreyer, I., Alcon, C., Jeanguenin, L., Sentenac, H., . . . Chérel, I. (2007). Increased functional diversity of plant K^+ channels by preferential heteromerization of the shaker-like subunits AKT2 and KAT2. *Journal of Biological Chemistry, 282*(1), 486-494.

Xiong, L., Schumaker, K. S., & Zhu, J.-K. (2002). Cell signaling during cold, drought, and salt stress. *The Plant Cell, 14*(suppl 1), S165-S183.

Xu, J., Li, H. D., Chen, L. Q., Wang, Y., Liu, L. L., He, L., & Wu, W. H. (2006). A protein kinase, interacting with two calcineurin B-like proteins, regulates K^+ transporter AKT1 in Arabidopsis. *Cell, 125*(7), 1347-1360.

Yang, T., Zhang, S., Hu, Y., Wu, F., Hu, Q., Chen, G., . . . Yu, L. (2014). The role of a potassium transporter OsHAK5 in potassium acquisition and transport from roots to shoots in rice at low potassium supply levels. *Plant Physiology, 166*(2), 945-959.

Yeo, A. (1998). Molecular biology of salt tolerance in the context of whole-plant physiology. *Journal of Experimental Botany, 49*(323), 915-929.

Yu, S.-M., Lo, S.-F., & Ho, T.-H. D. (2015). Source–sink communication: regulated by hormone, nutrient, and stress cross-signaling. *Trends in plant science, 20*(12), 844-857.

Zagotta, W. N., Hoshi, T., & Aldrich, R. W. (1990). Restoration of inactivation in mutants of Shaker potassium channels by a peptide derived from ShB. *Science, 250*(4980), 568-571.

Zakharyan, E., & Trchounian, A. (2001). K^+ influx by Kup in Escherichia coli is accompanied by a decrease in H^+ efflux. *FEMS microbiology letters, 204*(1), 61-64.

Zeng, L., & Shannon, M. C. (2000). Salinity effects on seedling growth and yield components of rice. *Crop Science, 40*(4), 996-1003.

Zheng, S., Pan, T., Fan, L., & Qiu, Q. S. (2013). A novel AtKEA gene family, homolog of bacterial K^+/H^+ antiporters, plays potential roles in K^+ homeostasis and osmotic adjustment in Arabidopsis. *PLoS One, 8*(11), e81463.

Zhu, X., Pan, T., Zhang, X., Fan, L., Quintero, F. J., Zhao, H., . . . Mendoza, I. (2018). K^+ efflux antiporters 4, 5, and 6 mediate pH and K^+ homeostasis in endomembrane compartments. *Plant Physiology, 178*(4), 1657-1678.

Annexes

Résumé long de la thèse en français

K^+, le cation inorganique le plus abondant dans les plantes, représente jusqu'à 10% du poids sec total de la plante (Véry & Sentenac, 2003). Il est très mobile à l'intérieur des plantes, et peut être transporté sur de longues distances, en effectuant des cycles au sein du système vasculaire. Il peut être rapidement remobilisé des tissus plus anciens vers les plus jeunes pour soutenir la croissance (Atwell & Steer, 1990 ; Proe, Midwood, & Craig, 2000).

De nombreux systèmes de transport de K^+ ont été identifiés chez les plantes modèles (Mäser et al., 2001; Véry et al., 2014). Ils possèdent différentes propriétés en termes de sélectivité ionique, d'affinité et d'énergétique de transport (transports passifs ou actifs de K^+ énergisé par un couplage avec d'autres ions, H^+ ou Na^+). Ces systèmes de transport de K^+ chez les plantes se répartissent en deux familles de canaux K^+, à savoir les familles Shaker et TPK, et trois familles de transporteurs de K^+, à savoir les familles HAK/KUP/KT, HKT et KEA/CPA (Véry et al., 2014). Les canaux K^+ Shaker assure la médiation de flux passifs de K^+ et constituent la conductance majeure à K^+ de la membrane plasmique dans la plupart des tissus et types cellulaires (Lebaudy, Véry, & Sentenac, 2007; Véry et al., 2014).

Les canaux Shaker des plantes qui sont des canaux K^+ "voltage-dépendants" (c.a.d., dont l'activité est régulée par le voltage) présentent une structure prédite très similaire à celle de leurs homologues chez les animaux (Véry & Sentenac, 2003). Les canaux Shaker végétaux fonctionnels sont des protéines tétramériques composées de quatre sous-unités α dont la partie transmembranaire est impliqué dans la perméation de K^+. Chaque sous-unité α contient six segments transmembranaires hydrophobes (S1-S6), un domaine "pore" (P) entre le cinquième et le sixième segment, et des extrémités N- et C-terminales, qui sont situées dans le cytosol. L'extrémité C-terminale contient plusieurs éléments régulateurs, dont le domaine de liaison des nucléotides cycliques (CNBD), le domaine homologue à l'ankyrine (Anky ; non présent dans tous les canaux), et le domaine riche en résidus hydrophobes et acides (KHA). Le domaine ankyrine peut agir comme un site de régulation fonctionnelle des canaux Shaker en interagissant avec des partenaires régulateurs (par exemple, des kinases ou des phosphatases) (Véry et al., 2014). Les canaux K^+ de Shaker présentent cinq groupes phylogénétiques et quatre types fonctionnels: canaux rectifiant entrants (spécialisés dans des influx de K^+ vers l'intérieur de la cellule), canaux rectifiant sortants (spécialisés dans des efflux de K^+ vers l'extérieur de la cellule), canaux faiblement rectifiant, canaux silencieux (c'est-à-dire qui ne médient pas de courant lorsqu'ils sont exprimés seuls). Chez le riz, la structure de la famille des canaux Shaker est très similaire à celle d'Arabidopsis (Pilot et al. 2003b).

Des systèmes d'absorption de K^+ à faible affinité (passifs) et à haute affinité (actifs) sont présents dans les couches périphériques des racines pour optimiser l'absorption de ce cation par la racine en fonction de la disponibilité externe de K^+ (Epstein, 1973; Epstein, Rains, & Elzam, 1963). K^+ absorbé par les racines est chargé dans le xylème, puis transloqué vers les parties aériennes via les vaisseaux du xylème, par la pression racinaire et la transpiration. Chez Arabidopsis, il a été démontré que le canal K^+ Shaker sortant SKOR joue un rôle majeur dans la sécrétion de K^+ dans la sève du xylème (Gaymard et al., 1998). SKOR est exprimé dans les cellules du péricycle de la racine et du parenchyme xylémien. Une approche de génétique inverse et la caractérisation électrophysiologique ont démontré que SKOR fonctionne comme un canal voltage-dépendant de type sortant et contribue à environ 50% de la translocation de K^+ vers les parties aériennes (Gaymard et al., 1998). L'identité moléculaire des autres systèmes contrôlant la charge en K^+ de la sève du xylème est jusqu'à présent peu

déterminée. Il a été démontré que le transporteur de nitrate NRT1.5, qui est exprimé dans le péricycle des racines (Lin et al., 2008), contribue légèrement à déterminer la concentration de K^+ dans la sève du xylème, en même temps que la concentration de nitrate, dans des plantes cultivées dans des conditions limitantes en K^+ (Li et al., 2017). De plus, AtKUP7, qui est exprimé de manière ubiquitaire et participe à l'absorption de K^+ par les racines, pourrait également être directement impliqué dans le contrôle de la charge en K^+ de la sève du xylème dans des plantes cultivées dans des conditions de faible disponibilité en K^+ (Han et al., 2016).

Chez le riz, le canal K^+ Shaker sortant OsK5.2 et les transporteurs de K^+ à haute affinité OsHAK5 sont considérés comme impliqués dans la charge en K^+ de la sève du xylème (Nguyen et al., 2017; Yang et al., 2014). OsK5.2 est exprimé dans les tissus vasculaires des racines et les stomates. Une approche de génétique inverse a révélé qu'OsK5.2 contribue fortement à la translocation de K^+ vers les parties aériennes, comme SKOR chez Arabidopsis (Nguyen et al., 2017). Les études sur *OsHAK5* ont montré en plus d'une large expression dans les couches périphériques des racines, une expression dans les tissus vasculaires, et une augmentation de l'expression dans des conditions limitantes en K^+, ce qui suggère qu'OsHAK5 peut avoir des rôles physiologiques dans les racines à la fois dans l'absorption de K^+ et la translocation de K^+ entre les racines et les parties aériennes, en particulier dans des conditions de faible disponibilité en K^+ dans le milieu externe (Yang et al., 2014). Une diminution de la concentration de K^+ dans la sève xylémienne chez les plantes mutantes pertes de fonction pour ce gène a été observée, spécifiquement dans des conditions de carence en K^+ (Yang et al., 2014). Cela pourrait provenir de l'absorption réduite par les racines, mais pourrait également indiquer une implication directe d'OsHAK5 dans la translocation de K^+ des racines vers les parties aériennes.

Les tissus vasculaires du phloème sont composés de cellules vivantes: les tubes criblés, qui ont dégradé la plupart de leurs organites, y compris le noyau, et les cellules compagnes étroitement associées avec les tubes criblés et reliées par de nombreux pores plasmodesmatiques pour former le complexe tube criblé-cellule compagne ("SE-CC") (Williams, Lemoine, & Sauer, 2000). Le phloème peut transporter les assimilats photosynthétiques depuis les sites de synthèse dans les organes sources (feuilles matures) jusqu'aux sites d'utilisation dans les organes puits (par exemple, les apex des racines et des pousses aériennes) (Patrick, 1997). En plus des hydrates de carbone, divers composés peuvent être trouvés dans l'exsudat du phloème tels que des ions, des protéines, des acides nucléiques, des hormones, des acides gras, en particulier comme signaux de régulation à longue distance entre les sources et les puits (Lucas, Yoo, & Kragler, 2001). On connaît peu de choses sur le mécanisme moléculaire du transport de K^+ dans le phloème des plantes. K^+ est le principal ion inorganique présent dans la sève du phloème (Deeken et al., 2008). Le contrôle du transport de K^+ dans le phloème joue un rôle dans la construction du gradient osmotique qui permet la translocation des assimilats photosynthétiques des organes sources (feuilles) vers les organes puits (Patrick, 1997). Chez Arabidopsis, AKT2, le seul canal Shaker K^+ caractérisé dans le phloème, est supposé, par le transport de K^+ qu'il occasionne, jouer un rôle crucial dans la régulation de la (re)charge en saccharose du phloème (Deeken et al., 2002 ; Gajdanowicz et al., 2011; Lacombe et al., 2000). Une approche de génétique inverse a démontré que AKT2 est en fait nécessaire à la polarisation électrique de la membrane du phloème (d'une manière dépendante de K^+) et à la charge en saccharose de la sève du phloème, probablement par son contrôle de la polarisation de la membrane des cellules du phloème (Deeken et al., 2002). En revanche, l'activité d'AKT2 s'est avérée avoir peu d'impact sur le contrôle des concentrations de K^+ dans la sève du phloème (Deeken et al., 2002). Chez le riz, on connaît peu de choses sur

le transport de K^+ dans le phloème. Récemment, par l'analyse de plantes de riz transgéniques exprimant le promoteur d'*OsAKT2* (*OsK3.1*) fusionné au gène rapporteur *GUS*, a été montré qu'OsAKT2, comme son homologue AKT2 d'Arabidopsis, est particulièrement exprimé dans les tissus vasculaires du phloème des parties aériennes (Shen et al., 2020). Le rôle physiologique d'OsAKT2 dans le transport de K^+ dans le phloème du riz reste en grande partie inconnu.

Le contrôle de l'ouverture stomatique permet d'optimiser les échanges gazeux entre les tissus internes de la feuille et l'atmosphère, notamment l'apport de CO2 pour la photosynthèse et la perte d'eau par transpiration. La transpiration des feuilles est un des paramètres qui modulent la translocation de K^+ vers les parties aériennes. Chez Arabidopsis, les canaux Shaker entrants KAT1 et KAT2 sont considérés comme les principaux systèmes qui médient l'influx de K^+ dans les cellules de garde pendant l'ouverture stomatique, tandis que le canal Shaker sortant GORK est le principal impliqué dans l'efflux de K^+ de ces cellules pendant la fermeture stomatique (Hosy et al., 2003; Lebaudy et al., 2008). Chez le riz, les mouvements stomatiques sont régulés par une navette d'ions entre les cellules de garde et les cellules subsidiaires adjacentes, qui forment le complexe stomatique (Mumm, Wolf, Fromm, Roelfsema, & Marten, 2011). À ce jour, il a été démontré que le canal K^+ Shaker sortant OsK5.2 joue un rôle dans la sécrétion de K^+ par les cellules de garde pour engendrer la fermeture stomatique (Nguyen et al., 2017).

La salinisation des sols favorisée par le changement climatique, est l'un des principaux facteurs contribuant à la dégradation des terres et à la désertification, et affecte de manière significative la production et la qualité des principales cultures, incluant les cultures céréalières dans le monde. La restriction de la croissance des plantes dans les sols salins est principalement due à des niveaux élevés de Na^+ et de Cl^-. Pour la majorité des plantes, Na^+ est considéré comme le principal ion toxique en cas de stress salin. Les dommages spécifiques à Na^+ sont souvent associés à une carence en K^+ et à d'autres déséquilibres en nutriments ioniques (Cramer, Lynch, Läuchli, & Epstein, 1987; Parida & Das, 2005). A court terme, l'exposition des plantes à la salinité abaisse le potentiel hydrique de la solution du sol. Les racines ont donc des difficultés à absorber l'eau de la solution externe du sol, ce qui entraîne un stress osmotique (Munns & Tester, 2008 ; van Zelm, Zhang, & Testerink, 2020). Une réponse adaptative pour faire face à ce stress est l'absorption par la racine de sels du sol. A long terme, l'exposition des plantes à la salinité, conduit à une arrivée massive d'ions, en particulier de Na^+, à un niveau toxique dans le cytoplasme des cellules foliaires via le flux de transpiration (Munns, 2005; Munns & Tester, 2008). Cet effet ultérieur spécifique de Na^+ apparaît généralement sur les vieilles feuilles en inhibant leur capacité photosynthétique (van Zelm et al., 2020). De plus, l'excès de Na^+ dans le sol entraîne un déficit plus ou moins grave d'absorption de K^+, Ca^{2+} et NO_3^- qui sont des ions essentiels pour la croissance et le développement des plantes, et peut finalement conduire à la mort des plantes (James et al., 2011). En réponse au stress salin, les plantes peuvent activer des mécanismes complexes aux niveaux physiologique et moléculaire. Les effets les plus délétères sur les plantes sous stress salin apparaissent dans la deuxième phase en raison de la perturbation de l'homéostasie ionique (Munns & Tester, 2008). Comme Na^+ et K^+ ont des propriétés physico-chimiques très similaires, ils peuvent entrer en compétition pour des sites de liaison dans des protéines impliquées dans des processus métaboliques clés du cytoplasme (Marschner, 1995). En tant que nutriment essentiel, K^+ est nécessaire à l'activation de plus de 60 enzymes cytoplasmiques, alors que Na^+ ne peut pas se substituer à K^+ dans ces fonctions spécifiques (Evans & Sorger, 1966; Suelter, 1970). De plus, la sensibilité au stress salin est largement attribuée à la

déficience en K^+ induite par le sel, d'autant plus que la concentration en K^+ dans le sol est généralement de l'ordre de 100 micromolaires (Véry & Sentenac, 2003), soit plusieurs ordres de grandeur inférieure à celle de Na^+. Par conséquent, l'accumulation de K^+ dans les parties aériennes et le maintien d'un rapport cytosolique K^+/Na^+ élevé dans les feuilles sont cruciaux pour la survie des plantes en condition de forte salinité (Hauser & Horie, 2010; Shabala & Cuin, 2008). Les membranes des cellules végétales contiennent un grand nombre de systèmes de transport qui sont responsables du transport de K^+ et de Na^+ à travers les membranes. Tous ces systèmes contribuent potentiellement à l'homéostasie K^+/Na^+ et à la tolérance des plantes au sel. Cependant, jusqu'à présent, seul le rôle des systèmes de transport de Na^+, en particulier les transporteurs de Na^+ de la famille HKT qui sont impliqués dans les QTL d'homéostasie K^+/Na^+, est bien documenté.

Objectifs de ma thèse

Il est d'une grande importance agronomique pour une culture alimentaire de base comme le riz de proposer des stratégies utiles pour améliorer la nutrition minérale de la plante, et donc potentiellement, la production de biomasse et de rendement et l'adaptation aux contraintes environnementales telles que la forte salinité du sol. La compréhension des mécanismes médiés par les systèmes de transport de K^+, par lesquels le riz peut absorber K^+ à partir de la solution externe du sol et répartir cet ion via le système vasculaire dans les tissus de la plante entière pour la croissance de la plante, et en condition de stress salin pour la prévention de la toxicité de Na^+, peut contribuer à atteindre cet objectif. Au niveau moléculaire, je me suis concentrée sur les deux canaux K^+ Shaker de type sortant du riz, OsK5.1 et OsK5.2, respectivement, supposé jouer un rôle dans le transport de K^+ à longues distances, ou connu pour être impliqué dans ce transport. Très peu d'information était disponible sur OsK5.1, à part le fait qu'il était exprimé dans le système vasculaire des racines (Kim et al., 2015). En revanche, OsK5.2 était déjà connu pour être impliqué dans la charge en K^+ de la sève du xylème et la sécrétion de K^+ par les cellules de garde pour la fermeture des stomates et ainsi dans le contrôle de la transpiration des feuilles (Nguyen et al., 2017).

1) La transpiration des feuilles étant, en plus de la sécrétion d'ions vers les vaisseaux du xylème, l'un des paramètres qui modulent la translocation des ions vers les parties aériennes, OsK5.2 semblait être un modèle intéressant pour évaluer le niveau de contribution de ces fonctions au contrôle de l'apport de K^+ et de Na^+ aux parties aériennes en conditions salines et à la tolérance des plantes au sel. En effet, bien que l'homéostasie de K^+ et Na^+ dans les feuilles soit considérée comme un paramètre clé de la tolérance au sel chez les plantes, les mécanismes sous-jacents ne sont pas entièrement identifiés. En particulier, la contribution des canaux K^+ à cette homéostasie a été peu examinée. **Cette étude sur le rôle des fonctions d'OsK5.2 dans la tolérance au sel des plantes de riz, basée sur une approche de génétique inverse, est présentée au chapitre III:**

La mutation perte de fonction (KO) d'*OsK5.2* n'a pas de conséquence notable sur le développement du riz (cv Nipponbare) lorsque les plantes sont cultivées dans un milieu hydroponique standard. De manière intéressante, j'ai observé que lorsque les plantes étaient soumises à des conditions salines (plantes de 6 semaines soumises à 100 mM NaCl pendant 7 jours), les plantes mutantes *osk5.2* présentaient alors une réduction sévère de la biomasse, alors que les plantes de génotype sauvage (WT) ne présentaient pas de réduction significative de biomasse. Ainsi, le canal K^+ à rectification sortante OsK5.2, impliqué dans la translocation de K^+ vers les parties aériennes et la sécrétion de K^+ par les cellules de garde pour la fermeture des stomates, est un déterminant important de la tolérance au sel du riz. Lors d'un

traitement salin, l'expression d'*OsK5.2* s'est révélée plutôt maintenue dans les racines. La fonction d'OsK5.2 dans la charge en K^+ de la sève du xylème s'est montrée maintenue, et même augmentée de façon transitoire, dans les racines. Ceci indique que les canaux K^+ peuvent fortement contribuer à la sécrétion de K^+ dans la sève du xylème en condition de stress salin, un point qui n'avait pas été clarifié auparavant. En effet, il est difficile d'obtenir des mesures fiables du potentiel membranaire et de la concentration apoplastique de K^+ des cellules stellaires. Ainsi, le fait qu'OsK5.2 puisse contribuer à la sécrétion de K^+ en cas de stress salin fournit une preuve définitive que la sécrétion passive (médiée par les canaux) de K^+ peut se produire dans les cellules stellaires des plantes de riz confrontées à des conditions salines. Cette conclusion, qui n'exclut pas une contribution des mécanismes actifs de transport de K^+ à la sécrétion de K^+ en conditions salines, signifie également que d'autres canaux qu'OsK5.2, soit sélectifs de K^+ et appartenant à la famille Shaker (Véry et al., 2014), soit peu sélectifs de K^+ comme les canaux NSCC identifiés dans les cellules stellaires par des expériences de patch clamp (Wegner & de Boer, 1997), pourraient également contribuer à la sécrétion de K^+ dans la sève du xylème dans de telles conditions. Mes résultats ont également montré qu'OsK5.2 était impliqué sélectivement dans le transport de K^+ dans les racines et n'était pas impliqué dans la charge en Na^+ de la sève du xylème, indiquant que le canal est sélectif de K^+, comme attendu, et que son activité n'a pas non plus d'effet indirect sur le transport de Na^+, par exemple par un effet sur le potentiel électrique de la membrane cellulaire.

Dans les parties aériennes, l'expression d'*OsK5.2* est régulée à la hausse dès le début du traitement salin. La fonction de sécrétion de K^+ d'OsK5.2 dans les cellules de garde s'est révélée permettre une réduction rapide de l'ouverture des stomates sous traitement salin, et donc une diminution du flux d'eau transpiratoire. La contribution réelle des canaux ioniques des cellules de garde au déclenchement de la fermeture des stomates lors d'un stress salin a été peu étudiée jusqu'à présent. Ici, mes données révèlent le rôle important de l'activité des canaux K^+ sortants dans le contrôle de l'ouverture des stomates lors d'un stress salin. Les données de transpiration de la plante entière indiquent en effet que l'activité d'OsK5.2 dans les stomates a contribué à la réduction de l'ouverture stomatique pendant toute la durée du traitement salin, et que cette activité est particulièrement importante au début du stress salin en permettant une réduction plus précoce de l'ouverture stomatique. La diminution du flux d'eau transpirationnel à travers l'activité d'OsK5.2 dans le stomate limite le flux de Na^+ à travers la plante et réduit l'accumulation de Na^+ dans les feuilles. La diminution du flux d'eau transpirationnel a cependant aussi un effet dépressif sur le flux volumétrique de translocation de K^+ de la sève du xylème. Mais mes analyses montrent que la contribution d'OsK5.2 à la charge en K^+ de la sève du xylème surpasse l'effet "négatif" résultant de la réduction du flux volumique du xylème. Ainsi, dans l'ensemble, les fonctions d'OsK5.2 permettent la nutrition en K^+ des parties aériennes tout en minimisant l'arrivée de Na^+, et sont apparues très bénéfiques pour l'homéostasie K^+/Na^+ des feuilles, l'évitement de la toxicité saline et le maintien de la croissance des plantes.

Étant donné qu'assurer une absorption efficace de K^+ à partir de la solution du sol par les racines semble être le principal moyen d'assurer l'alimentation en K^+ des parties aériennes, la plupart des études visant à identifier les déterminants de la tolérance au sel parmi des systèmes de transport du K^+ se sont concentrées sur les systèmes d'absorption racinaires. Il a été démontré que plusieurs transporteurs HAK sont impliqués dans l'absorption de K^+ par les racines et contribuent ainsi à la tolérance au sel des plantes: AtHAK5 chez Arabidopsis (Nieves-Cordones et al., 2010), et OsHAK1, OsHAK5, OsHAK16 et OsHAK21 chez le riz

(Chen et al., 2015; Feng et al., 2019; Shen et al., 2015; Yang et al., 2014). D'autre part, d'autres mécanismes de tolérance au sel chez les plantes médiés par le transport de K^+ et en particulier des mécanismes impliquant des canaux K^+, ont été rapportés mais n'ont pas encore été décryptés. En particulier, les rôles des deux homologues d'OsK5.2 chez Arabidopsis, SKOR et GORK, dans la tolérance au sel d'Arabidopsis n'avaient pas encore été caractérisés. Ici, je montre que les deux fonctions d'OsK5.2, c'est-à-dire le contrôle de l'ouverture stomatique et la sécrétion de K^+ dans la sève du xylème, sous-tendent ensemble la contribution du canal à la tolérance au sel. En plus de mettre en évidence des mécanismes de tolérance au sel médiés par des canaux K^+, ces résultats fournissent une nouvelle cible possible pour les sélectionneurs en vue de l'amélioration de la tolérance au stress salin chez le riz.

(2) En approfondissant l'étude de l'expression d'OsK5.2 dans le système vasculaire, j'ai localisé l'expression d'OsK5.2 dans les tissus du phloème des plantes de riz. Cette nouvelle découverte a suscité des questions sur la façon dont OsK5.2 contrôle la concentration de K^+ dans la sève du xylème et sur le rôle de ce canal dans la circulation globale de K^+ dans la plante. **L'étude des rôles d'OsK5.2 dans la circulation de K^+ à travers le xylème et le phloème dans la plante entière du riz, en utilisant une approche de génétique inverse, est rapportée dans le chapitre IV.**
En effectuant une coloration GUS de sections transversales de racines, de feuilles et de gaines foliaires, j'ai révélé la localisation de l'activité du promoteur d'*OsK5.2* en particulier dans les tissus du phloème. Dans les coupes transversales de racines, l'activité GUS a été détectée dans les cellules compagnes du phloème et le parenchyme du xylème. Dans les coupes transversales de feuilles, l'activité GUS a été détectée dans les cellules compagnes du phloème et le parenchyme vasculaire. L'analyse par qRT-PCR a montré que l'expression d'*OsK5.2* était détectée à la fois dans les racines et dans les feuilles, mais que les transcrits d'*OsK5.2* étaient 4 fois plus abondants dans les racines, chez des plantes âgées de 5 semaines. Après avoir observé qu'*OsK5.2* est exprimé dans les tissus du phloème, le rôle d'OsK5.2 dans le phloème a d'abord été étudié en analysant la sève du phloème dans des plantes WT et mutantes *osk5.2*. Des limbes de feuilles matures ont été utilisés, et afin d'empêcher l'obturation des tubes criblés du phloème par la coupure, une solution d'EDTA a été appliquée pour faciliter l'écoulement continu de la sève du phloème (King & Zeevaart, 1974).

Les concentrations de K^+ se sont révélées significativement réduites dans la sève du phloème des plantes mutantes *osk5.2*, d'environ 30%. Ainsi, la perte de fonction d'*OsK5.2* a été identifiée comme entraînant à la fois un défaut dans la concentration de K^+ dans la sève du xylème (chapitre 3; Nguyen et al., 2007), un défaut dans la teneur en K^+ des feuilles et un défaut dans la concentration de K^+ dans la sève du phloème. Par conséquent, le défaut relatif à K^+ chez les plantes mutantes *osk5.2* semble concerner l'ensemble de la boucle de circulation de K^+ entre les racines et les parties aériennes, et donc le rôle précis du canal OsK5.2 et l'origine du défaut n'étaient plus aussi clairs. Comme OsK5.2 est principalement exprimé dans la racine, je me suis d'abord concentrée sur cet organe pour compléter l'analyse des fonctions d'OsK5.2. OsK5.2 étant exprimé à la fois dans le parenchyme du xylème et dans les cellules compagnes du phloème dans la racine, il pourrait jouer un rôle dans la charge en K^+ de la sève du xylème de deux manières distinctes: (1) être impliqué dans la sécrétion "directe" vers la sève du xylème depuis le parenchyme xylémien de K^+ arrivant du flux d'absorption de la racine, et (2) être impliqué dans la décharge de K^+ de la sève du phloème, ce K^+ sécrété étant capable de recirculer dans le xylème (Wegner & de Boer, 1997). Afin de discriminer ces

deux rôles, j'ai opté pour la mise en place d'une série d'expériences de traçage de K^+ en utilisant l'analogue de K^+, Rb^+. Les rapports des concentrations de Rb^+ et K^+ dans les sèves du xylème et du phloème ont permis d'estimer dans quelle mesure Rb^+ avait été sécrété dans la sève et avait recirculé dans la plante par le phloème. J'ai déterminé que 5 heures après l'apport de Rb^+ dans le milieu externe, Rb^+ dans la sève du xylème proviendrait principalement du flux externe, et j'ai donc fixé ce temps pour une étude plus approfondie. Des conditions d'humidité relative de 70% ou de 90% ont été appliquées pendant la période d'apport de RbCl, afin d'examiner les différences possibles dans le transport de Rb^+ entre les plantes transpirantes et les plantes "non" transpirantes. Sous 90 % d'humidité relative, la concentration de Rb^+ dans la sève du xylème des plantes mutantes *osk5.2* s'est avérée significativement réduite par rapport à celle des plantes WT. Ceci indique que dans les plantes "non"-transpirantes, OsK5.2 contribue fortement à la sécrétion directe de K^+ dans la sève du xylème à partir du flux d'absorption. Sous une HR de 70 %, les concentrations de Rb^+ et de K^+ dans la sève du xylème des plantes WT ont clairement augmenté, toutes deux d'environ 66%, ce qui suggère que le taux de sécrétion de K^+ dans la sève du xylème augmente dans les plantes transpirantes. Chez les plantes mutantes osk5.2, la concentration moyenne de Rb^+ dans la sève du xylème, après l'apport de RbCl, n'a été réduite que d'environ 20 % par rapport à celle des plantes WT. Ainsi, sous une HR de 70 % par rapport à une HR de 90 %, la contribution des autres systèmes de transport de K^+ à la sécrétion directe de K^+ dans la sève du xylème a fortement augmenté, et la contribution relative d'OsK5.2 est devenue mineure. Puisque les concentrations de K^+ mesurées dans les mêmes échantillons de sève de xylème sous 70 % d'humidité relative, contrastent fortement avec celles de Rb^+ (fortement inférieures dans les plantes mutantes), cela indique qu'une grande partie de la concentration de K^+ dans la sève xylémienne à l'état stationnaire dans les plantes transpirantes provient de la recirculation de K^+ déchargé du phloème, dépendante de l'activité d'OsK5.2 dans ce tissu. J'ai donc émis l'hypothèse qu'OsK5.2 dans la membrane des cellules compagnes est impliqué dans la décharge de K^+ de la sève du phloème.

Puisque des connexions existent entre le transport de K^+ et le transport des photoassimilats dans le phloème, j'ai examiné l'effet d'une réduction de la durée de la phase lumineuse journalière sur le phénotype de croissance des plantes mutantes *osk5.2* et WT cultivées en hydroponie sur un milieu standard. Dans des conditions de jour court (cycle de 8 h de lumière/16 h de nuit), les plantes mutantes *osk5.2* ont montré des différences de croissance claires par rapport aux plantes WT correspondantes. La réduction de croissance des plantes mutantes *osk5.2* concernait à la fois les racines et les parties aériennes des plantes âgées de 5 semaines. Chez les plantes cultivées dans des conditions de longueur de jour normale, d'autre part, la teneur en fructose s'est avérée significativement diminuée dans les feuilles analysées des plantes mutantes par rapport aux plantes WT. La prochaine étape dans cette étude des connexions possibles entre l'activité d'OsK5.2 dans le phloème et le transport des glucides, sera d'analyser la translocation des sucres solubles vers les organes puits dans la sève du phloème de plantes WT et mutantes *osk5.2*.

En fin de compte, avec les études précédentes (Kim et al., 2015 ; Nguyen et al., 2017), les données qui sont maintenant disponibles fournissent une vision assez complète des fonctions d'OsK5.2, et en particulier de son rôle dans la circulation de K^+ dans toute la plante. OsK5.2 était connu pour être impliqué dans la charge de la sève du xylème en K^+, comme SKOR. Sauf dans le cas particulier des plantes "non" transpirantes, j'ai mis en évidence qu'OsK5.2 réalise cette charge en K^+ de la sève du xylème d'une manière différente de SKOR. Une contribution physiologique importante d'OsK5.2 à la décharge de K^+ du phloème dans

les racines a été mise en évidence. Ceci constitue une fonction nouvellement mise en évidence pour un canal K^+ sortant. L'observation d'un phénotype de croissance chez les plantes mutantes *osk5.2* dans des conditions de jours courts suggère de plus un rôle important d'OsK5.2 dans le transport des photoassimilats, qui devra être étudié plus en détail à l'avenir.

(3) *OsK5.1*, l'autre gène Shaker de canal K^+ sortant chez le riz, est annoté comme orthologue d'*AtSKOR* dans le génome du riz. Mes études d'expression tissulaire soutiennent l'hypothèse qu'*OsK5.1* est un orthologue potentiel du canal K^+ *SKOR* d'Arabidopsis, avec une expression conjointe dans le péricyle de la racine et le parenchyme du xylème. La fonction d'OsK5.1 a été analysée chez le riz en utilisant une approche de génétique inverse, et dans des contextes hétérologues, par complémentation du mutant perte de fonction *atskor* pour des analyses phénotypiques et par expression transitoire dans des cellules COS de mammifères pour comprendre les propriétés fonctionnelles du canal. OsK5.2 a été analysé en parallèle dans les systèmes d'expression hétérologue pour comparaison. **Ce travail sur les fonctions d'OsK5.1 et d'OsK.2 dans les systèmes d'expression hétérologue est rapporté dans le chapitre V.**
L'activité GUS, sous le contrôle du promoteur d'*OsK5.1*, s'est montrée très faible dans les limbes et les gaines des feuilles mais forte dans les racines, en accord avec les données d'expériences de qRT-PCR. Des coupes transversales des racines colorées par l'activité GUS ont montré que cette activité était principalement détectée dans le péricycle des racines, le parenchyme du métaxylème précoce et le phloème. Aucune activité GUS n'a été détectée dans le parenchyme central du métaxylème tardif. Dans l'ensemble, le patron d'expression observé pour *OsK5.1* permet de soutenir l'hypothèse selon laquelle *OsK5.1* serait un orthologue d'*AtSKOR*, et on pourrait donc prédire qu'OsK5.1 partage les fonctions d'AtSKOR dans la translocation de K^+ des racines vers les parties aériennes. De manière surprenante, deux lignées KO *osk5.1*analysées n'ont pas présenté de phénotype dans la translocation de K^+. Puisque chez le riz, contrairement à Arabidopsis, un autre canal Shaker, OsK5.2, contribue à la translocation de K^+ des racines vers les parties aériennes, j'ai émis l'hypothèse que l'absence de phénotype chez les plantes mutantes *osk5.1* pourrait être due à une redondance de fonction entre les deux gènes. La complémentation de la lignée mutante *skor* d'Arabidopsis avec la région codante d'*OsK5.1* sous le contrôle du promoteur *AtSKOR* a cependant rétabli la concentration de K^+ dans la sève du xylème, ce qui indique qu'OsK5.1, comme SKOR, est capable de sécréter K^+ dans la sève du xylème lorsqu'il est "introduit" dans les tissus où *SKOR* est exprimé dans la racine d'Arabidopsis. Ceci a permis de faire l'hypothèse qu'OsK5.1 est un canal K^+ de type sortant, semblable à SKOR. L'obtention d'informations fonctionnelles plus détaillées a été tentée par expression transitoire d'OsK5.1 dans la lignée cellulaire mammalienne COS-7. Bien que le canal K^+ Shaker GORK de type sortant d'Arabidopsis ait pu être exprimé fonctionnellement et caractérisé par la technique du patch-clamp en mode cellule entière, OsK5.1 s'est montré électriquement silencieux dans les cellules COS-7 en utilisant la technique du patch-clamp. Ma tentative d'exprimer fonctionnellement OsK5.2 dans des cellules COS-7 a également échoué. Ceci a suggéré de manière intéressante une régulation post-traductionnelle particulière dans ces canaux Shaker de riz, nécessaire à leur fonctionnement, contrairement aux canaux homologues d'Arabidopsis. J'ai commencé à examiner l'hypothèse selon laquelle la région N-terminale cytosolique pourrait être le siège de certaines de ces régulations, en concevant un canal chimérique NterGORK-OsK5.2 où la séquence N-terminale d'OsK5.2 a été échangée avec celle de GORK. Il est intéressant de noter que le canal chimérique s'est montré fonctionnel, médiant des courants K^+ sortants lorsqu'il a été exprimé dans les cellules COS-7. Ceci a ouvert la voie à d'autres analyses

fonctionnelles de ce canal et à l'identification des bases structurales de cette régulation particulière de l’activité de ce canal.